EVALUATION OF THE ENGINEERING PROPERTIES OF CLAYS WITH THE PIEZOCONE PENETROMETER

by

SETH PHILIP GADINSKY

B.S.C.E., Tufts University
(1980)

Submitted to the Department of
Civil Engineering
in Partial Fulfillment of the
Requirements of the Degree of

MASTER OF SCIENCE IN CIVIL ENGINEERING

at the

MASSACHUSETTS INSTITUTE OF TECHNOLOGY

February 1983

Signature of Author: _____
Department of Civil Engineering,
February 28, 1983

Certified by: _____
Amr S. Azzouz
Thesis Supervisor

Accepted by: _____
Francois M.M. Morel
Chairman, Civil Engineering Department Committee

EVALUATION OF THE ENGINEERING PROPERTIES OF CLAYS WITH THE PIEZOCONE PENETROMETER

by

SETH P. GADINSKY

Submitted to the Department of Civil Engineering on February 28, 1983 in partial fulfillment of the requirements for the degree of Master of Science in Civil Engineering

ABSTRACT

This thesis evaluates the adequacy of the recently developed Piezocone Penetrometer as an in situ testing device. A literature review documents previous experience with the piezocone in evaluating such diverse engineering properties as stress history, undrained shear strength, and coefficient of consolidation. This review is updated by results of a recent geotechnical investigation program performed on the MIT campus.

Simultaneous measurements of the cone resistance, q_c, and pore pressures, u, during piezocone penetration, obtained from several soil deposits, show the device to be extremely useful in the determination of soil stratification and identification. Furthermore, u and q_c measurements may be used to evaluate the stress history of a clay deposit. Results show that the ratio u/q_c is related to the overconsolidation ratio; high u/q_c associated with low OCR and vice-versa. More research is necessary, however, so as to establish a data base that can be relied upon for the estimation of the stress history of cohesive deposits.

Use of the piezocone penetrometer to evaluate the undrained shear strength, s_u, of clays has been approached both theoretically and empirically. Direct measurement of s_u from the cone penetration logs is possible through the use of one of the many theoretical solutions for the cone factor, N_K. Due to the many uncertainties involved in the application of those theories, however, empirical solutions are more extensively employed.

Once penetration is interrupted, pore pressure dissipation ensues. Solutions are currently available for predicting the consolidation and flow characteristics of cohesive deposits from the dissipation records. Evaluation of these theories by means of various case studies indicates that the solution developed by Baligh and Levadoux (1980) provides good estimates of the horizontal consolidation coefficient for use in problems involving unloading and possibly reloading of overconsolidated deposits.

Thesis Supervisor: Amr S. Azzouz
Title: Assistant Professor of Civil Engineering

ACKNOWLEDGEMENTS

I would like to acknowledge the persons for whom a great deal of appreciation is owed for helping me to complete this thesis. Their constant support and understanding enriched my tenure at MIT:

Professor Amr S. Azzouz, my thesis supervisor, whose input, guidance, and friendship throughout this long and painstaking process were a very special part of my MIT education.

All of my friends at MIT who didn't think that I would remember them in my acknowledgements.

Ronnie Schwartz and Terri Demeris for typing my thesis and for putting up with all of the rewrites and general harassment throughout the typing process.

Liebe Grace, only I can appreciate the difference her constant love and support have made in my life over the last three years; and Bill Schlosser, my roommate, who always managed to keep it all in perspective for me.

Finally, my family, whose love is a very special part of my life; especially my father, Edward, we should all be blessed with fathers like him.

TABLE OF CONTENTS

LIST OF TABLES

LIST OF FIGURES

LIST OF FIGURES - Cont.

LIST OF FIGURES - Cont.

LIST OF FIGURES - Cont.

LIST OF FIGURES - Cont.

LIST OF FIGURES - Cont.

CHAPTER 1

INTRODUCTION

1.1 Background

In situ testing has a long history in foundation engineering. The standard penetration test and earlier forms of the Dutch cone test, both in use before 1930, represented the main methods for early subsurface exploration and eventually led to the widely used design procedures based on empirical correlations. Development of the field vane test in Sweden during the 1940's enabled the first "simple" measurement of in situ undrained strength. Evaluation of these tests and developments of new, more sophisticated in situ testing techniques have recently become the subject of renewed interest and research.

The recently developed electric Piezocone Penetrometer represents an example of such new developments. Being able to simultaneously measure the cone resistance, pore pressure and sleeve friction during penetration, this device provides information which previously required two separate probes. Now, in addition to the evaluation of the undrained shear strength, the Piezocone can be utilized to evaluate engineering properties as diverse as stress history and coefficient of consolidation.

1.2 Scope and Objectives

In the fall of 1981, a geotechnical investigation was initiated at the vicinity of the Solar House located on the campus of the Massachusetts Institute of Technology, M.I.T.

The study was intended to establish a permanent on-campus facility for carrying out geotechnical in situ testing. The field investigation involved Piezocone Penetrometer borings, Field Vane testing, and undisturbed sampling. Subsequently, laboratory index-classification, consolidation and strength tests were performed on the undisturbed clay tube samples.

The objective of this thesis is to evaluate the adequacy of the Piezocone Penetrometer as an in situ device for determining the strength and consolidation characteristics of clays. The main body of the thesis reviews past studies reported in the literature concerning the Piezocone and details the findings resulting from the field and laboratory programs initiated at M.I.T. A breakdown of the topics covered in the thesis by chapter is as follows:

Chapter 2: Review of In Situ Tests for Evaluation of Engineering Properties of Clays.

Discussion in this chapter concerns the pros and cons of in situ versus laboratory testing and how in situ tests, such as the field vane, pressuremeter, and cone penetration tests can be utilized to evaluate the strength and consolidation characteristics of clays.

Chapter 3: Review of Soil Properties Underlying the M.I.T. Campus

Over the years, soil investigations were performed at various locations on the M.I.T. campus. This chapter

brings all of these studies together, tying in the results of the recent Solar House investigation program. Included are summaries of the index, strength, and consolidation test results from the various studies.

The last two chapters discuss how the Piezocone is used to evaluate the strength and consolidation properties of clays.

Chapter 4: Evaluation of Cone Resistance and Pore Pressure Measurements During Penetration

This chapter studies how cone resistance, q_c, measurements are used to evaluate the undrained shear strength and how simultaneous q_c and generated pore pressure, u, measurements can lead to predictions of stress history of clay deposits. The chapter also discusses the usefulness of cone penetration data in establishing soil stratifications and identifications.

Chapter 5: Evaluation of Pore Pressure Dissipation after Penetration

When penetration stops, the generated pore pressures dissipate. Herein will be demonstrated how the dissipation records, when used in conjunction with the existing theoretical solutions, can lead to estimations of the compressibility and flow characteristics of clays.

1.3 Findings and Conclusions

The extensive study performed herein has shown that the piezocone penetrometer has a great potential in establishing soil stratifications and identifications. Predictions of the undrained shear strength can be made from the cone resistance, q_c, data through empirical cone factors, N_k. Needless to say, a universal N_k value for all clays does not exist, although the values tend to fall within a certain range. Extreme caution is necessary, however, in applying these average values to sites for which no analysis has yet been made.

Theoretical solutions are currently available for predicting the consolidation and flow characteristics of fine-grained soils based on the pore pressure decay data when penetration stops. Evaluations in a variety of soil deposits show that the solutions provide reasonable estimates of coefficients of consolidation and permeability.

CHAPTER 2

REVIEW OF IN SITU TESTS FOR EVALUATION OF ENGINEERING PROPERTIES OF CLAYS

Many different types of tests currently exist, both in situ (e.g., the field vane, pressuremeter, Dutch cone, etc.) and laboratory, for evaluating the strength and consolidation characteristics of clays. Each test has advantages and limitations with regard to its use and applicability. Recently, much interest has been given to the use of the Piezocone Penetrometer as an in situ device for measuring the engineering properties of clays. This chapter will outline the pros and cons of in situ versus laboratory testing and present how some in situ tests are utilized to evaluate the strength and consolidation properties of clays.

2.1 In Situ Versus Laboratory Testing

In situ and laboratory testing provide two alternative approaches for evaluation of engineering properties of clays. Ladd et al. (1977) discussed the advantages and disadvantages of both forms of testing. A synopsis of this discussion is presented herein.

In situ testing (e.g., penetration and field vane tests) has the advantage of making measurements on relatively undisturbed soil at substantial savings in time and cost compared to laboratory tests, but interpretation of the data is highly empirical and often subject to substantial uncertainty. Also, in situ tests suffer in that the soil being tested cannot be seen. The more sophisticated, but also

more expensive, in situ testing devices (e.g., the pressuremeter) have the potential of yielding more easily interpreted and reliable data. Interest in in situ testing has greatly increased in recent years, this being directed towards development of improved equipment and new devices and at a better understanding of the simpler and more empirical testing procedures.

Laboratory testing offers the advantage of having well defined and directly controllable boundary conditions. This makes interpretation of the data relatively straightforward, although assessment of the applicability of the results to in situ conditions may still present problems, especially regarding predictions of undrained modulus and creep behavior. But such problems are now at least recognized. Most of the recent developments in laboratory testing have been directed towards an improved ability to model the in situ stress conditions, including both the initial stresses and variations resulting from applied loadings for representative elements within the foundation soil.

A major problem still facing most laboratory testing is the influence of sample disturbance. Disturbance reduces predictions of maximum past pressures, $\bar{\sigma}_{vm}$, from consolidation tests and lowers the measured undrained shear strengths, s_u.

2.2 In Situ Tests For Evaluation of Engineering Properties of Clays.

The field vane, pressuremeter, and cone penetration tests are the most commonly employed in situ tests used to evaluate the strength and consolidation characteristics of clays. These tests are quick, easy, and economical to perform and will yield semi-continuous to continuous records at a given investigation site. However, since the behavior of most clays is anisotropic and strain-rate dependent (Ladd et al. 1977), the undrained shear strength, s_u, measured using these devices will likely be different. While all three tests can be employed to predict s_u, only the cone penetration test, supplemented with pore pressure measurements (e.g., the piezo-cone penetrometer) can be used to predict the consolidation characteristics of clays. The procedures for performing the tests and interpreting soil properties in the case of the field vane, pressuremeter, and cone penetration tests will be outlined in the next few sections.

2.2.1 Field Vane Test, FVT

The field vane test is probably the most widely used in situ strength test in the U.S.A. The torque required to rotate the blades of the vane at a constant rate of 6°/min is used to backfigure the undrained shear strength as follows:

$$s_u = \frac{\text{maximum torque}}{\pi \left(\frac{d^2 h}{2} + \frac{d^3}{6}\right)} \qquad (2.1)$$

where, d = vane diameter

h = vane height

A schematic drawing of a typical rectangular field vane is shown in Fig. 2.1.

The test is relatively easy and inexpensive to use, and will yield undisturbed as well as remolded s_u profiles. It is, however, difficult to assess the failure mode associated with this test. Shearing on a vertical cylindrical surface involves severe rotation of principal planes with a stress system unlike that encountered with any actual failures of practical interest (Ladd, 1971). Also, use of the vane is limited to homogeneous soft clays without shells, stones, fibers, sand pockets, etc.

Figure 2.2 shows the field vane correction factor developed by Bjerrum (1972) as a function of the plasticity index of the clay. This correction factor is to be used along with the field vane undrained shear strength in designing embankments on cohesive foundations.

2.2.2 Pressuremeter Test

The pressuremeter tests, both the Menard Pressuremeter Test (MPT) and the Self-Boring Pressuremeter Test (SBPT), are used widely in France and England for the design of both shallow and deep foundations, but have found limited use

elsewhere. The MPT consists of a cylindrical probe (D ≈ 6cm), Fig. 2.3a, connected to a pressure loading and volume measurement system. A measurement cell is lowered into a predrilled borehole and the test performed by monitoring the volume of water injected into the cell as a result of pressure increments applied at one minute intervals.

In theory, the MPT was thought to yield four soil parameters: the in situ total horizontal stress; the pressuremeter modulus; the pressure corresponding to initial yielding; and the pressure limit used to estimate the strength of the soil. In practice, however, interpretation of MPT data has proven to be very complex due to the influence of disturbance, the substantial end effects at high strains, indeterminate drainage conditions, and variations in the cell membrane calibration curve (Ladd et al., 1977).

The SBPT device is based on the same measurement concept as the Menard pressuremeter. However, the SBPT incorporates a small rotating cutting tool near the hollow cylindrical tip of the apparatus, the soil being carried to the surface in slurried form via an inner tube (see Fig. 2.3b). By controlling the rate of advance (0.1 to 1 m/min), the device can be inserted with far less disturbance than caused by predrilling a hole.

The SBPT offers the capability of making in situ measurements of strength-deformation properties of soils in greater detail and more accurately than heretofore possible (Ladd et al., 1977). A study of the suitability of the SBPT

test in predicting the stress-strain-strength properties of Boston Blue Clay has recently been completed (see Ladd et al., 1979, for details). They concluded that the initial pressure recorded after self-boring was generally much less than the in situ total horizontal stress, σ_{ho}, perhaps mainly due to improper installation techniques. However, available interpretation methods (e.g., the Marsland-Randolph graphical method, 1977) yielded quite reasonable estimates of σ_{ho}, especially in "stiff" clay, and this technique should be further evaluated via SBPT programs in other clay deposits.

Values of undrained shear strength, s_u, obtained from elastic-plastic and various derived methods of analysis were very sensitive to the input data, often showed considerable scatter and generally exceeded the in situ s_u appropriate for bearing capacity and stability analyses. In particular, derived peak strengths in the "soft" clay were too high by a factor of two or more. However, most of the tests did give reasonable estimates of undrained shear modulus.

2.2.3 Cone Penetration Test, CPT

There are many types of cone penetrometers, the quasi-static devices being superior to the dynamic types for producing data for quantitative design. The quasi-static devices developed in the Netherlands are most widely used. These "Dutch" cones have a base area of 10 cm^2, an apex angle of 60°, and employ a penetration rate of 1 to 2 cm/sec (Ladd et al., 1977). Continuous measurements of penetration

resistance, q_c, and sleeve friction, f_s, are recorded as the cone is statically penetrated through the clay strata.

Dutch cone test, DCT, data are primarily used to predict the undrained strength of clays and the friction angle and compressibility of sands. Several correlations have been developed for identification of soil types based on the ratio f_s/q_c (e.g., Begemann, 1965), but these must be used with caution unless verified by local experience (Ladd et al., 1977).

Estimates of undrained shear strength, s_u, from DCT results usually employ an equation of the following form:

$$q_c = N_k S_u + \sigma_o \qquad (2.2)$$

where σ_o is the in situ total vertical, horizontal or octahedral stress and N_k the cone factor. Theoretical solutions for N_k are currently available (see Chapter 4 for details). However, additional development is needed before these solutions can be used with reliability. As a result, N_k is generally obtained from empirical correlations, the reference s_u usually being measured via unconsolidated undrained, UU, triaxial compression or field vane tests (Schmertmann, 1975; Lunne et al., 1976; Baligh et al., 1978; de Ruiter, 1982 and others).

In 1975, Wissa et al. (1975) and Torstensson (1975) independently developed the piezometer probe. It consists of a fine porous element located on a conical tip connected hydraulically to an electro-mechanical pressure transducer

which transmits the signal to the recording equipment at the surface. Compared to existing piezometers, this probe has a much shorter response time (essentially instantaneous) and hence provides wider capabilities. As an illustration, the excess pore pressures, u, measured during penetration in a deposit consisting of clay, loose sand and varved clay are shown in Fig. 2.4. The measured u values can give an indication of the soil type and of changes in relative consistency or density. In addition, variations in the coefficient of consolidation of the soil layers can also be inferred from rates of pore pressure dissipation.

Since 1975, the electric cone penetrometers and piezometer probe have been used in various field testing programs involving different clay deposits (Baligh et al., 1978). The results showed that combining them provides an excellent potential for soil identification as well. This has led a number of institutions (e.g., University of British Columbia, Laval University, the Norwegian Institute of Technology, as well as several geotechnical engineering consultants) to develop a single cone that can measure q_c and u simultaneously - The Piezocone Penetrometer.

2.3 The Piezocone Penetrometer

The major thrust of this report concerns the piezocone penetrometer as a tool to be used for the evaluation of engineering properties of clays. The piezocone, illustrated in Fig. 2.5, is shaped like the Dutch cone, but contains a porous

stainless steel tip which is hydraulically connected to a pressure transducer for measuring the pore water pressure, u. The force required to push the cone is measured by a load cell located behind the porous stone (see Fig. 2.5). The friction sleeve consists of a freely rotating hollow cylinder of area 225 cm^2 and is equipped with a load cell for measuring the sleeve friction, f_s.

In addition to its use in providing estimates of the stress history, strength and consolidation characteristics of soil (which will be explained in detail in Chapters 4 and 5), the piezocone can also be used in a variety of other applications:

(a) Detection of Failure Planes

Soil around earthen failure planes will exhibit reduced strength due to its partly remolded state. When landslides or embankment failures are investigated with the piezocone, these failure zones will appear on the penetration logs as zones of reduced tip resistance and reduced pore pressure because of the increase in permeability from remolding (Wissa et al., 1975).

(b) Evaluation of Equilibrium Groundwater Conditions

Equilibrium pore pressures obtained after dissipation will yield information about the degree of consolidation below embankments. This is particularly useful for stability analyses in determining the rate of embankment construction. Equilization of pore pressures also yields information about the groundwater seepage characteristics below foundations.

(c) Material Classification

Jones and Van Zyl (1981) feel that from results previously published, it appears highly likely that a parameter based on pore pressure response will be much more sensitive than the friction ratio, f_s/q_c (Begemann, 1965), for materials identification. With this in mind, they performed a piezocone investigation on a mine tailings impoundment and derived a soil classification chart utilizing the Δu and q_c data, Fig. 2.6. The tailings heterogeneous nature makes it an ideal deposit with which to study a wide range of soil types. Excess pore pressure, $\Delta u=u-u_o$, was used because they feel it is a more sensitive measure than u, and it will indicate dilatant materials, e.g., dense sands. As expected, due to the differences in permeabilities, soft clays plot close to the Δu axis, sands close to the q_c axis, and intermediate materials graph rationally between the two.

From the classification chart, Jones and Van Zyl conclude that the fairly narrow band of results, with comparatively small overlap of different materials within the band, suggests that this plot can usefully be developed as an indication of the effective grain size of the material. They also note that the results are a function of cone shape, filter position, and rate of penetration.

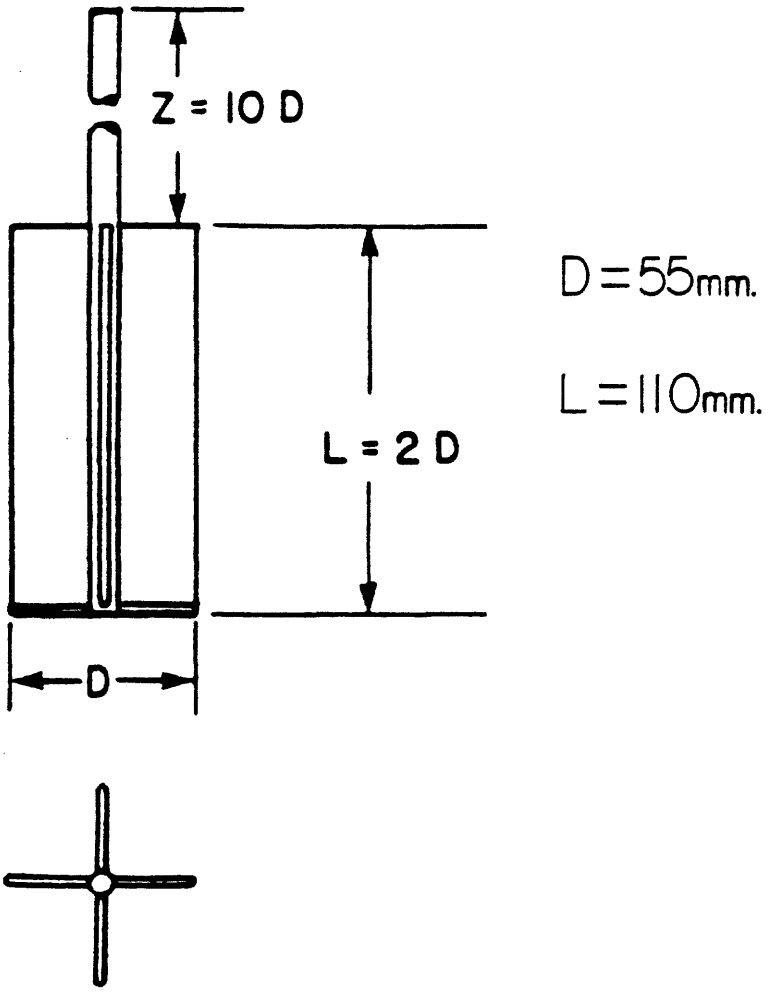

Figure 2.1 Geometry of Field Vane

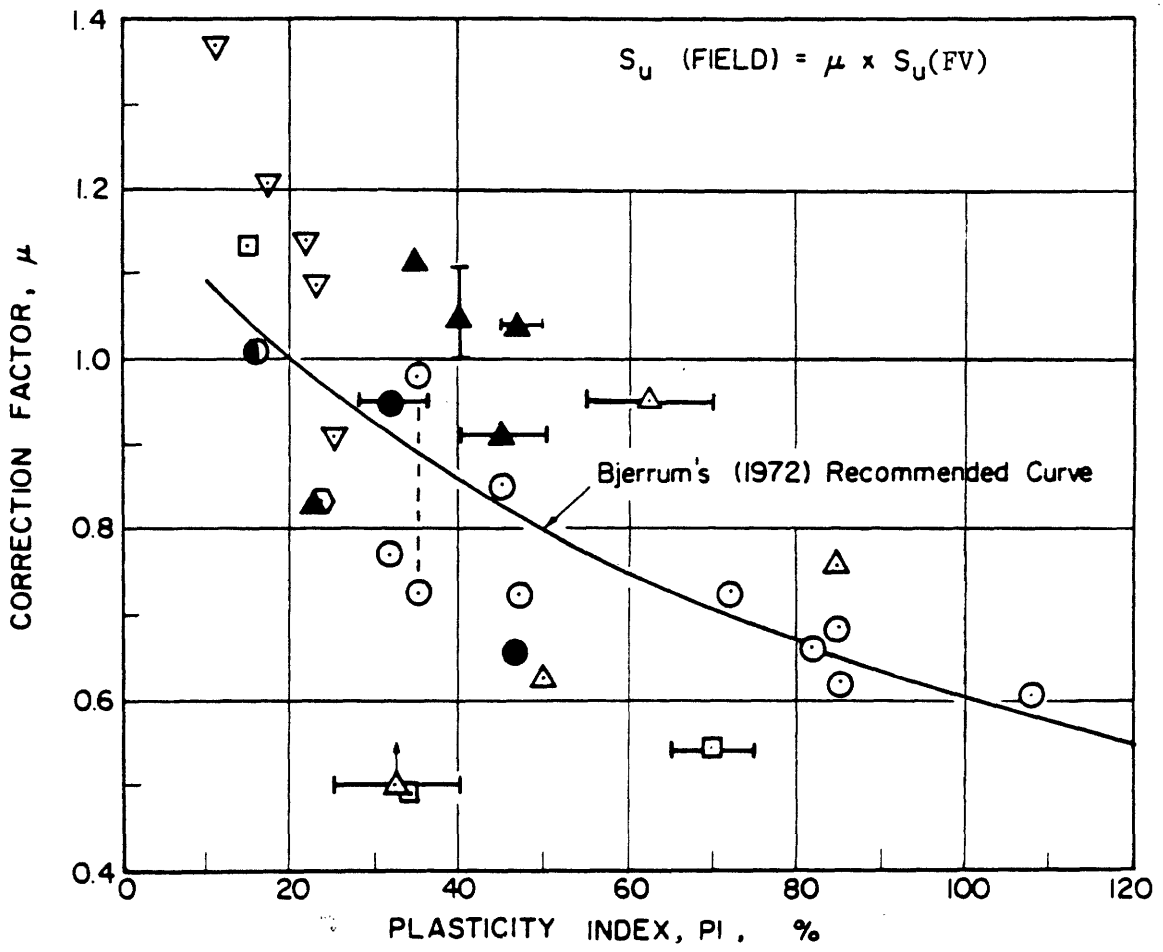

Figure 2.2 Empirical Correction Factor Derived from Embankment Failures for the Field Vane Test (from Ladd, 1975)

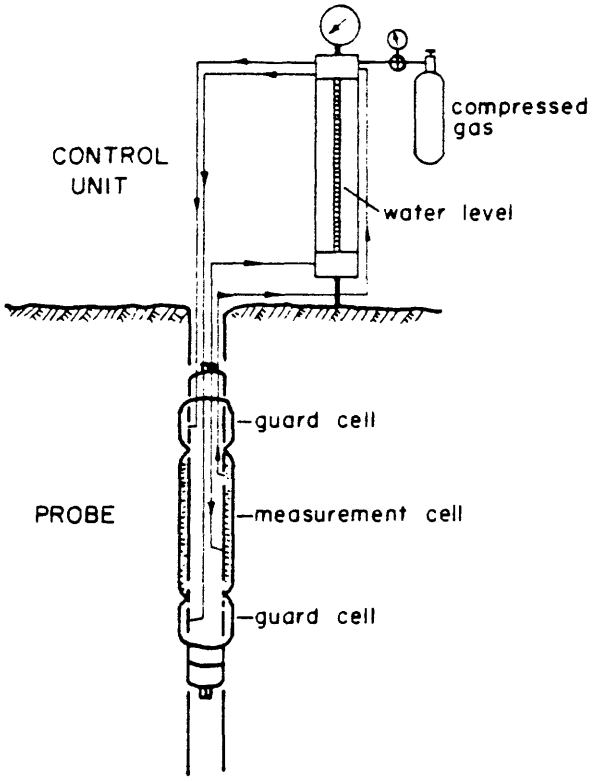

a) Menard Pressuremeter

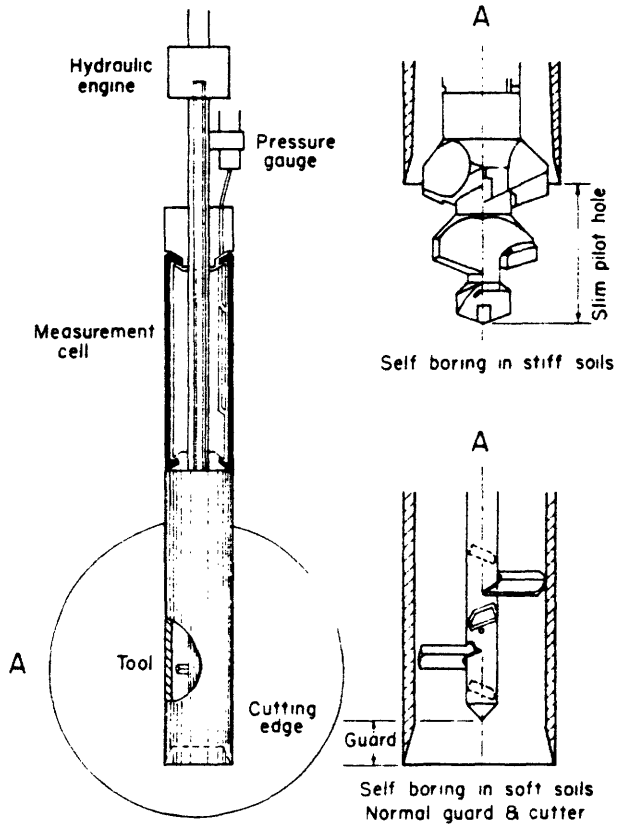

b) Self-Boring Pressuremeter (SBP)

Figure 2.3 Schematic of Pressuremeter (from Ladd et al.,1977)

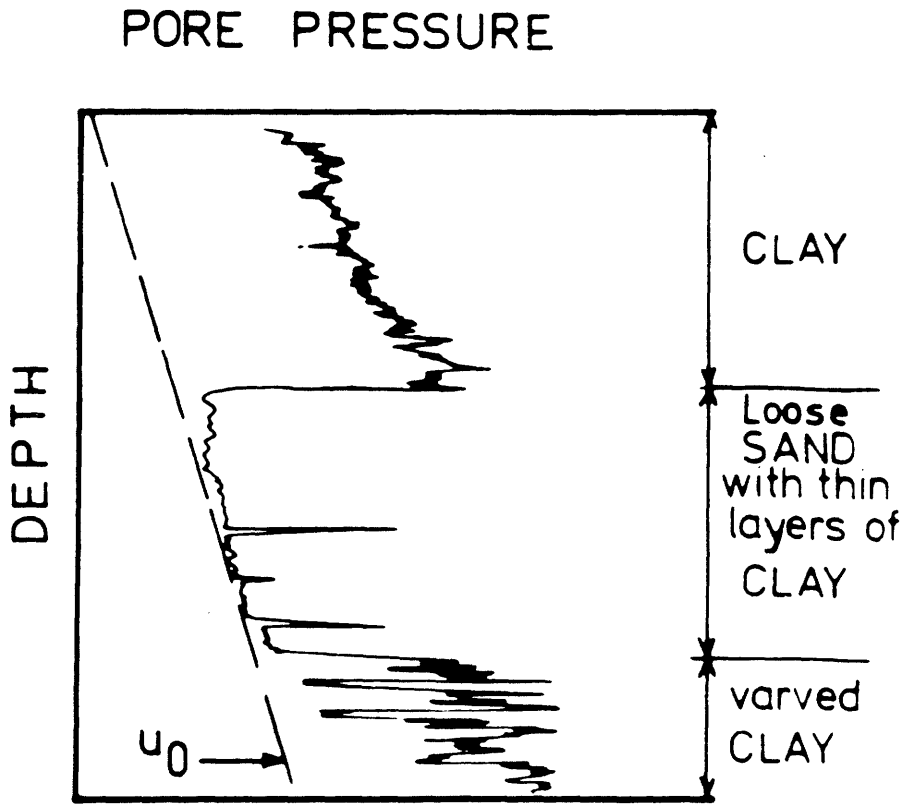

Figure 2.4 Typical Pore Pressure Response in a Layered Soil (from Torstensson, 1975)

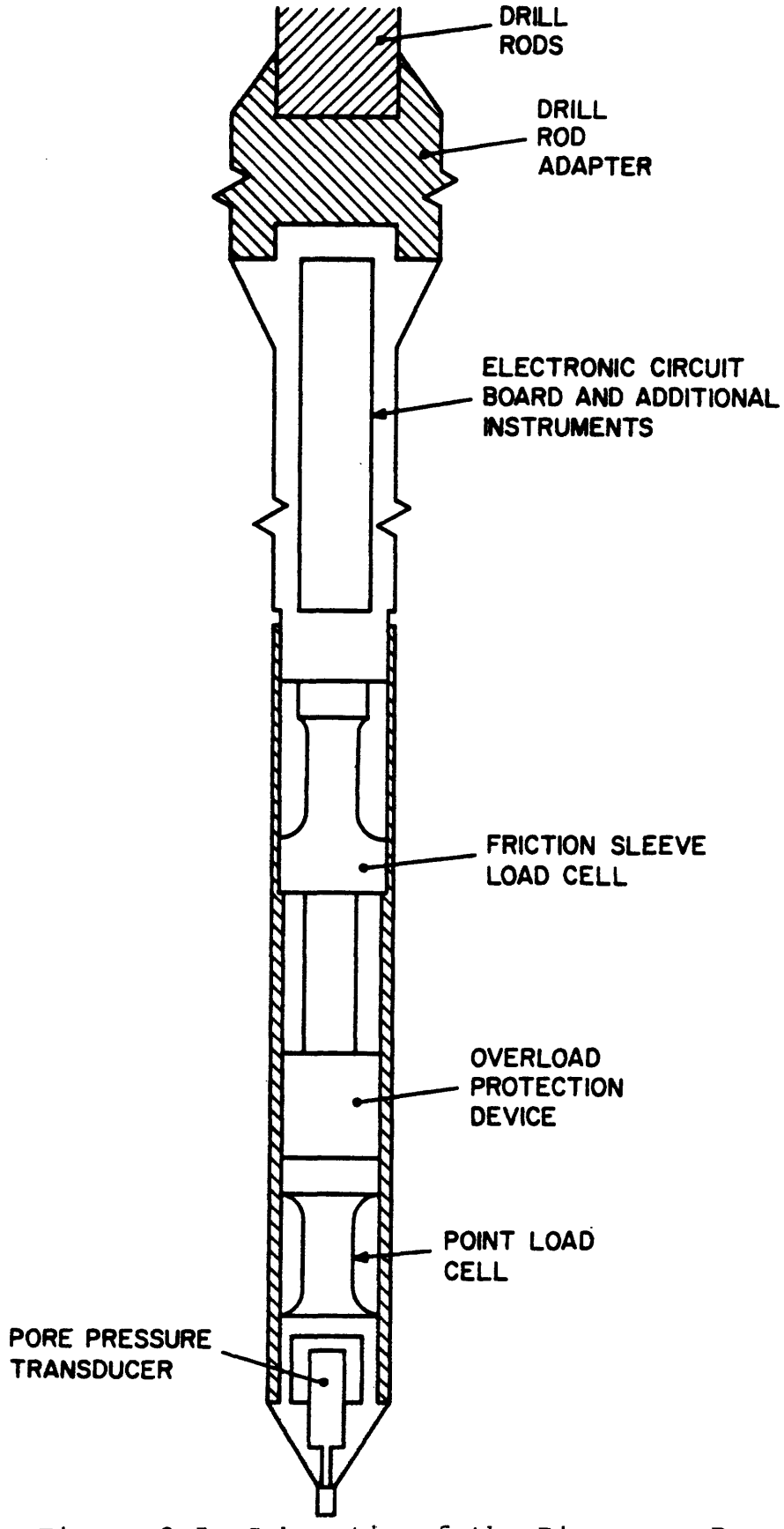

Figure 2.5 Schematic of the Piezocone Penetrometer

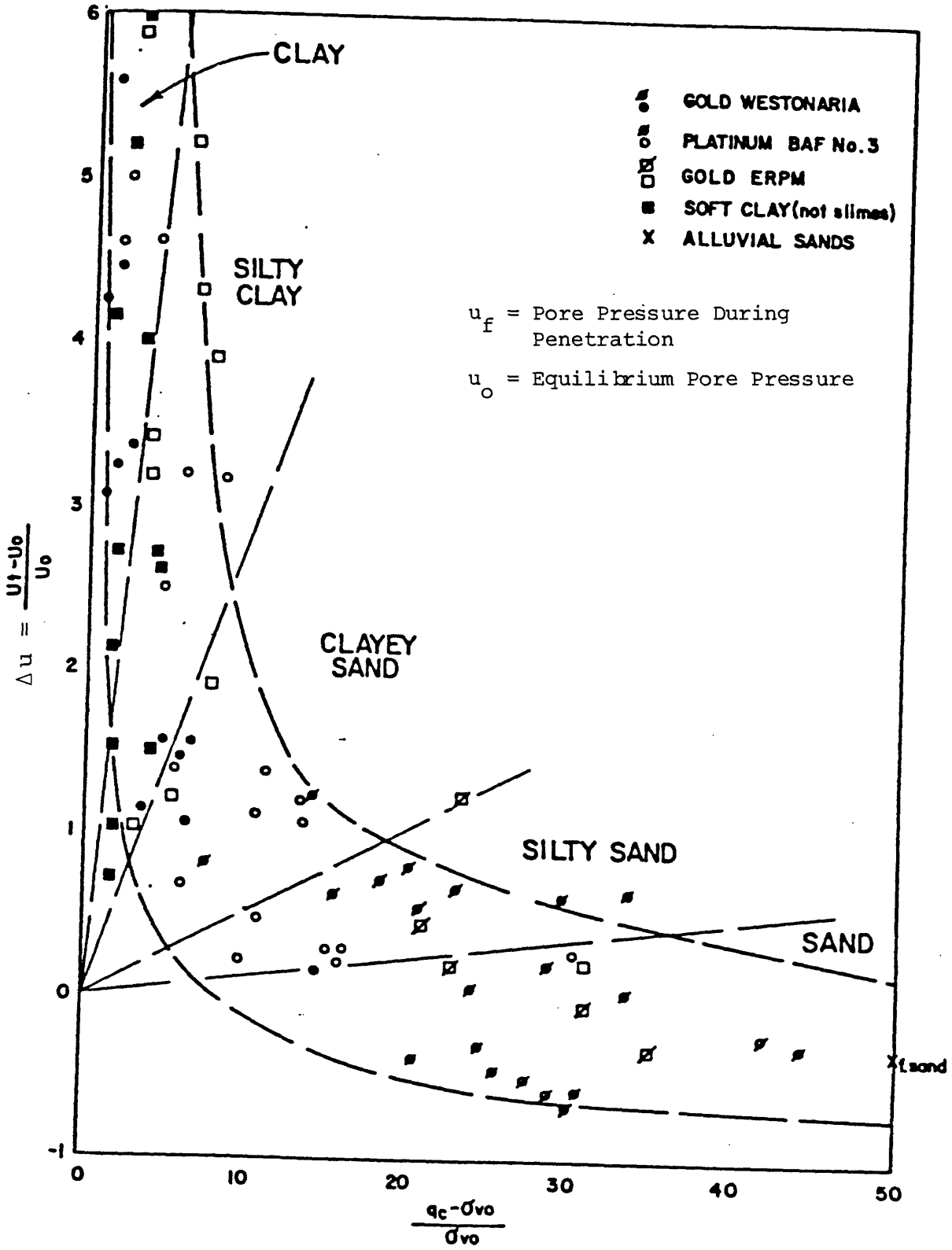

Figure 2.6 Soil Identification for Mine Tailings with with Pore Pressure and Tip Resistance Values (from Jones and Van Zyl, 1981)

CHAPTER 3

ENGINEERING PROPERTIES OF SOILS UNDERLYING THE MIT CAMPUS

3.1 Introduction

Ladd and Luscher (1965) summarized the engineering properties of the soils at several locations on the MIT campus, which in chronological order are:

Hayden Library and near vicinity

Materials Center

Life Sciences Building

Student Center

Center for Advanced Engineering Study (CAES)

The data included in this report are the index properties (natural water content, specific gravity, Atterberg limits, etc.), stress history, as well as the compressibility, consolidation and strength characteristics. Since that time, soils investigations have been performed for the Married Student Housing, McCormick Hall, Space Center, and Sloan Building (The locations of these sites are shown in Fig. 3.1). However, aside from soil profiles, not much information regarding the engineering properties of the underlying clays was obtained from these studies.

In the fall of 1981, a geotechnical investigation was initiated adjacent to the Solar House, which is located on the West End of the MIT campus (see Fig. 3.1) as part of a research program intended to establish a permanent facility for carrying out geotechnical in situ testing. The objectives

of this investigation were to establish a site with known soil profile and engineering properties to be used for educational purposes and for future evaluation and calibration of newly developed in situ tests. In the past, the site of the abandoned I-95 embankment in Saugus, Massachusetts, about 11 miles north of Boston, served these purposes, but it now suffers the drawback of environmental restrictions (the area is now a wildlife sanctuary). Combined with problems of security and access, there was a great need for a closely located and more permanent site.

The in situ testing program at the MIT Solar House consisted of a total of 8 bore holes; 4 for piezocone penetration, 3 for field vane testing and one hole for undisturbed sampling. The boring locations are illustrated in Fig. 3.2. In addition, a well and a deep piezometer of the M206 type (at elevation -76.5 ft) were installed for monitoring the ground water conditions.

High quality undisturbed samples were obtained at 11 depths within the Solar House clay stratum with a 3 1/2-inch diameter fixed piston Shelby tube sampler. The tubes were sealed at both ends with cellophane, a coating of a wax-paraffin mixture, aluminum foil, and a final coating of the wax-paraffin mixture. The tubes were stored for subsequent radiography and laboratory testing. The disposition of samples for laboratory testing for the Solar House clays is presented in Table 3.1.

This chapter will update the Ladd and Luscher report with the results of the different investigation programs performed after the publication of that report and detail the field and laboratory testing program adopted to obtain the results of the Solar House investigation.

3.2 Stratigraphy

Geologically, the MIT campus overlies the Boston Blue Clay formation which was formed during the wane of the late Pleistocene ice age (about 14,000 years ago) under a marine environment in the Boston Basin, probably not very far from the ice margin. The clay deposit overlays a glacial till which covers the bedrock, and has a typical thickness in excess of 50 to 125 ft depending on the topography of the till. It includes numerous lenses of fine sands, isolated sand pockets and occasional stones or pebbles. Subsequent to clay deposition, movements of the earth crust and of the sea level resulted in emergence of the clay above the sea, followed by extensive weathering, desiccation, and erosion of the upper part of the deposit. This was in turn followed by at least two periods of submergence and deposition, of lesser significance, in which outwash sand, peat and silt were deposited above the clay.

The investigations at the nine sites mentioned above disclosed subsurface conditions compatible with the geologic site description given above. Typical soil profiles for the nine locations are presented in Fig. 3.3 in the west to east sequence as they appear on campus. The overburden soil

profile for the top 40 ft at the Solar House was inferred from profiles of surrounding sites. The sequence of soil types is very similar, although thicknesses and elevations vary. The generalized soil profile is:

Fill - mostly hydraulic, but some dumped

Loose organic silts and fine sand - some pockets of peat

Firm sand and gravel - widely varying in thickess.

Boston Blue Clay - of medium consistency in higher elevations, soft in lower elevations; the lowest 10 ft or so may be medium again and contain considerable amounts of sand.

Glacial till - mixture of gravel, sand, silt and clay; usually very dense.

Shale or slate - often weathered and/or fractured near the upper surface.

The groundwater table elevations vary from +10.5 to +16.5 ft and appear to increase from west to east, with the Solar House having the lowest water level and the Hayden Library the highest. Pore pressure conditions are hydrostatic for all the sites.

3.3 Index Properties

Figure 3.4 plots versus elevation the Atterberg Limits and total unit weights from the CAES, Materials Center, Student Center, and Solar House sites. As is consistent with past limits tests on BBC, the Plasticity Index ($I_p=w_L-w_p$) is approximately 20%. Total unit weights were either directly measured, backcalculated from water content measurements using

weight-volume relationships, or estimated. For the Solar House site, the total unit weights were calculated directly from the weights of the oedometer clay samples.

Prior to performing any tests on the Solar House clays, all sample tubes were radiographed at MIT in order to assess their quality. After several trials, the procedure adopted consisted of placing the sample about 6 ft from the X-ray head, exposing it for 5 minutes using a 260 KV input voltage with a current of 3.9 mA, and developing the film for about 15 minutes. Each tube was radiographed in 10 inch sections.

Radiography is useful in detecting gas pockets or cracks, sand lenses and zones of excessive sample disturbance. Such information proves essential in estimating the amount of suitable material in each tube and in selecting the best portions for the consolidation and strength tests. In this case, the negatives of the radiographed tubes exposed the clay to be homogeneous in nature and absent of sand lenses or excessive disturbance.

3.4. Consolidation and Stress History

One-dimensional consolidation tests were run on undisturbed clay samples recovered from different depths at the CAES, Student Center, Materials Center, Hayden Library, and Solar House sites. The tests were run in brass fixed ring oedometer cells (D = 2.5-2.75 in, H = 0.6-1.0 in) according to the procedures described in Lambe (1951), except that:

1. Load increment ratios less than unity were used on some tests in order to well define the break in the compression curve and therefore the $\bar{\sigma}_{vm}$ estimate.
2. Vertical strain (ε_v) rather than void ratio was used since compression curves based on strain yield more consistent and reliable estimates of compressibility and maximum past pressure (Ladd, 1973).
3. The maximum past pressure was estimated from compression curves based on strains corresponding to the end of primary consolidation, as recommended by Ladd (1973), such strains being determined from dial readings versus log time data. Also, most load increments were applied for time intervals only of sufficient duration to enable determination of the end of primary consolidation.
4. Tests were run with changing temperature in order to monitor its effects on compression characteristics.

Figure 3.5 presents typical compression curves from oedometer tests performed on Solar House clays at three representative depths.

Stress history refers to the existing in situ effective stresses and the degree of overconsolidation:

$$OCR = \frac{\bar{\sigma}_{vm}}{\bar{\sigma}_{vo}} \qquad (3.1)$$

where, OCR = overconsolidation ratio

$\bar{\sigma}_{vm}$ = maximum effective past pressure

$\bar{\sigma}_{vo}$ = in situ effective vertical stress

In situ vertical effective stresses, $\bar{\sigma}_{vo}$, are calculated from the total unit weight measurements and assuming hydrostatic initial pore pressure conditions. The values are tabulated in Table 3.2 and plotted versus depth in Fig. 3.6 for four sites. A sample calculation of $\bar{\sigma}_{vo}$ is shown in Table 3.3 for the CAES site. The $\bar{\sigma}_{vm}$ values are obtained from the laboratory compression curves and are plotted, together with $\bar{\sigma}_{vo}$, vs. depth in Fig. 3.7.

The data in Fig. 3.7 show that the clay is overconsolidated above elevation about -60 ft, with the maximum past pressure increasing as one goes up. The increased amount of precompression at the higher elevations is thought to be the result of desiccation of the upper portion of the clay stratum. The wide scatter in values of maximum past pressure may result partially from inaccuracies in determination of values of $\bar{\sigma}_{vm}$ from the compression curves and partially from varying degrees of desiccation. However, there does not appear to be any consistent variation in the degree of precompression with location, except that the clay at the Solar House may be somewhat more overconsolidated than usual above elevation -37 ft (see Fig. 3.8 for details). This may be a result of recovering higher quality samples from the Solar House site as compared to other sites, which is further

substantiated by the lower RR values obtained at this location as will be shown below (Ladd, 1973, states that sample disturbance decreases $\bar{\sigma}_{vm}$ and increases RR). Detailed tabulated data and compression curves for the Solar House tests are given in Appendix A.

Compression data from the oedometer tests from the different sites are plotted in Fig. 3.7 and tabulated in Table 3.2. Included are data on the following indices:

$$\text{CR, SR, or RR} = \frac{\Delta e/1+e_o}{\Delta \log \text{ stress}}$$

1. CR = compression ratio for initial loading in the virgin compression range of stresses (i.e., greater than $\bar{\sigma}_{vm}$)
2. SR = Swelling ratio for rebound from $\bar{\sigma}_{vm}$ over one cycle
3. RR = Recompression ratio for initial loading and recompression between $\bar{\sigma}_{vm}$ of 6 to 8 kg/cm^2 and 1 kg/cm^2.

Values of the coefficient of consolidation in the normally consolidated range, c_v (NC), are tabulated in Table 3.4 and plotted in Fig. 3.9 for oedometer test results from the CAES and Solar House sites. The values represent an average of the square root time and log time curve fitting methods. The data in Fig. 3.9 show that c_v (NC) averages 10.5 x 10^{-4} cm^2/sec below elevation -29 ft, discounting the values

at elevation -79 ft. At this location, the clay is interspersed with sand which increases the rate of consolidation. Data on c_v in the overconsolidated range for both swelling and recompression are detailed in Ladd and Luscher (1965).

3.5 Laboratory Undrained Strength Testing

The strength testing program for the Solar House investigation consisted of twelve one-dimensionally consolidated undrained Direct Simple Shear (CK_oUDSS) tests. The tests were run using the Geonor DSS device, Fig. 3.10, according to the SHANSEP (an acronym for Stress History and Normalized Soil Engineering Properties) procedure.

The SHANSEP method (Ladd and Foott, 1974) takes advantage of the well recognized fact that the in situ stress-strain-strength properties of most cohesive sediments are primarily controlled by the stress history of the deposit. Furthermore, many cohesive soils exhibit "normalized behavior", at least reasonably so from a practical design viewpoint, such that normalized soil parameters (NSP) like $s_u/\bar{\sigma}_{vo}$ can be uniquely related to OCR, independent of the actual values of $\bar{\sigma}_{vo}$ and $\bar{\sigma}_{vm}$. Ladd and Foott (1974) recommended that NSP be measured on test specimens one-dimensionally (K_o) reconsolidated to $\bar{\sigma}_{vc}$ values greater than the in situ $\bar{\sigma}_{vm}$ in order to minimize the effects of sample disturbance. Subsequent experience at MIT suggests that this procedure yields: (1) much more reliable results than reconsolidation

to the in situ $\bar{\sigma}_{vo}$ when testing tube samples of low OCR clays, especially those typically obtained offshore; and (2) reasonable estimates of the in situ $s_u/\bar{\sigma}_{vo}$ versus OCR relationship (less true for undrained modulus) for those sedimentary deposits which are not highly sensitive (i.e., naturally cemented and/or leached clays possessing a high liquidity index) such that reconsolidation beyond the in situ $\bar{\sigma}_{vm}$ will obviously alter the natural clay structure.

Ten SHANSEP type tests with nominal sample heights of 2.54cm were run at four levels of OCR (1,2,4, and 8). Normalized stress paths, normalized stress-strain curves, and undrained moduli curves for the ten tests are presented in Figs. 3.11, 3.12, and 3.13, respectively. Figure 3.14 presents the results of these tests in the form of normalized shear strength, $s_u/\bar{\sigma}_{vc}$, versus overconsolidation ratio, OCR.

Two additional DSS tests were run at OCR=1 to study the influence of sample height and consolidation procedure on the observed results. The first test was a SHANSEP type test (i.e., $\bar{\sigma}_{vc}$=1.5 to 2 $\bar{\sigma}_{vm}$) except that a reduced sample height (1.46cm as opposed to 2.54cm) was used. The second test was run at $\bar{\sigma}_{vc}=\bar{\sigma}_{vo}=\bar{\sigma}_{vm}$ to check on the possible destruction of the clay structure that may be caused by consolidating 1.5 to 2 times past $\bar{\sigma}_{vm}$, as per the SHANSEP procedure. The results of the two tests were in accordance with those of the other ten SHANSEP tests. The sample with the reduced height produced identical results with what had been obtained. Although the

normalized shear strength was slightly higher (0.190 vs. 0.176) when the sample was consolidated to $\bar{\sigma}_{vo}$, the preshear OCR could easily have been greater than one due to the uncertainty in predicting $\bar{\sigma}_{vo}$ and $\bar{\sigma}_{vm}$ and hence the increase in $s_u/\bar{\sigma}_{vc}$. Therefore, it was concluded that consolidation past $\bar{\sigma}_{vm}$ does not significantly alter the structure of the Boston Blue Clay samples.

Table 3.5 summarizes the results of the DSS testing program. Further detailed test summaries, stress-strain and undrained modulus curves, and stress paths are presented in Appendix B.

Seven different types of undrained shear strength tests were run on samples from seven different locations on the MIT campus. The strength tests and corresponding locations are summarized as follows:

Location	Type Shear Test
Hayden Library	U
Nuclear Physics Lab	U
Materials Center	U, LV, $\overline{CIU}$
CAES	UU, LV, $\overline{CIU}$, $\overline{CK_oTC}$
Life Sciences	$\overline{CIU}$, $\overline{CK_oTC}$
Student Center	UU, LV
Solar House	FV, $\overline{CK_oUDSS}$

where, U = Unconfined Compression Test

UU = Unconsolidated Undrained Compression Test

$\overline{CIU}$ = Consolidated Isotropically Undrained Compression Test with Pore Pressure Measurements

$\overline{CK_oTC}$ = K_o Consolidated Undrained Compression Test with Pore Pressure Measurements

$\overline{CK_oUDSS}$ = K_o Consolidated Undrained Direct Simple Shear Test

LV = Lab Vane

FV = Field Vane

The triaxial and LV test procedures are outlined in Ladd and Luscher (1965). The test results (see Fig. 3.15), illustrate the amount of scatter obtained from tests run with different boundary conditions, modes of deformation, and strain rates. Average strength profiles for all of the shear tests run on BBC below the MIT campus will be presented and discussed at the end of the chapter.

3.6 In Situ Testing

3.6.1 Piezocone Penetration

The piezocone penetrometer used for the Solar House program is illustrated in Fig. 2.5. The piezocone was penetrated at a steady rate of 2 cm/sec in the clay stratum (i.e., starting from a depth of 40 ft below ground surface) at four different locations within the Solar House site. During penetration, depth was recorded as an electrical signal and

all cone resistance, pore pressure, and friction sleeve measurements were displayed on multi-channel high-speed strip chart recorders for observations during field operations and were also recorded on magnetic tapes using a data logger for subsequent computer processing.

An essential requirement for the successful use of the piezocone is careful deairing of the porous element aimed at the removal of all gases from the pore pressure measuring system. Failure to properly deair the porous stone would lead to severe inaccuracies in both the pore pressure measured during penetration as well as the measured dissipation of excess pore pressures after penetration has stopped. Methods of proper deairing are described in detail in Baligh et al. (1980).

It has been shown (Baligh et al., 1981 and Zuideberg et al., 1982) that the cone resistance measurements, especially in soft clays, can be significantly reduced due to the pore pressure acting on the base behind the cone. The existence of an O-ring seal on a groove located between the cone base and the housing mounted behind it reduces the effective cone area and allows the free access of water to an area at the base of the cone. The correction for this occurrence was made by adding the pore pressure on the grovve to q_c measured, as follows:

$$q_c \text{ (corrected)} = q_c \text{ (measured)} + \bar{\alpha} u_{base} \qquad (3.2)$$

where, u_{base} = measured pore pressure at cone base

$\bar{\alpha}$ = ratio of groove area to base area

Values of $\bar{\alpha}$ differ from one cone to another. For the one used in this study $\bar{\alpha} = 0.33$. Also, since the pore pressures in this investigation were measured at the cone tip, it would be more convenient to use u_{tip} in Eq. 3.2 instead of u_{base}. Based on the results of an extensive testing program, Baligh et al., (1979), show that for Boston Blue Clay, the pore pressures at the cone base are approximately 10% smaller than those generated at the tip. Combining this with $\bar{\alpha}$ value of 0.33, (q_c) corrected was computed in this study from the following relationship:

$$(q_c)\text{corrected} = (q_c)\text{measured} + 0.30\ u_{tip} \qquad (3.3)$$

Plots of corrected cone resistance, q_c, and pore pressure, u, versus depth for two of the four piezocone holes are shown in Figs. 3.16 and 3.17. Holes MP3 and MP4 experienced some mechanical difficulties and yielded unreliable results. As expected, the stiffer, more overconsolidated clays are characterized by higher point resistances and lower pore pressures than the softer, normally consolidated clays, where q_c and u exhibit linear increases with in situ effective stress and hydrostatic pore pressure, respectively. At the present time, the reliability of skin friction measurements in clay deposits seems to be questionable (Baligh et al., 1981). A plot of skin friction, f_s, versus depth is presented in Fig. 3.18;

however, f_s values were not incorporated into any subsequent analyses.

Subsequent to penetration, dissipation of generated pore pressures occurs. Dissipation tests were run at 12 depths below 53 ft. Figure 3.19a illustrates typical pore pressure versus time curves recorded at depths 58 and 78 ft. Baligh and Levadoux (1980), Torstensson (1977), and others have developed theories to predict the horizontal coefficient of consolidation, c_h, from measurements of pore pressure versus time. In order to utilize these theoretical solutions, the pore pressure dissipation data must be presented in a normalized form:

$$\bar{u} = \frac{u-u_o}{u_i-u_o} \qquad (3.4)$$

where, u = pore pressure at time t

u_i = pore pressure at the end of penetration

u_o = hydrostatic pore pressure

Figure 3.19b presents the curves in the normalized format. Dissipation curves for eleven tests below 53 ft are illustrated in Fig. 3.20. Chapter 5 will be devoted to the study of these dissipation curves to predict c_h.

3.6.2 Field Vane Testing

Thirty eight field vane tests were performed with the Geonor Field Vane, described in Chapter 2, within the three vane test holes at the Solar House. Peak and Remolded shear

strengths were measured according to ASTM (1965) specifications. Table 3.6 presents the shear strengths measured and sensitivity of the clay, and Fig. 3.21 profiles the results versus elevation.

3.7 Undrained Shear Test Profiles

Figure 3.22 plots average strength profiles versus elevation for all but the LV tests. Some points of interest regarding the strength profiles are:

1) The CK_oTC strength is higher than that measured from the DSS test throughout the deposit. This is consistent with the data reported in Table 4.1 and indicates that BBC is anisotropic.

2) Similarly, the FV profile is consistently higher than the DSS profile. In the upper clays the difference is about 0.20 kg/cm^2 and increases to a maximum of 0.40 kg/cm^2 at elevation -80 ft. FV strengths higher than those measured by the Direct Simple Shear test contradict existing data on Boston Blue Clay especially in the normally to slightly overconsolidated region. The reason for this discrepancy is not clear. However, it should be mentioned that the DSS results reported herein represent the first set of data on "undisturbed" BBC samples. Previous data (Ladd and Edgers, 1972) were obtained from residemented samples. As shown in Chapter 3, the $s_u/\bar{\sigma}_{vo}$ value for N.C. "undisturbed" BBC is about 0.18 whereas from residemented samples, Ladd and Edgers

obtained 0.20. Further work on this aspect is still needed.

3) The U and UU profiles don't show any consistent trend with the overconsolidation profile of the clay. Furthermore, as is shown in Fig. 3.15, tremendous scatter is associated with these average profiles. For example, the results in Fig. 3.15 show that at any given depth, the strength can vary by a factor of 4 to 6 which is clearly unacceptable.

For more detailed information regarding stress-strain behavior, undrained moduli, and A_f values for the triaxial and LV tests, consult Ladd & Luscher (1965).

Sample #	Depth (ft)	Type Test
MUD 1-1	40.5-42.5	oedometer 1-1a, DSS-16
MUD 1-2	45-47	oedometer 1-2a, DSS-11,13,19
MUD 1-3	50-52	oedometer 1-3a
MUD 1-4	58-60	oedometer 1-4b, DSS-10,12
MUD 1-5	66-68	oedometer 1-5, DSS-20
MUD 1-6	74-76	oedometer 1-6
MUD 1-7	84-86	oedometer 1-7a, DGL-1 DSS-1,2a
MUD 1-8	90-92	oedometer 1-8, DSS-X1
MUD 1-9	95-97	oedometer DGL-4, 1-9 DSS-5,X2
MUD 1-10	100-102	oedometer DGL-2, 1-10a
MUD 1-11	105-107	oedometer DGL-3, 1-11

* Limits tests performed on samples from each tube

Table 3.1 Disposition of Samples for Engineering Properties Tests at the Solar House Site

Location	Elev. (ft)	w_N%	$\bar{\sigma}_{vo}$ (kg/cm^2)	$\bar{\sigma}_{vm}$ (kg/cm^2)	OCR	CR ( ) Denotes Average Value	RR	SR
CAES	-30.0	-	1.58	4.0± 0.3	2.53 ± 0.19	0.181 ± 0.014	0.030	0.032
	-38.5	-	1.82	3.1± 0.4	1.70 ± 0.22	0.163	0.024	0.025
	-45.5	-	2.00	3.8± 0.2	1.90 ± 0.10	0.173	0.025	0.025
	-54.0	-	2.21	3.1± 0.1	1.40 ± 0.05	0.201 ± 0.014	0.038	0.032
						(0.180)	(0.0295)	(0.0285)
Materials Center	-14.8	34.7	1.25	6.0 ± 1.0	4.80 ± 0.80	0.155	-	0.024
	-26.3	39.6	1.55	4.8 ± 0.3	3.10 ± 0.19	0.209	-	0.032
	-38.3	36.7	1.90	4.0 ± 0.3	2.11 ± 0.16	0.192	-	0.025
	-50.3	32.5	2.20	3.5 ± 0.3	1.59 ± 0.14	0.219	-	0.024
	-62.3	41.8	2.50	2.5 ± 0.2	1.00 ± 0.08	0.206	-	0.023
						(0.195)		(0.0255)
Hayden Library	-19.6	-	1.20	4.9	4.08	0.143	-	0.030
	-22.0	-	1.36	5.1	3.75	0.137	-	0.027
	-28.5	-	1.54	5.2	3.38	0.164	-	0.027
	-32.1	-	1.64	5.4	3.29	0.161	-	0.021
	-35.5	-	1.75	3.6	2.06	0.178	-	0.029
	-42.1	-	1.92	3.7	1.93	0.225	-	0.033
	-51.1	-	2.20	3.1	1.41	0.199	-	0.027
	-57.1	-	2.38	2.9	1.22	0.147	-	0.016
	-63.3	-	2.56	2.5	0.98	0.189	-	0.024
	-72.6	-	2.80	2.4	0.86	0.170	-	0.024
	-79.1	-	3.00	2.4	0.80	0.157	-	0.018
						(0.170)		(0.0250)
Student Center	-16.5	32.80	1.52	4.1 ± 0.7	2.70 ± 0.46	0.174	0.029	0.028
	-22.0	38.70	1.66	6.1 ± 0.5	3.67 ± 0.30	0.218	0.036	0.039
	-22.0	39.70	1.66	6.1 ± 0.5	3.67 ± 0.30	0.208	0.036	0.036
	-26.5	39.70	1.78	4.0 ± 0.3	2.25 ± 0.17	0.188	0.037	0.028
	-31.5	47.00	1.91	5.0 ± 0.5	2.62 ± 0.26	0.250	0.044	0.039
	-41.5	32.26	2.20	2.7 ± 0.2	1.23 ± 0.09	0.154	0.017	0.021
	-41.5	40.50	2.20	2.0 ± 2.0	-	0.167	-	0.026
	-51.5	36.00	2.46	2.0 ± 0.2	0.81 ± 0.08	0.141	0.017	0.018
	-51.5	41.00	2.46	1.6 ± 0.1	0.65 ± 0.04	0.167	0.021	0.019
	-63.5	41.50	2.80	-	-	0.140	0.026	0.023
						(0.181)	(0.0290)	(0.0280)
Solar House	-19.5	30.19	1.50	8.60± 0.40	5.74 ± 0.26	0.132	0.019	0.026
	-24.0	41.12	1.60	6.60± 0.20	4.12 ± 0.12	0.184	0.013	0.033
	-29.0	46.20	1.75	5.85± 0.15	3.34 ± 0.12	0.196	0.015	0.043
	-37.0	39.10	1.95	5.00± 0.20	2.56 ± 0.10	0.175	0.017	0.034
	-44.5	-	2.15	3.30± 0.20	1.53 ± 0.10	0.275	0.023	0.035
	-52.5	40.79	2.38	2.80± 0.20	1.17 ± 0.09	0.185	0.028	0.027
	-63.0	48.73	2.58	2.90± 0.20	1.12 ± 0.08	0.212	0.031	0.038
	-63.0	51.20	2.58	2.85± 0.10	1.10 ± 0.04	0.265	0.026	0.035
	-68.5	47.07	2.72	2.53± 0.13	0.93 ± 0.04	0.272	0.018	0.032
	-73.5	37.80	2.85	3.68± 0.18	1.29 ± 0.06	0.246	0.015	0.025
	-73.5	40.44	2.85	2.70± 0.10	0.94 ± 0.04	0.238	0.018	0.032
	-79.0	26.70	3.00	4.05± 0.15	1.35 ± 0.05	0.131	0.015	0.006
	-79.0	26.10	3.00	2.65± 0.15	0.88 ± 0.05	0.109	0.024	0.012
	-83.5	24.60	3.12	2.72± 0.22	0.87 ± 0.07	0.065	0.016	0.005
	-83.5	36.82	3.12	2.95± 0.15	0.95 ± 0.05	0.187	0.027	0.022
						(0.198)	(0.0201)	(0.0246)
Average for all locations						(0.185)	(0.0243)	(0.0258)

Table 3.2 Summary of Compression Data for BBC Below MIT Campus

	Thickness (ft)	γ_t (lb/ft^3)	$\Delta\sigma_v$ (kg/cm^2)	σ_v (kg/cm^2)	u (kg/cm^2)	$\bar{\sigma}_v$ (kg/cm^2)	Remarks
+21.0							
	8.5	125	0.52				
+12.5				0.52	0	0.52	γ_t estimated
+12.0	0.5	101	0.02	0.54	0	0.54	Avg. 16 tests (γ_t=71-120)
	18	101	0.89				
-6.0				1.43	0.55	0.88	
	4	135	0.26				No measurements but min.w_n=15%
-10.0				1.69	0.67	1.02	
	30	119	1.75				Avg. with range γ_t=114-124
-40.0				3.44	1.58	1.86	
	25	117	1.43				Avg. with range γ_t=113-123
-65.0				4.87	2.35	2.52	
	25	123	1.50				Avg. with range γ_t=116-137
-90.9				6.37	3.11	3.26	

Table 3.3 Computation of Vertical Stresses - CAES

Location	Elevation (ft)	$\bar{\sigma}_{vo}$ (kg/cm^2)	$\bar{\sigma}_{vm}$ (kg/cm^2)	c_v(NC) x 10^{-4} cm^2/sec — Initial Compression from 8-16 (kg/cm^2)
CAES	-30.0	1.58	4.0 ± 0.3	9
	-38.5	1.82	3.1 ± 0.4	20
	-45.5	2.00	3.8 ± 0.2	20
	-54.0	2.21	3.1 ± 0.1	20

Location	Elevation (ft)	$\bar{\sigma}_{vo}$ (kg/cm^2)	$\bar{\sigma}_{vm}$ (kg/cm^2)	Initial Compression: Load Increment (kg/cm^2)	Initial Compression: c_v(NC) (x 10^{-4} cm^2/sec)
Solar House	-19.5	1.50	8.60± 0.40	14.2-24.14	51.00
	-24.0	1.60	6.60± 0.20	14.2-24.14	23.50
	-29.0	1.75	5.85± 0.15	14.2-24.14	12.60
	-37.0	1.95	5.00± 0.20	14.2-24.14	17.20
	-44.5	2.15	3.30± 0.20	4-8	6.30
	-52.5	2.38	2.80± 0.20	4-8	11.40
	-63.0	2.58	2.85± 0.10	4.75-8-16	4.45
	-63.0	2.58	2.90± 0.20	8.35-14.2	12.50
	-63.0	2.58	4.00± 0.10	4-8	6.50
	-68.5	2.72	2.53± 0.13	4-8	6.33
	-73.5	2.85	2.70± 0.10	4-8	8.25
	-73.5	2.85	3.68± 0.18	4.75-8	6.84
	-79.0	3.00	2.65± 0.15	8.35-14.2	53.80
	-79.0	3.00	-	4-8	61.50
	-83.5	3.12	2.72± 0.22	3-4.75-8-16	151.00
	-83.5	3.12	2.95± 0.15	4-8	8.00

Table 3.4 Coefficient of Consolidation, Normally Consolidated - MIT Campus

Test No.	w_N%	At Consolidation					At τ_h maximum					
		OCR	$\bar{\sigma}_{vc}$	$\bar{\sigma}_{vm}$	t_c (days)	ε_v%	γ%	$\tau_h/\bar{\sigma}_{vc}$	$\tau_h/\bar{\sigma}_{vm}$	$\bar{\sigma}_v/\bar{\sigma}_{vc}$	$\bar{\sigma}_v/\bar{\sigma}_{vm}$	ϕ°
1	40.1	1.00	4.57	4.57	0.66	9.5	4.50	0.179	0.179	0.553	0.553	17.9
2a	41.4	1.00	6.04	6.04	0.50	17.4	6.42	0.173	0.173	0.583	0.583	16.5
5	37.6	1.00	4.54	4.54	0.90	11.7	3.69	0.177	0.177	0.684	0.684	14.5
10	34.0	2.01	4.51	9.06	0.76	8.7	8.3	0.318	0.158	0.847	0.422	20.5
12	37.6	2.00	4.52	9.02	0.81	9.8	5.97	0.334	0.167	0.959	0.480	19.2
20	39.0	2.01	3.50	7.03	0.86	11.95	6.50	0.322	0.160	0.900	0.447	19.7
11	34.9	3.95	2.70	10.66	0.73	8.3	9.60	0.538	0.136	1.258	0.317	23.2
13	34.2	4.04	3.22	13.00	0.83	9.0	9.96	0.531	0.131	1.312	0.325	22.0
16	39.8	8.03	1.74	14.00	1.50	9.2	10.57	0.894	0.111	1.814	0.226	26.2
19	35.3	7.97	1.79	14.29	0.97	10.2	10.90	0.870	0.109	1.827	0.229	25.5
X-1	43.0	1.00	2.68	2.68	1.03	4.2	3.76	0.190	0.190	0.674	0.674	15.7
X-2	41.1	1.00	4.68	4.68	0.92	10.3	4.50	0.172	0.172	0.646	0.646	14.6

NOTE: Test X-1, $\bar{\sigma}_{vc} = \bar{\sigma}_{vo}$
Test X-2 was run with a reduced sample height

Table 3.5 Summary of $CK_o\overline{UDSS}$ Tests

Hole #	Depth (ft)	s_u(Undisturbed) (kg/cm^2)	s_u(Remolded) (kg/cm^2)	$S_t = s_u(U)/s_u(R)$
	45	1.182	0.358	3.30
	51	1.086	0.325	3.34
	55.5	0.840	0.243	3.46
	61	0.955	0.293	3.26
FV 1	65.5	1.031	0.320	3.22
	71.5	0.738	0.249	2.96
	75.5	0.673	0.195	3.45
	81	0.732	0.239	3.06
	86.5	0.564	0.230	2.45
	90.7	0.738	0.268	2.75
	96.5	0.848	0.285	2.98
	101	0.901	0.252	3.58
	106	1.101	0.369	2.98
	42	1.109	0.545	2.04
	47	0.906	0.277	3.27
	53	1.085	0.342	3.17
	58	0.700	0.212	3.30
	63	0.998	0.325	3.07
	68	0.812	0.217	3.74
FV 2	73	0.754	0.222	3.40
	78	0.597	0.271	2.20
	83	0.727	0.225	3.23
	88	0.667	0.212	3.15
	93	0.765	0.298	2.57
	98	0.943	0.404	2.33
	103.5	0.786	0.249	3.16
	106	1.052	0.222	4.74
	80	0.628	0.203	3.09
	85	0.694	0.269	2.58
	90	0.786	0.342	2.30
	93.4	0.900	0.391	2.30
FV 3	96.7	0.974	0.440	2.21
	101.5	0.938	0.235	3.99
	102.5	0.873	0.466	1.87
	104	0.976	0.445	2.19

Table 3.6 Summary of Field Vane Tests

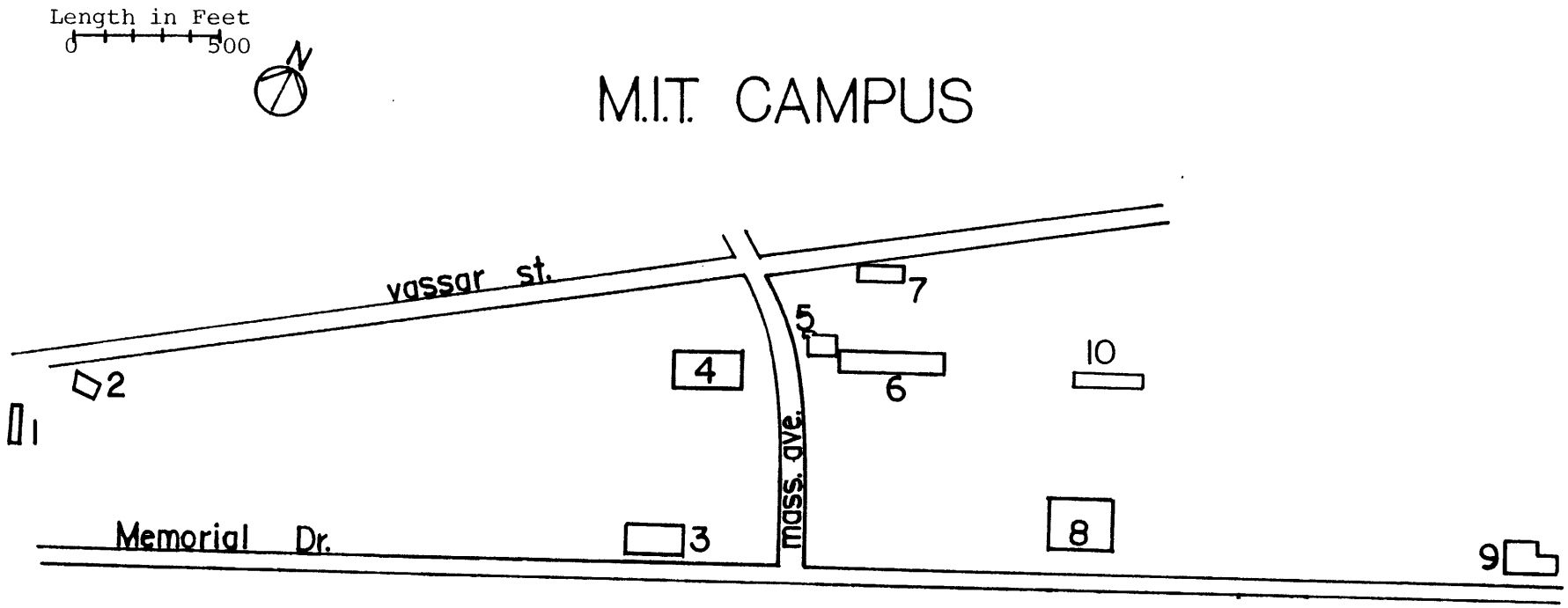

1. Married Student Housing
2. Solar House
3. McCormick Hall
4. Student Center
5. C.A.E.S.
6. Materials Center
7. Space Center
8. Hayden Library
9. Sloan Building
10. Life Sciences Building

Figure 3.1 Locations of Soil Investigations

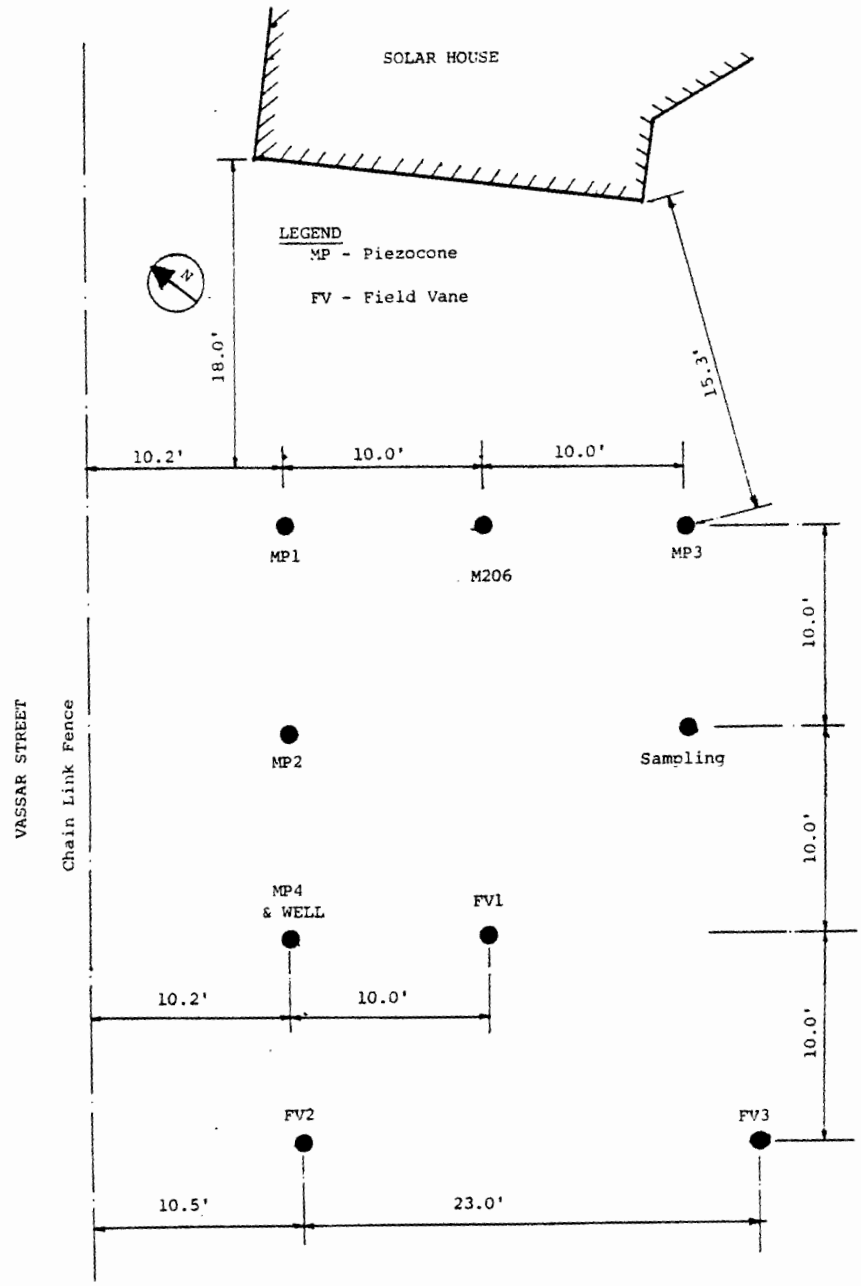

Figure 3.2 Boring Location Plan at the Solar House

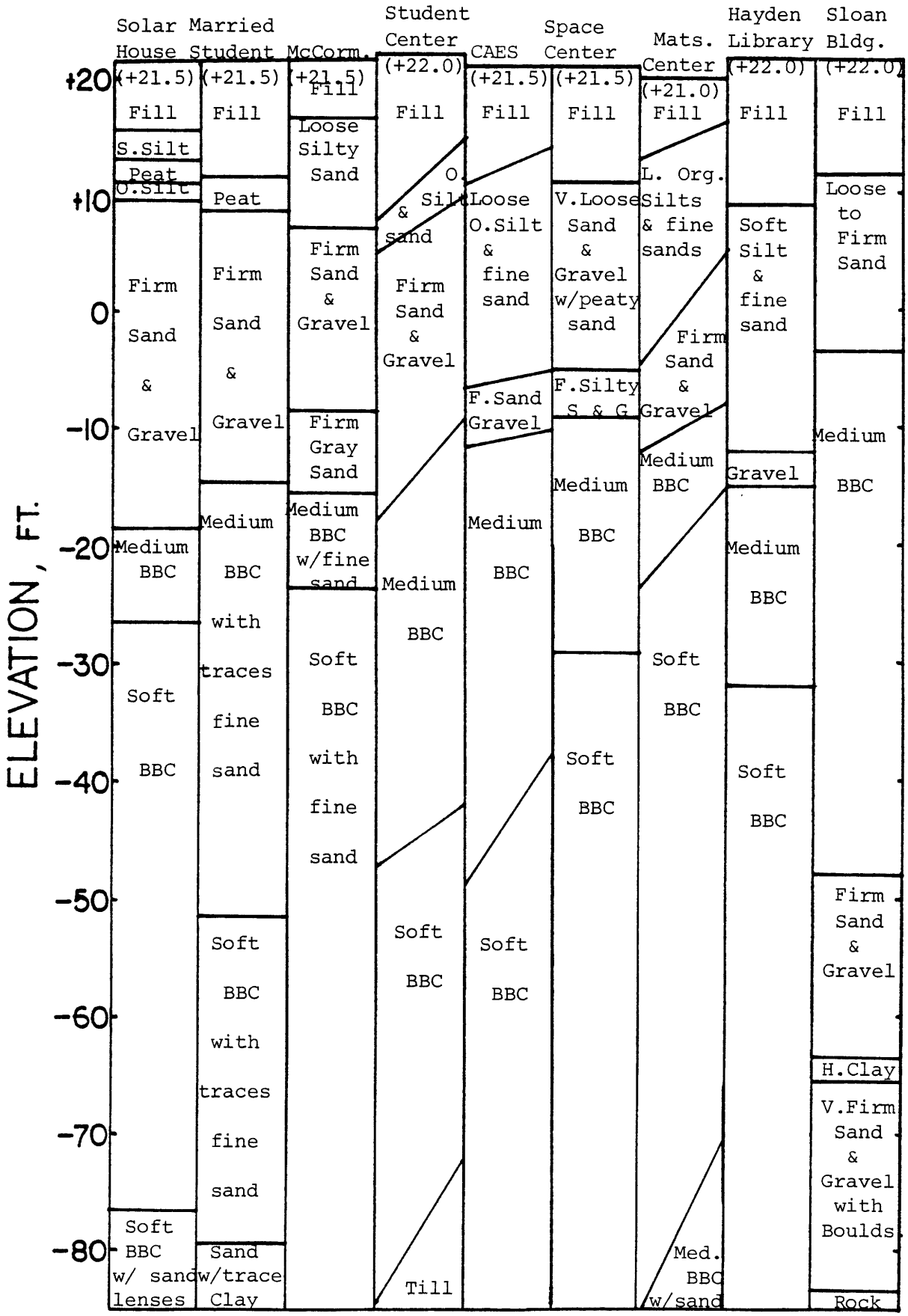

Figure 3.3 Typical Soil Profiles on the MIT Campus

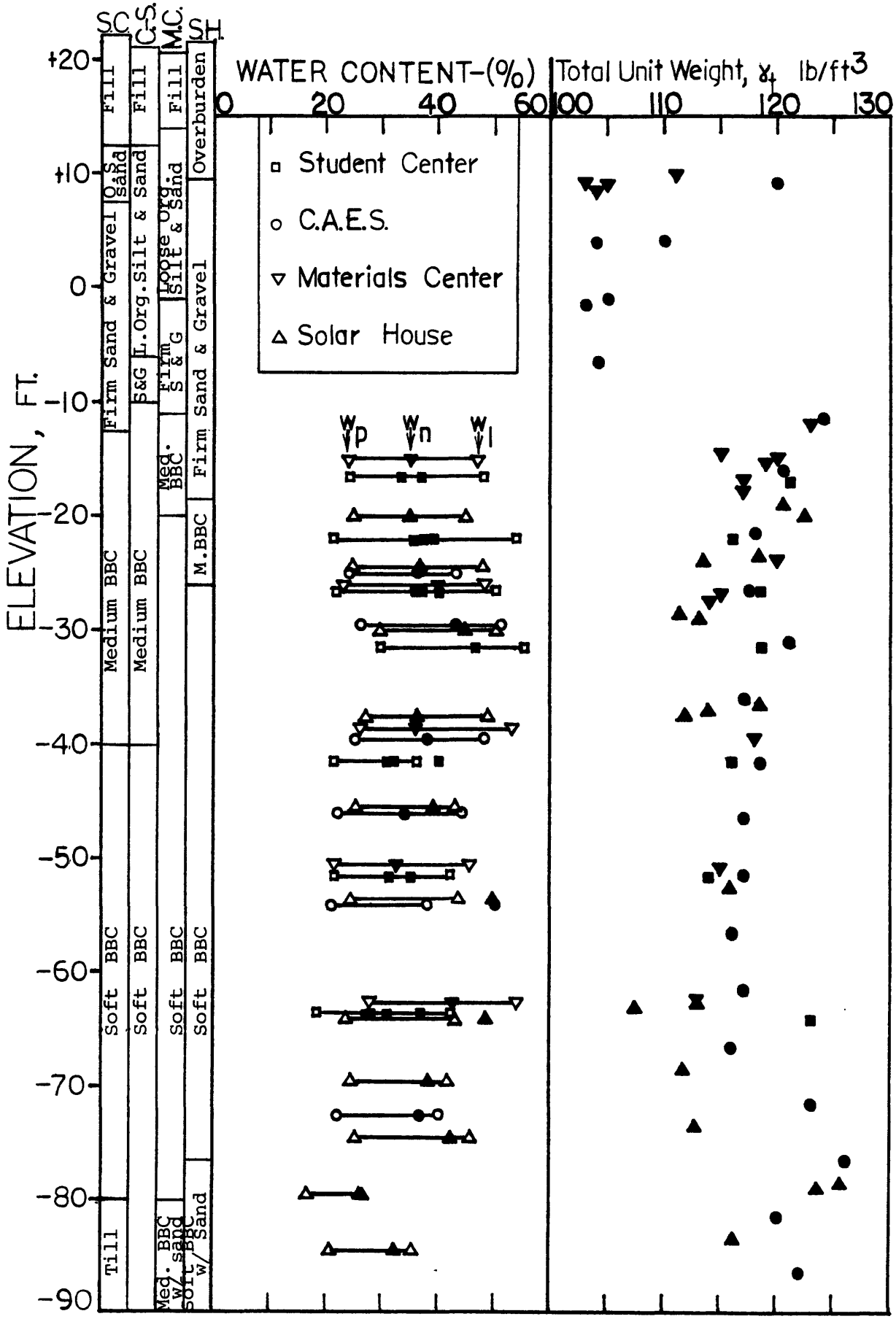

Figure 3.4 Atterberg Limits and Total Unit Weights

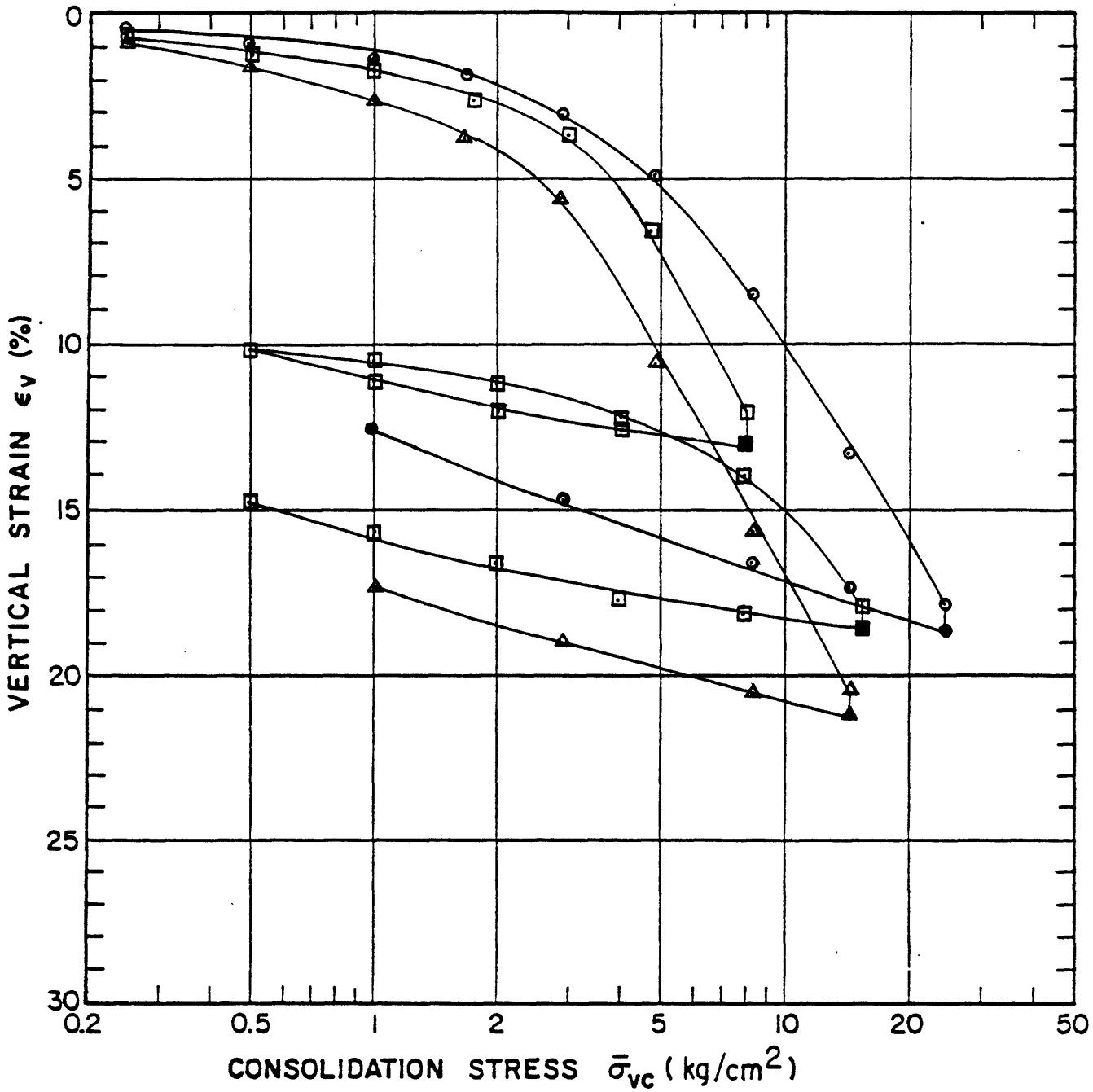

SYMBOL	DEPTH(ft)	$\bar{\sigma}_{vo}$	$\bar{\sigma}_{vm}$
○	51	1.75	5.85
△	85	2.58	2.90
□	95	2.85	3.68

Figure 3.5 Typical Compression Curves from Oedometer Tests on BBC (Solar House)

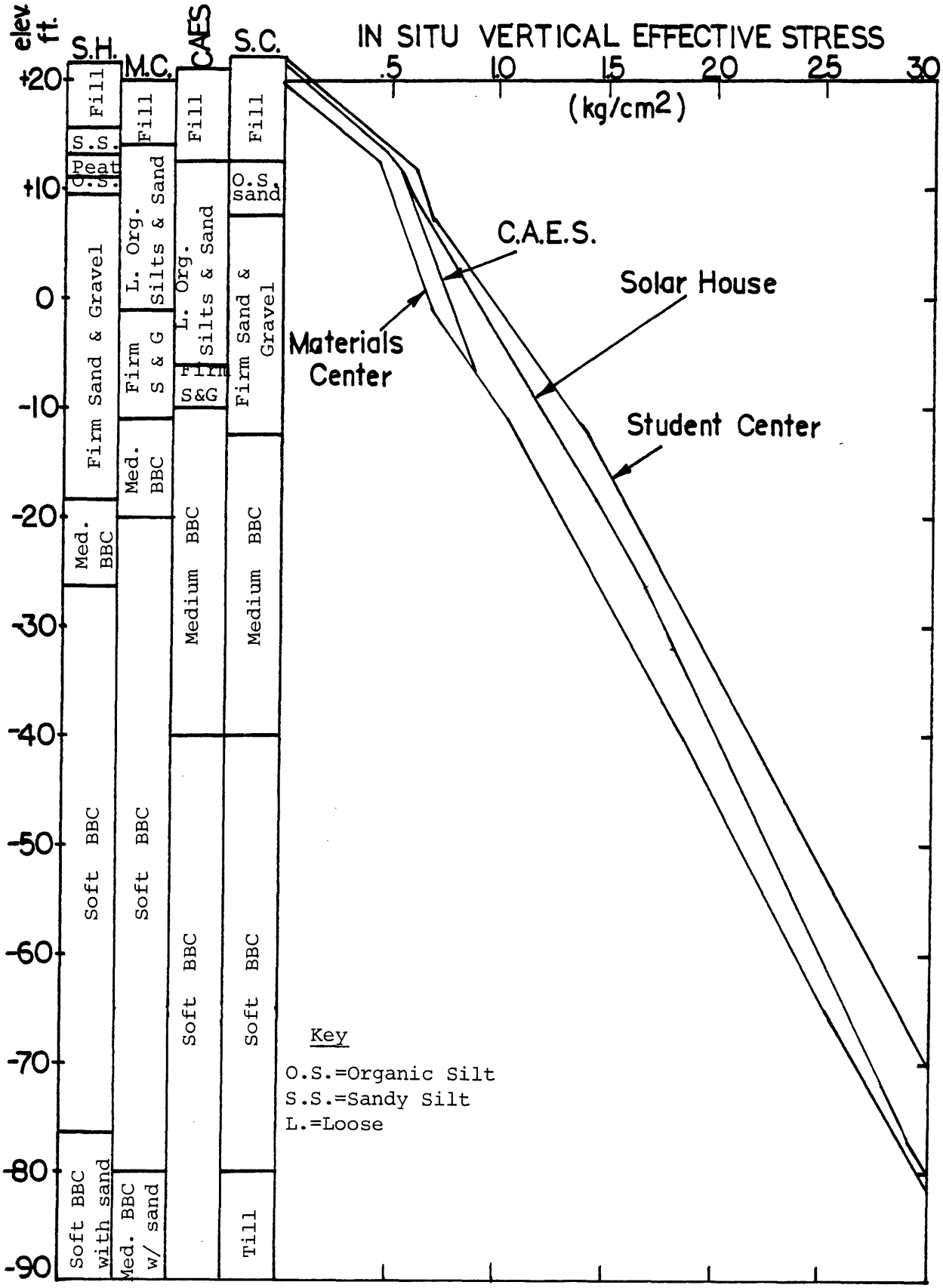

Figure 3.6 In Situ Vertical Effective Stresses

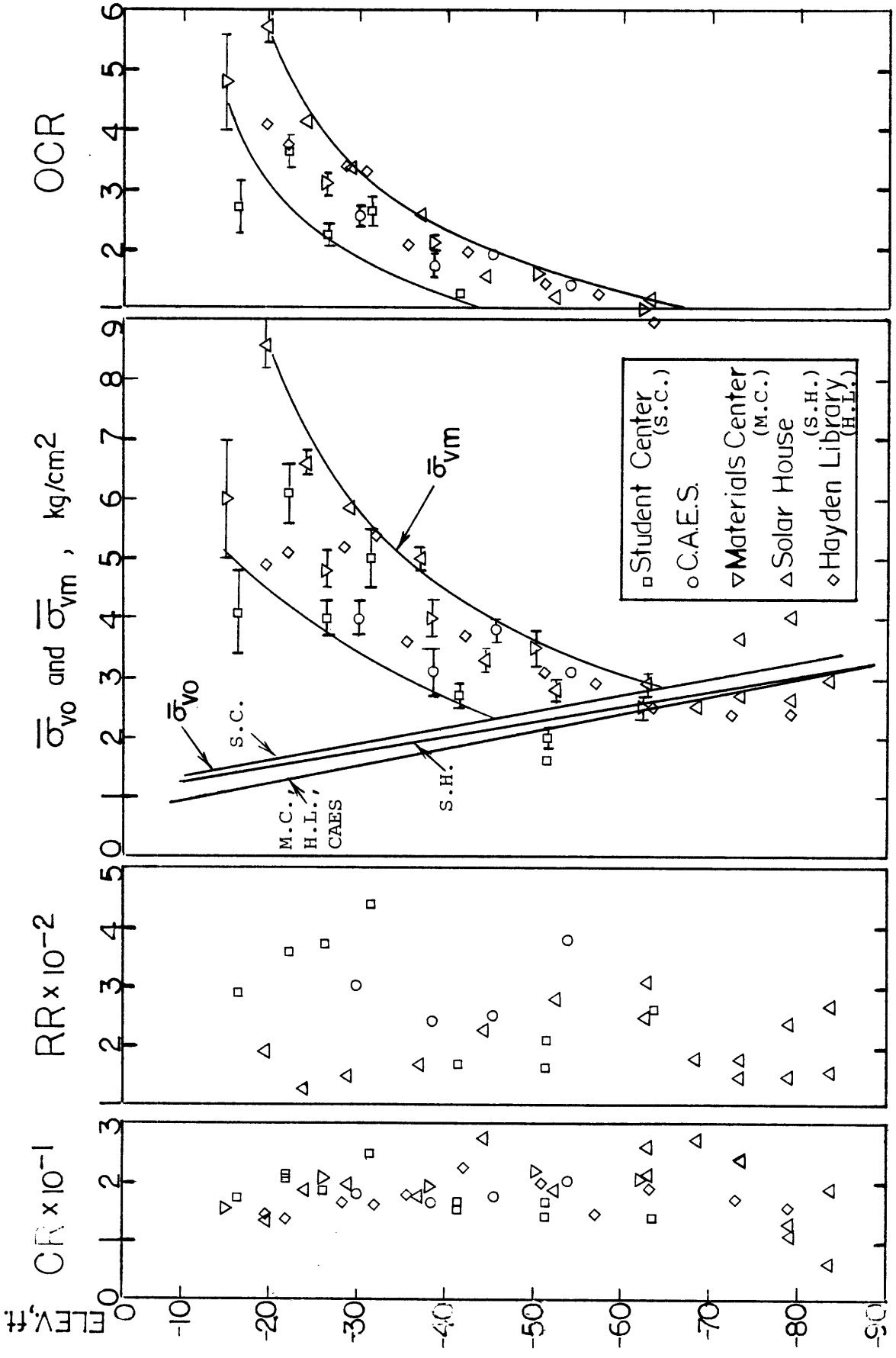

Figure 3.7 Compression Data on BBC Underlying the MIT Campus

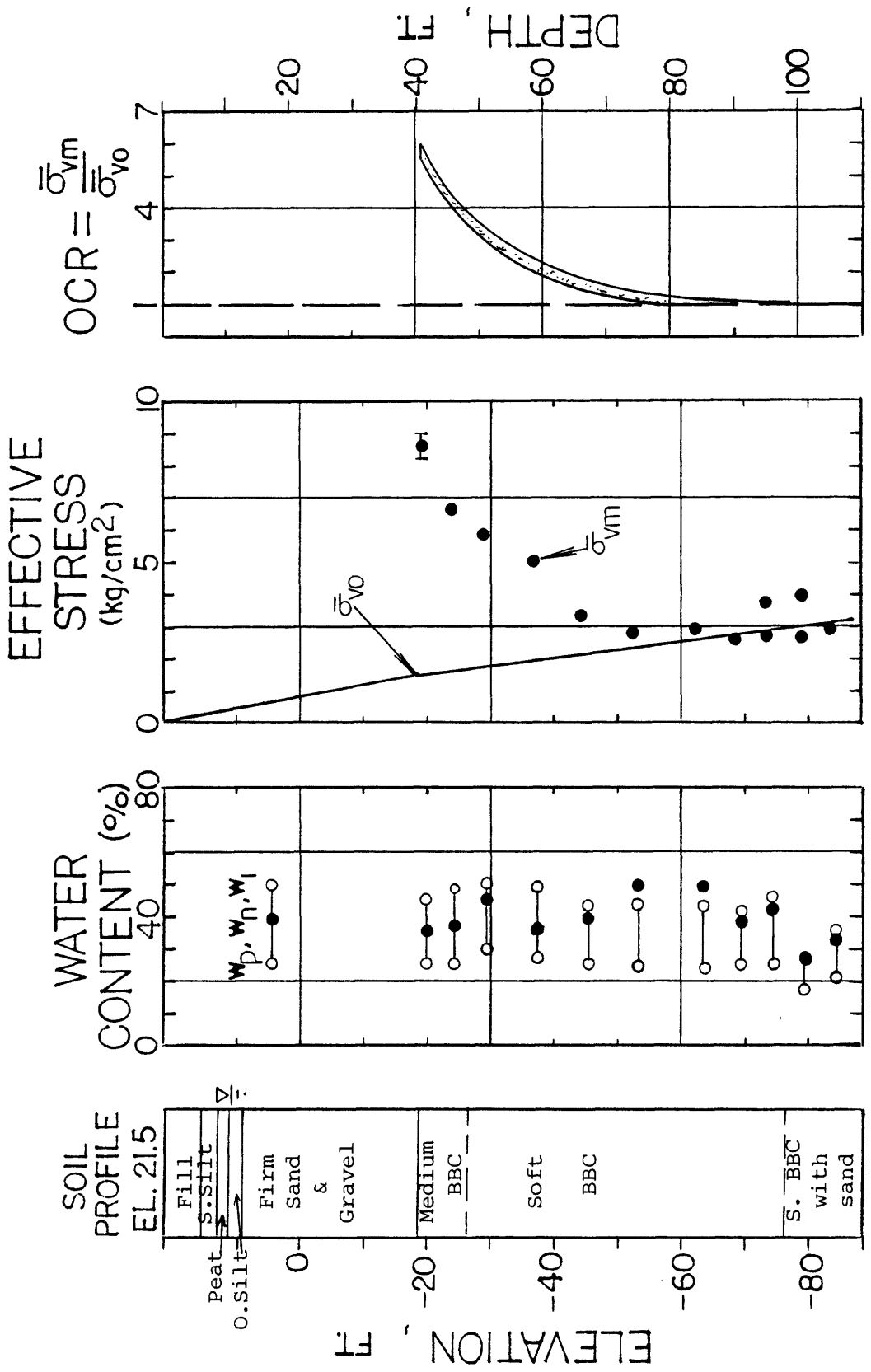

Figure 3.8 Soil Conditions at the Solar House Site

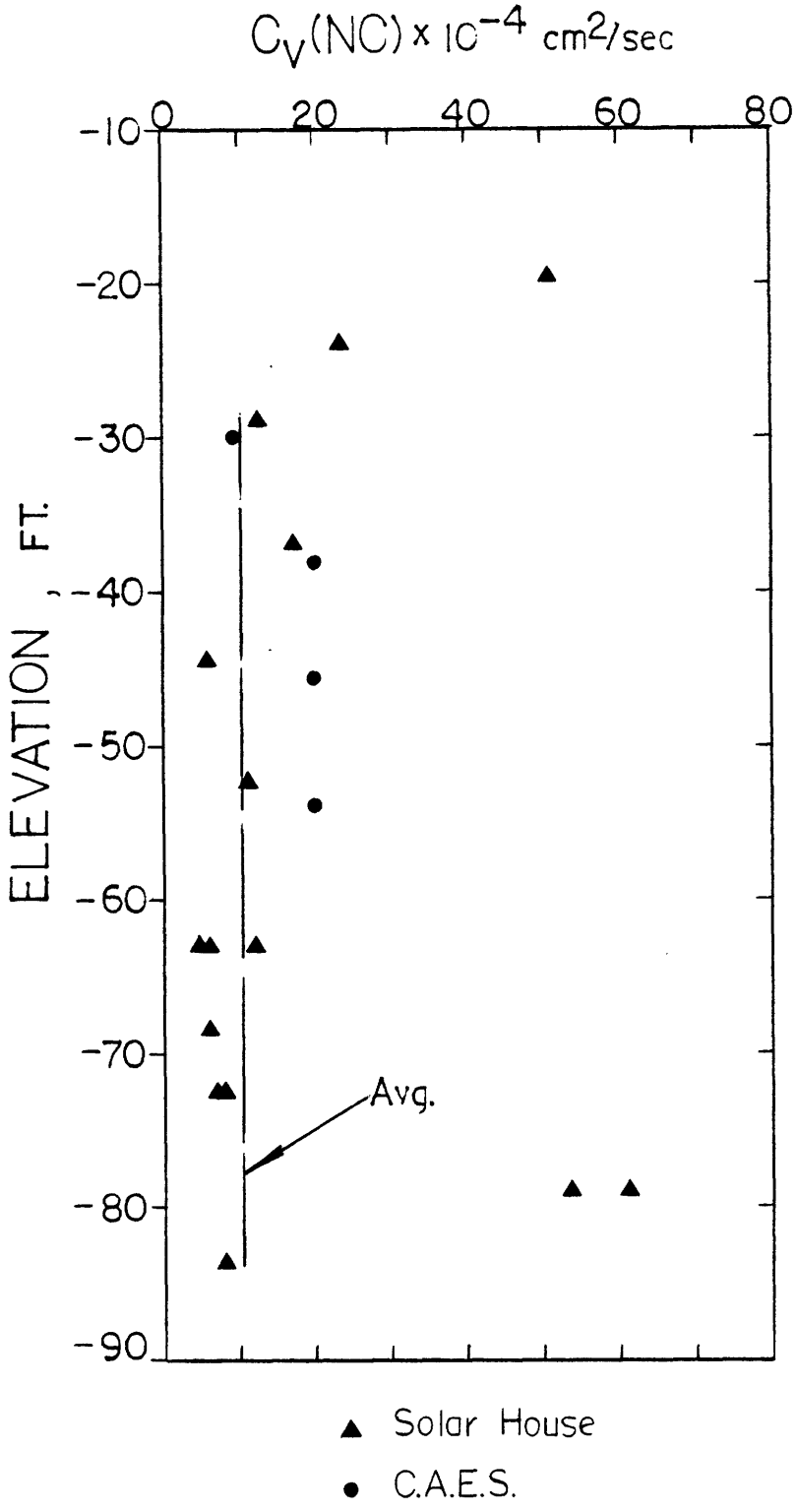

Figure 3.9 Vertical Coefficient of Consolidation

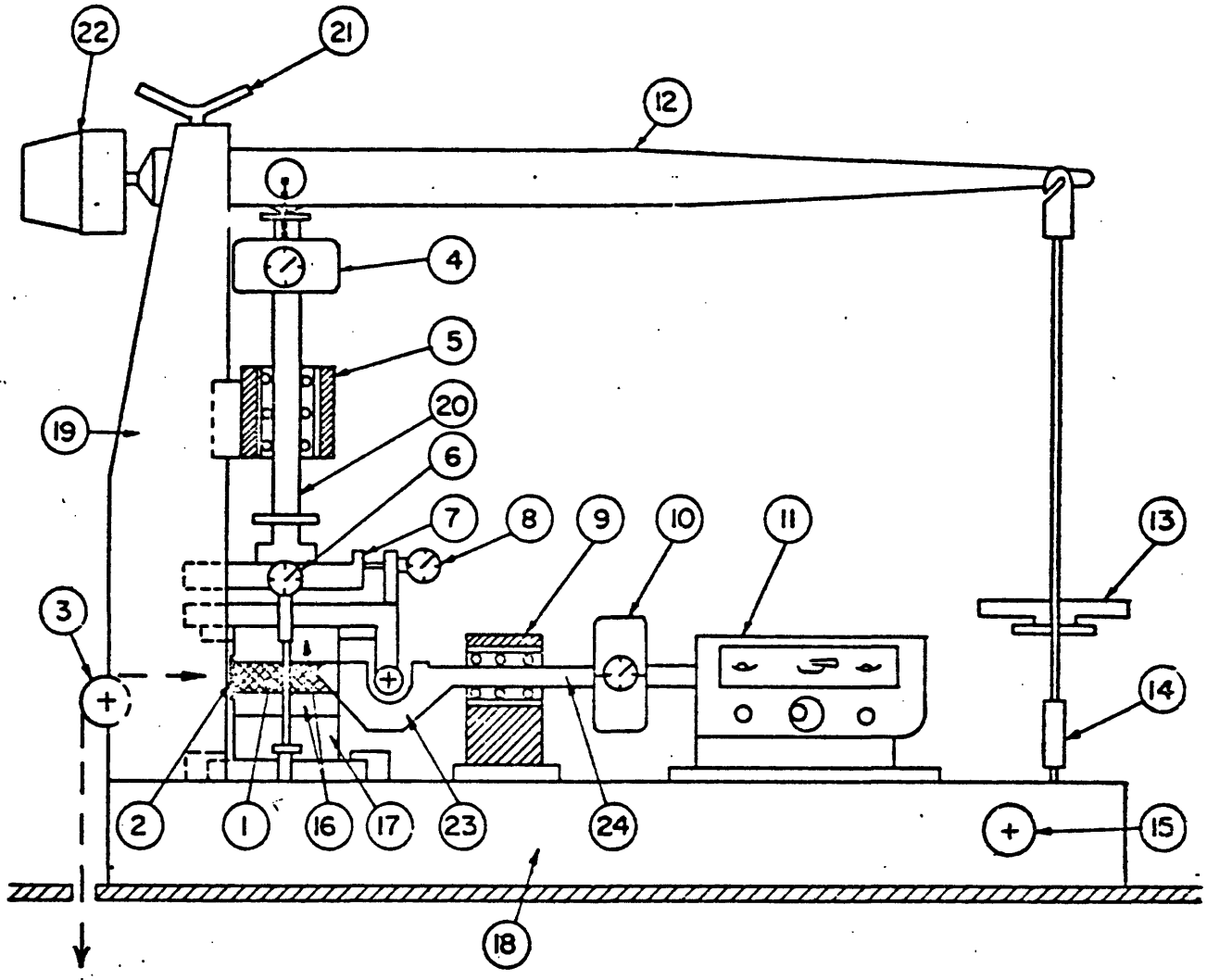

(1) Sample (2) Reinforced rubber membrane (3) Wheels for applying dead load (4) Load gauge for vertical load (5) Ball bushing (6) Dial gauge for measurement of vertical deformation (7) Sliding box (8) Dial gauge for measurement of horizontal deformation (9) Ball bushing (10) Load gauge for horizontal force (11) Gear box (12) Lever arm (13) Weights (14)-(15) Clamping and adjusting mechanism used for constant volume tests (16) Lower and upper filter holders (17) Pedestal (18) Base (19) Tower (20)Vertical piston (21) Adjusting mechanism (22)Counterweight (23) Connection fork (24) Horizontal piston

Figure 3.10 Drawing of Geonor Direct-Simple Shear Apparatus, Model 4

Test No.	Sample No.	Depth (ft)	w_N (%)	$\bar{\sigma}_{vc}$ (kg/cm^2)	$\bar{\sigma}_{vm}$ (kg/cm^2)	OCR	Symbol
1	1-7	85.0	40.1	4.57	4.57	1	●
2a	1-7	85.0	41.4	6.04	6.04	1	◁
5	1-9	96.0	36.6	4.54	4.54	1	▷
12	1-4	59.0	37.6	4.52	9.03	2	◇
20	1-5	67.0	39.0	3.50	7.03	2	▽
11	1-2	46.0	34.9	2.70	10.66	3.95	⬡
13	1-2	46.0	34.2	3.22	13.00	4.04	□
16	1-1	41.5	39.8	1.74	14.00	8.03	○
19	1-2	46.0	35.3	1.79	14.29	7.97	△

GEOTECHNICAL LABORATORY
DEPT. OF CIVIL ENGR., M.I.T.

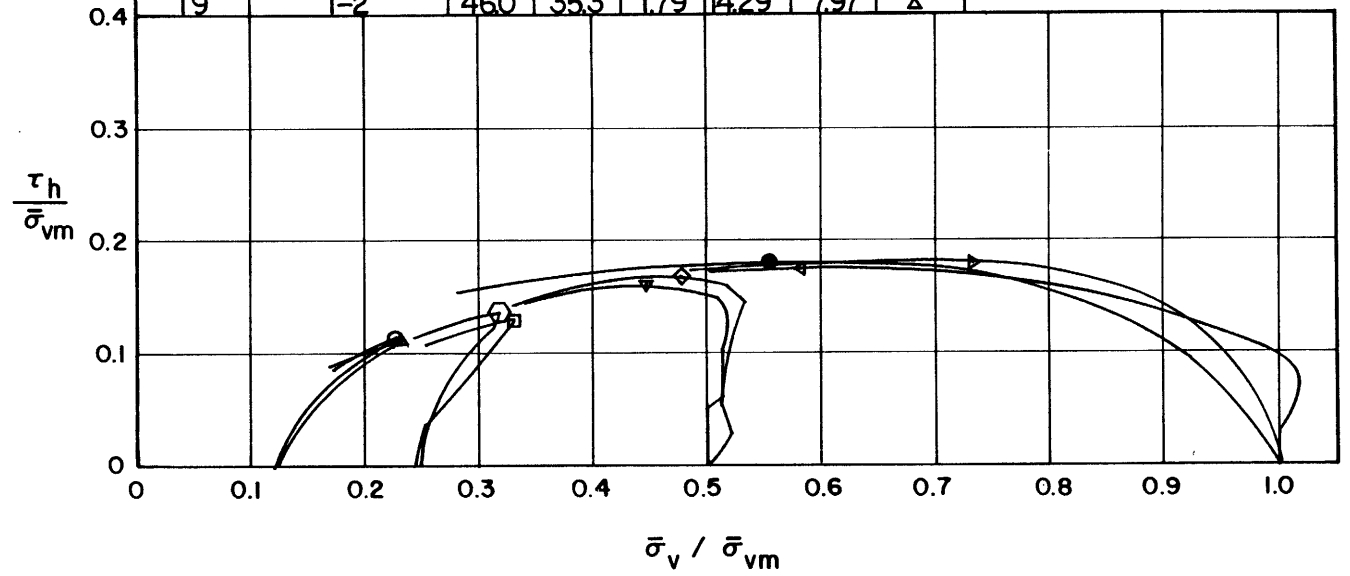

FIGURE

Figure 3.11 NORMALIZED STRESS PATHS FROM CK_oUDSS TESTS (Solar House)

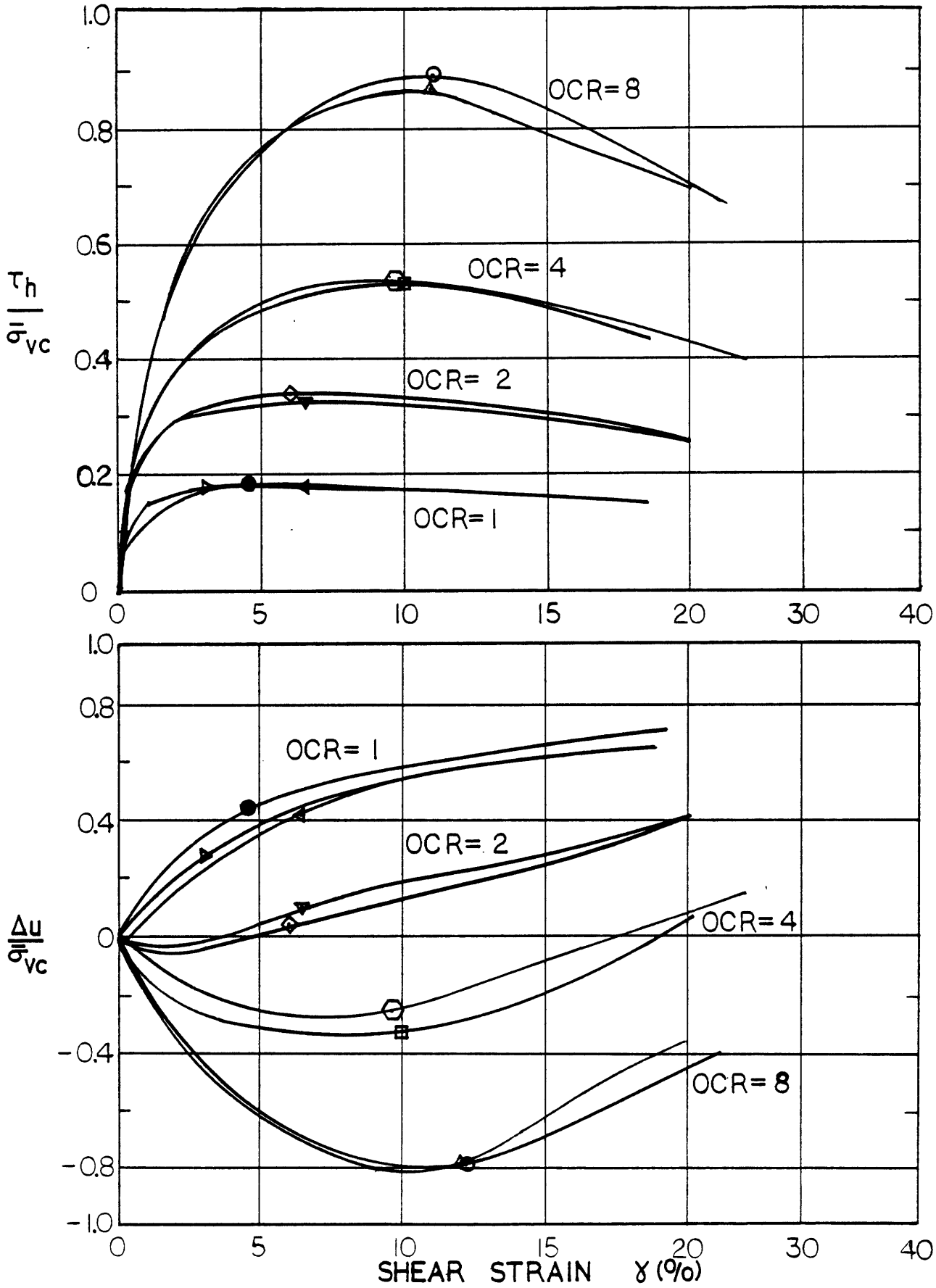

*See Fig. 3.11 for a list of symbols and test numbers

Figure 3.12 Normalized Stress vs. Strain From CK_oUDSS Tests (Solar House)

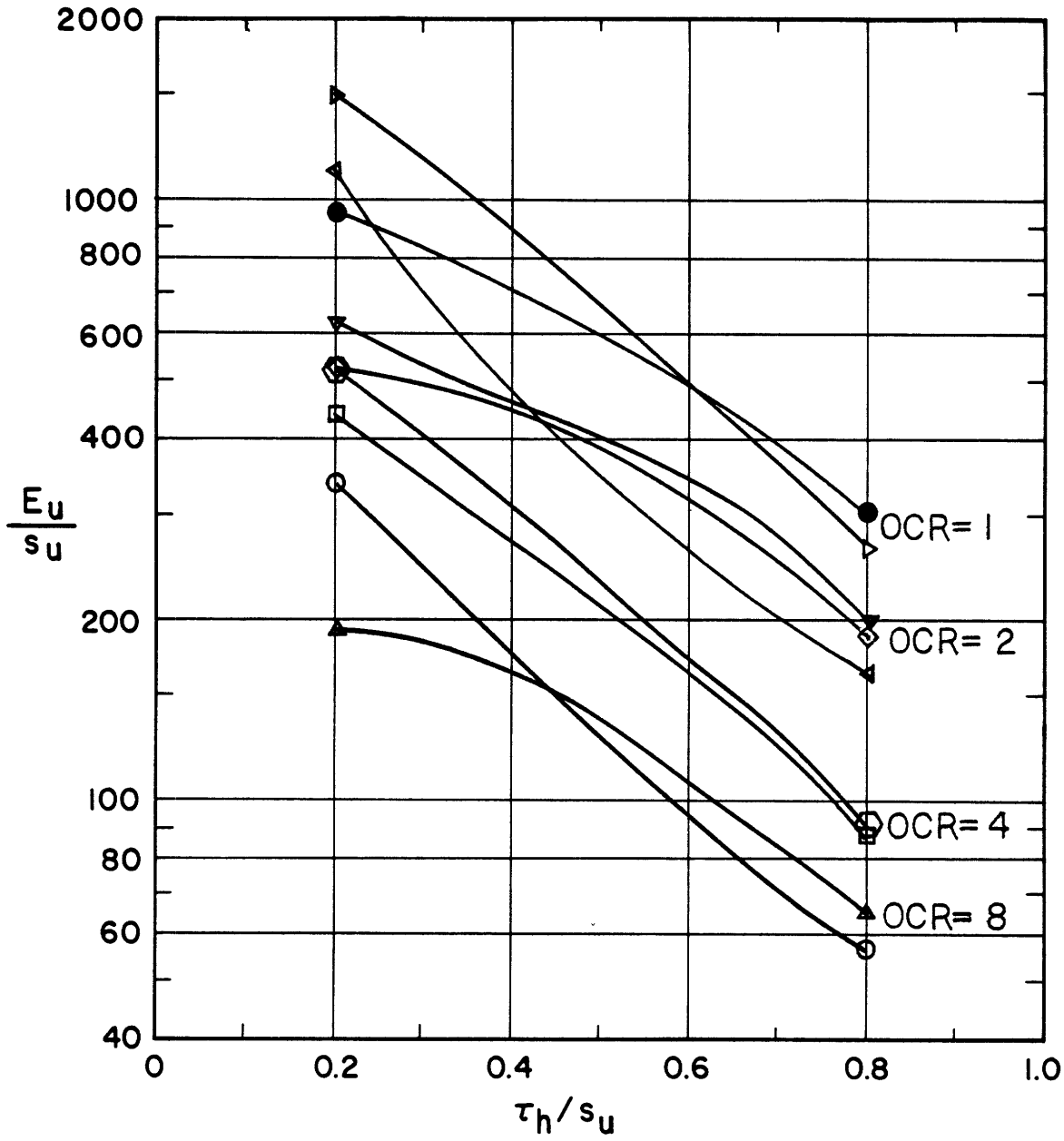

*See Fig. 3.11 for a list of symbols and test numbers

Figure 3.13 Normalized Modulus from CK_oUDSS Tests (Solar House)

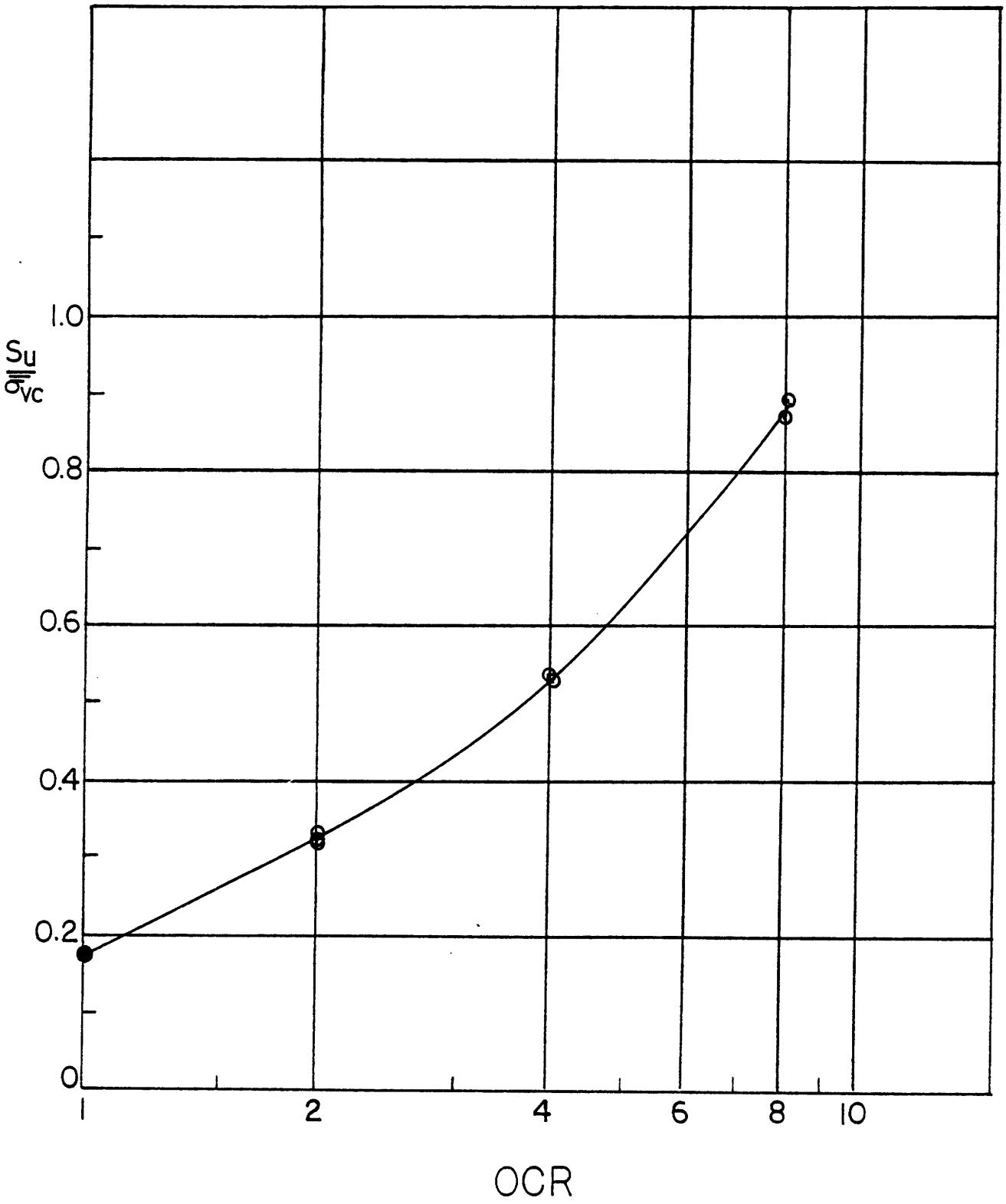

Figure 3.14 SHANSEP CK$_0$UDSS Parameters for BBC at the Solar House Site

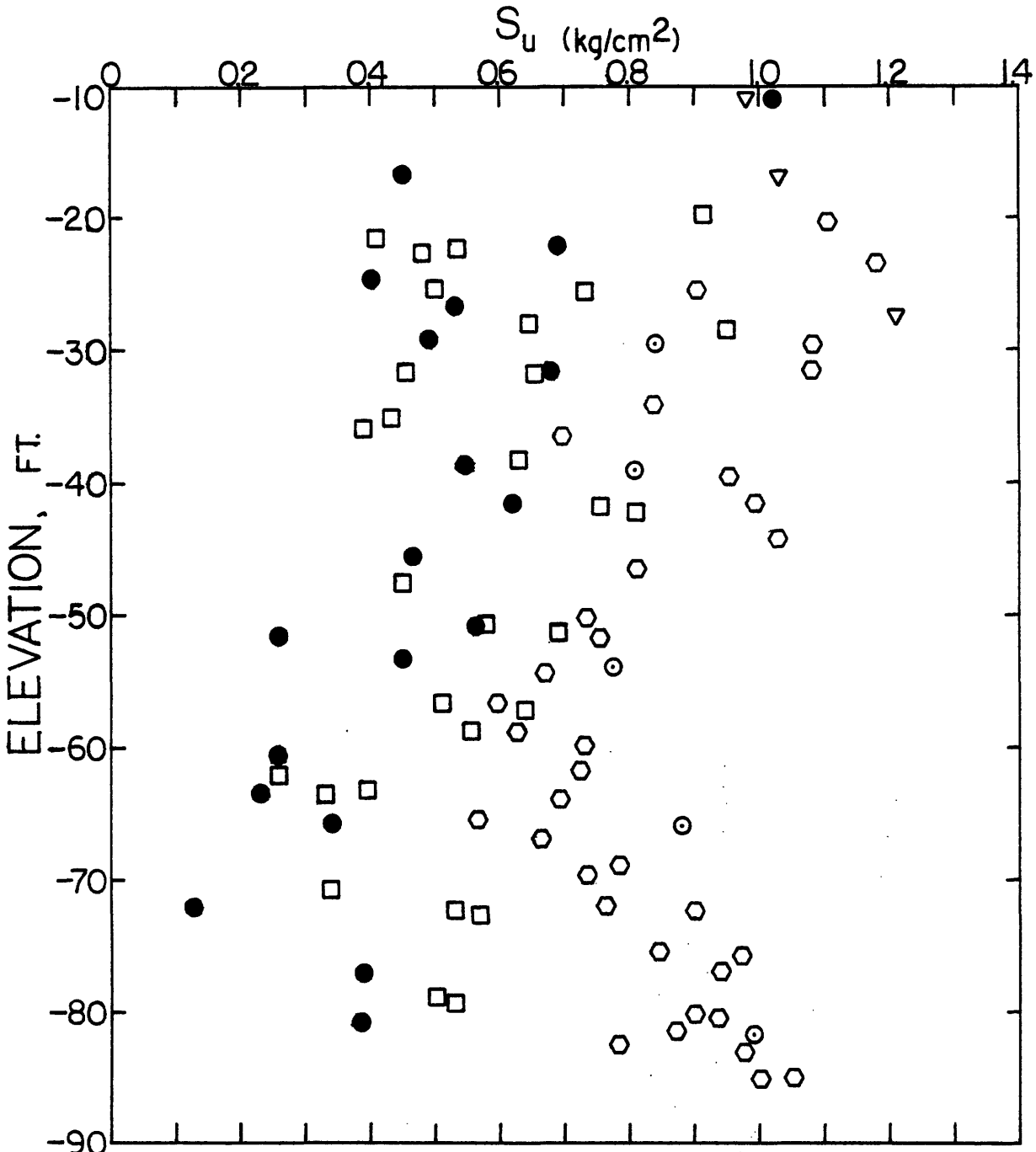

Figure 3.15 Peak Undrained Shear Strengths for Tests on BBC Below the MIT Campus

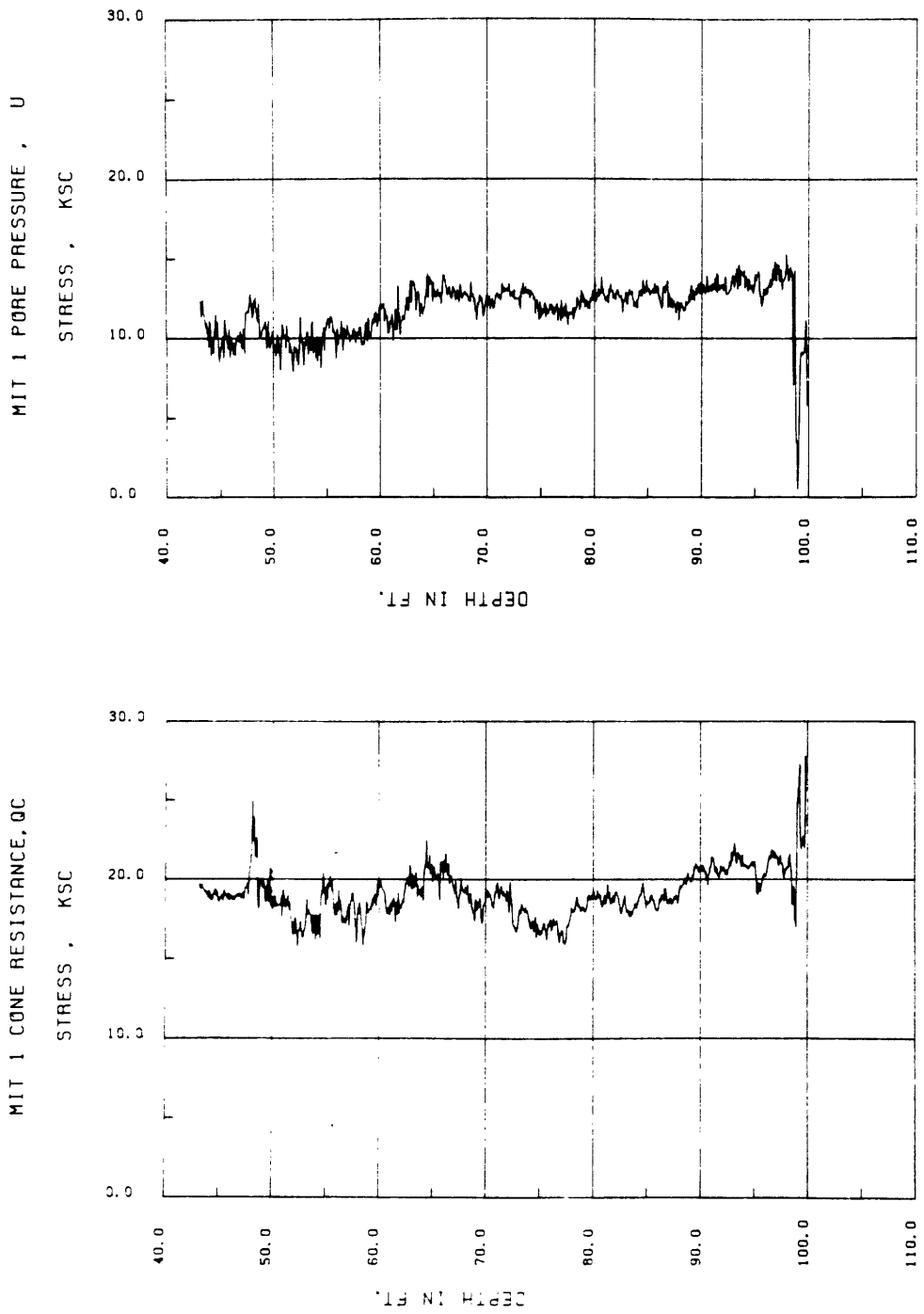

Figure 3.16 Cone Penetration and Pore Pressure Measurements Obtained with the Piezocone: Solar House, Hole MP1

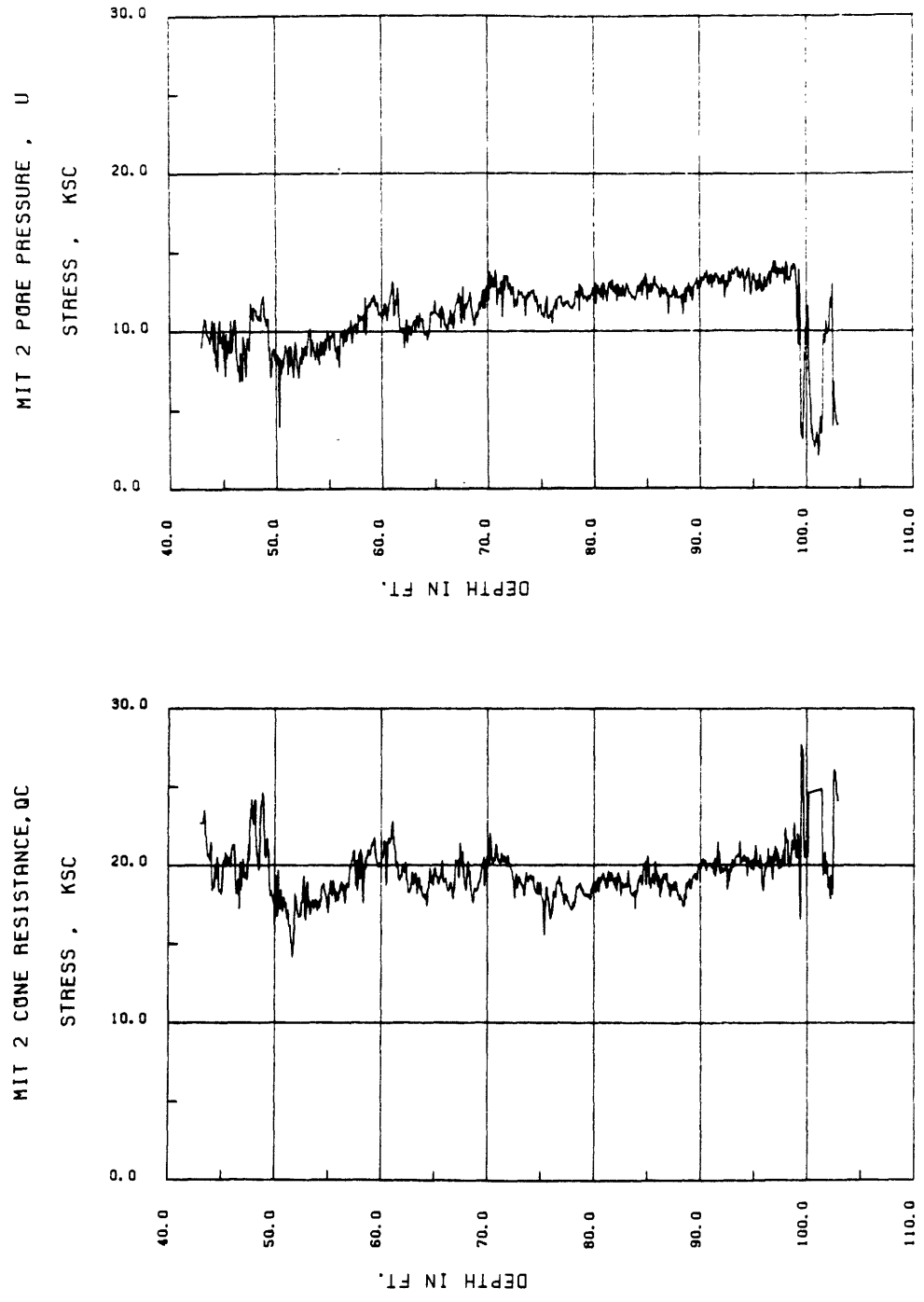

Figure 3.17 Cone Resistance and Pore Pressure Measurements Obtained with the Piezocone: Solar House, Hole MP2

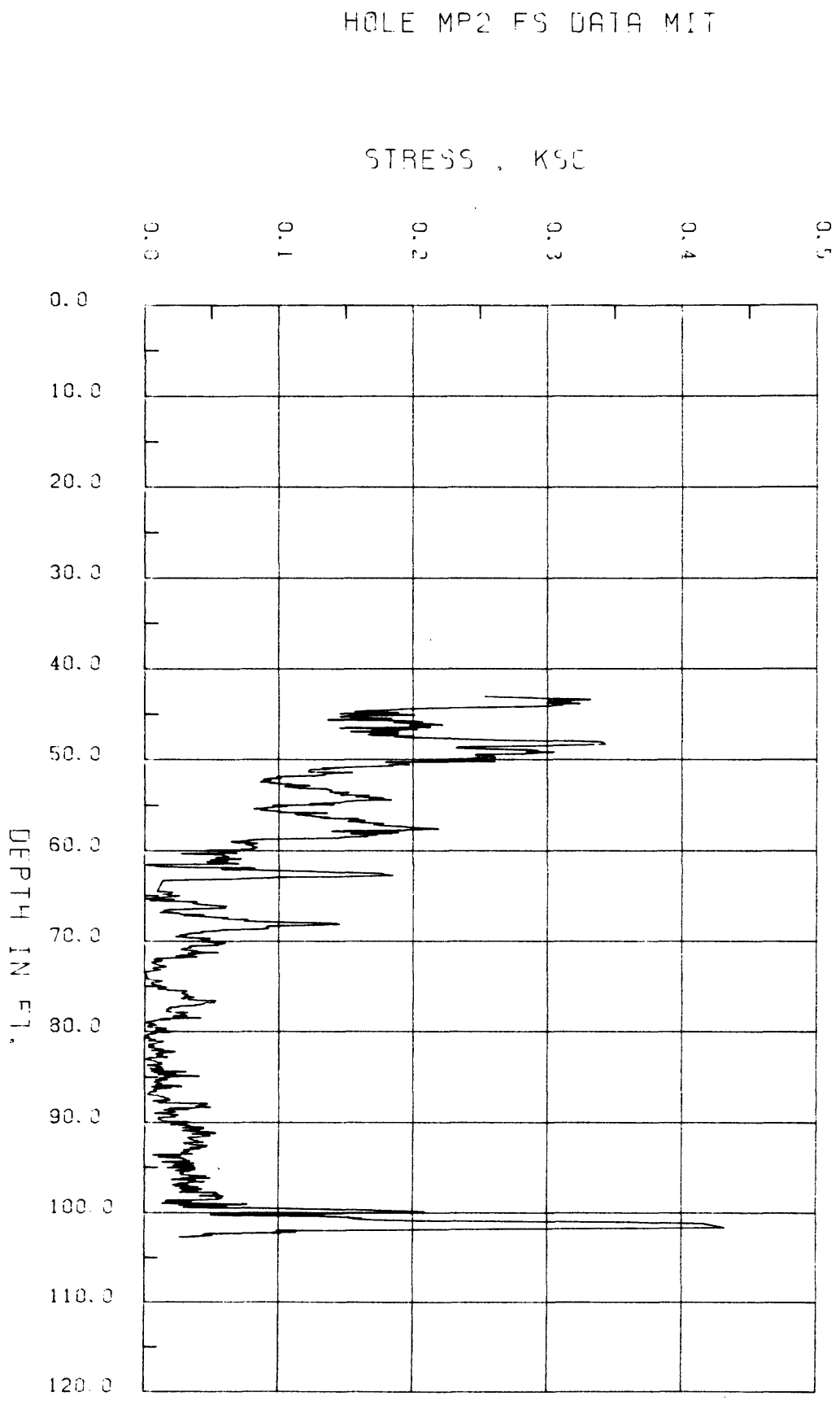

Figure 3.18 Skin Friction Measurement Obtained with the Piezocone at the Solar House, Hole MP2

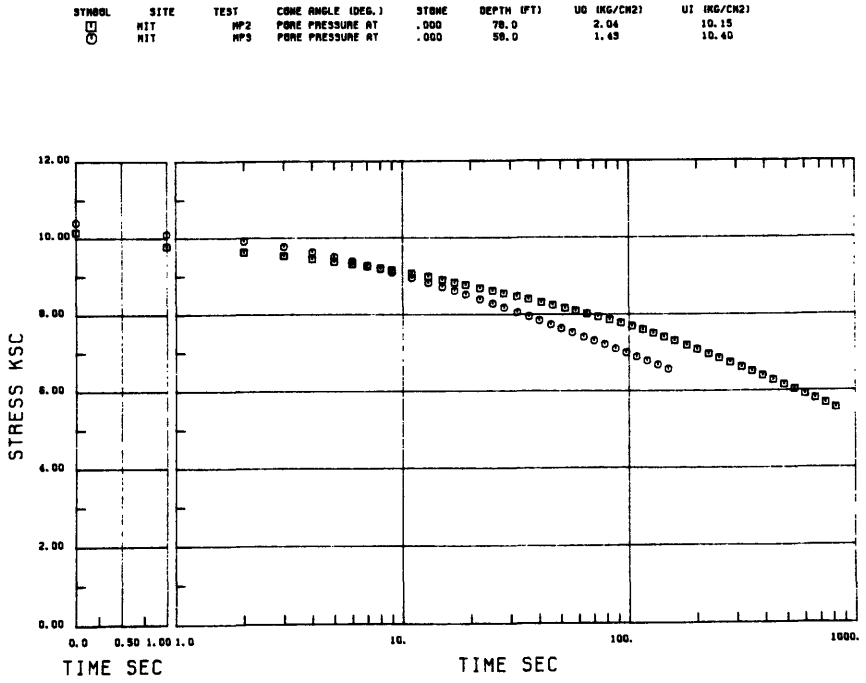

a) Measured

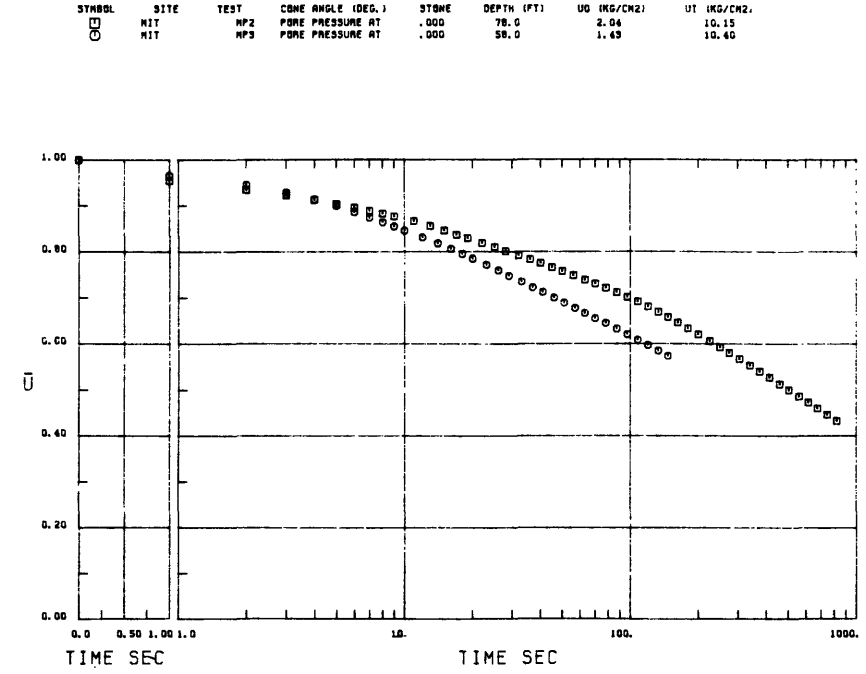

b) Normalized

Figure 3.19 Measured and Normalized Pore Pressure Dissipation Curves

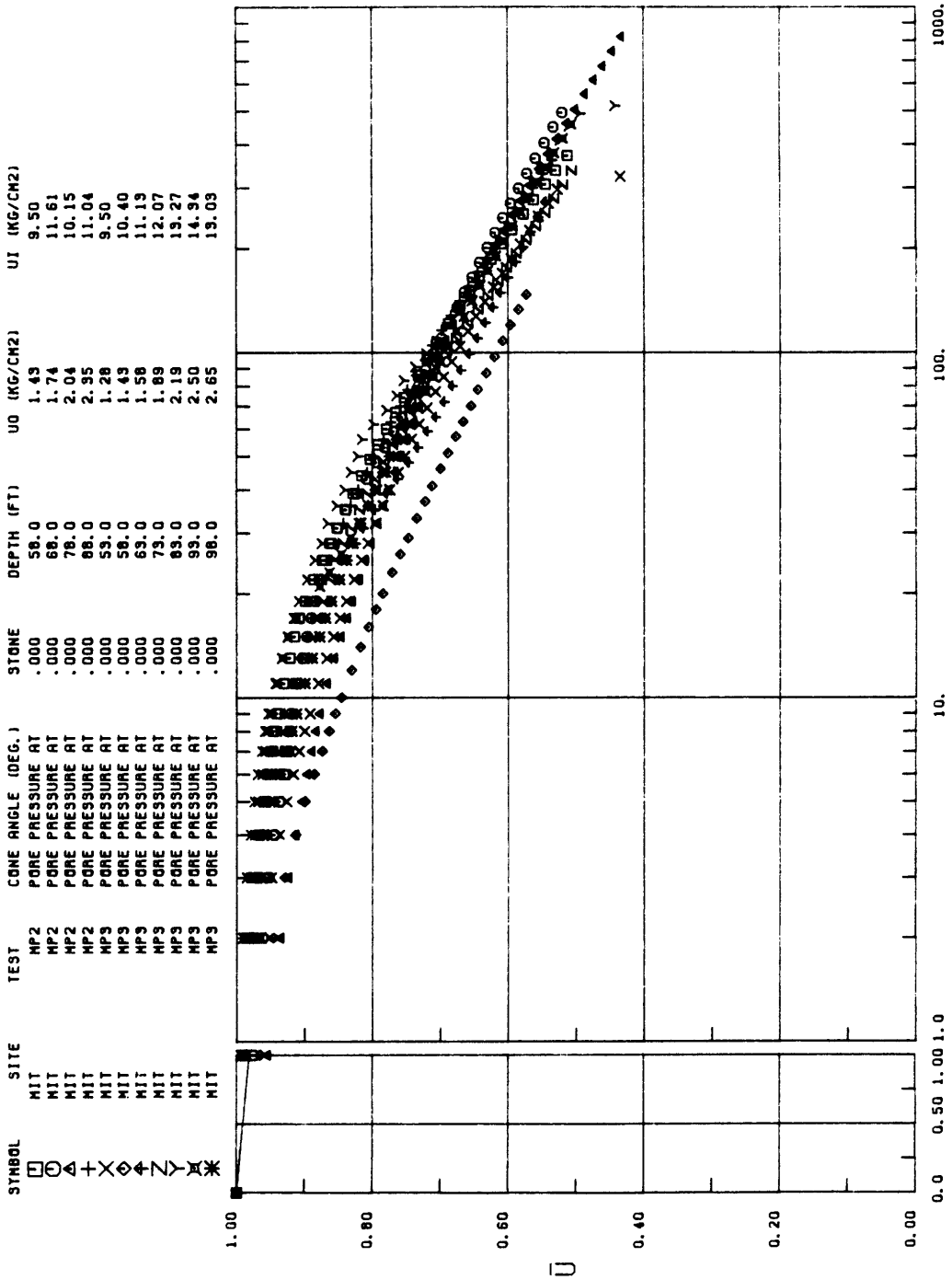

Figure 3.20 Normalized Dissipation Records for the Solar House Investigation

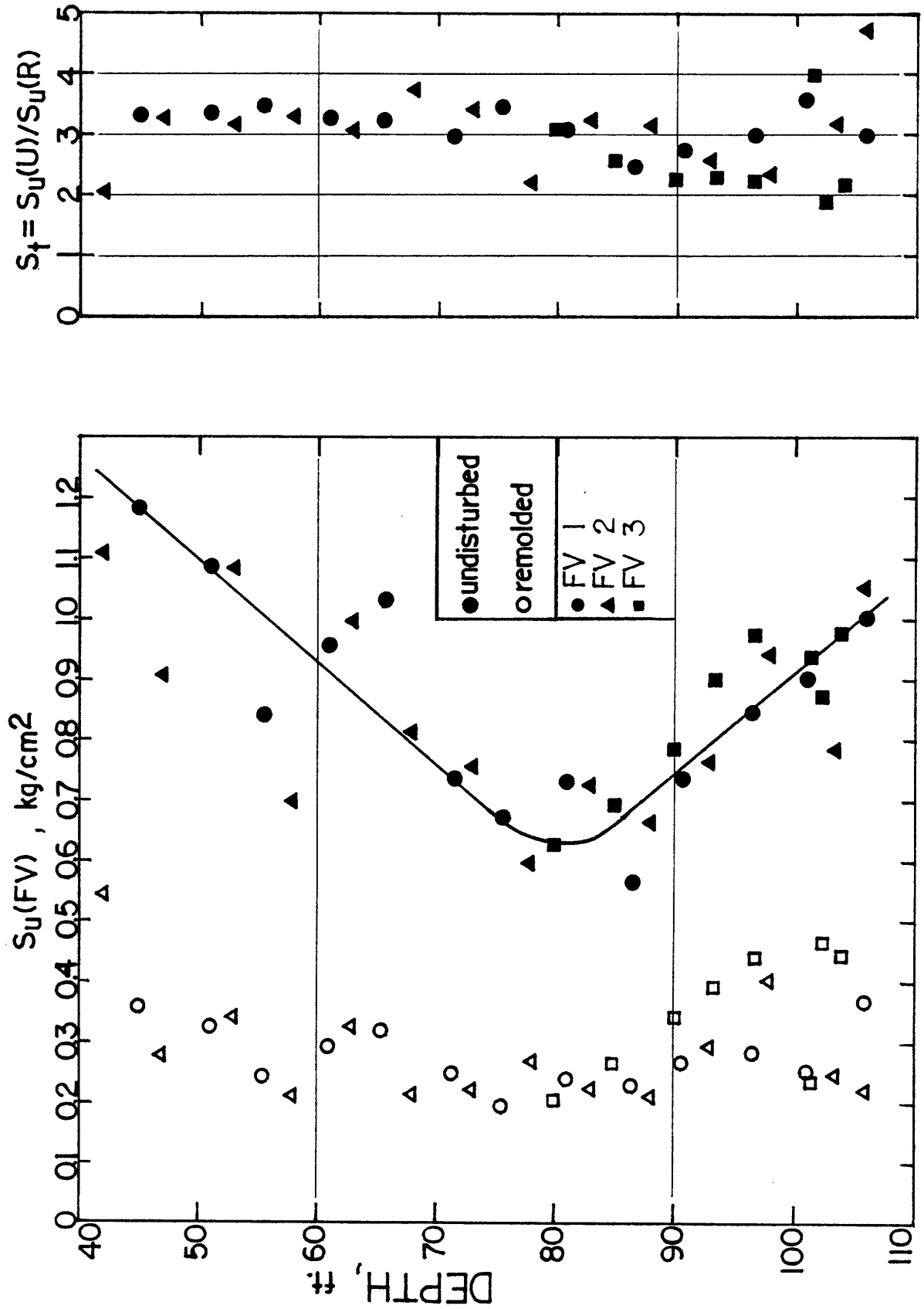

Figure 3.21 Field Vane Strength and Sensitivity Profiles at the Solar House Site

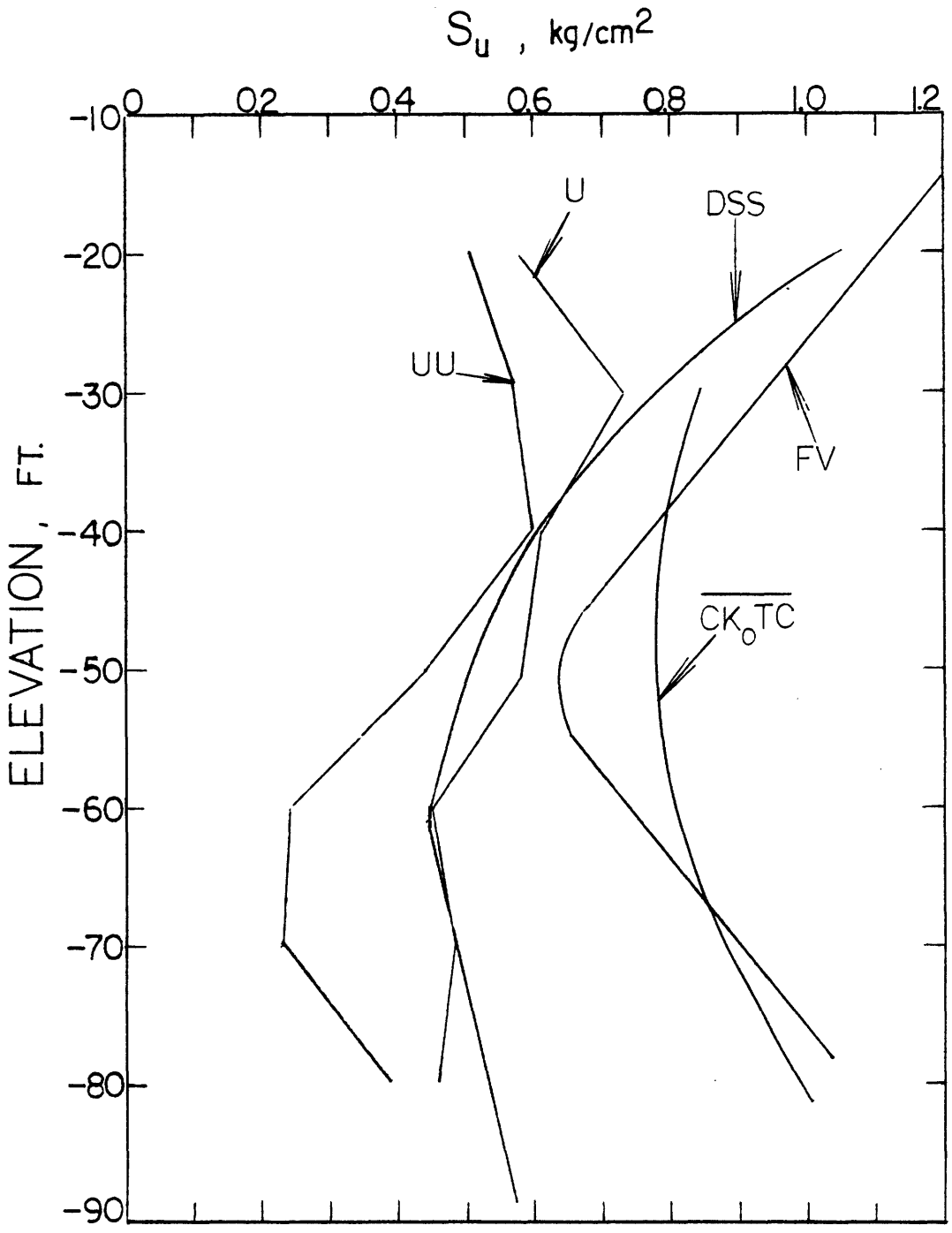

Figure 3.22 Average Undrained Strength Profiles for BBC Below the MIT Campus

CHAPTER 4

EVALUATION OF CONE RESISTANCE AND PORE PRESSURE MEASUREMENTS DURING PENETRATION

4.1 Introduction

As presented in section 2.2.3, cone resistance measurements during penetration can be utilized to predict the undrained shear strength of clays. Simultaneous pore pressure and cone resistance measurements allow further evaluation of the stratigraphy, stress history, and consolidation characteristics of soils. This chapter will detail past applications of the piezocone in the evaluation of stratigraphy, stress history, and shear strength as well as present the results from the MIT Solar House investigation. The topic of consolidation characteristics of soils will be discussed in Chapter 5.

4.2 Stratigraphic Logging

4.2.1 Background

As discussed in Chapter 2, simultaneous measurements of the cone resistance, q_c, and pore pressures, u, during cone penetration are useful in establishing soil stratification and identification. This section presents examples from different soil deposits to help illustrate this point.

In 1978, Baligh and his co-workers at MIT conducted an extensive study at a site located in Saugus, Mass. about 11 miles north of Boston. The soil profile illustrated in Fig. 4.1 consists of about 25 ft of peat, sand, and stiff clay

which overlie 130 ft of Boston Blue Clay, BBC. Based on laboratory estimates of the maximum past pressure, $\overline{\sigma}_{vm}$, the clay above a depth of 75 ft is significantly overconsolidated.

Figure 4.2 shows the cone resistance, q_c, and the penetration pore pressure, u, obtained in the upper 25 ft. Individually, q_c and u detect major changes in strata, but jointly they have an excellent potential for soil identification as well. For example, in the peat, q_c is low and u is high, whereas in the relatively clean sand, q_c is high and u is very close to the hydrostatic value, u_o.

The q_c and u records obtained during the next 120 ft are illustrated in Fig. 4.3 where we note:

(1) The sharp increase in q_c and decrease in u at depths of 25, 51, 99 and 117 ft suggest the presence of sand lenses at these depths. Such information is essential for the determination of drainage boundaries for problems involving the dissipation of excess pore pressures.

(2) At a depth of approximately 140 ft, a sharp increase in q_c is accompanied by a sharp decrease in u. This corresponds to the interface with the glacial till. In fact, the u record suggests the presence of a small transition zone overlying the till.

Campanella et al., (1982) define the heterogeneous soil profile for the Annacis site near Vancouver, British Columbia, with the use of cone resistance, pore pressure and friction resistance logs, Fig. 4.4. As mentioned before, low resistances and high pore pressures characterize the silt

layers, whereas low pore pressures and high cone resistances indicate sand lenses. Silty sand layers are distinguished by responses intermediate of the two.

A useful soil identification parameter in heterogeneous deposits is the time to reach 50% dissipation, t_{50} (Campanella et al., 1982), which is usually achieved in silty sand mediums during breaks to extend the drilling rods. Equilization of pore pressures in sands, with relatively high coefficients of permeability, will occur in a few minutes, whereas for clays, the time required may be a few hours. For silty soils, the time required for equilization is between the two extremes. Times to 50% dissipation at the Annacis site are also shown in Fig. 4.4.

Azzouz et al., (1982) present the results of a comprehensive soil investigation program performed on soft offshore Venezuelan clays from the Gulf of Paria and Orinoco Delta regions. In addition to the "conventional" index-strength tests, the investigation involved a sophisticated SHANSEP laboratory testing program together with continuous in situ measurements of q_c and u. This represents the first time penetration pore pressures were measured offshore.

The SHANSEP strength profile obtained from the Direct Simple Shear test is shown in Fig. 4.5 together with the results of the "conventional" strength tests performed onboard ship. As can be seen from the figure, the SHANSEP profile undergoes an abrupt change at a depth of about 75-80 ft below the mud line. At this depth, the normalized strength ratio,

$s_u/\bar{\sigma}_{vo}$, decreases from 0.235 ± 0.01 to 0.200 ± 0.005, which was entirely unexpected since it was not accompanied by significant changes in the plasticity index or mineralogy of the clay.

Figure 4.6 shows the cone resistance, q_c, and penetration pore pressure, u, measured during cone penetration. Also shown in this figure is the normalized pore pressure record $(u-u_o)/\bar{\sigma}_{vo}$. The results show:

(1) The values of q_c are only slightly higher than u, which suggests, based on experience with other deposits, that the clay at this site is soft. This agrees well with the stress history derived from the results of the laboratory testing program (Azzouz et al., 1982).

(2) The top 134 ft, which are described as soft to stiff clay based on the onboard classification tests, can be further divided into three sublayers:

a) Sublayer B, Z=75 to 130 ft, has a significantly different rate of increase of u with depth compared to A and C. This is consistent with the SHANSEP strength variation with depth illustrated in Fig. 4.5

b) Sublayer C, Z=130 to 134 ft, is characterized by a clear drop in u which is accompanied by a very slight increase in q_c.

A transition sublayer between 75 and 85 ft could also have been added.

(3) The variation in properties between the "upper" and "lower" clays can be further illustrated by studying the variation of the normalized pore pressure ratio with depth. For Z<75 ft, this ratio is in the range of 3 to 3.5, except from Z=25 to 35 ft where it ranges from 3.5 to 6. For Z=75 to 125 ft, $(u-u_o)/\bar{\sigma}_{vo}$ ranges between 2.5 to 3.

In summary, study of the penetration logs can reveal useful information regarding different stratifications within the stratum. These stratifications will yield a detailed picture of soil variability which may help explain and/or verify laboratory test variability.

4.2.2 Solar House Investigation

From review of the u and q_c plots, and the normalized pore pressure, Figs. 4.7 and 4.8, it would appear that the clay underlying the Solar House can be divided into four sublayers as follows:

Layer	Depth (ft)	Characteristics
A	40-50	u, q_c, and $(u-u_o)/\bar{\sigma}_{vo}$ decreasing
B	50-65	All values increasing
C	65-77.5	All parameters decreasing
D	77.5-98	u and q_c increasing, $(u-u_o)/\bar{\sigma}_{vo}$ constant

Layers A-C clearly indicate the "upper" clays where the soil is overconsolidated and exhibits variable behavior with

depth. Below 77.5 ft, layer D, are the "lower" clays where u and q_c increase with u_o and $\bar{\sigma}_{vo}$, respectively, and $(u-u_o)/\bar{\sigma}_{vo}$ remains relatively constant. The OCR in layer D ranges from 1.5 to 1. Also, the ratio of u/q_c below 77.5 ft is near unity, characteristic behavior of softer clays.

The sharp drop in u and increase in q_c at 98 ft suggests the interface of a clayey sand or sandy clay layer at that depth. Index classification of the soil below 98 ft confirms the presence of sand interspersed with the clay by the reduced values of the plasticity index below that depth (P.I. ≈ 12%).

4.3 Stress History

Simultaneous u and q_c measurements can be used to evaluate the stress history of a clay deposit. The relationship between u/q_c, and overconsolidation ratio was first hypothesized by Baligh et al. (1980):

> "Cone penetration in clays causes severe undrained straining of the soil well beyond the peak strength. For soft clays with low OCR, undrained shearing results in decreased effective stresses. This implies that pore pressures near the cone must increase not only to resist the compressive stresses caused by penetration, (i.e., to satisfy equilibrium), but also because of the large shear strains. On the other hand, more overconsolidated clays will develop smaller pore pressures during cone penetration, but because of the compressive stresses, the pore pressure during cone penetration need not be negative."

In order to check this hypothesis, the ratio of u to q_c is examined. High values of u/q_c should be associated with low OCR and vice-versa. Figure 4a presents the u/q_c profile for the BBC located at the Saugus site (see Fig. 4.1) which shows u/q_c to increase with depth down to approximately 80 ft and then remains constant. This agrees well with the OCR profile presented in Fig. 4.9 which shows OCR to decrease from a value of about 7 at depth 25 ft to about 1.2 at depth 80 ft and remains constant thereafter. Furthermore, since u and q_c are measured simultaneously by means of the piezocone, the ratio u/q_c is also useful in the determination of soil stratification. For example, the u/q_c profile clearly detects the sand lenses at depths 51, 99, and 117 ft as well as the location of the glacial till.

Many studies have since been performed to further advance the usefulness and applicability of the u/q_c-stress history relationship. Lacasse and Lunne (1981) and Zuideberg et al. (1982) both show that the relative trend of the relationship matches the expectations, i.e., the increase in OCR corresponds to a decrease in u/q_c; however, the absolute figures need as yet further discussion and research. Tumay et al. (1981), through a field study, and Smits (1982), through lab penetration tests, present results relating u/q_c and OCR (Fig. 4.10), but arrive at different conclusions regarding their usefulness. Tumay agrees that u/q_c is a good indicator of OCR, provided a region-specific calibration exists. On the

other hand, Smits, using $(u-u_o)/(q_c-u_o)$ instead of u/q_c, states that the wide band of data points, in combination with a small slope of the straight lines, indicates that such a relation is not very useful in practice to obtain information on the stress history of the clay. He arrives at this conclusion even after showing the existence of a unique relationship for $\Delta u/q_c-u_o$ for normally consolidated clays, which may suggest the possibility of unique values of $\Delta u/q_c-u_o$ for different overconsolidation ratios.

It is believed that anytime u is greater than q_c (or $u/q_c > 1$), measurement inaccuracies exist. These inaccuracies are caused by the free flow of water behind the cone which acts to reduce the effective q_c measured. It can be seen from Tumay's study, in Fig. 4.10a, that u/q_c for the enlarged cone (D/d=2) is considerably greater than for the regular cone (D/d=1). This makes sense since the area behind the base of an enlarged cone allows considerably more water flow than a regular cone, which reduces q_c to an even greater extent. In the case when u/q_c is greater than unity, q_c must be corrected for the pressure behind the cone base by the method outlined in section 3.5.1.

While Smits was the only dissenter on the applicability of the pore pressure-cone resistance ratio, many authors disagree on how the pore pressure should be expressed; either as the generated value, u, or as the excess pore pressure, $\Delta u=(u-u_o)$. Campanella et al., (1982) expect $\Delta u/q_c$ to relate

more uniquely to the stress history of a clay deposit. They feel that u/q_c will only be constant with depth for normally consolidated clays if u_o is hydrostatic, i.e., linear with depth. A disadvantage of using Δu is that knowledge of hydrostatic conditions must exist to define it, even though u_o can be obtained after allowing for excess pore pressure dissipation, this takes a considerable amount of time and expense.

Plots of u/q_c for the Solar House investigation are presented in Figs. 4.11 and 4.12. These plots show the means and standard deviations of the u/q_c data points from each two foot increment of depth. The relative trend of the plots supports Baligh's hypothesis; that is, as OCR decreases, u/q_c increases. When the clay becomes normally consolidated, u/q_c becomes constant at approximately 0.67. However, being that the location of the porous stone, the cone angle, and the cone shape all affect u and q_c measurements; further research is needed before u/q_c can be quantitatively related to stress history.

4.4 Undrained Shear Strength, s_u

It has been well established, based on field and laboratory studies, that the stress-strain-strength characteristics of soft saturated clays are influenced by the mode of failure and the rate of strain (Ladd, 1975). This is extremely evident with regard to the undrained shear strength. Table 4.1 illustrates, through 4 different strength tests on BBC, that s_u is not a unique value, but depends on the stress

system, direction of shear, type of consolidation (isotropic or one-dimensional), and rate of loading. Therefore, a problem exists in interpreting the "field strength" being measured from cone penetration tests.

Use of the cone penetration test (CPT) to evaluate the undrained shear strength of clays has been approached both theoretically and empirically. The theoretical approach utilizes one of the many solutions for the cone factor, N_k, for application into the equation:

$$q_c = N_k s_u + \sigma_o \qquad (4.1)$$

where, q_c = penetration resistance

s_u = undrained shear strength

σ_o = in situ total vertical, horizontal or octahedral stress

The empirical approach to cone penetration, in lieu of directly predicting s_u utilizing a predetermined theoretical cone factor, employs a reference s_u that is determined from laboratory or field tests, to backfigure N_k utilizing equation 4.1. This N_k value will then be used in subsequent investigations to predict s_u from penetration resistance logs.

4.4.1 Theoretical Approach to Cone Penetration

Baligh et al. (1979) present a comprehensive overview of the existing theoretical methods for penetration resistance interpretation, Table 4.2. The theoretical solutions are based on three approaches that can be grouped as follows: plane strain slip-line, expansion of cavities, and steady

penetration. All of the approaches rely on modifications of more rigorous solutions to simplified problems. The simplifications are made with respect to problem geometry, stress-strain behavior of soil, and the mode of deformation. Factors which were not rigorously considered, totally neglected, or not able to be accounted for simultaneously by theoretical predictions include: anisotropy in shear strength and initial stresses, soil deformation prior to yield, soil compressibility, strain softening, strain rate, cone angle, relative depth, and reduced friction at the soil-cone interface, all of which are known to influence the ultimate cone resistance (Baligh et. al., 1979; Durgunoglo and Mitchell, 1975).

The cavity expansion and steady penetration approaches require computation of a rigidity index, I_R, in order to obtain a cone factor value. The rigidity index, I_R, is defined as:

$$I_R = G/s_u \qquad (4.2)$$

where, G = undrained shear modulus

Baligh (1975) presents a chart of N_K versus I_R for various cone angles, Fig. 4.13, to be used in his steady penetration approach. Over the full range of likely clay rigidities (i.e., G/s_u = 6-400), $N_c = 16 \pm 2$ for a 60° cone.

In addition to the solutions presented in Table 4.2, Levadoux and Baligh (1980) introduced a new two-dimensional

method to be used in deep foundation problems (e.g., cone penetration and piles). The strain path method is based on concepts similar to the well known stress path method (Lambe, 1967) and consists of four basic steps:

a) estimate the initial stresses

b) estimate an approximate strain field satisfying conservation of volume, compatibility and boundary velocity requirements

c) evaluate the deviatoric stresses at a selected number of elements by performing laboratory tests on samples subjected to the same strain paths, or alternatively, by using an appropriate soil model; and

d) estimate the octahedral (isotropic) stresses by integrating the equilibrium equations.

Levadoux and Baligh (1980) applied the strain path method to predict the cone resistance profile for the Saugus site shown in Fig. 4.1. The predictions are in reasonable agreement with the measurements. However, the method is sophisticated and requires a significant effort in selecting the input parameters for the soil model described in step (c) above. As a result, their technique cannot be used readily in interpreting the q_c records in practice.

Several investigators have attempted to evaluate the adequacy of some of the methods presented in Table 4.2 in predicting the undrained shear strength from the q_c measurements. Lacasse and Lunne (1982) report results from two test sites in Norway. They concluded that the Baligh (1975)

theory, with an N_k=16, produced s_u profiles which are in very close agreement with the field vane strength profiles (see Fig. 4.14). Jamiolkowski et al., (1982) obtained undrained shear strengths and rigidity indices from field pressuremeter and laboratory Direct Simple Shear and Triaxial tests at three Italian sites in order to predict penetration resistance, q_c, utilizing the available theoretical solutions for cone factors. Figure 4.15 illustrates the results of these studies.

From the above results, it is difficult to make conclusions about the applicability of the theoretical solutions to predict s_u. Although Baligh's approach looks promising at the Norway sites and at the Taranto site (Italy), it greatly over-predicts q_c at Montalto di Castro (Italy). Except for the Lacasse and Lunne study, which utilized a range for N_K, the other studies relied upon laboratory testing to arrive at values for I_R (needed to obtain N_c in the cavity expansion solution) and s_u. In a way, this reduces these studies to a quasi-theoretical approach to the problem. Also, are we to assume that the cone measures the field vane strength because of the good agreement at the two Norway sites? Obviously, more of these kinds of studies are necessary to answer what "field strength" the cone measures and which of the theoretical approaches, if any, is better suited to predict the undrained shear strength of clays.

4.4.2 Empirical Approach to Cone Penetration

The most widely reported test to estimate a reference s_u is the field vane test. Plate load, laboratory triaxial and Direct Simple Shear tests have also been used. Table 4.3 summarizes the N_k values reported in the literature. Cone factors vary from 5-33 depending upon the testing method used to predict s_u and the different clay region. For the Solar House site, cone factors were calculated using field vane as well as DSS strength results, and fall within a range of 13 -22 and 18-32, respectively. Figures 4.16 through 4.19 present cone factor, N_k, profiles for the site calculated using equation 4.1 and the respective reference strength tests. These plots show the means and standard deviations of the N_K data points from each two foot increment of depth. It can be seen from these figures that below 65 ft (OCR=2), the N_k values plot within a fairly narrow band, 18-22 for s_u(FV) and 26-32 for s_u(DSS).

Figure 4.20a presents results compiled at numerous sites for N_k versus P.I. for s_u(FV) uncorrected. It is seen that N_k decreases as plasticity increases; however, Fig. 4.20b shows that after applying Bjerrum's correction factor, (see Fig. 2.2), most of the N_k values fall within a range of 14 $\pm$ 3. Because μ=1 for P.I.=20%, the Solar House N_k values remained unchanged. Bjerrum's correction factor helps to reduce the scatter in the cone factor values, but cannot totally account for the dependence of N_k on some of the inherent limitations of the empirical approach.

Clearly, because of the scatter of N_k values and the limitations of the empirical analysis, no single N_k value exists that will cover all types of clays, penetrometers, and test conditions. However, for a given clay deposit, a given penetrometer, and given test conditions, it seems likely that there should be a unique relationship between cone tip resistance and s_u (Kjekstad, 1978). However, it must be remembered that if field vane tests are used to backfigure a cone factor, any subsequent penetration tests using that cone factor will yield a field vane strength profile. Because of the non-uniqueness of s_u, when a cone factor is used, it is important to understand what type of strength profile it will yield (i.e., field vane, DSS, etc.).

4.4.2.1 Prediction of s_u Using Generated Pore Pressures

Only recently have empirical studies been performed to relate $\Delta u(u-u_o)$ to s_u via a cone factor $N_{\Delta u}$:

$$\Delta u = N_{\Delta u} S_u \qquad (4.3)$$

Tavenas et al. (1982) found at the Batiscan site in Quebec, Canada, that $N_{\Delta u}$ seems to be controlled more by the liquidity index, I_L, as opposed to P.I. as is the case with N_K. For the porous filter located at the cone base, and using field vane strengths, they determined that:

$$N_{\Delta u} = 7.9 \pm 0.7 \quad \text{for } 0.8 < I_L < 2$$

$$N_{\Delta u} = 11.7 \pm 2.0 \quad \text{for } I_L > 2$$

They feel these correlations are still too scattered to permit an accurate evaluation of s_u for design; however, they believe that $N_{\Delta u}$ should be constant in a given clay formation.

Using field vane strengths, Roy et al. (1982) found at the St. Alban site in Quebec:

$N_{\Delta u}$ = 7.4 for filters located at the tip

$N_{\Delta u}$ = 4.7 for filters located up the shaft

In order for $N_{\Delta u}$ to be constant, Δu and s_u need to increase at similar rates. In a normally consolidated clay, a constant $N_{\Delta u}$ is to be expected because Δu increases with u_o and s_u increases with $\bar{\sigma}_{vo}$, both of which increases at similar rates. However, in a clay deposit such as BBC, where the OCR undergoes marked changes with depth, a constant $N_{\Delta u}$ is not to be expected. The excess pore pressure, $u-u_o$, remains relatively constant during penetration, increasing slightly as OCR decreases; whereas s_u undergoes a steady decrease as OCR decreases. Therefore, because OCR decreases with depth, one would expect an opposite effect of $\Delta u/s_u$. Results from the Solar House site support this reasoning. Figure 4.21 illustrates Δu with depth and Figs. 4.22 and 4.23 show $\Delta u/s_u$(FV) for the three test holes. As expected, $\Delta u/s_u$ decreases until a depth of about 80 ft (OCR=1) where $N_{\Delta u}$ becomes constant. It is clear, therefore, that this relationship is not adequate for BBC nor for deposits with similar stress histories.

Undrained Shear Strength Determined From	OCR $\frac{\bar{\sigma}_{vm}}{\bar{\sigma}_{vc}}$	Undrained Strength Ratio		
		$\frac{s_u(ave)}{\bar{\sigma}_{vc}}$	$\frac{s_u(V)}{\bar{\sigma}_{vc}}$	$\frac{s_u(H)}{\bar{\sigma}_{vc}}$
$\overline{CK_oU}$ (1) Plane Strain Active & Passive	1	0.26^5	0.34	0.19
	2	0.47	0.57	0.37
	4	0.81	0.95	0.67
$\overline{CIU}$ (1) Triaxial Compression	1	0.32^5	0.32^5	-
	2	0.55^5	0.55^5	-
	4	0.90	0.90	-
$\overline{CK_oU}$ (2) Direct-Simple Shear	1	0.20	-	-
	2	0.37	-	-
	4	0.61	-	-
$\overline{UU}$ (1) Triaxial Compression	1	0.18	0.18	
	2	0.36	0.36	
	4	0.60	0.60	

(1) $s_u = q_f = \frac{1}{2}(\sigma_1 - \sigma_3)_f$

(2) $s_u = \tau_h$ maximum

Table 4.1 Predicted vs Measured Ultimate Bearing Capacity of Strip Footing on Boston Blue Clay (from Ladd, 1971)

Type of Approach	Reference	$q_c = N_c s_u + p_o$ Expression for N_c	N_c for 2 δ = 60°		p_o
			G/s_u = 100	G/s_u = 400	
Bearing Capacity	Terzaghi (1943) Meyerhof (1951)	(shape factor)(depth factor) x 5.14	9.25	same	σ_{vo}
Bearing Capacity	Mitchell and Dorgunoglu (1973)	(shape factor)(depth factor) x (2.57 + 2 δ cot δ)	9.63	same	σ_{vo}
Bearing Capacity	Meyerhof (1961)	(1.09 to 1.15) x (6.28 + 2 δ + cot δ)	10.2	same	σ_{vo}
Bearing Capacity	Begemann (1965)	(shape factor)(2) x 5.14	13.4	same	σ_{vo}
Bearing Capacity	Anagnostopolous (1974)	(shape factor) x 14.88	17	same	σ_{vo}
Cavity Expansion	Bishop et al (1945)	1.33(1 + ℓn G/s_u)	7.47	9.30	unspecified
Cavity Expansion	Gibson (1950)	1.33(1 + ℓn G/s_u) + cot δ	9.21	11.03	σ_{vo}
Cavity Expansion	Vesic (1975, 1977)	1.33(1 + ℓn G/s_u) + 2.57	10.04	11.87	σ_{oct}
Cavity Expansion	Al Awkati (1975)	(correction factor) x (1 + ℓn G/s_u)	10.65	13.28	σ_{oct}
Steady Penetration	Baligh (1975)	1.2(5.71 + 3.33 δ + cot δ) + (1 + ℓn G/s_u)	11.02 + 5.61 =16.63	11.02 +6.99 =18.01	σ_{ho}

Table 4.2 Summary of Existing Theories of Cone Penetration in Clays (Baligh 1979)

Reference	Region of Clay	Cone Factor N or N*	Soil Properties			Correlation by	Penetrometer Type
			W_N%	W_L%	I_p%		
Thomas (1965)	London Clay	18.0*	20-30	80-85	55	UC	M (Dutch)
Ward, et al.(1965)	London Clay	15.5	22-26	60-71	36-43	UU	M (Dutch)
Meigh & Corbett (1969)	Arabian Gulf Soft Clay	16.0	30-47	38-62	20-35	--	--
Ladanyi & Eden (1969)	Leda Clay (Gloucester)	7.5	50-70	50	23	FV	E (Borros)
Ladanyi & Eden (1969)	Leda Clay (Ottowa)	5.5	72-84	40	20	FV	E (Borros)
Pham (1972)	Soft Bangkok Clay	16.0	60-70	70-80	40-50	--	----
Anaonastopoulos (1974)	Patras Clay	17.0*	30	35	18	UC	H (Gouda)
Brand, et al. (1974)	Soft Bangkok Clay (Bangpli)	19.0	60-130	60-130	60-120	FV	M (Dutch)
Brand, et al. (1974)	Weathered Bangkok Clay (Bangpli)	14.0	100-130	100-135	60-80	FV	M (Dutch)
Ricceri, et al. (1974)	Venetia Cohesive Soils	23/21*	---	30-85	10-50	UC	H (Goudsche)
Genevois & Luzzolini (1974)	Rome & Tirrenian Clays	10.0 q_c 5kg/cm^2 18.0 q_c 27kg/cm^2	40-70	40-120	20-60	FV	M (Dutch)
Milovich (1974)	Nicolet Clay	10.0 7.0	63	63	8-23	UC FV	---
Marsland (1974)	London	14-18.5 12-16 17.5-21					Triaxial Triaxial Plate
Eide (1974)	Drammen, Onsoy, Goteborg	12-20*			11-50	FV	E (Fugro)
	Aarhus, Sandines	8-12*			9-67	FV	E (Fugro)
Lunne, et al. (1976)	Drammen Clay	14-19*	---	---	9-30	FV	E (Fugro)
	Drammen Clay	12-15*	---	---	10-35	FV	E (Fugro)
	Onsoy	14-18*	---	---	25-36	FV	E (Fugro)
	Goteborg	14-20*	---	---	40-60	FV	E (Fugro)
	Ska-Edeby	10-15*	---	---	35-50	FV	E (Fugro)
Koutsoftas & Fischer (1976)	New Jersey	16 ± 3*	45-75		30-50	FV	M(Dutch)
		16 ± 3*	25-50		9-27	FV	
Kjekstad, et al. (1979)	Norway North Sea	17.9* 15.7* 17.5*	15-25	---	17-26	CIU UU UC	E (Fugro)
Baligh, et al. (1979)	Boston Blue Clay	9-15*	40-50	20-50	24	FV	E (Fugro)
	Atchafalaya Basin	9-17*	40-70	20-90	60-80	FV	E (Fugro)
	Connect. Varved Clay	10-14*	60-80	20-70	30	FV	E (Fugro)
Tezcan, et al. (1979)	Izmir, Soft Clays	13-15	33-70	60-80	20-30	LV/UU	M (Begemann)
Marsland (1979)	London	9.25 24-29					Triaxial Plate

Table 4.3 Some Cone Factors Determined for Cohesive Soils

Table 4.3 Page 2

Reference	Region of Clay	Cone Factor N or N*	Soil Properties W_N%	W_L%	I_p%	Correlation by	Penetrometer Type
Yilmaz (1981)	Louisiana Cohesive Soils - Lake Charles	24.0*	20-40	60-70	25-45	UU	E (Fugro)
		19.0*				UC	
		17.0*				LV	
		9.0*				FV	
	- Erwinville	31.0*	40-50	70-100	30-60	UU	E (Fugro)
		10.0*				LV	
		9.3*				FV	
	- Laplace	9.3*	60-90	60-80	34-45	UU	E (Fugro)
		10.4*				UC	
		8.5*				LV	
		5.0*				FV	
Tavenas et al. (1981)	James Bay (Canada)	16-21			7-18		Piezocone
Lacasse & Lunne (1982)	Onsoy	12.1-17.5*			23-36	FV (cor)	Piezocone
		11.8-18.8*			10-28	FV (cor)	
Jamilkowski et al. (1982)	Porto Tello	12 ± 4*				FV	E (Fugro)
		11 ± 3*				FV (cor)	
	Montalto di Castro	9 ± 1*				$\overline{CK_oUC}$	E (Fugro)
	Taranto	16 ± 2*				$\overline{CK_oUC}$	E (Fugro)
Cancelli et al. (1982)	Modena	25.2*				UU &	M(Goudsche)
		28.5				UUC	E(Goudsche)
Roy et al.(1982)	St. Lawrence Lowlands	14.7*			10-30	FV	E (Fugro)
Tumay et al.(1982)	Louisiana	5.9*				$\overline{CIU}$	Piezocone
		6.7*				FV	
		11.2*				LV	
		12.8*				UC	
Azzouz et al. (1982)	Venezuela (Orinoco)	11-19	50-70	65-100	35-65	$\overline{CK_oUDSS}$	Piezocone
Gadinsky (1983)	BBC (MIT)	13-22*				FV (cor)	Piezocone
		18-32*				$\overline{CK_oUDSS}$	
	BBC (Saugus)	10-20*				$\overline{CK_oUDSS}$	
		10-19*				FV (cor)	

LEGEND

Soil Properties
- w_N - Natural Water Content
- W_L - Liquid Limit
- I_p - Plasticity Index
- S_u - Undrained Shear Strength
- S_t - Sensitivity

Cone Factor
- $N = q_c/S_u$
- $N^* = (q_c - \sigma_v)/S_u$
- q_c = Tip Resistance
- σ_v = Overburden Stress

Tests
- UC - Unconfined Compression
- UU - Undrained Unconsolidated
- LV - Lab Vane
- FV - Field Vane
- $\overline{CK_oUC}$ - K_o consolidated undrained compression
- $\overline{CK_oUDSS}$ - K_o consolidated undrained

Penetration
- E - Electrical
- M - Mechanical
- H - Mechanical (Hydraulic)

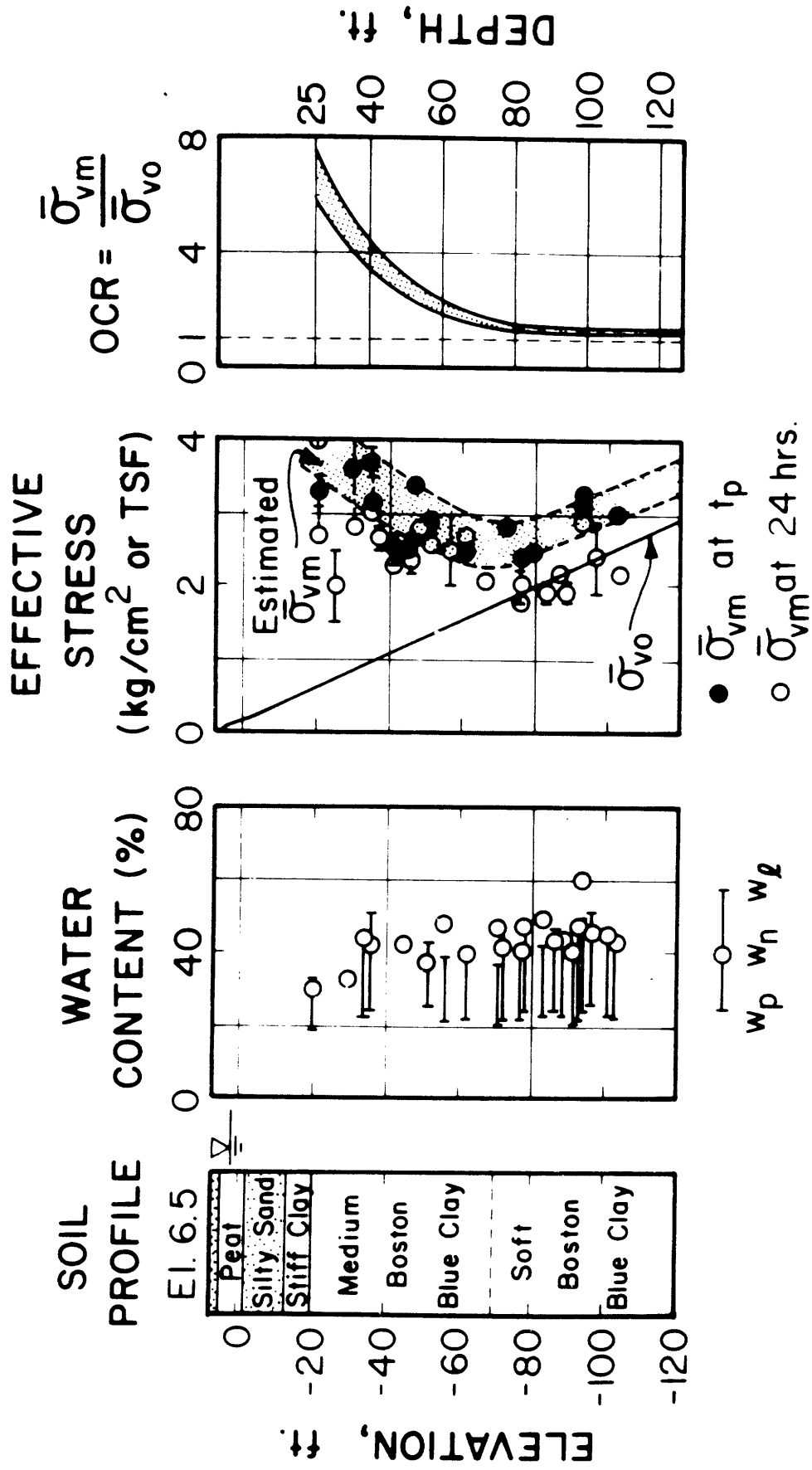

Figure 4.1 Soil Profile in Boston Blue Clay at Station 246 (from Baligh et al., 1981)

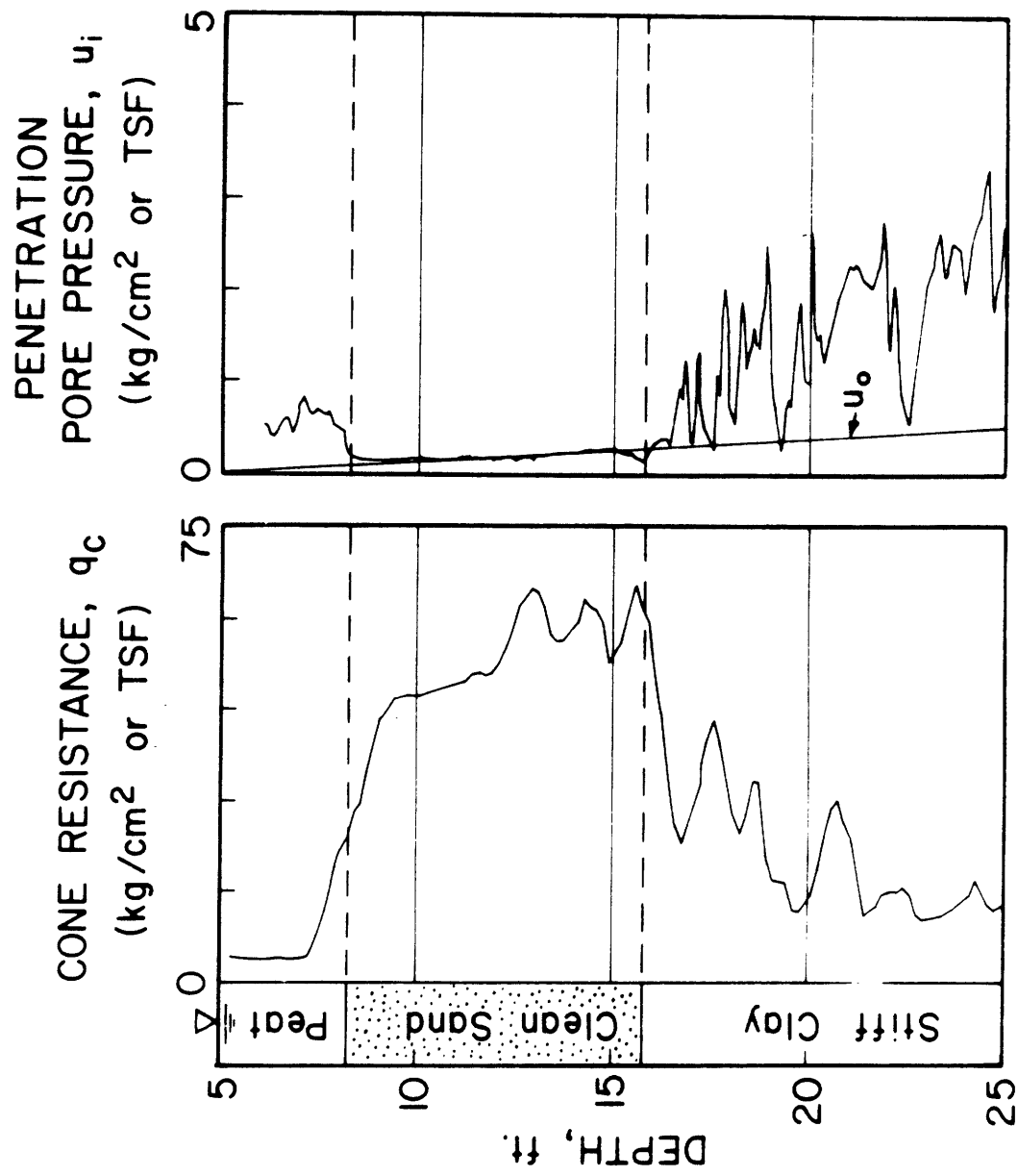

Figure 4.2 Cone Penetration in Soil Stratification and Identification (from Baligh and Levadoux, 1980)

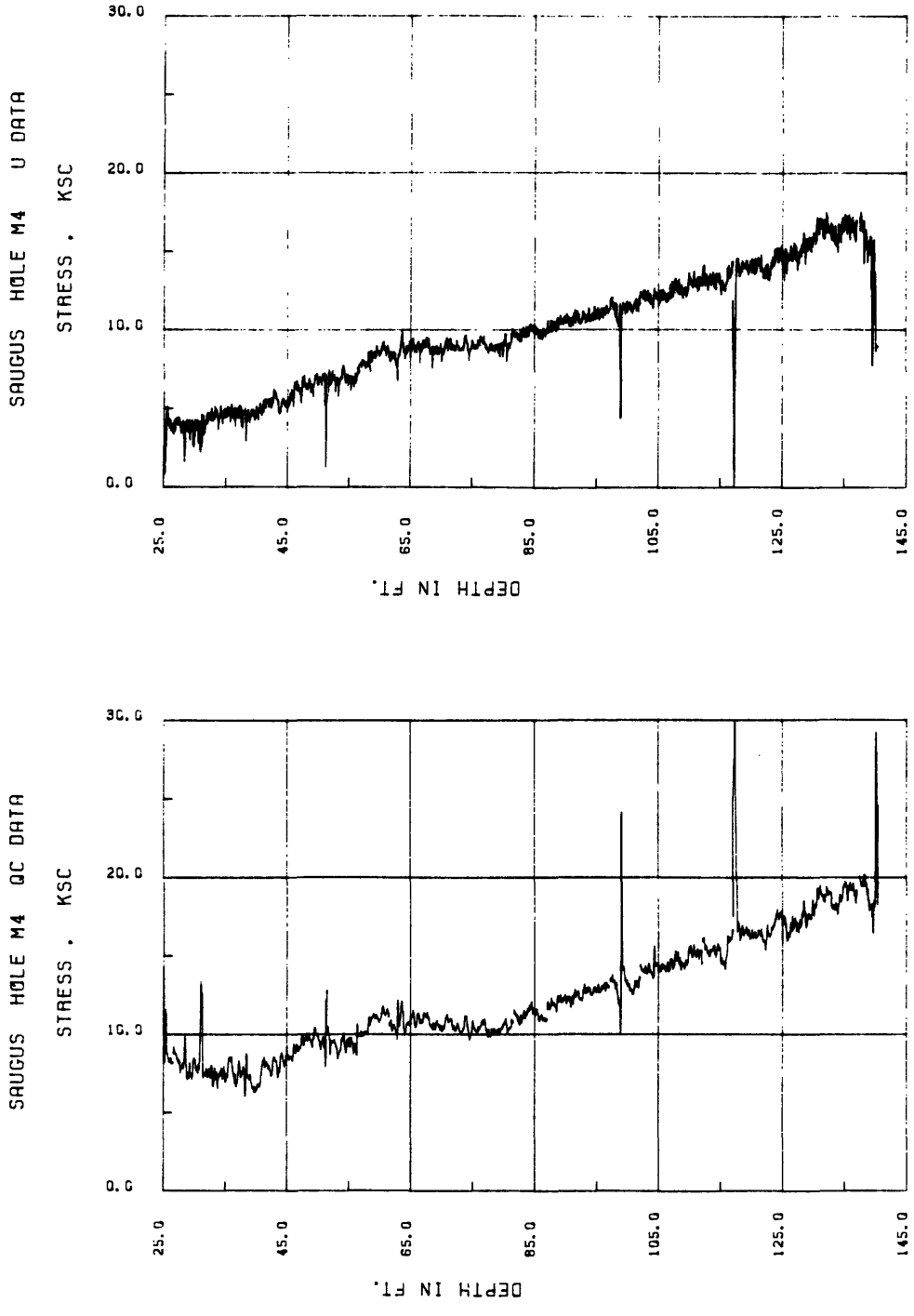

Figure 4.3 Cone Resistance and Pore Pressure Measurements Obtained with the Piezocone: Saugus Site

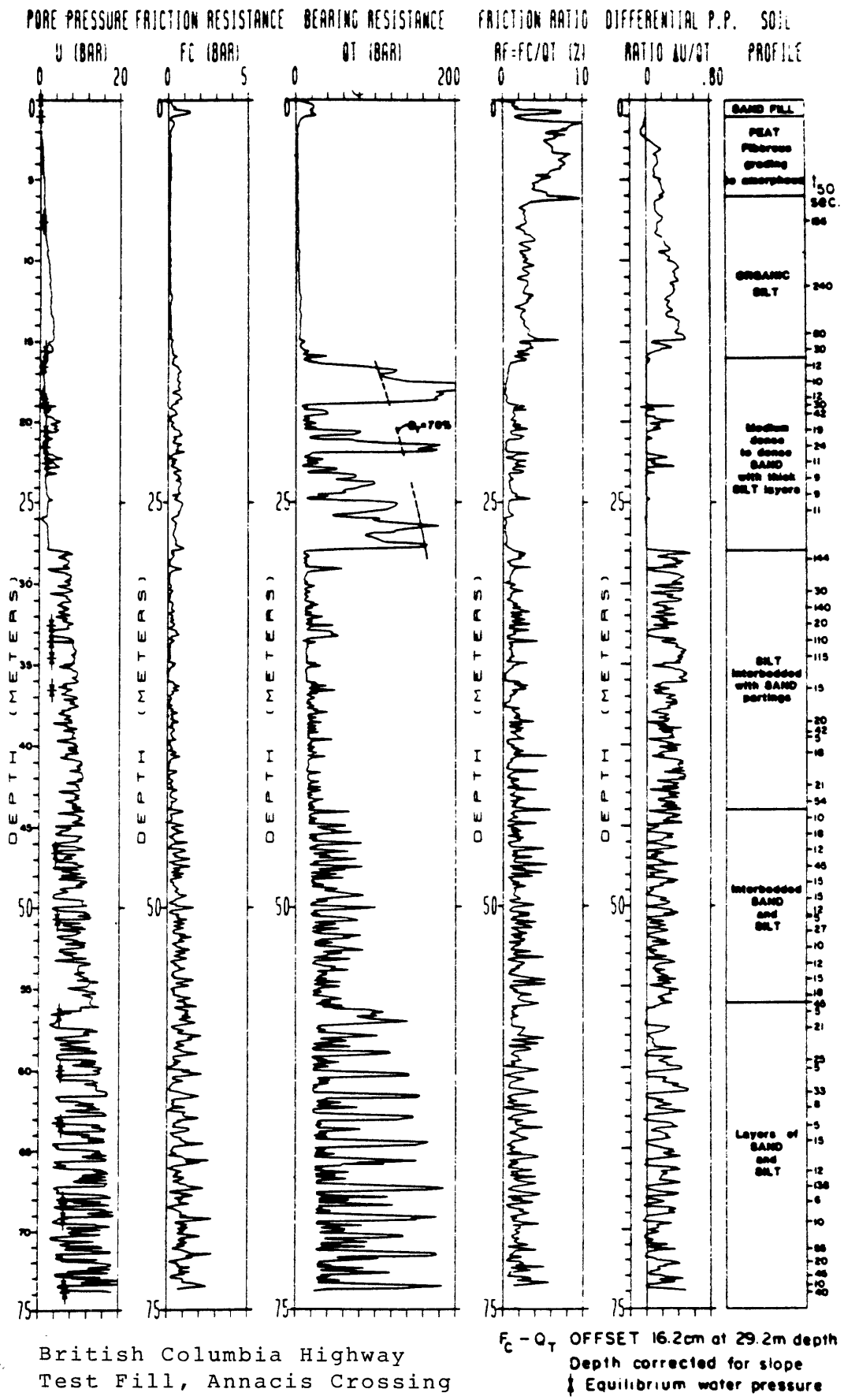

Figure 4.4 Example of Piezocone Logging in Stratified Soils (from Campanella et al., 1982)

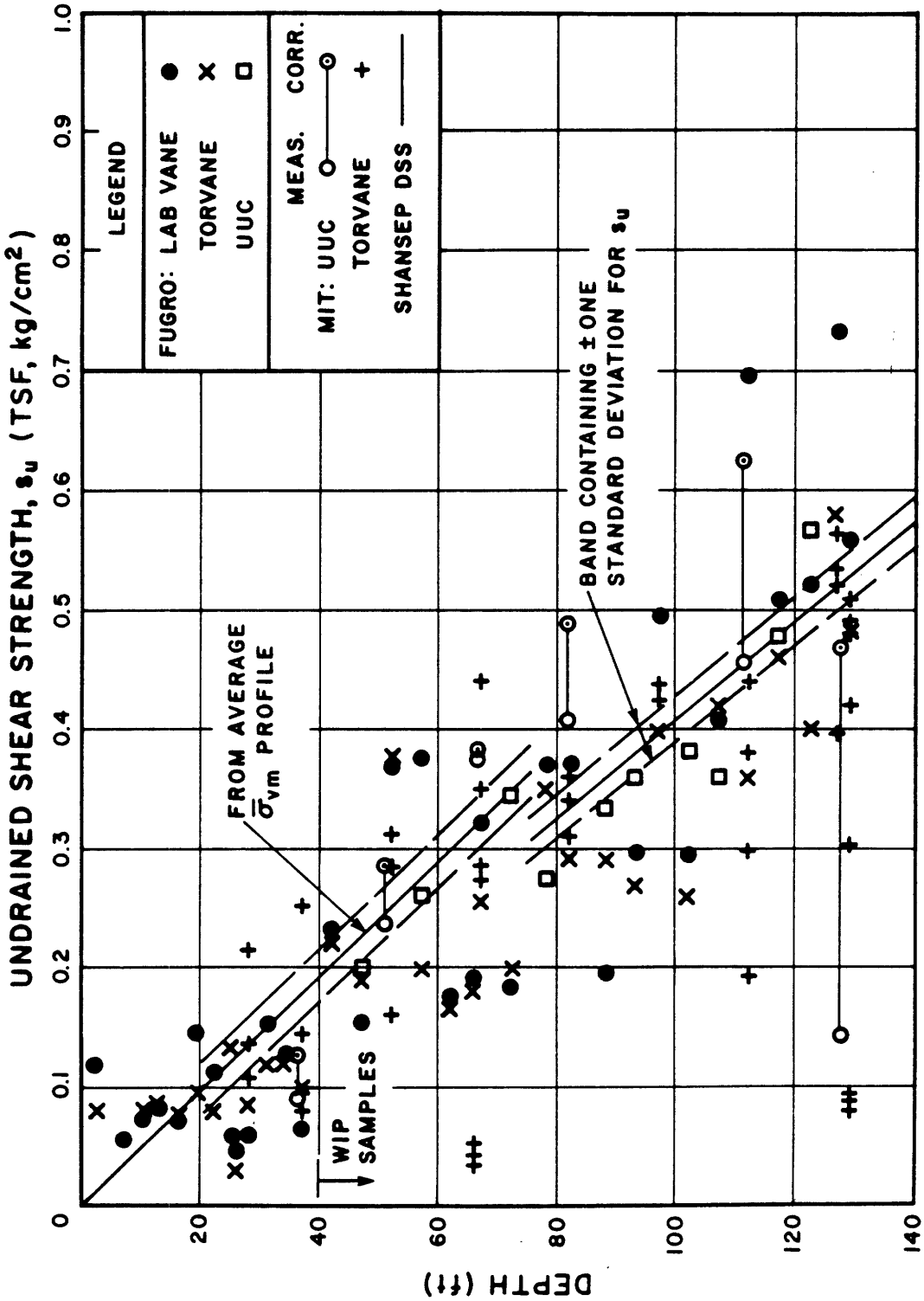

Figure 4.5 Comparison of Undrained Strength Data: Orinoco Clay, Boring F1 (from Azzouz et al., 1982)

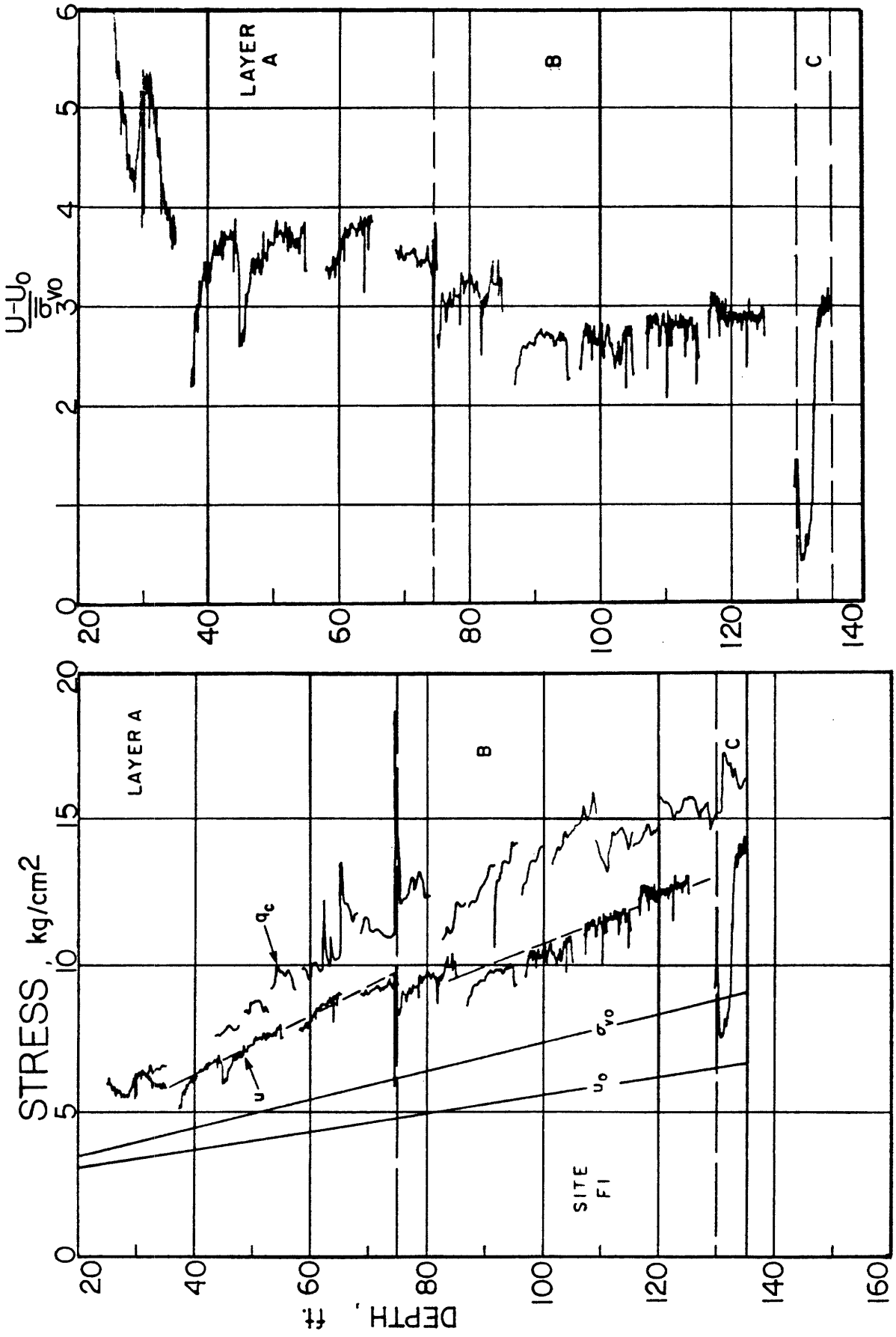

Figure 4.6 Determination of Stratigraphy Using Piezocone Logs: Orinoco Clay, Boring F1 (from Azzouz et al., 1982)

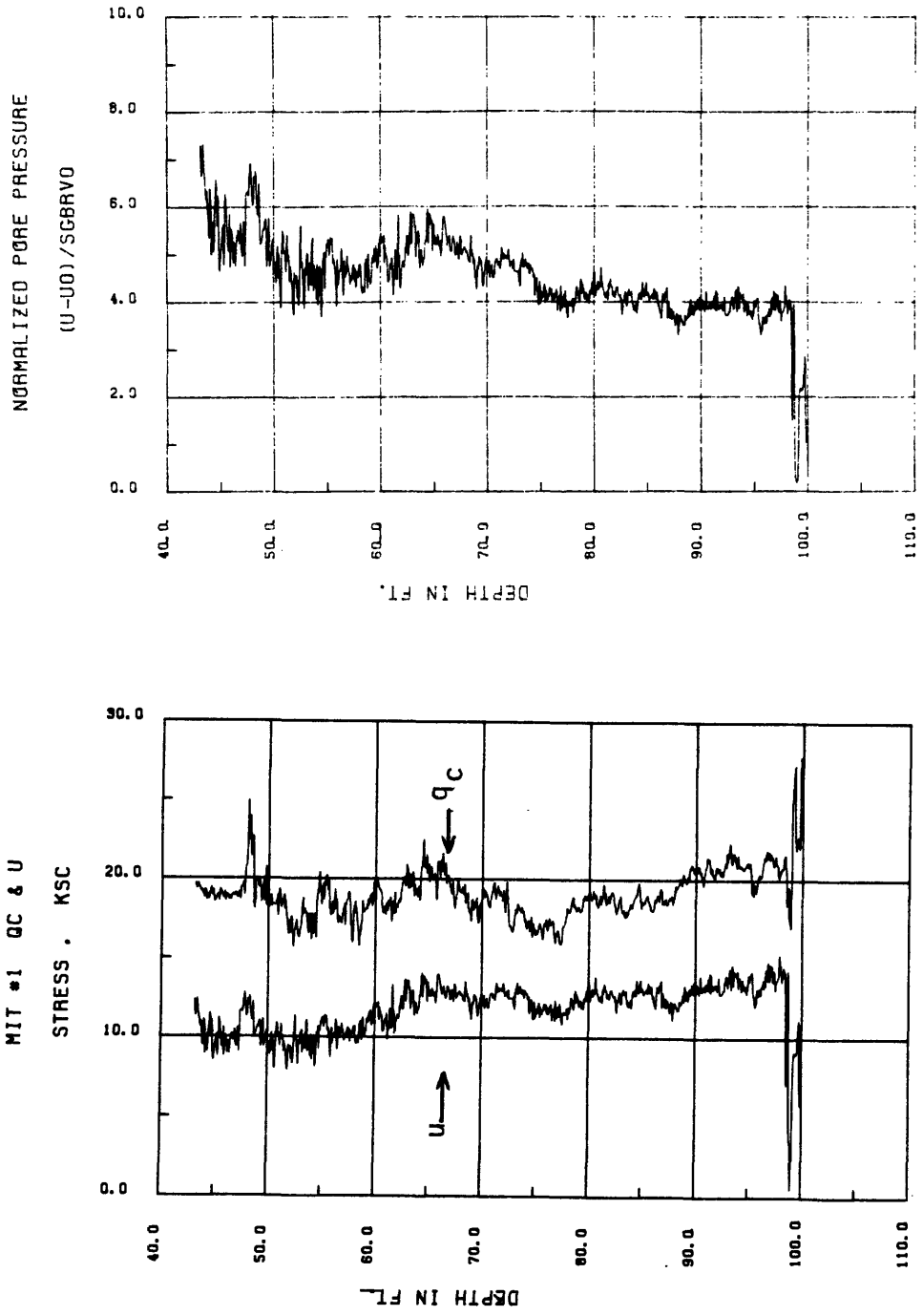

Figure 4.7 Cone Penetration, Pore Pressure, and Normalized Pore Pressure Data: Solar House, Hole MP1

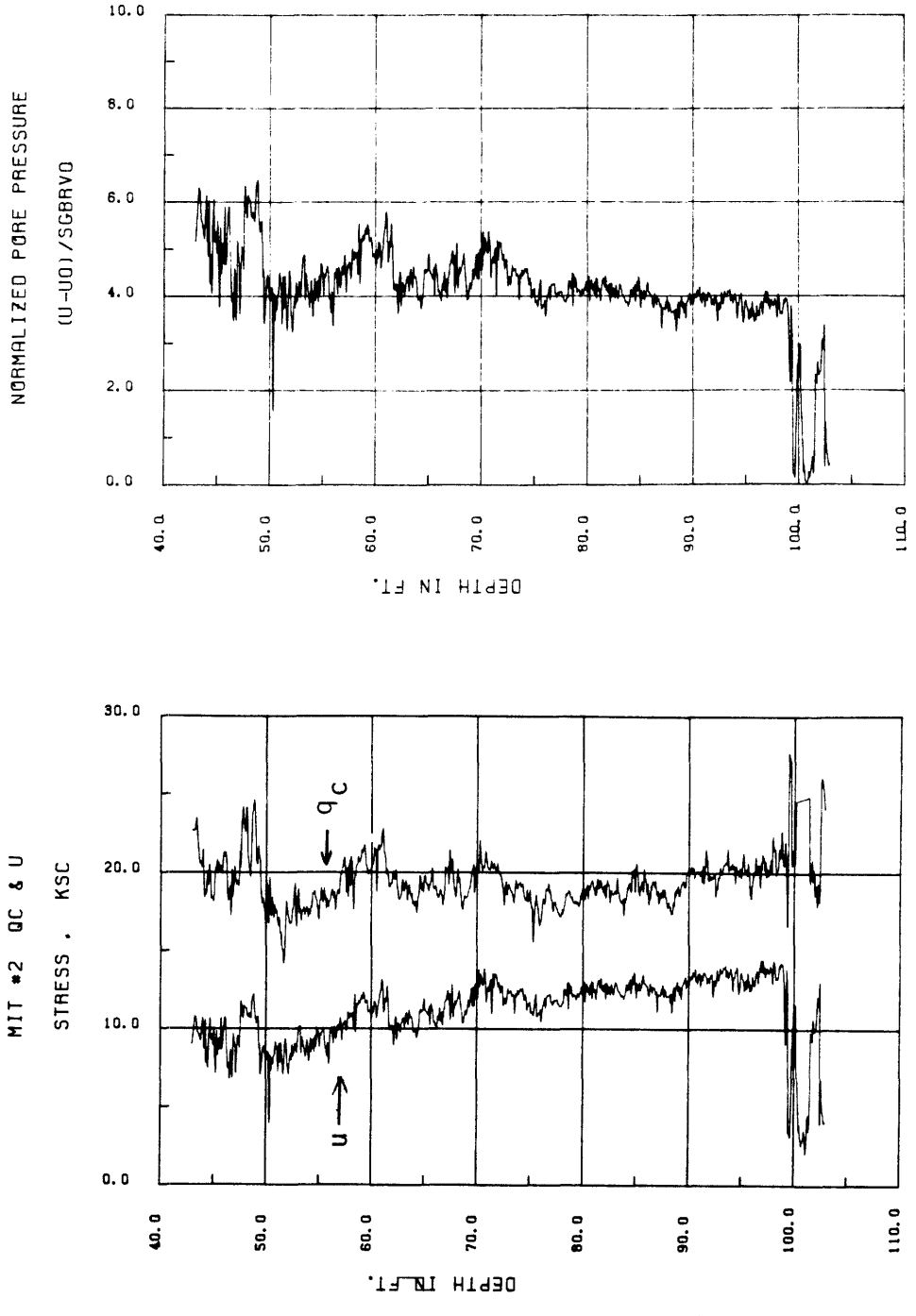

Figure 4.8 Cone Penetration, Pore Pressure, and Normalized Pore Pressure Data: Solar House, Hole MP2

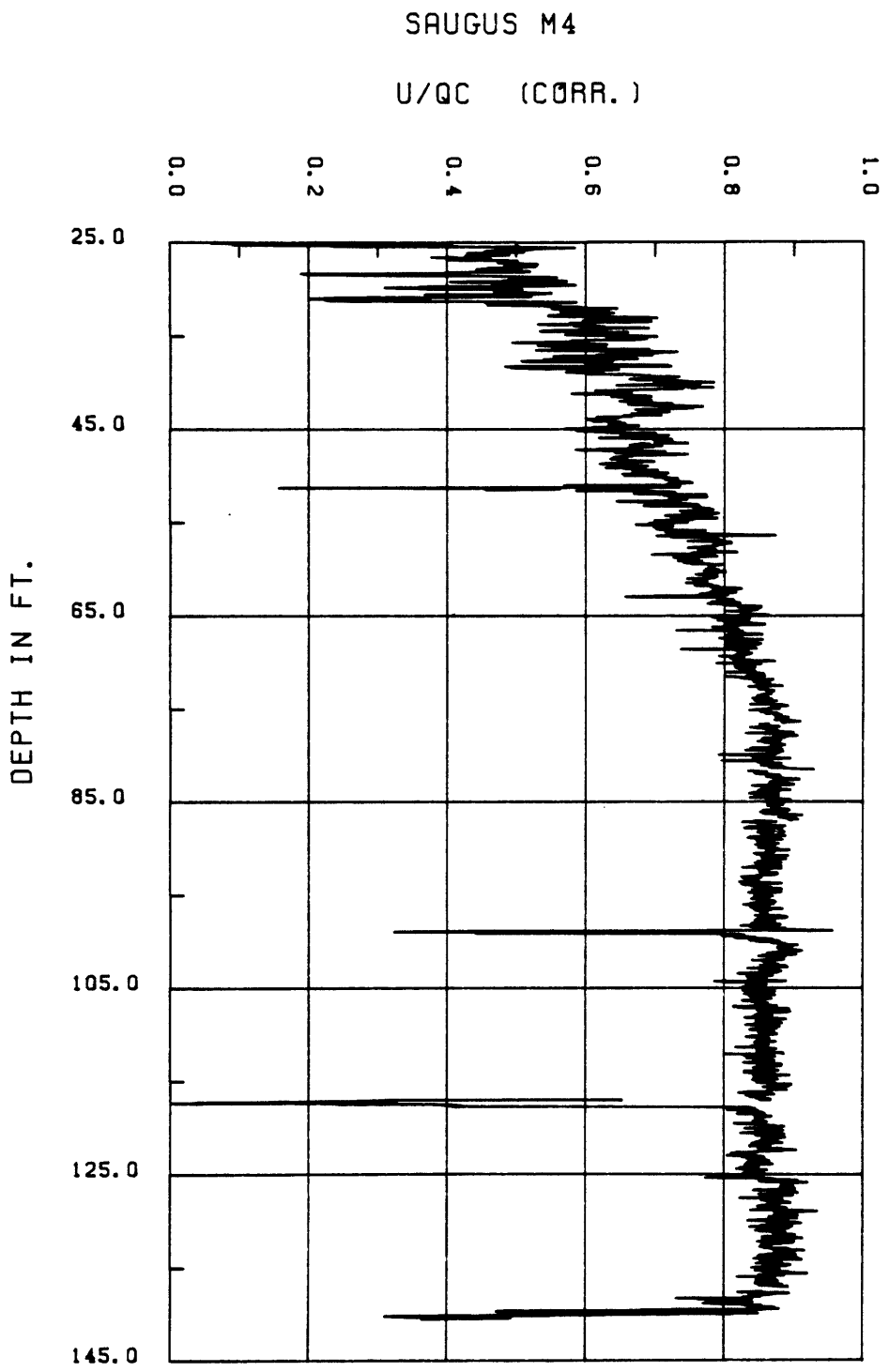

Figure 4.9 Pore Pressure to Cone Resistance Ratio: Saugus Site

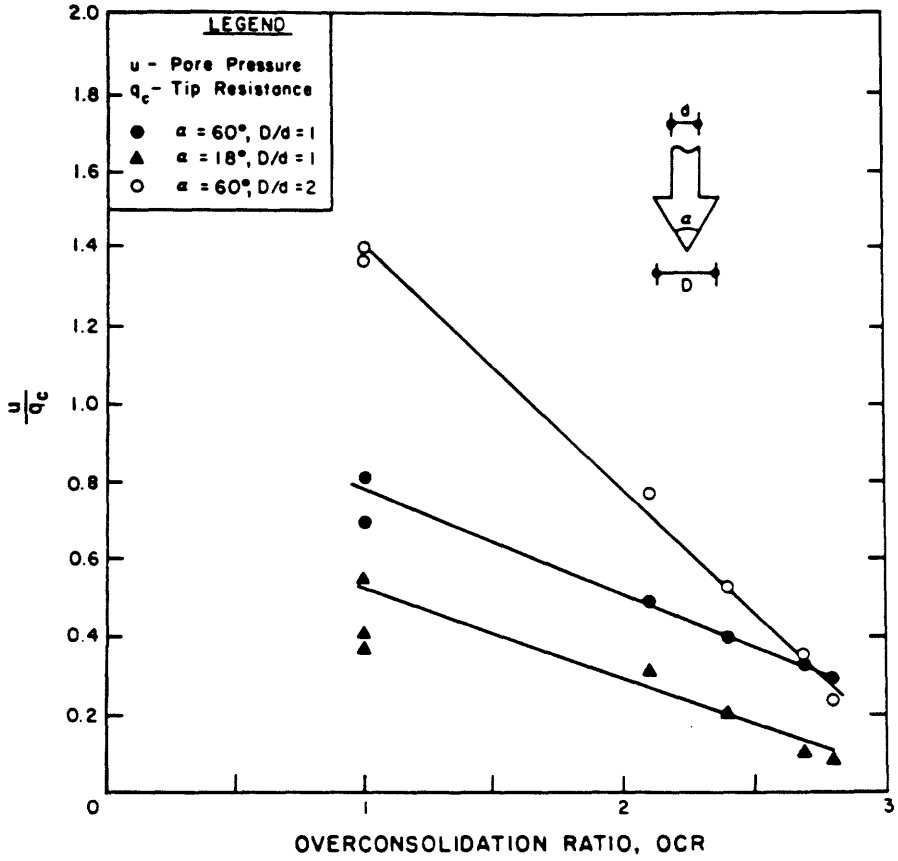

a) Field Penetration Tests in Louisiana Cohesive Soils (from Tumay et al., 1981)

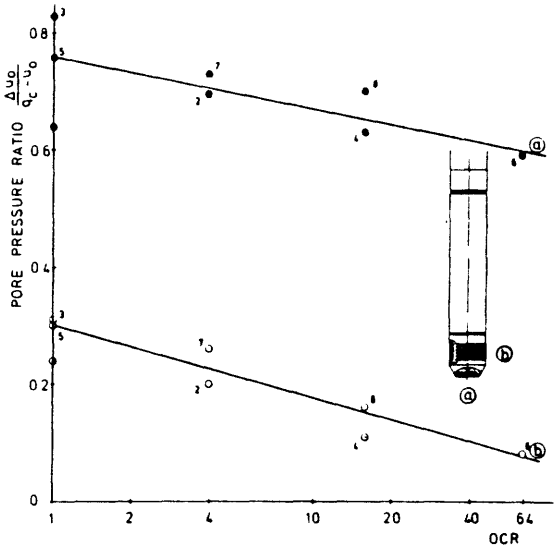

b) Laboratory Penetration Tests (from Smits, 1982)

Figure 4.10 Variation of Pore Pressure to Cone Resistance Ratio with Overconsolidation

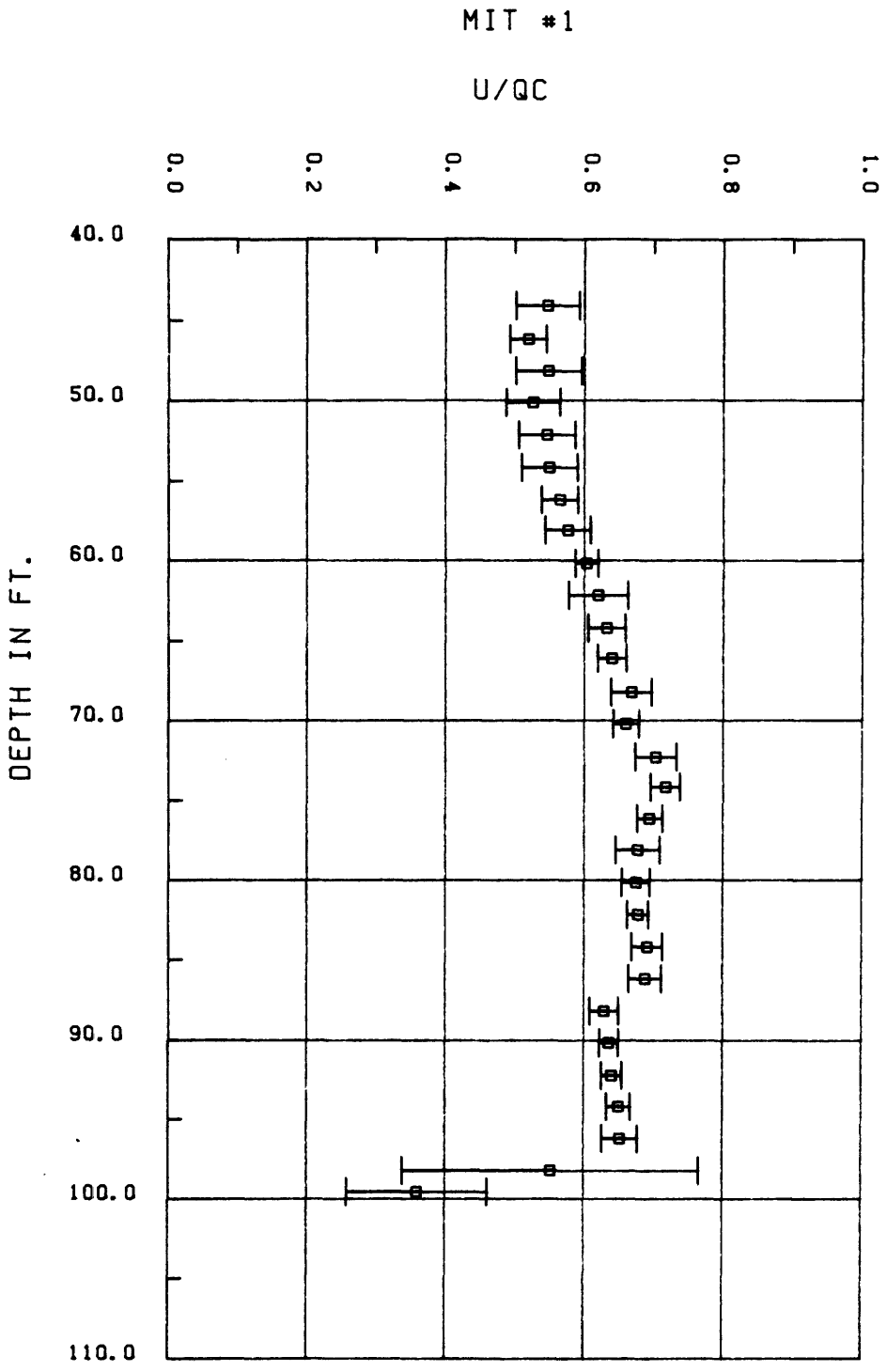

Figure 4.11 Pore Pressure to Cone Resistance Ratio: Solar House, Hole MP1

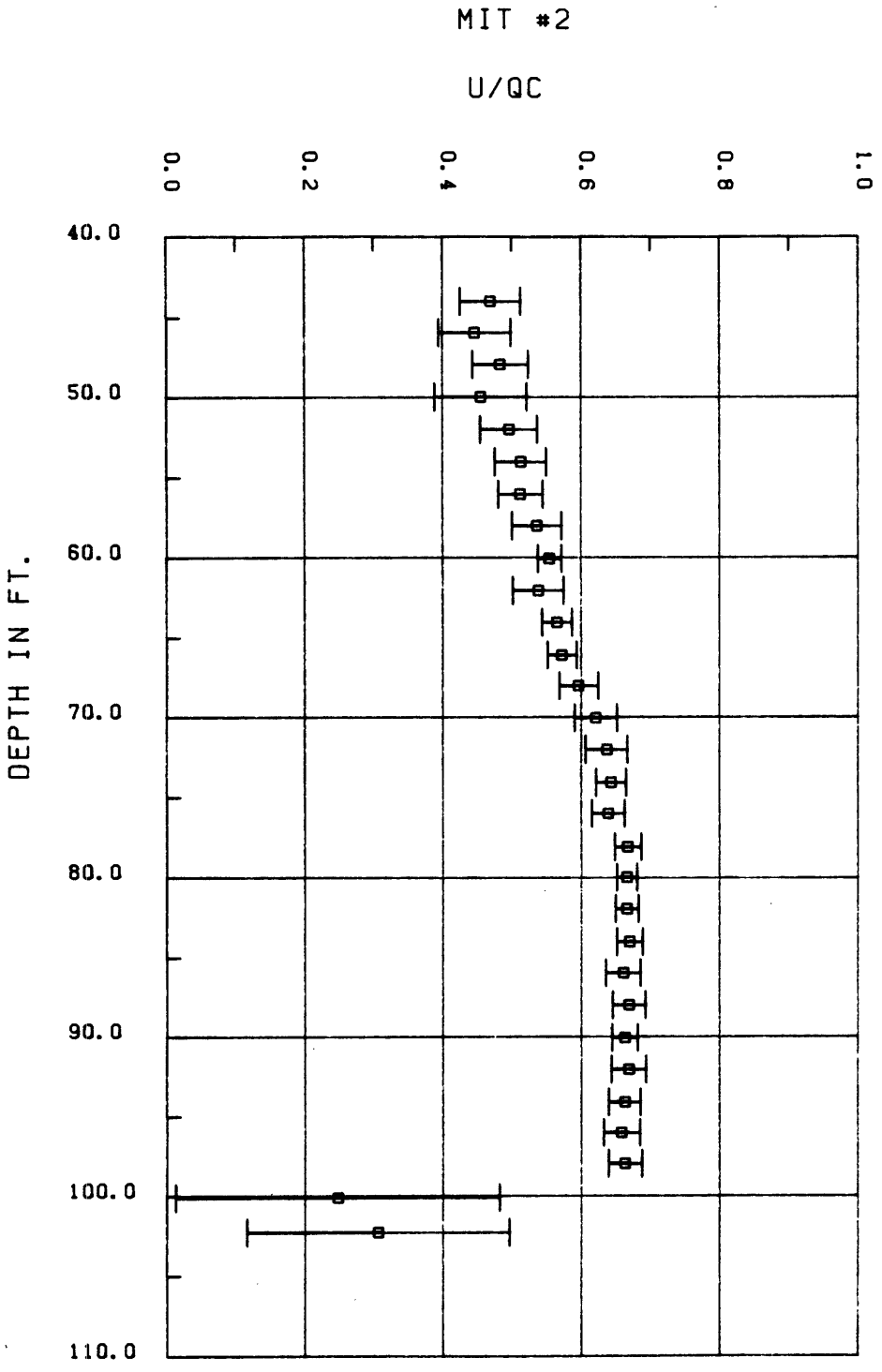

Figure 4.12 Pore Pressure to Cone Resistance Ratio: Solar House, Hole MP2

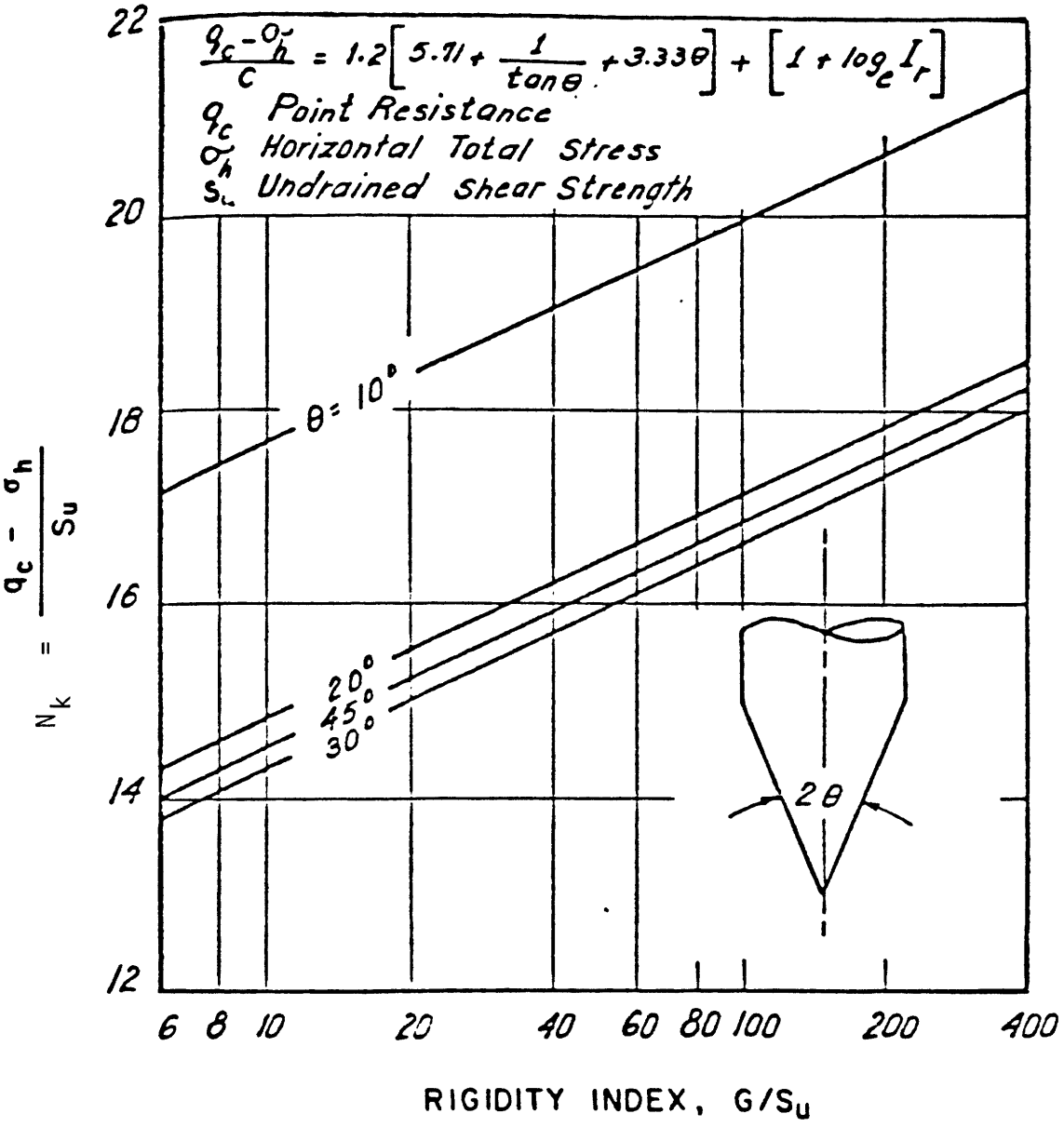

Figure 4.13 Effect of Rigidity Index and Cone Angle on the Penetration Resistance of Clay (from Baligh, 1975)

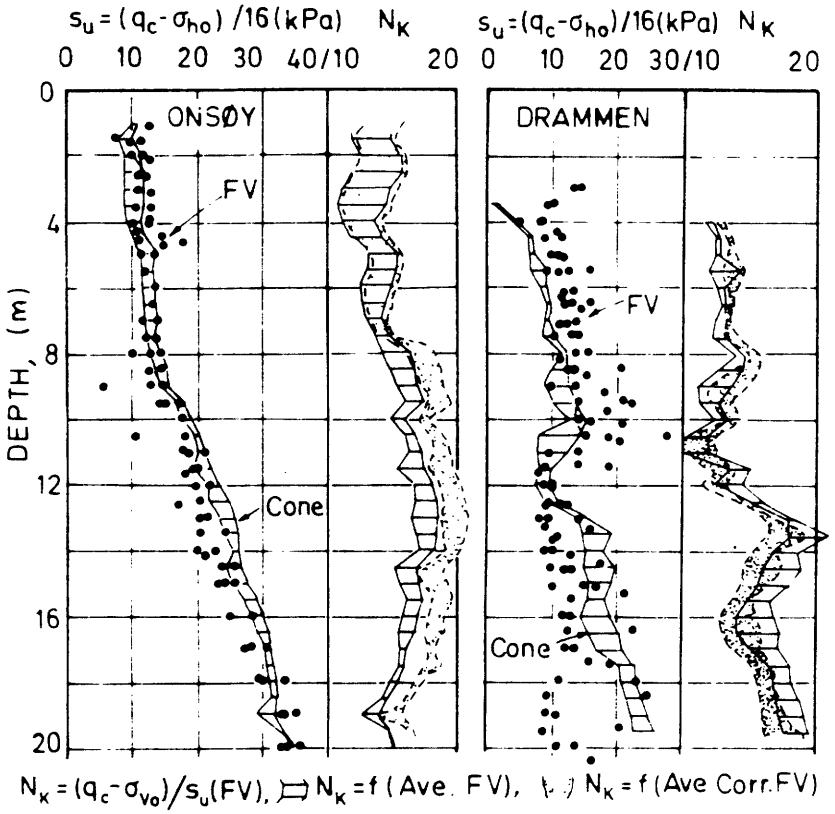

Figure 4.14 Undrained Shear Strength from Cone Resistance (from LaCasse and Lunne, 1982)

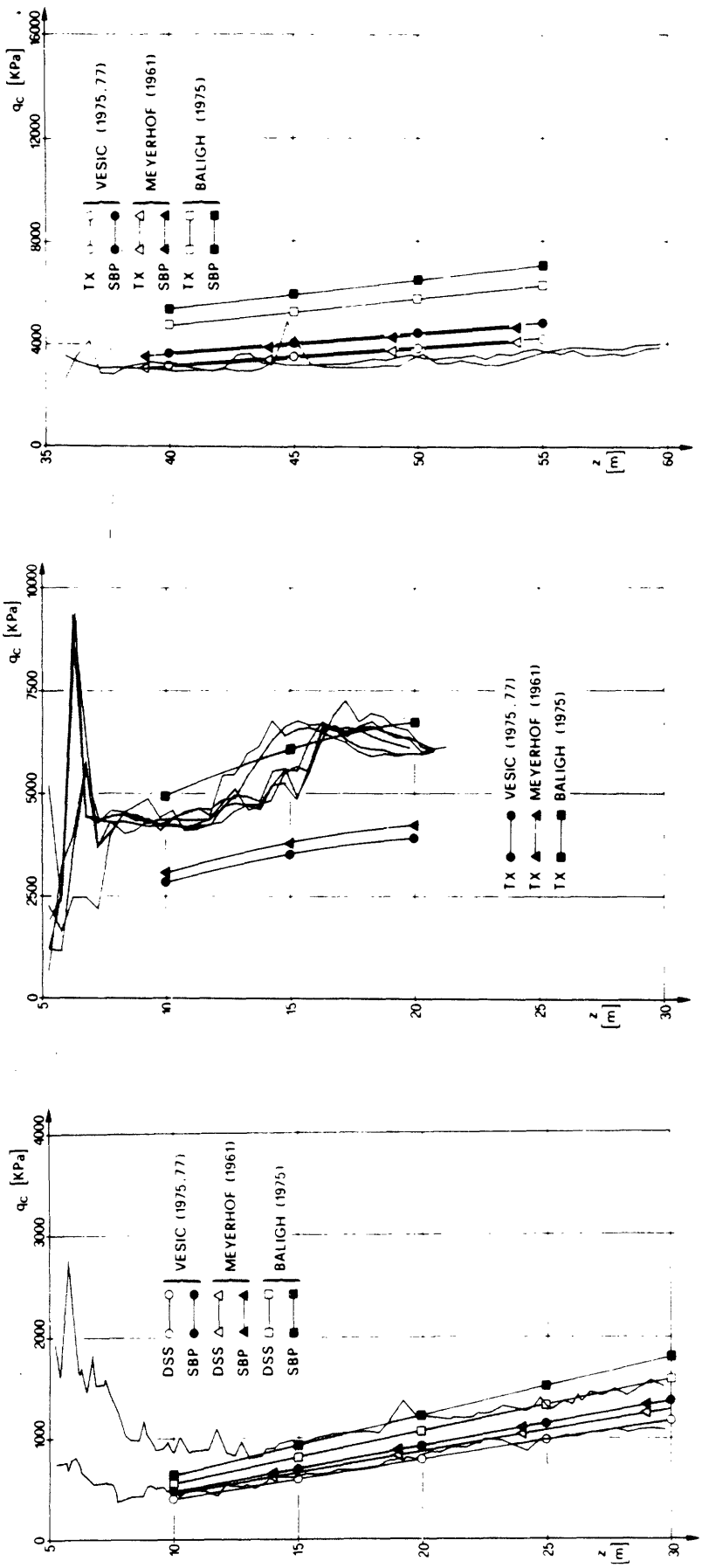

Figure 4.15 Comparison Between Measured and Predicted q_c Values at Three Italian Sites (from Jamiolkowski et al., 1982)

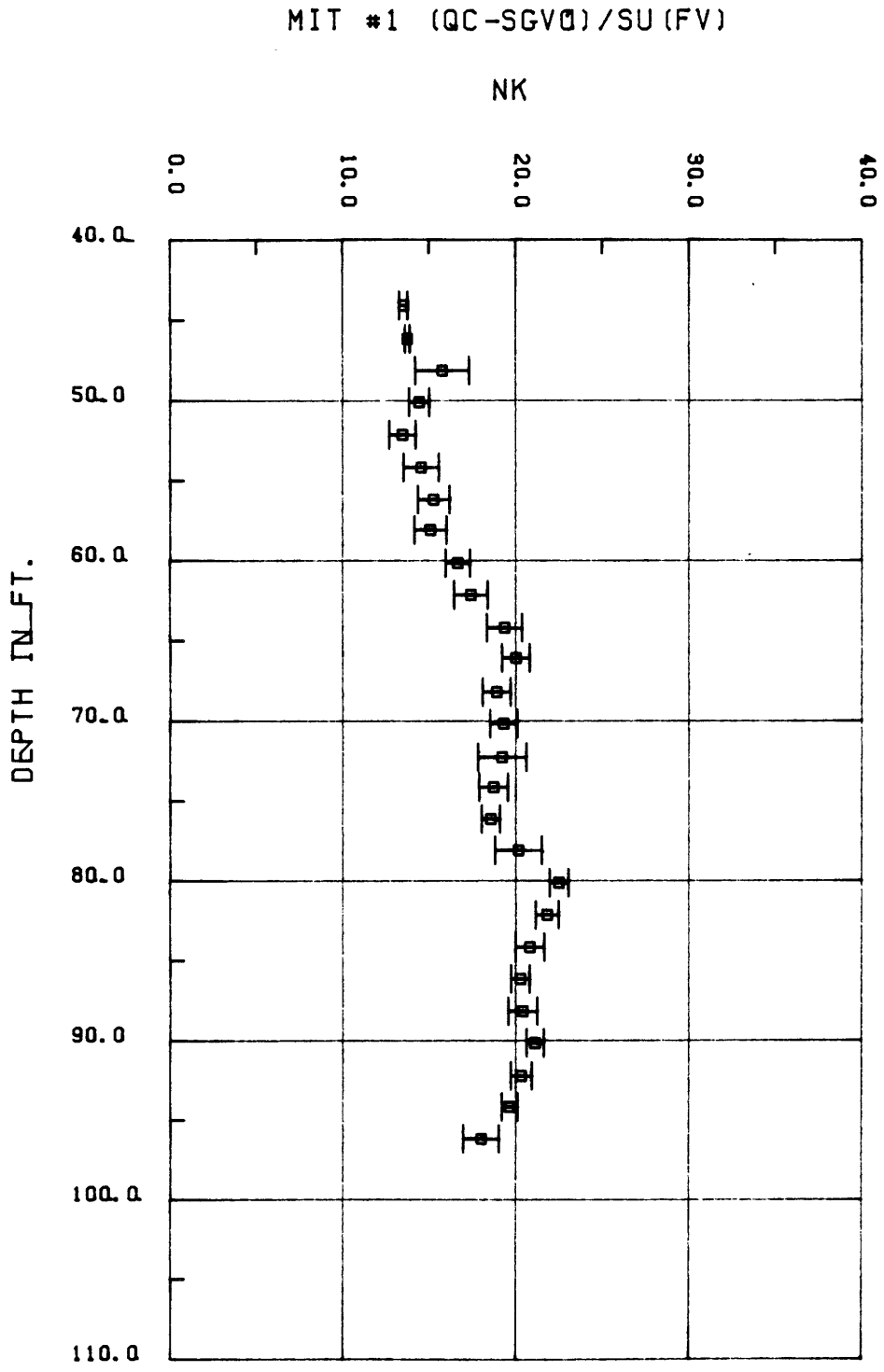

Figure 4.16 Empirical Cone Factor, N_k(FV), versus Depth: Solar House, Hole MP1

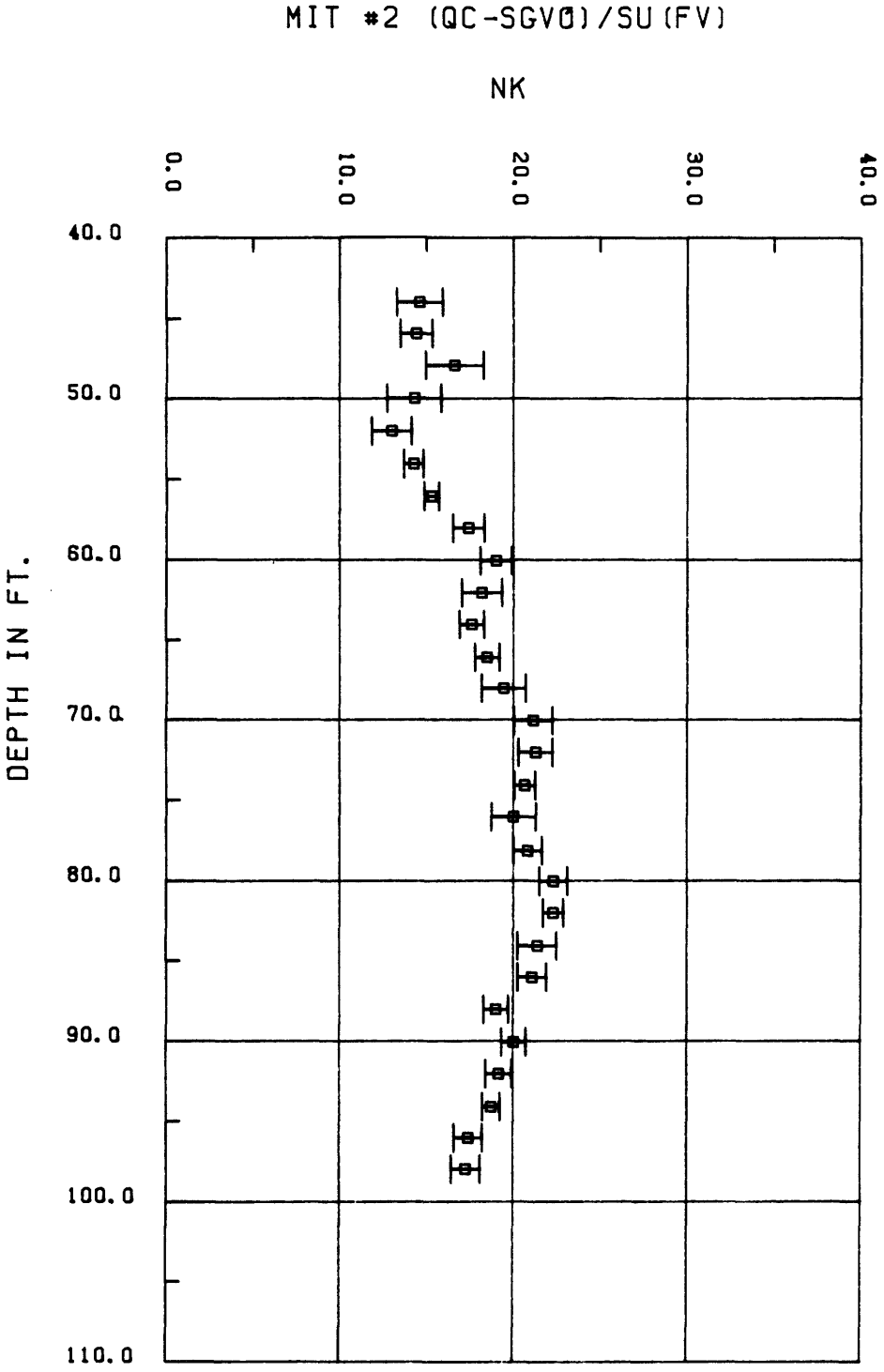

Figure 4.17 Empirical Cone Factor, N_k(FV), versus Depth: Solar House, Hole MP2

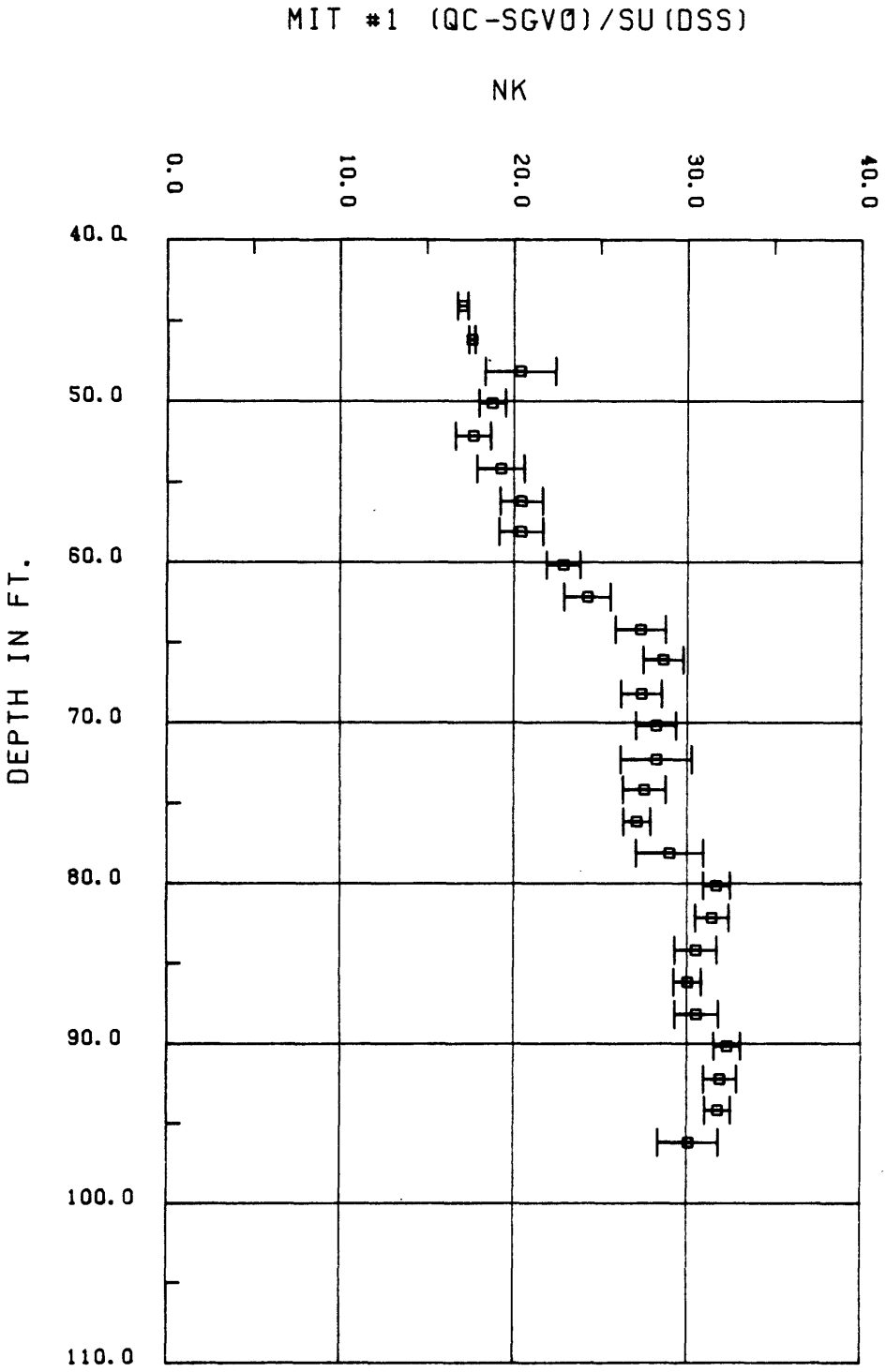

Figure 4.18 Empirical Cone Factor, N_k(DSS), versus Depth: Solar House, Hole MP1

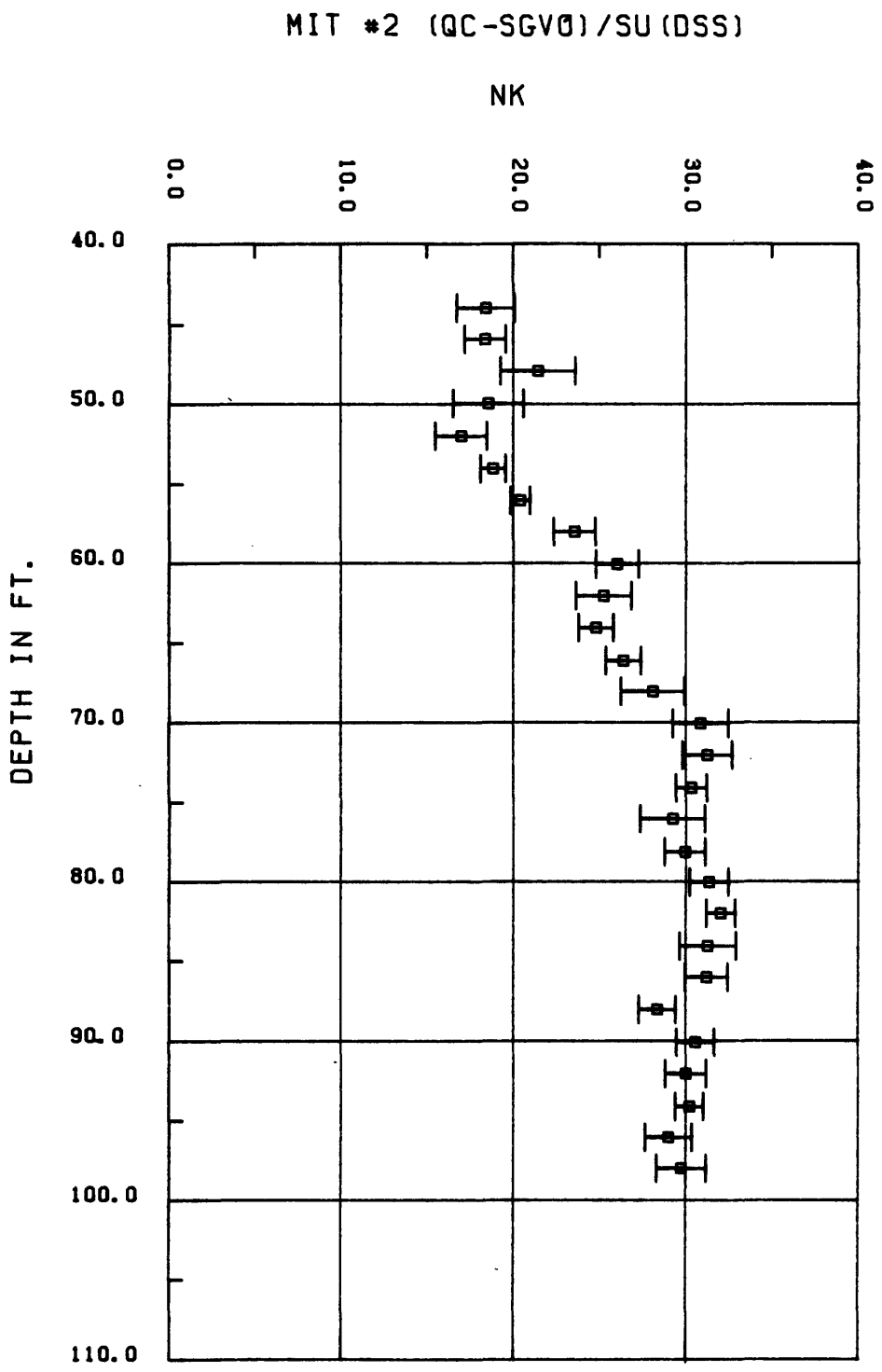

Figure 4.19 Empirical Cone Factor, N_k(DSS), versus Depth: Solar House, Hole MP2

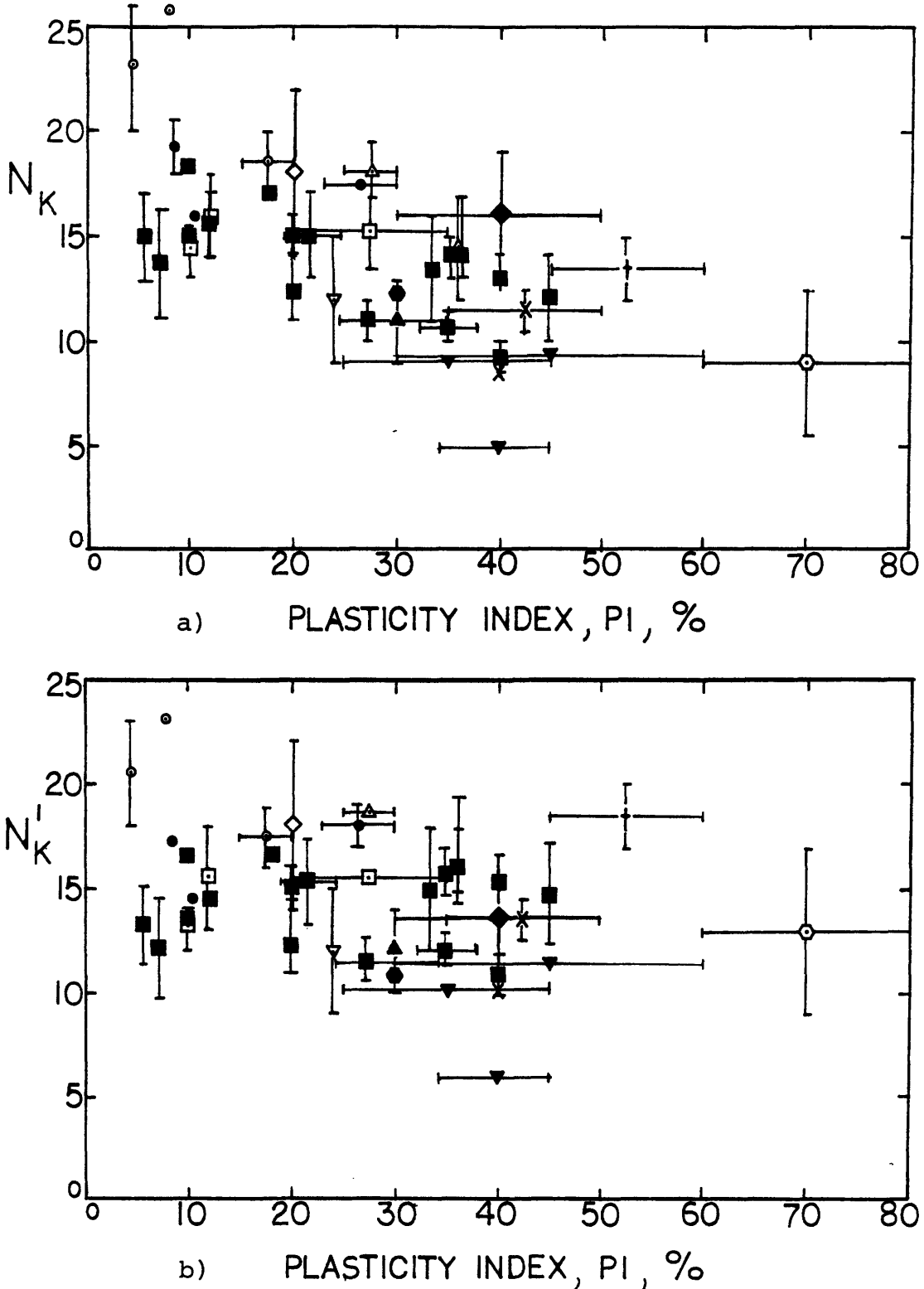

Figure 4.20 Empirical Cone Factor, N_k(FV) and N'_k(FV), for Very Soft to Medium Clays

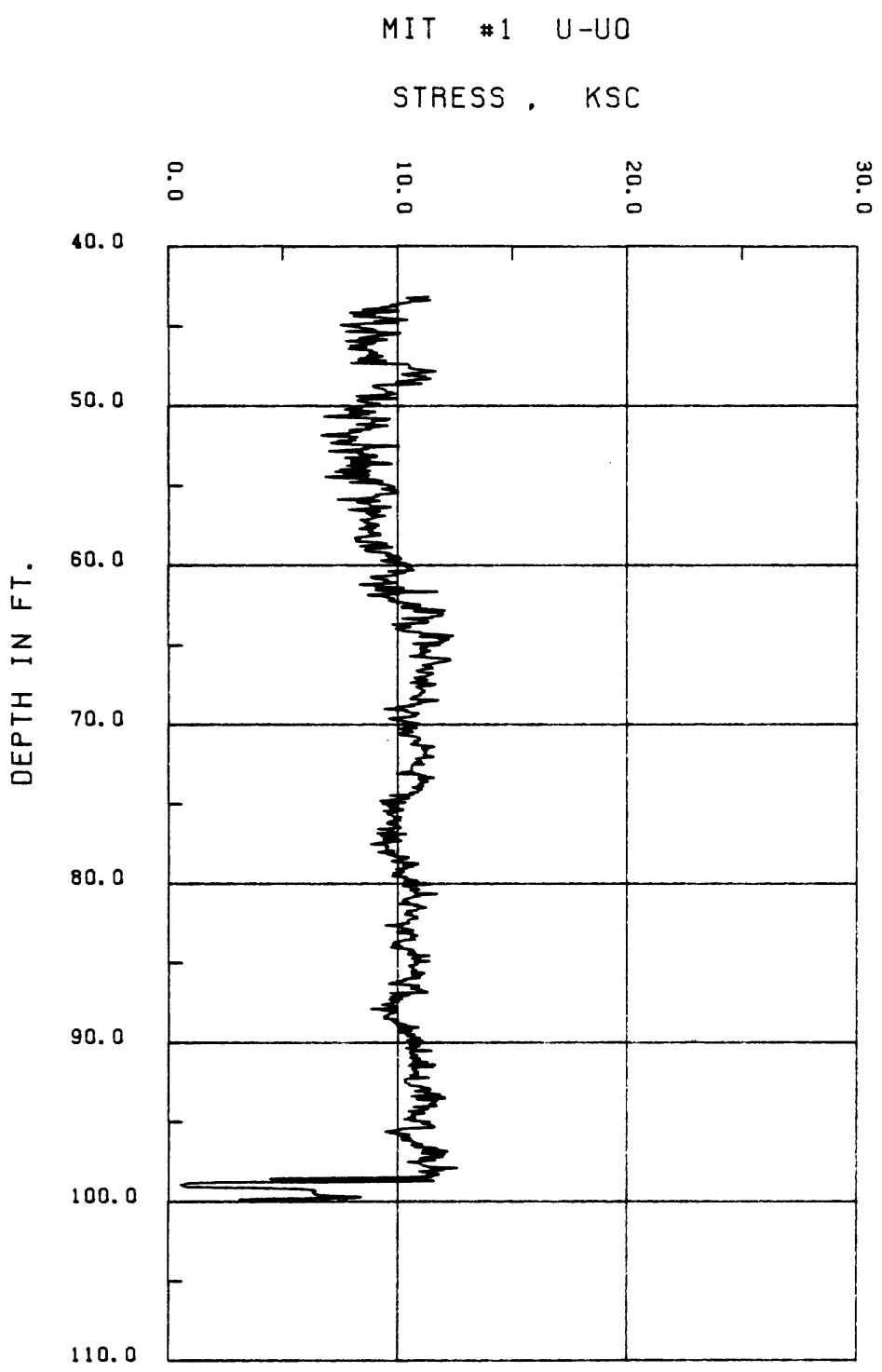

Figure 4.21 Excess Pore Pressure Measurement Versus Depth: Solar House, Hole MP1

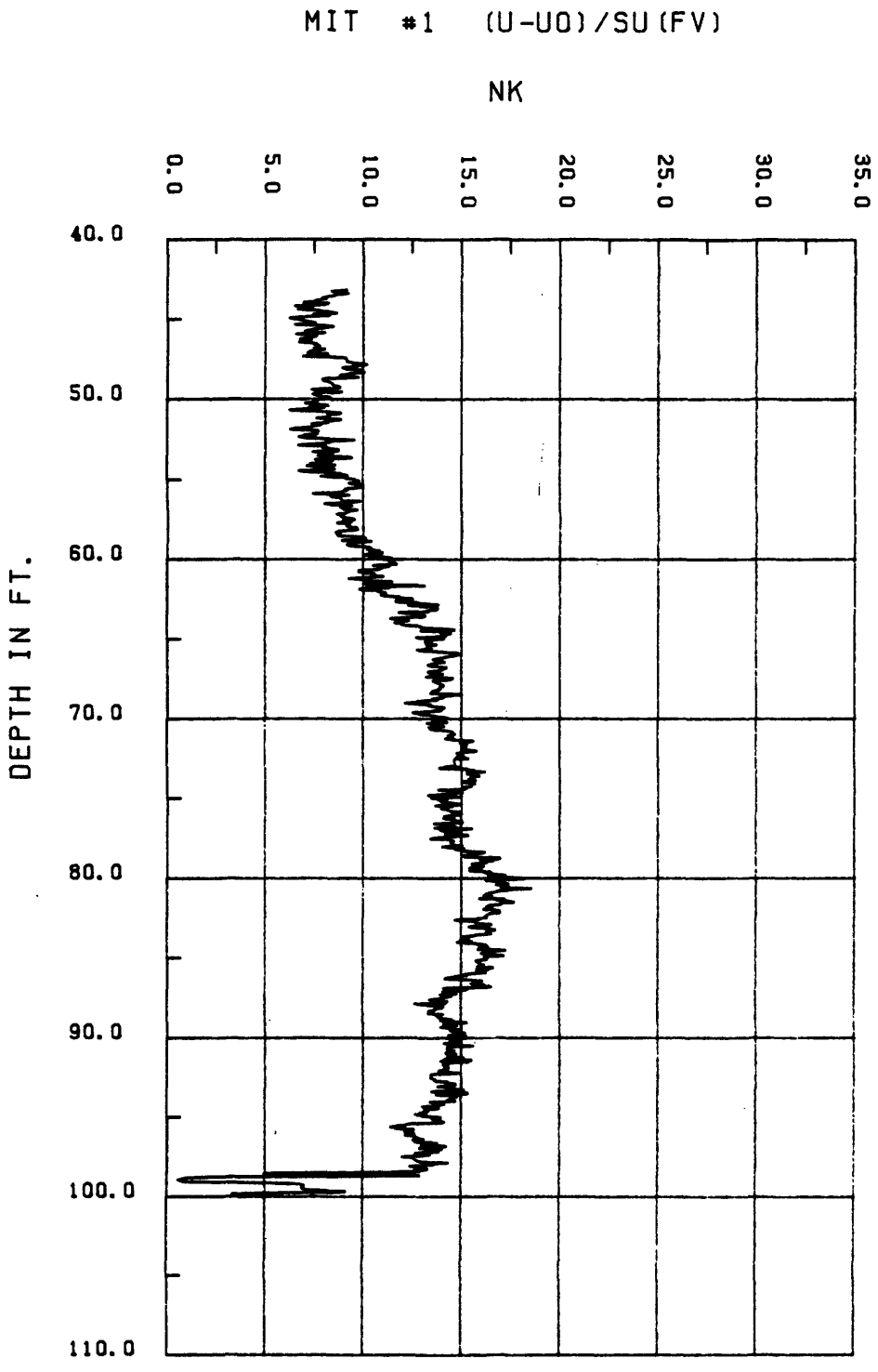

Figure 4.22 Empirical Cone Factor, $N_{\Delta u}(FV)$, versus Depth: Solar House, Hole MP1

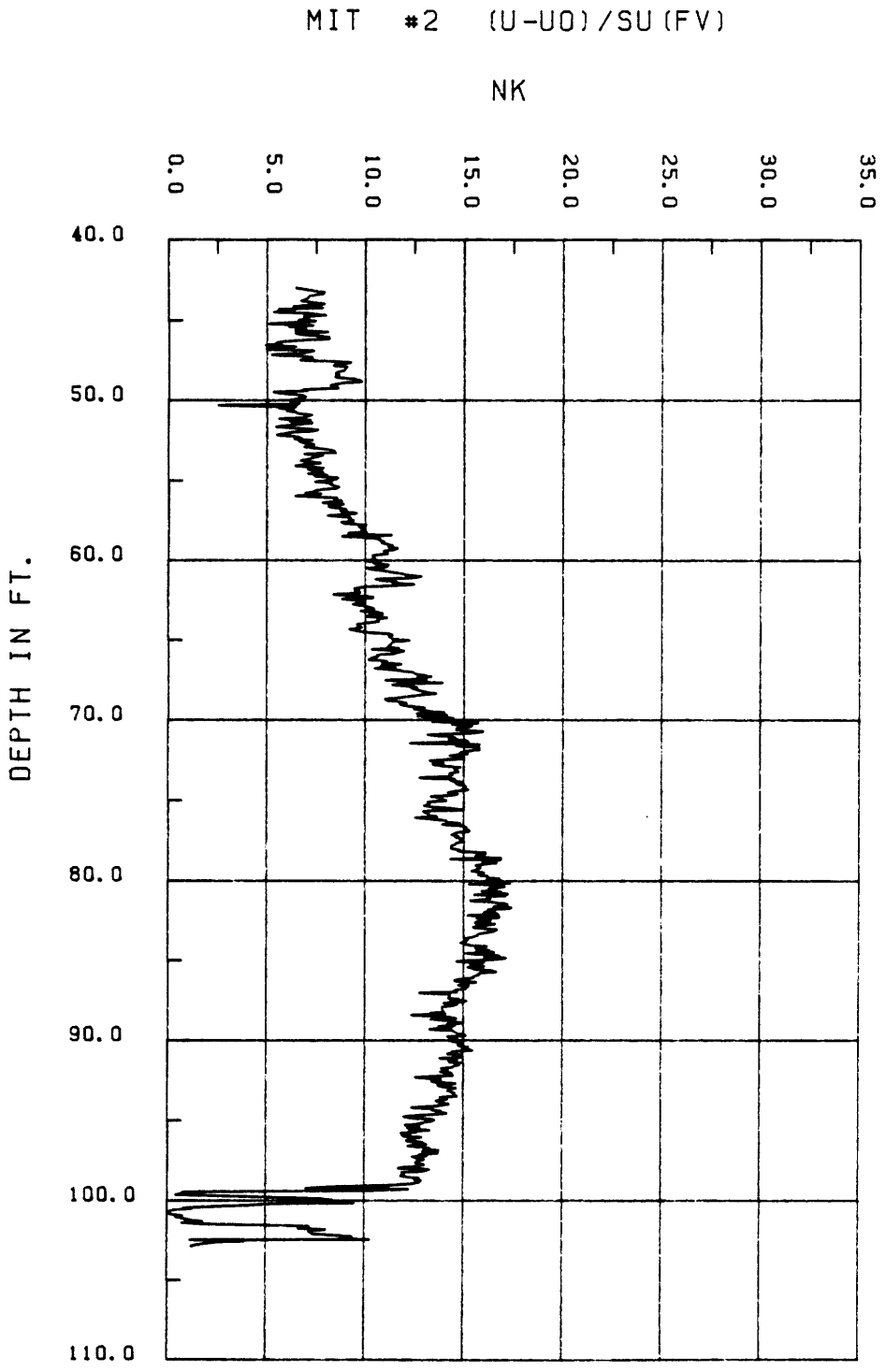

Figure 4.23 Empirical Cone Factor, $N_{\Delta u}(FV)$, versus Depth: Solar House, Hole MP2

CHAPTER 5

PORE PRESSURE DISSIPATION AFTER CONE PENETRATION

5.1 Introduction

Steady cone penetration in saturated clays causes undrained shearing and develops excess pore pressures in the soil. Once penetration is interrupted, these pore pressures will dissipate and eventually reach the equilibrium value u_o (typical dissipation curves were presented in Fig. 3.20). Many authors (Soderberg, 1962; Torstensson, 1977; Randolph and Wroth, 1979; Baligh and Levadoux, 1980; Battaglio et al., 1981; and Tumay et al., 1982) have developed solutions to predict the consolidation and flow characteristics of cohesive deposits from the pore pressure dissipation data. This chapter will discuss the consolidation process around probes, the existing dissipation solutions, the shortcomings of their interpretation, as well as compare their results to laboratory consolidation coefficients. Finally, a study of some case histories and a discussion of the applicability of the theoretical solutions in these cases will be presented.

5.2 Available Theoretical Pore Pressure Dissipation Solutions

Deep steady cone penetration causes very large shearing strains in the soil, especially in the immediate vicinity of the tip. In normally consolidated to slightly overconsolidated clay, these strains produce a failure zone

extending to a radial distance equal to 6.5 times the shaft radius (Levadoux and Baligh, 1980).

When shearing strains are applied to a normally consolidated clay, positive shear-induced pore pressures, Δu_s, develop resulting in a negative mean effective stress change, $\Delta\bar{\sigma}_{oct}$ (= - Δu_s). With regards to clay consolidation, the reduction in mean effective stress at a constant void ratio due to undrained shearing can be viewed as an artificial overconsolidation of the clay. Therefore, pore pressure dissipation during early stages of consolidation around cones takes place in a recompression mode (as opposed to virgin compression) for both normally consolidated and slightly overconsolidated clays with OCR$\leq$4 (Baligh and Levadoux, 1980; and Gillespie and Campanella, 1981). The consolidation characteristics of clays will be studied with respect to this phenomenon.

Theoretical methods for predicting the consolidation characteristics of cohesive desposits usually require the solution of two separate problems: 1) estimation of the initial pore pressure distribution within the soil mass due to cone penetration; 2) estimation of changes in soil properties and stresses during the subsequent consolidation phase. In the following presentation of the available methods for the interpretation of the pore pressure dissipation records, an emphasis will be placed on how these two problems are dealt with as well as on how each method is applied in practice.

5.2.1 Torstensson's Method (1977)

Torstensson (1977) suggests that the pore pressures in the soil caused by steady cone penetration can be estimated by one-dimensional (radial) solutions corresponding to cylindrical and spherical cavities (Soderberg, 1962; Ladanyi, 1963). During cavity expansion he assumes the soil to be isotropic, initially subjected to an isotropic state of stress, and elastic (linear prior to yielding) with a shear modulus, G, perfectly plastic (after yielding) with an undrained shear strength, s_u. Neglecting shear induced pore pressures, the cavity expansion model adopted by Torstensson predicts the following expressions for the initial pore pressure distribution, $\Delta u(r)$, and the zone over which it acts, λ:

a) For a cylindrical cavity

$$\Delta u(r) = 2s_u \cdot \ln \left(\frac{\lambda R}{r}\right) \qquad (5.1)$$

$$\lambda = (G/s_u)^{1/2}$$

b) For a spherical cavity

$$\Delta u(r) = 4s_u \cdot \ln \left(\frac{\lambda R}{r}\right) \qquad (5.2)$$

$$\lambda = (G/s_u)^{1/3}$$

Torstensson utilizes linear uncoupled one-dimensional finite difference consolidation analyses to estimate the normalized excess pore pressure dissipation curves in Fig. 5.1 ($\bar{u}$ vs. log T; $T = ct/R^2$). In order to estimate the coefficient of consolidation, c, he proposes matching of

predictions and measurements at 50% consolidation ($\bar{u} = 0.5$) and hence uses the expression:

$$c = \frac{T_{50}}{t_{50}} R^2 \qquad (5.3)$$

where T_{50} is the predicted time factor at $\bar{u} = 0.5$ (Fig. 5.1) for an appropriate value of E/s_u. E is the "equivalent" of Young's modulus of the clay. For undrained shearing $E = 3G \cdot t_{50}$ is the measured time to achieve 50% consolidation, and R is an "equivalent" radius that simulates the cavity radius.

Hence, the determination of c using Torstensson's method requires estimates of the rigidity index E/s_u, the equivalent radius, R, and the type of cavity (cylindrical or spherical). Baligh and Levadoux (1980) discuss the difficulties associated with the selection of these variables. For example, the shear modulus (or E) for a given clay can easily vary by one order of magnitude depending on the strain level, overconsolidation ratio and the mode of shearing. Similarly, the selection of an appropriate shear strength, s_u, is not an easy task (see Table 4.1 which shows that s_u for Boston Blue Clay depends on the stress system, strain rate and consolidation stresses). Furthermore, the selection of the type of cavity is difficult. Cavity expansion solutions are one-dimensional whereas cone penetration is two-dimensional, and hence the geometrical analogy between the two problems

is not clear. For a given clay (G/s_u fixed), spherical cavity solutions predict much faster dissipation (T_{50} smaller) than cylindrical cavities and hence predict smaller values of the coefficient of consolidation, c. From Fig. 5.1, the ratio of c estimated by the two methods is about 5.

5.2.2 Randolph and Wroth (1978)

Randolph and Wroth (1978) developed a method for analyzing the change in stresses and soil properties around piles and interpreting the results of the presuremeter test. The initial excess pore pressure distribution is obtained by the one-dimensional cylindrical cavity solution, Eq. 5.1, assuming the soil also to behave as an elastic-perfectly plastic material. They utilize a closed form analytical consolidation analysis to estimate the normalized excess pore pressure dissipation curves similar to those in Fig. 5.1.

5.2.3 Baligh and Levadoux (1980)

Baligh and Levadoux (1980) analyze the deep cone penetration in clays as an axisymmetric two-dimensional steady state problem that is essentially strain-controlled, i.e., strains and deformations in the soil are primarily imposed by kinematic requirements. They then use the strain path method described in Chapter 4 to estimate the normalized excess pore pressures due to cone penetration on the basis of laboratory data on normally consolidated Boston Blue Clay.

Figures 5.2 and 5.3 present a comparison between the pore pressures predicted by the strain path and cavity expansion methods and measurements obtained by Baligh et al., (1978) and Roy et al., (1979). The results show the following:

1) Predictions of pore pressures by the strain path method are in good agreement with in situ measurements on the face and shaft behind 18° and 60° cones in a Boston Blue Clay deposit having $1.3<OCR<3$ as well as in the soil surrounding a jacked pile in Champlain clay.

2) By neglecting the two-dimensional nature of the problem, cavity expansion solutions cannot provide the distribution of pore pressures along the shaft of the probe. Moreover, in the radial direction, the solution predicts unrealistic distributions, especially in the immediate vicinity of the probe (r/R = 1 to 5).

3) The measurements of pore pressures around the jacked pile in Champlain Clay are very similar to a number of other clays of different types and stress histories. Therefore, it seems possible that the predicted distribution of the normalized excess pore pressure by the strain path method for normally consolidated BBC will prove satisfactory in other clays as well.

Having developed the initial excess pore pressures, Baligh and Levadoux then use two-dimensional linear uncoupled finite element analyses to obtain the variation

of pore pressures with time. Figure 5.4 shows plots of normalized excess pore pressure, $\bar{u}$, versus time factor, T, at four selected locations along the tip and the shaft of 18° and 60° probes. $\bar{u}$ is defined as:

$$\bar{u} = \frac{u-u_o}{u_i-u_o} \tag{5.4}$$

where,

u = pore pressure recorded at time t

u_o = static or equilibrium pore pressure

u_i = initial pore pressure at end of penetration (t_{50}).

The results in Fig. 5.4 show that the time required to achieve a given degree of dissipation, $\bar{u}$, increases for points further away from the apex of the cone. Moreover, dissipation rates are affected by the probe angle.

Parametric studies were carried out by Baligh and Levadoux to investigate the effects of the initial excess pore pressure distribution, the anisotropy of the soil and the coupling between pore pressures and total stresses on the theoretical dissipation curves presented in Fig. 5.4. Their results show that:

1) dissipation times are significantly influenced by the initial excess pore pressure distribution

2) a reduction in the vertical coefficient of consolidation, c_v, from c_h to 0.1 c_h causes little delay in the uncoupled pore pressure dissipation at 4 selected

locations along the tip and shaft of an 18° piezometer probe provided that the time factor is defined as $T=c_h t/R^2$. This suggests that c_h governs consolidation around piezometer probes. Similar conclusions were arrived at by Gillespie and Campanella (1981) and Tumay et al., (1982).

3) The effect of linear coupling between total stresses and pore pressures is small except at early stages of consolidation especially near the apex of an 18° cone. This suggests that uncoupled solutions can provide reasonably accurate predictions away from the apex and after sufficient dissipation has taken place.

Finally, Baligh and Levadoux (1980) recommend the following procedure for the application of their method to predict the coefficient of consolidation of cohesive deposits:

1. Normalization of dissipation records and plotting $\bar{u}$ vs. log t:

   $\bar{u}$ is defined in Eq. 5.4

2. Choice of Records

   Identify and eliminate unusual dissipation records caused by high soil variability or improper performance of the piezometer probe. This requires engineering judgement and some experience. Unusual records are characterized by:

   a) A much higher or lower initial pore pressure, u_i, that may be easily detected in a plot of penetration pore pressure versus depth.

b) A fluctuation or an increase in pore pressure (or $\bar{u}$) for a significant period of time (greater than 10 seconds) after penetration stops.

3. Applicability of Predictions

This can be achieved graphically by comparing the measured normalized dissipation ($\bar{u}$ vs. log t) curves to the recommended curves of $\bar{u}$ vs. log T ($T=c_h t/R^2$, R=shaft radius) in Fig. 5.4. The measured dissipation curve ($\bar{u}$ vs. log t) is plotted to the same scale of $\bar{u}$ vs. log T and translated horizontally with respect to the predicted curve (while maintaining equality of $\bar{u}$) until the best agreement is achieved. According to linear uncoupled analyses, the horizontal translation reflects changes in c_h whereas the shape of the dissipation curve depends on the initial excess pore pressure distribution around the probe. Therefore, a good agreement between the measured and recommended normalized dissipation curves provides a strong indication of the applicability of the prediction method to the soil at hand.

4. Evaluation of c_h (Probe)

At a given degree of consolidation, the predicted c_h(probe) is obtained from the expression:

$$c_h \text{ (probe)} = \frac{R^2 T}{t} \qquad (5.5)$$

where, R = radius of the cone shaft

t = measured time to reach this degree of consolidation

T = time factor

An analytical method to check the validity of the prediction method consists of determining c_h at different $\bar{u}$. Large differences between c_h at various degrees of consolidation indicate an inadequate initial distribution of excess pore pressure or significant coupling or creep behavior.

The estimated values of c_h (probe) at 50% dissipation can be used in foundation problems involving horizontal water flow due to unloading or reloading of clays. For problems involving vertical water flow in the overconsolidated range, c_v (probe) can be estimated from the expression:

$$c_v \text{ (Probe)} = \frac{k_v}{k_H} \; c_h \text{ (probe)} \qquad (5.6)$$

where, k_v and k_h are the vertical and horizontal coefficients of permeability, respectively. Due to the lack of reliability of the estimates of k_h/k_v in the laboratory, rough estimates of k_h/k_v for different clays are presented in Table 5.1. Baligh and Levadoux (1980) also provide a technique for predicting k_h and c_v(NC) from the probe measurements.

Table 5.2 summarizes Figs. 5.1 and 5.4 in a more workable fashion.

5.3 Empirical and Curve Fitting Dissipation Solutions

In addition to the theoretical solutions presented in Section 5.2, several empirical and curve fitting procedures have been developed over the last few years.

5.3.1 Battaglio et al., (1981)

Battaglio and his co-workers use a trial and error method to obtain a dimensionless $\bar{u}$ vs. T relationship which best matches the field dissipation curves. The initial excess pore pressures are estimated using the one-dimensional cavity expansion solutions and the consolidation process is modeled by means of a one-dimensional finite difference solution to Terzaghi's Equation. The steps required to use their approach is as follows:

1) Compute the excess pore pressure distribution. For this, one needs to select the cavity shape, the rigidity index, I_R, and the pore pressure parameter at failure, A_f.

2) Solve, by the finite difference method, using a trial c_h value, the simple one-dimensional diffusion Terzaghi-type consolidation theory, which for radial flow is governed by the following partial differential equation:

$$\frac{\delta u}{\delta t} = c \left(\frac{\delta^2 u}{\delta r^2} + \frac{\beta}{r} \cdot \frac{\delta u}{\delta r}\right) \qquad (5.7)$$

where, β = 1 for cylindrical cavity ($c=c_h$)

β = 2 for spherical cavity ($c=c_{av}$; $c_v<c_{av}<c_h$)

u = excess pore pressure

r = radius of probe

3) Evaluate the standard deviation, Δ, between computed and observed curves of the excess pore pressure decay with time.

4) Repeat steps 2 and 3 until a c_h value which corresponds to the minimum value of the standard deviation Δ is obtained.

Examples of application of this procedure for two test sites are shown in Fig. 5.5. In these tests, the cylindrical cavity shape was adopted and the value of I_R was estimated from Direct Simple Shear tests.

5.3.2 Jones and Van Zyl, (1981)

Their empirical approach simply plots time to 50% dissipation, t_{50}, versus the reciprocal of the vertical coefficient of consolidation obtained from laboratory oedometer tests. A straight line fit through the origin of the results as in Fig. 5.6a yields the equation:

$$t_{50}\ (\text{min}) = \frac{50}{c_v}\ (m^2/yr) \qquad (5.8)$$

5.3.3 Tavenas et al., (1982)

They state that c_h should be a function of the permeability k and the modulus of deformability of the intact clay M. In overconsolidated clays, M is related to the maximum past pressure, $\overline{\sigma}_{vm}$, by $M=m\overline{\sigma}_{vm}$ so that c_h would be more or less constant and equal to:

$$c_h = \frac{K\bar{\sigma}_{vm}\, m}{\gamma_w} \quad . \tag{5.9}$$

The steps required to get c_h are:

1) Obtain k from direct permeability tests

2) Obtain $\bar{\sigma}_{vm}$ from oedometer tests

3) Plot t_{50} vs. $\frac{k\bar{\sigma}_{vm}}{\gamma_w}$

4) Correlate t_{50} to T_{50} in a manner similar to that presented in Figure 5.6b.

5.3.4 Tumay et al., (1982)

Tumay et al., (1982) recommend a curve fitting procedure for predicting the consolidation coefficient of cohesive deposits. The initial pore pressure distributions along the shaft and in the radial direction, a sufficient distance behind the tip, were obtained from the results and measurements obtained by Levadoux and Baligh (1980) and Roy et al., (1979), respectively. Linear uncoupled finite element consolidation analyses were then performed to obtain the theoretical dissipation curves.

Typical theoretical dissipation curves are shown in Fig. 5.7 where we note that there is a straight line portion of every dissipation curve. Each of these straight lines, when extended, meet at 90% consolidation; the point of intersection called T'_{90}. Also, Tumay et al., (1982) observed that all the parameters that affect dissipation,

i.e., anisotropy, disturbed zone around the cone, location of piezometric element, and cone angle, will be least pronounced during the final stages of consolidation. It can be seen from Fig. 5.7 that the anisotropic effects disappeared at about 90% consolidation. In other words, they feel that all dissipation curves will converge at about 90% consolidation and called this converging point T_{90}. The procedure adopted to compute the consolidation coefficient using Tumay's method is as follows:

1) Calculate the ratio of $\frac{\log T_{90}}{\log T'_{90}}$ which equals a constant A

2) Estimate t_{90} by the expression:

$$t_{90} = 10^{A \log t'_{90}}$$

where, t'_{90}=time of 90% dissipation at the straight line portion

t_{90}= actual time of 90% dissipation

3) Calculate c_h by the expression:

$$c_h = \frac{T_{90}}{t_{90}} (R^2)$$

Using the expression for t_{90} in step 2 will save time in field operations by not having to wait until pore pressures have completely dissipated. Once the dissipation curve has reached its straight line portion, a coefficient of consolidation can be estimated. For their analysis, A=1.13 and T_{90}=240.

The Tumay, Jones, and Tavenas solutions are all limited to predicting c_h at one level of dissipation. This violates one of the criteria for a solution to be applicable. That is, an acceptable solution to dissipation must be able to predict the same c_h value at all levels of dissipation.

Another limitation of the Tumay solution is that there seems to be no indication that t_{90} calculated using their procedure would match t_{90} from the actual field dissipation curves. They do not present dissipation curves carried to 90% dissipation in order to verify the curve fitting assumptions.

The empirical solutions of Jones and Tavenas rely mainly on laboratory test results for c_h and permeability. As will be shown in the following section, c_h values from consolidation tests can vary depending on the type of test, loading cycle, and stress level. One must first understand the consolidation process around probes and also understand the limitations of c_h(lab) values before an attempt to draw empirical relationships from the two measuring systems can be made.

Although the Battaglio solution appears to reasonably predict c_h at all levels of dissipation, and compares well with reference c_h values, use of the solution is complex and time-consuming. The beauty of the theoretical solutions is that the hard analytical work has been reduced

to a series of curves which makes for easy application. However, the Battaglio solution requires the equipment and knowledge to run a finite difference analysis. Clearly, this is impractical as comparable c_h values can be predicted at a fraction of the time and cost using the theoretical solutions.

Due to all of the limitations in the applicability of the above curve fitting and empirical solutions to dissipation of pore pressures, they will be left out of any subsequent analyses. Of the four procedures, Battaglio is the most promising if and when the hardware and software needed to perform such an analysis becomes more readily available.

5.4 Evaluation of c_h From Laboratory Tests

5.4.1 Background

Since consolidation takes place in the overconsolidated state (see Section 5.2), the objective of a laboratory testing program should be to evaluate c_h(probe) with lab measurements of c_h obtained from tests when the soil is in the overconsolidated range, i.e., c_h(OC). In consolidation tests, this would be during an unload or a reload cycle. Initial loading is largely influenced by sample disturbance which lowers c_h(OC), Ladd (1973), and is therefore not suitable for use in evaluating c_h(probe).

Consolidation tests, either the standard incremental oedometer or the constant rate of strain consolidation,

CRSC, (Wissa et al., 1971) are the laboratory techniques most widely used to evaluate c_h(OC). CRSC tests run on horizontal samples allow measurement of c_h(OC) at small stress increments. On the other hand, for the range of OCR of interest (estimated to be $\leq$ 3), the oedometer test is inadequate to evaluate c_h(OC) for the following reasons:

1) The very high gradients at the start of an unload or a reload cycle are overlooked by the curve fitting procedures used to calculate c_h which tend to emphasize the data towards the middle of the load increment.

2) Oedometer tests can only yield average values for an increment of loading.

It can be seen from Fig. 5.8 that c_h(OC) during unloading, as measured in the oedometer test in the range of OCR from 2-4, is five to ten times lower than that from a CRSC test run on samples from the same tube.

The degree of overconsolidation at which dissipation takes place in not presently known. However, it is felt that the value of c_h at the in situ OCR is a good starting point from which to evaluate c_h(probe) until further information on this subject is known.

Furthermore, one would want to compare c_h(probe) values with c_h(lab) values measured at the in situ OCR during a <u>reload</u> cycle, since this best simulates the actual field occurrence. However, as will be shown below, attempts to evaluate c_h(lab) during recompression will lead to erroneous results because at a given OCR, c_h(reload) is

a function of the size of the unload cycle. Instead, it is felt that c_h measured during unloading will yield proper values for comparison with c_h(probe).

5.4.2 Why c_h(OC) during unload?

To prove that the c_h measured during the unload cycle is appropriate to evaluate c_h(probe), first it must be established that c_h during reloading is affected by the amount of unloading, and second, that at a given OCR, c_h will be the same whether it is measured during unload or reload.

1) Dependence of c_h(reload) on magnitude of unloading

By definition, $$c_h = \frac{k_h}{m_v \gamma_w} \qquad (5.10)$$

where, k_h = horizontal coefficient of permeability

m_v = coefficient of volume change

γ_w = unit weight of water

From Baligh and Levadoux (1980),

$$m_v = \frac{RR}{2.3\ \bar{\sigma}_v} \quad \text{for small increments of stress} \qquad (5.11)$$

where,

RR = recompression ratio

By combining Eqs. 5.10 and 5.11, we arrive at the relationship:

$$c_h = \frac{2.3\ k_h \bar{\sigma}_v}{RR} \qquad (5.12)$$

The dependency of c_h (reload) on the degree of unloading can be shown by studying how the parameters k_h, $\bar{\sigma}_v$, and RR are affected when evaluated at the same $\bar{\sigma}_v$, during reloading, for two tests with the same $\bar{\sigma}_{vm}$ unloaded to different levels of OCR. From the results of two CRSC tests run on horizontal samples of BBC in Fig. 5.9, it can be seen that log k_h is proportional to the void ratio, e. Because of the steepness of the slopes, small changes in e will not considerably change k_h. Therefore, since e does not change much during an unload-reload cycle, k_h should remain relatively constant regardless of the degree of unloading. Also, comparing c_h for two tests at a given OCR means that $\bar{\sigma}_v$ will be the same for both tests. Therefore, since k_h and $\bar{\sigma}_v$ are constant, c_h is inversely related to RR by Eq. 5.12. Figure 5.10 shows that at any OCR during reloading, RR is greater for test A which experienced a greater degree of unloading. As a result, c_h at any OCR would be lower for test A than B because of the degree of unloading associated with each test.

Because of this phenomenon, one is faced with the question, "what is the correct degree to which I should unload my sample?" Unfortunately, this question cannot be answered because it is not yet known exactly how much unloading takes place upon probe penetration in clays.

2) $\underline{c_h(\text{unload}) = c_h(\text{reload})}$

Once penetration stops, pore pressures begin to dissipate. The values measured therefore take place during

the beginning of reloading where the compressibility is low; and as the effective stress increases, RR increases. Assuming that small unload-reload cycles (OCR ≈ 1-4) closely simulate the probe penetration and subsequent consolidation, the shapes of the unload-reload loops will be more or less symmetric. Because of this symmetry, the beginning of unloading is characterized by the same low compressibility and subsequent increase in the swelling ratio, SR.

Although k_h will be slightly higher during early stages of reloading, $\overline{\sigma}_v$ will be slightly lower. Therefore, the compensating decrease in k_h and increase in $\overline{\sigma}_v$ and vice-versa should keep the product $k_h(\overline{\sigma}_v)$ relatively constant at similar locations on the unload or reload part of the cycle. Therefore, c_h measured during the early stages of unloading should compare well with c_h during early portions of reloading. Since c_h(unload) is easier to measure and is not dependent on degrees of unloading, it is felt that this is the parameter to evaluate with c_h(probe).

5.5. Case Histories

5.5.1 Introduction

The applicability of the Baligh and Levadoux (1980) and Torstensson's (1977) cylindrical and spherical solutions to dissipation of excess pore pressures will be evaluated in this section through a series of case studies.

The first two cases represent research done at MIT (including the Solar House study) and the final two represent research reported in the literature. Included in each study will be the soil characteristics, dissipation curves, comparisons of c_h predicted by the different solutions, and any laboratory c_h data presented as reference values.

5.5.2 Presentation of Case Histories

1. Saugus, Massachusetts (Baligh et al., 1980,1981)

The piezocone was used at a site in Saugus, Mass., 160 to 200 ft to the east of the unfinished Interstate-95 embankment certerline at a location designated station 246. This site has been comprehensively studied by M.I.T. over the last two decades.

As presented in Chapter 4, the soil profile at the test site consists of 25 ft of peat, sand and stiff clay layers which overlie about 120 ft of Boston Blue Clay, (BBC), (see Fig. 5.11). Estimates of the maximum past pressure, $\bar{\sigma}_{vm}$, from conventional oedometer and CRSC tests indicate that the clay above a depth of 60 ft is significantly overconsolidated.

A series of dissipation tests were run between 1979 and 1980 using different probe geometries and porous stone locations. Table 5.3 outlines the probe geometries and respective number of tests. The results of all dissipation tests are presented in Fig. 5.12 to 5.14 as bands of normalized excess pore pressure versus time. Included on

these Figs. are the Baligh and Levadoux solutions corresponding to c_h(probe)=0.04 cm^2/sec. Tables 5.4 to 5.6 present c_h(probe) at various degrees of dissipation evaluated by the three theories mentioned above.

Ghantos (1982) ran a series of CRSC tests on undisturbed horizontal BBC samples. His results for c_h (swelling) versus OCR are shown in Fig. 5.15. From this curve he was able to plot c_h(swelling), at the in situ OCR versus depth in Fig. 5.16. This figure shows that the c_h(probe) value of 0.04 cm^2/sec, predicted with the Baligh and Levadoux solution, falls nicely within a band of 0.014 to 0.06 cm^2/sec for c_h(swelling). This band represents the uncertainty in the prediction of OCR.

Utilizing Torstensson's method for predicting c_h(probe) requires knowledge of three parameters, the rigidity index ($I_R = G/s_u = \frac{\overline{E}u}{3s_u}$), the type of cavity expansion (cylindrical or spherical), and the probe radius, R. Tables 5.4 through 5.6 show that the spherical solution at best underpredicts c_h(probe) by a factor of five. Therefore, it is felt that this solution does not accurately model pore pressure dissipation and will not be discussed further. The cylindrical solution appears to predict c_h(probe) well for E_u/s_u between 400 and 500; however, there is an inaccuracy involved in utilizing these

normalized modulus values to predict c_h(probe) in soft clays which will be discussed below.

Baligh and Levadoux (1980) present excess pore pressure measurements due to pile installation in eight clay deposits, Fig. 5.17a. Important properties of the eight clays and pile types are summarized in Fig. 5.17a and Table 5.7; and cover a wide range of soil types. They note in Fig. 5.17a that:

1) Significant excess pore pressures [$\Delta u_i(r) > 0.2\ \overline{\sigma}_{vo}$, say] develop within a radius r = 20R (i.e., $\lambda = 20$) around the pile and measurable excess pore pressures extend to r = 50R or even 80R.

2) In spite of the very different conditions (soil and pile) in cases a, b, c, d, g and h, results between r = 5R and r = 20R fall within a well defined band and suggest that $\lambda \simeq 20R$.

Figure 5.17b shows the band including most of the test data for r > 5R. A reasonably good fitting of the data between r = 5R and r = 20R can be achieved by either a logarithmic distribution or a linear distribution.

Noting that the logarithmic initial excess pore pressure distribution is derived by elasto-plastic cylindrical cavity expansion solutions; according to Eq. 5.1, the straight line in Fig. 5.17b corresponds to a clay with $E_u/s_u = 1200$ and $s_u/\overline{\sigma}_{vo} = 0.68$ (i.e., $G/\overline{\sigma}_{vo} = 272$). This ratio of E_u/s_u is much higher than estimated by Torstensson in analyzing cavity expansion problems even

though $s_u = 0.68\ \bar{\sigma}_{vo}$ is excessively high especially for the soft clays (OCR ≃ 1) in cases a and b. Therefore, Torstensson's cylindrical solution, even with $E_u/s_u = 500$, cannot accurately predict the initial excess pore pressure distribution needed to model pore pressure dissipation. Judging by the trend, (c_h(probe) increases as E_u/s_u increases), a solution for $E_u/s_u = 1200$ would severly over-predict c_h(probe).

Since the Baligh and Levadoux solution accurately predicts c_h for all types of probe geometries and stone locations, and does not rely upon evaluating E_u/s_u nor a type of cavity expansion, it will be the solution applied to predict c_h(probe) for the remainder of the case studies.

2. M.I.T. Solar House

Dissipation tests were part of the in situ testing program outlined in Chapter 3. The band of dissipation curves representing 12 tests run below depths of 53 ft (OCR < 3) are shown in Fig. 5.18 along with the Baligh and Levadoux solution for c_h (probe) = 0.04 cm^2/sec. When compared with dissipation curves obtained at Saugus with the same radius cone, an almost identical band of dissipations is obtained. Because of this phenomenon, the lab results obtained for the Saugus site will also be applied to the Solar House site and a c_h of 0.04 cm^2/sec adopted.

3. Canadian Clays (Campanella et al., 1982)

A. McDonald's Farm, Richmond, British Columbia

The soil profile at the site consists of approximately 15 meters of clay and sand overlying a deposit of soft, normally consolidated clayey SILT, Fig. 5.19. A dissipation test was run at a depth of 20.5 meters with a 60° piezocone with the porous stone located at its base. Fig. 5.20 presents the dissipation curve and a band of curves representing c_h(probe) = 0.05 to 0.08 cm^2/sec obtained from the Baligh and Levadoux solution.

CRSC tests run on vertical and horizontal samples predict $c_h(OC) = c_v(OC) = 0.058$ cm^2/sec which falls within the band of c_h(probe) predictions.

B. Burnaby, B.C.

One dissipation test was performed at a depth of 15.5m in a soft silty clay deposit located at Burnaby, B.C. This test utilized a 60° cone with the porous element located at the cone base as well. Figure 5.21 presents the dissipation curve and a band of curves representing c_h(probe) = 0.005 to 0.007 cm^2/sec obtained from the Baligh and Levadoux solution.

CRSC tests performed on vertical samples yielded $c_v(OC)$ equal to 0.01 cm^2/sec, slightly higher than the c_h(probe) predictions.

4. Italian Clays (Battaglio et al., 1981)

Dissipation tests were performed in two Italian clays using an 18° piezometer probe with the porous element

located slightly above the tip.

A. Porto Tolle Site

The Porto Tolle clay is a normally consolidated silty clay, the soil profile and stress history of which are presented in Fig. 5.22a. A dissipation test was run within the clay and is shown in Fig. 5.23, bounded by curves representing c_h(probe) = 0.015 to 0.030 cm^2/sec as obtained by the Baligh and Levadoux solution. These c_h values compare favorably with those calculated by different laboratory and field procedures shown in Table 5.8.

B. Trieste Site

Figure 5.22b shows the soil profile and stress history of the Trieste clay, which is a soft normally consolidated organic clay with shell fragments. The dissipation curve performed at this site is shown in Fig. 5.24, bounded by curves representing c_h(probe) = 0.007 to 0.011 cm^2/sec as obtained by the Baligh and Levadoux solution. No laboratory c_h values accompanied this case in the literature.

In conclusion, from review of these case studies, it is apparent that the Baligh and Levadoux solution can predict the horizontal coefficient of consolidation of cohesive deposits with reasonable accuracy. It should be noted that this coefficient should be used in problems involving unloading or reloading.

Anisotropic Permeability of Clays

	Nature of Clay	k_h/k_v
1.	No evidence of layering	1.2 ± 0.2
2.	Slight layering, e.g., sedimentary clays with occasional silt dustings to random lenses	2 to 5
3.	Varved clays in north-eastern U.S.	10 ± 5

Table 5.1 Anisotropic Permeability of Clays (from Baligh and Levadoux, 1980)

TIME FACTOR T

Degree Dissipation	10%	20%	40%	50%	60%	80%	90%
Baligh & Levadoux							
60°,tip	0.12	0.44	1.90	3.65	6.50	27.00	82.20
60°,mid-height	0.12	0.51	1.90	3.65	6.50	27.00	82.20
60°,base	0.18	0.68	3.09	5.75	10.72	39.80	04.70
18°,tip	0.04	0.16	1.35	3.00	6.00	30.80	74.50
18°,mid-height	0.13	0.52	2.60	4.70	8.20	34.00	84.00
Torstensson spherical							
E_u/s_u=500		0.11	0.46	0.81	1.26	3.28	5.74
E_u/s_u=400		0.10	0.40	0.68	1.13	2.85	4.70
E_u/s_u=300		0.085	0.35	0.61	0.98	2.36	4.01
E_u/s_u=200		0.067	0.28	0.47	0.77	1.91	3.04
E_u/s_u=100		0.057	0.20	0.32	0.50	1.16	1.89
Torstensson cylindrical							
E_u/s_u=500		0.34	2.14	4.29	8.33	23.61	38.57
E_u/s_u=400		0.30	1.75	3.57	6.79	20.20	31.62
E_u/s_u=300		0.24	1.38	2.81	5.37	16.29	26.98
E_u/s_u=200		0.18	1.06	2.32	3.82	10.13	17.43
E_u/s_u=100		0.14	0.83	1.37	2.49	6.03	10.00

Table 5.2 Time Factors for Theoretical Solutions at Different Percent Dissipation

Year	Cone Angle	Stone Location	Cone Radius (cm)	No. of Tests
1979	60°	Tip	1.91	9
1979	18°	Mid-Height	1.91	6
1979	18°	Tip	1.91	17

Table 5.3 Piezocone Studies Performed at Saugus, Mass.

SAUGUS (18°, MID-HEIGHT)

$c_h \times 10^{-2}$ (cm^2/sec)

% Dissipation	10	20	40	50	60
t (sec)	7.4-16	31-51	210-310	440-650	910-1250
Baligh & Levadoux	2.96-6.41	3.72-6.12	3.06-4.52	2.64-3.90	2.39-3.29
Torstensson spherical					
E_u/s_u=500		0.79-1.29	0.54-0.80	0.45-0.67	0.37-0.51
E_u/s_u=400		0.72-1.18	0.47-0.69	0.38-0.56	0.33-0.45
E_u/s_u=300		0.61-1.00	0.41-0.61	0.34-0.51	0.29-0.39
E_u/s_u=200		0.48-0.79	0.33-0.49	0.26-0.39	0.22-0.31
E_u/s_u=100		0.41-0.67	0.24-0.35	0.20-0.27	0.15-0.20
Torstensson cylindrical					
E_u/s_u=500		2.43-4.00	2.52-3.72	2.41-3.56	2.43-3.34
E_u/s_u=400		2.15-3.53	2.06-3.04	2.00-2.96	1.98-2.72
E_u/s_u=300		1.72-2.82	1.62-2.40	1.58-2.33	1.57-2.15
E_u/s_u=200		1.29-2.12	1.25-1.84	1.30-1.92	1.11-1.53
E_u/s_u=100		1.00-1.65	0.98-1.44	0.77-1.14	0.73-1.00

Band of 6 tests below 60 ft (OCR < 2)

R = 1.91 cm

Table 5.4 Prediction of c_h(probe) by Theoretical Solutions

SAUGUS (18°, TIP)

$c_h \times 10^{-2}$ (cm^2/sec)

% Dissipation	10	20	40	50	(4 tests) 60
t (sec)	2.3-10.5	15-38	106-175	209-360	430-800
Baligh & Levadoux	1.39-6.34	1.54-3.89	2.81-4.65	3.04-5.24	2.74-5.09
Torstensson spherical					
E_u/s_u=500		1.06-2.68	0.96-1.58	0.82-1.41	0.57-1.07
E_u/s_u=400		0.96-2.43	0.83-1.38	0.69-1.19	0.52-0.96
E_u/s_u=300		0.82-2.07	0.73-1.20	0.62-1.06	0.45-0.83
E_u/s_u=200		0.64-1.63	0.58-0.96	0.48-0.82	0.35-0.65
E_u/s_u=100		0.55-1.39	0.42-0.69	0.32-0.56	0.23-0.42
Torstensson cylindrical					
E_u/s_u=500		3.26-8.27	4.46-7.37	4.35-7.49	3.80-7.07
E_u/s_u=400		2.88-7.30	3.65-6.02	3.62-6.23	3.10-5.76
E_u/s_u=300		2.30-5.84	2.88-4.75	2.85-4.90	2.45-4.56
E_u/s_u=200		1.73-4.38	2.21-3.65	2.35-4.05	1.74-3.24
E_u/s_u=100		1.34-3.40	1.73-2.86	1.39-2.39	1.14-2.11

Band of 17 tests below 60 ft (OCR < 2)

R = 1.91 cm

Table 5.5 Prediction of c_h(probe) by Theoretical Solutions

SAUGUS (60°, TIP)

$c_h \times 10^{-2}$ (cm^2/sec)

% Dissipation	10	20	40	50	60
t (sec)	1.5-15	7.6-60	125-280	295-530	630-1100
Baligh & Levadoux	2.92-29.18	2.68-21.2	2.48-5.55	2.51-4.51	2.16-3.76
Torstensson spherical					
E_u/s_u=500		0.67-5.28	0.60-1.34	0.56-1.00	0.42-0.73
E_u/s_u=400		0.61-4.80	0.52-1.17	0.47-0.84	0.37-0.65
E_u/s_u=300		0.52-4.08	0.46-1.02	0.42-0.75	0.33-0.57
E_u/s_u=200		0.41-3.22	0.36-0.82	0.32-0.58	0.26-0.45
E_u/s_u=100		0.35-2.74	0.28-0.58	0.22-0.40	0.17-0.30
Torstensson cylindrical					
E_u/s_u=500		2.07-16.32	2.79-6.25	2.95-5.31	2.76-4.82
E_u/s_u=400		1.82-14.40	2.28-5.11	2.46-4.41	2.25-3.93
E_u/s_u=300		1.46-11.52	1.80-4.03	1.93-3.47	1.78-3.11
E_u/s_u=200		1.09-8.64	1.38-3.09	1.60-2.87	1.27-2.21
E_u/s_u=100		0.85-6.72	1.08-2.42	0.94-1.69	0.83-1.44

Band of 9 tests below 60 ft. (OCR<2)

R = 1.91 cm

Table 5.6 Prediction of c_h(probe) by Theoretical Solutions

Case	a	b	c	d	e	f	g	h
Reference	Bjerrum and Johannessen (1960)	Lo and Stermac (1965)	Koizumi and Ito (1967)	Roy et al (1979)	Baligh et al (1978)	Airhart et al (1969)	Ismael and Klym (1979)	Soderman and Milligan (1961)
1) Site	Southern Norway	Wallecsburg Ontario, Canada	Otemachi Tokyo, Japan	Saint Alban Quebec, Canada	Saugus Massachusetts, USA	Beaumont Texas, USA	Pickering Ontario, Canada	Big Pic River Canada
2) Soil 2-a Type and description	Soft Marine clay	Soft to firm silty clay	Very sensitive slightly organic silty clay	Very sensitive Marine soft silty Champlain Clay	Marine illitic Boston Blue Clay	Highly over-consolidated	Firm clayey-sandy silt	Medium to stiff varved silty clay
2-b Plasticity Index (PI)	25	20	60	20	20	40	10	37 clay, 7 silt
2-c Overconsolidation ratio (OCR)	= 1	= 1	= 2.5 (5)	2.2 to 2.4	1.2 to 4	OCR = 7 (5)	High sand content	OCR = 3 (5)
2-d Undrained Strength (s_u)	2 to 2.5 TSM (1)	2 to 2.5 TSM (1)	3 to 3.5 TSM (2)	1.2 to 2 (1)	3.5 to 5.5TSM (1)	11 TSM (3)	No OCR & s_u meas.	2.5 to 4.5 TSM
2-e Sensitivity (S_t)	6 to 8 (1)	4 to 6 (1)	v. high	16	6			
3) Pile: 3-a type	Steel Hollow Box	Steel pipe	Steel pipe	Steel pipe	Steel cylinder	Steel pipe	H-pile	H-pile
3-b Cross section	20 x 20 cms	ϕ = 8.9 cm	ϕ = 30 cm	ϕ = 21.9 cm	ϕ = 3.8 cm	ϕ = 40.7 cm	12"x 53 lb.	12" x 53 lb.
3-c Length	= 20 m	15 m	5.5 m	7.5 m	Variable	16.2 m	7.6 m	16.8 to 50.6 m
3-d Installation	Driving	Driving	Jacking	Jacking	Jacking	Driving	Driving	Driving
4) Pore Pressures Measurements 4-a Device	MGI piezometer	not reported	Cells on piles and piezometers	Gloetzl cell on pile & Geonor electric piezometer in soil	Electric Transducer	Pressure Transducer	Gage at surface for pressure on pile and geonor piezometer in soil	Casagrande open tube
4-b Quality	Good		Fair	Very Good	Very Good	Fair	Fair	Questionable
5) Notes	No measurements of u_i close to pile	Significant scatter. Pore pressures still rising after 1 hr when second pile was driven	Significant scatter. Comprehensive study (4)	Very repeatable	Very repeatable	Pore pressure still rising after 8 hours. No data on G.W. level.		

(1) Field Vane Test (3) Unconfined Test (5) Estimated

(2) Dutch Cone Test (4) Important uncertainty in $\bar{\sigma}_{vo}$ due to 1.5m excavation. We assume wide excavation and pore pressure equalization. Otherwise $\bar{\sigma}_{vo}$ doubles at depth = 5m.

Table 5.7 Summary of Case Histories Where Excess Pore Pressures were Measured During Pile Installation in Clay (from Baligh and Levadoux, 1980)

S O U R C E	$c_h \times 10^{-3}$ (cm^2/sec)
IL Oedometer test	1.7 - 2.5
Piezometer probe dissipation tests	8 (I_R = 110)
Constant head permeability tests	9.7
Self boring permeameter	1.86 - 14.8
Back analyses of trial embankment with vertical drains	6 - 21

Table 5.8 Comparison Between c_h Values by Different Procedures at the Porto Tolle Site (from Battaglio, et al. 1981)

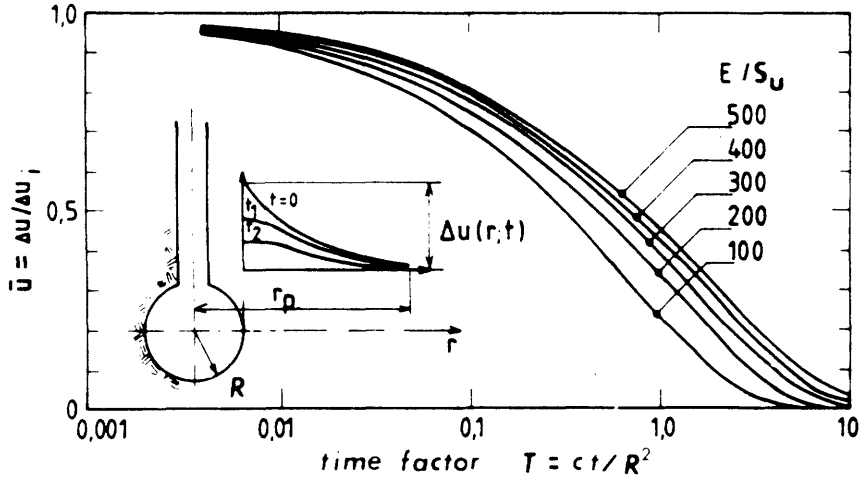

R = radius of pore pressure probe
c = coefficient of consolidation

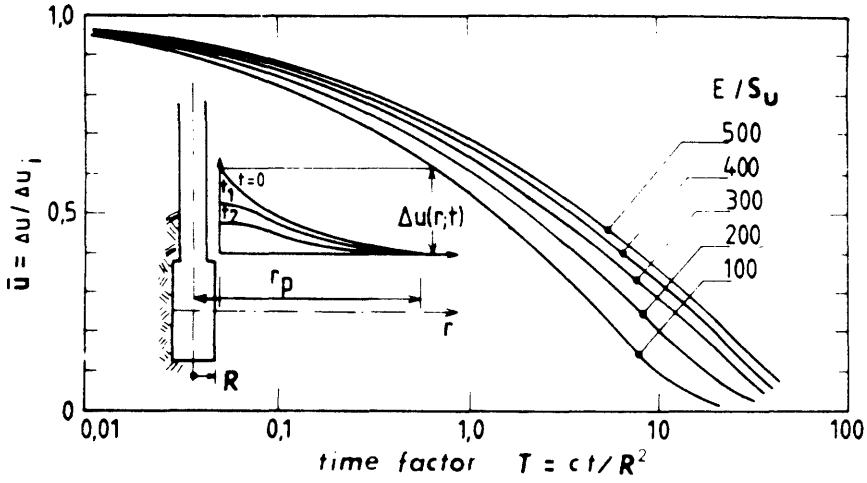

R = radius of pore pressure probe
c = coefficient of consolidation

Figure 5.1 Pore Pressure Dissipation Around Spherical and Cylindrical Pore Pressure Probes Predicted by Torstensson, 1977

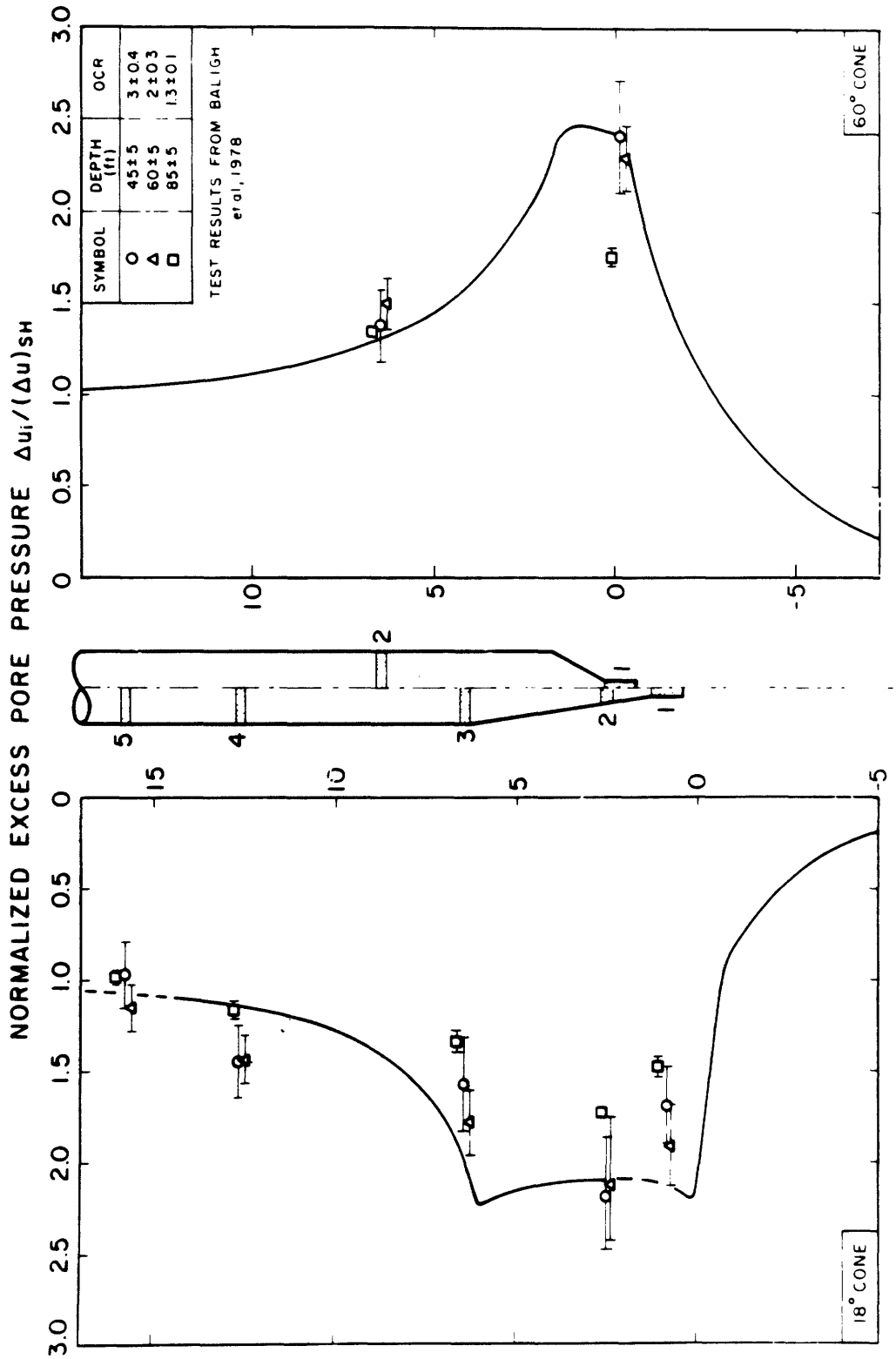

Figure 5.2 Predicted vs. Measured Normalized Excess Pore Pressures Along the Face and Shaft of 18° and 60° Cones During Steady Penetration in Boston Blue Clay (from Baligh and Levadoux, 1980)

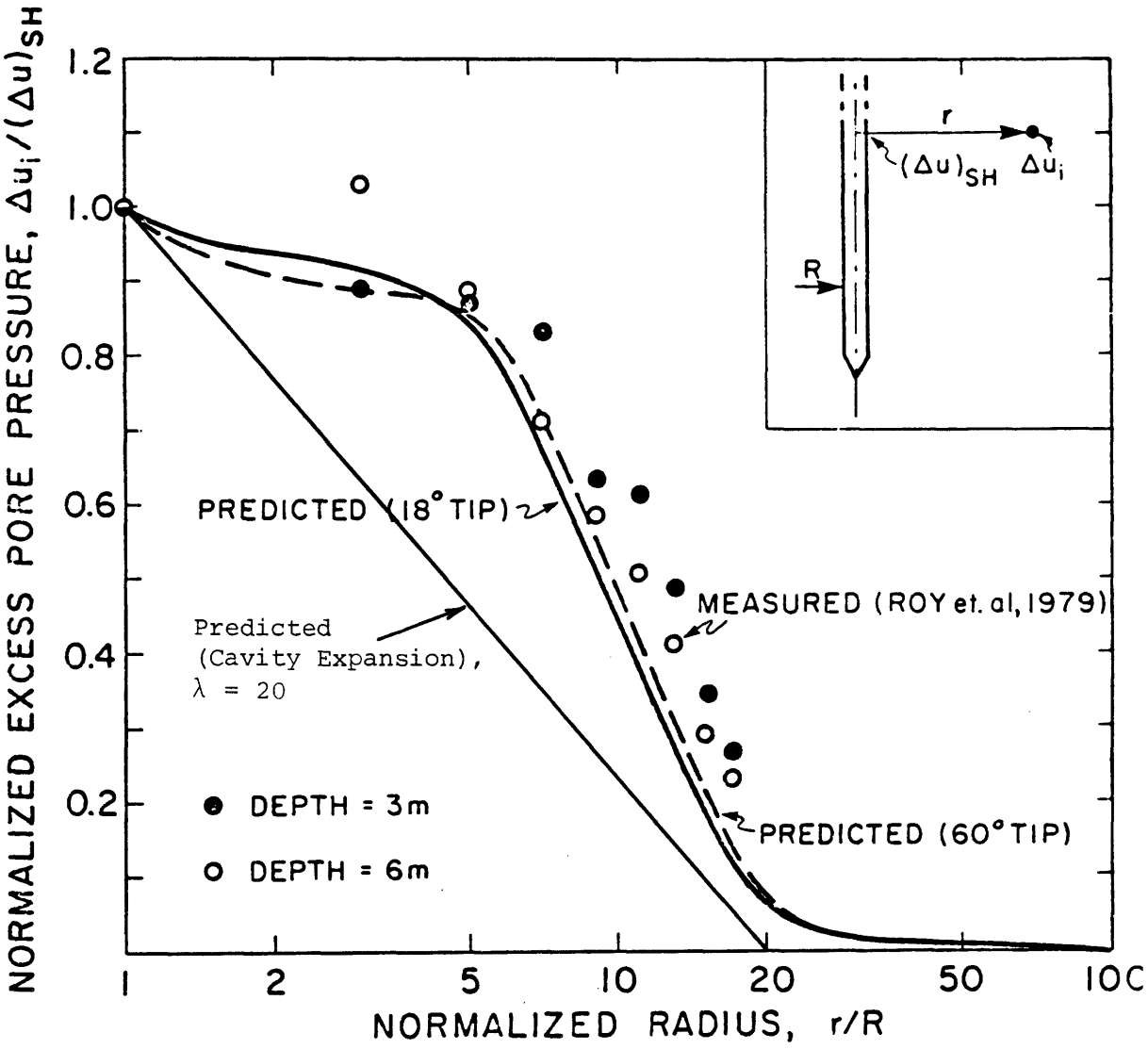

Figure 5.3 Predicted vs. Measured Distribution of Normalized Excess Pore Pressures During Penetration in Clays (from Baligh and Levadoux, 1980)

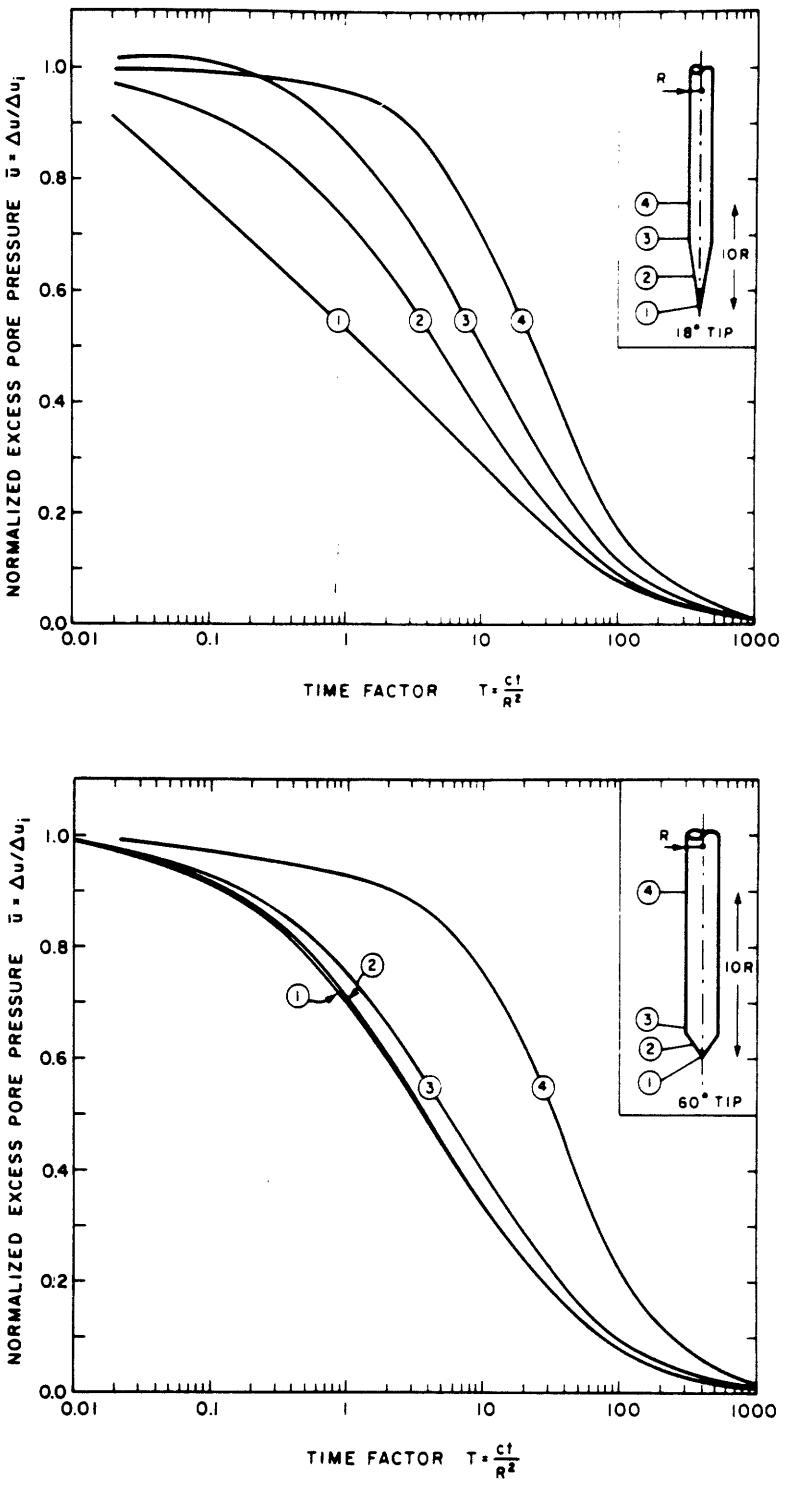

Figure 5.4 Dissipation Curves for an 18° and a 60° Cone According to Linear Isotropic Uncoupled Solutions (from Baligh and Levadoux, 1980)

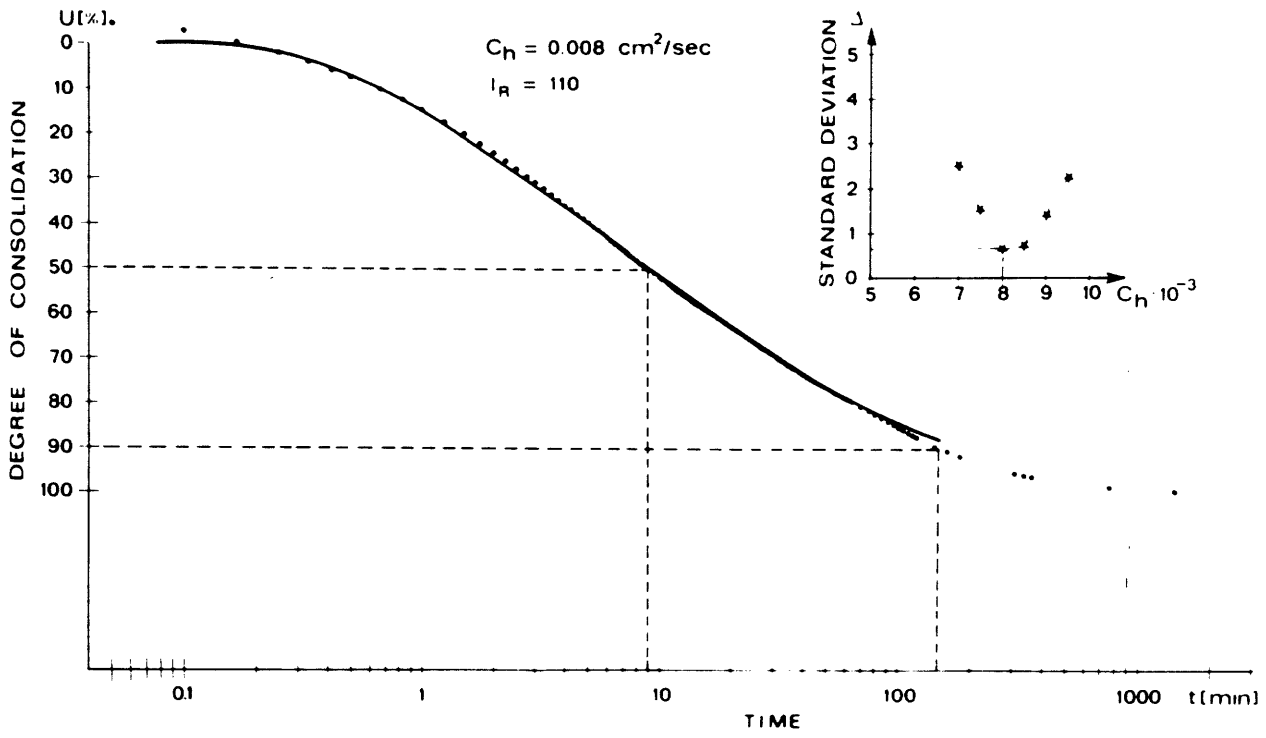

a) Porto Tolle Site

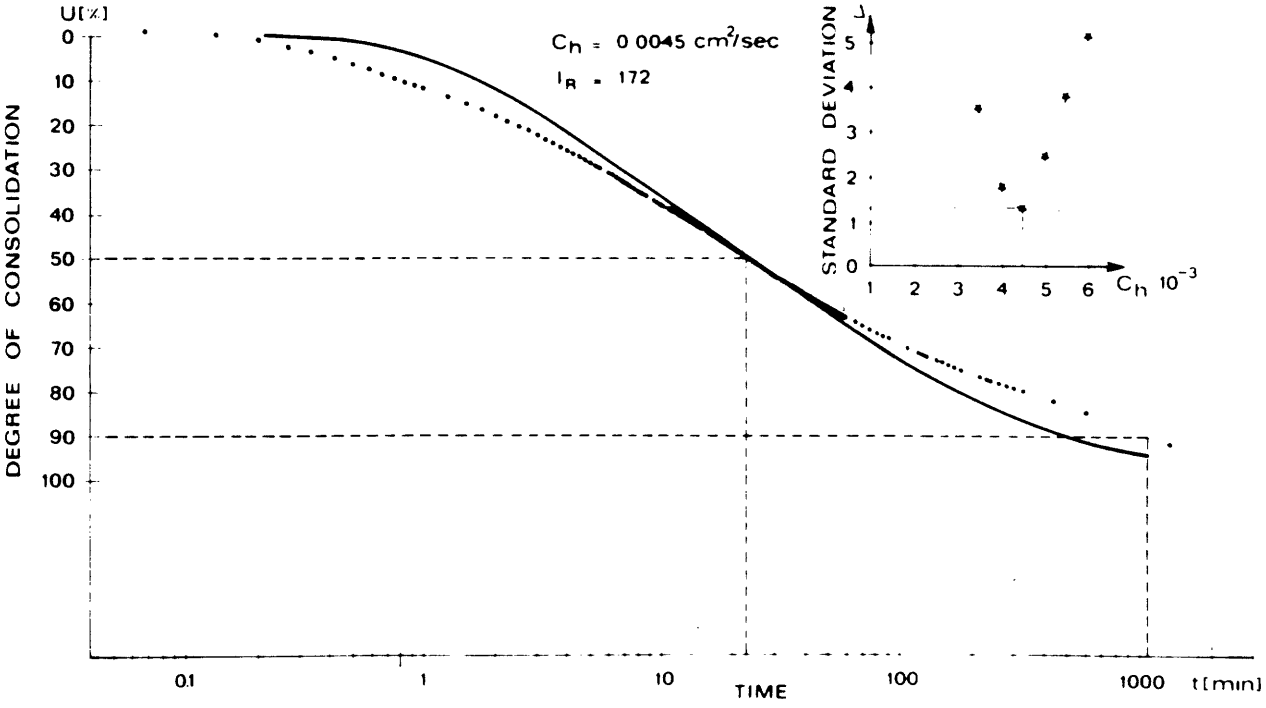

b) Trieste Site

Figure 5.5 Comparison Between Predicted and Measured Pore Pressure Decay at Two Italian Sites (from Battaglio et al., 1981)

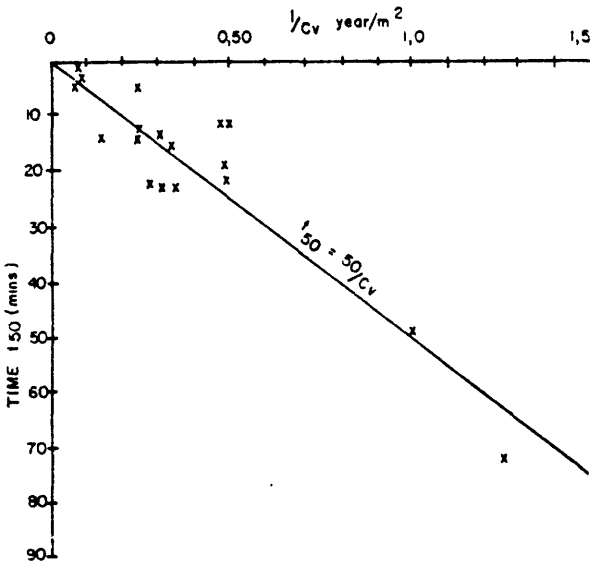

Figure 5.6a Correlation of Field Dissipation Times with Laboratory Consolidation Data (from Jones and Van Zyl, 1981)

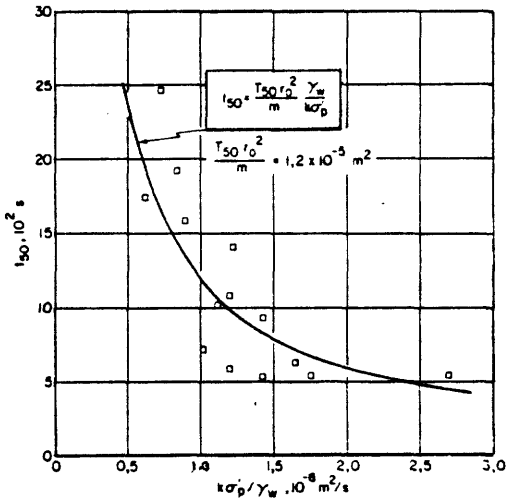

Figure 5.6b Empirical Correlation Between t_{50} and $k\bar{\sigma}_{vm}/\gamma_w$ in Chamlain Sea Clays, Canada (from Tavenas et al., 1982)

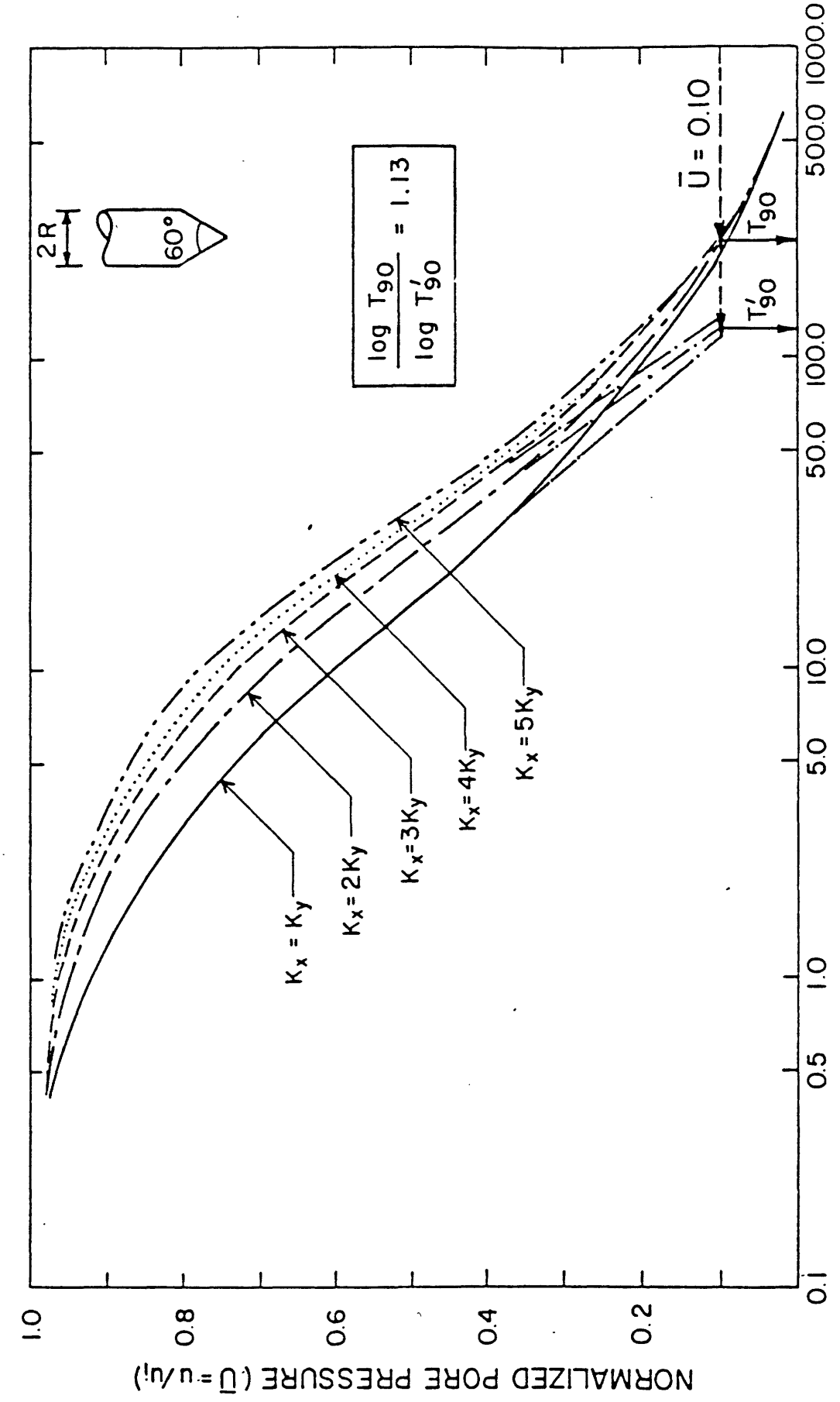

Figure 5.7 Interpretation Method for Estimation of 90 percent Dissipation Time (from Tumay et al., 1982)

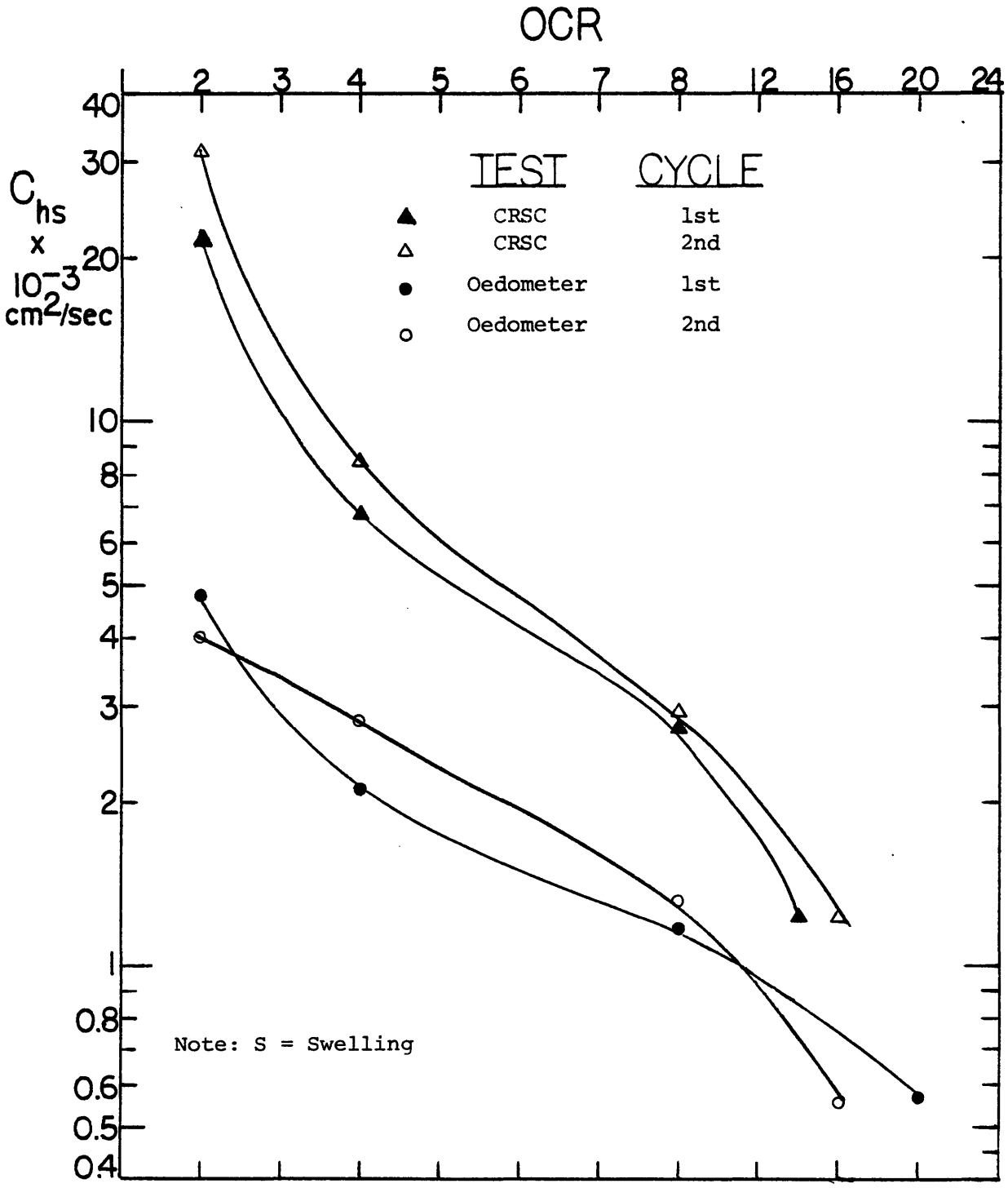

Figure 5.8 c_h Versus OCR from CRSC and Oedometer Tests

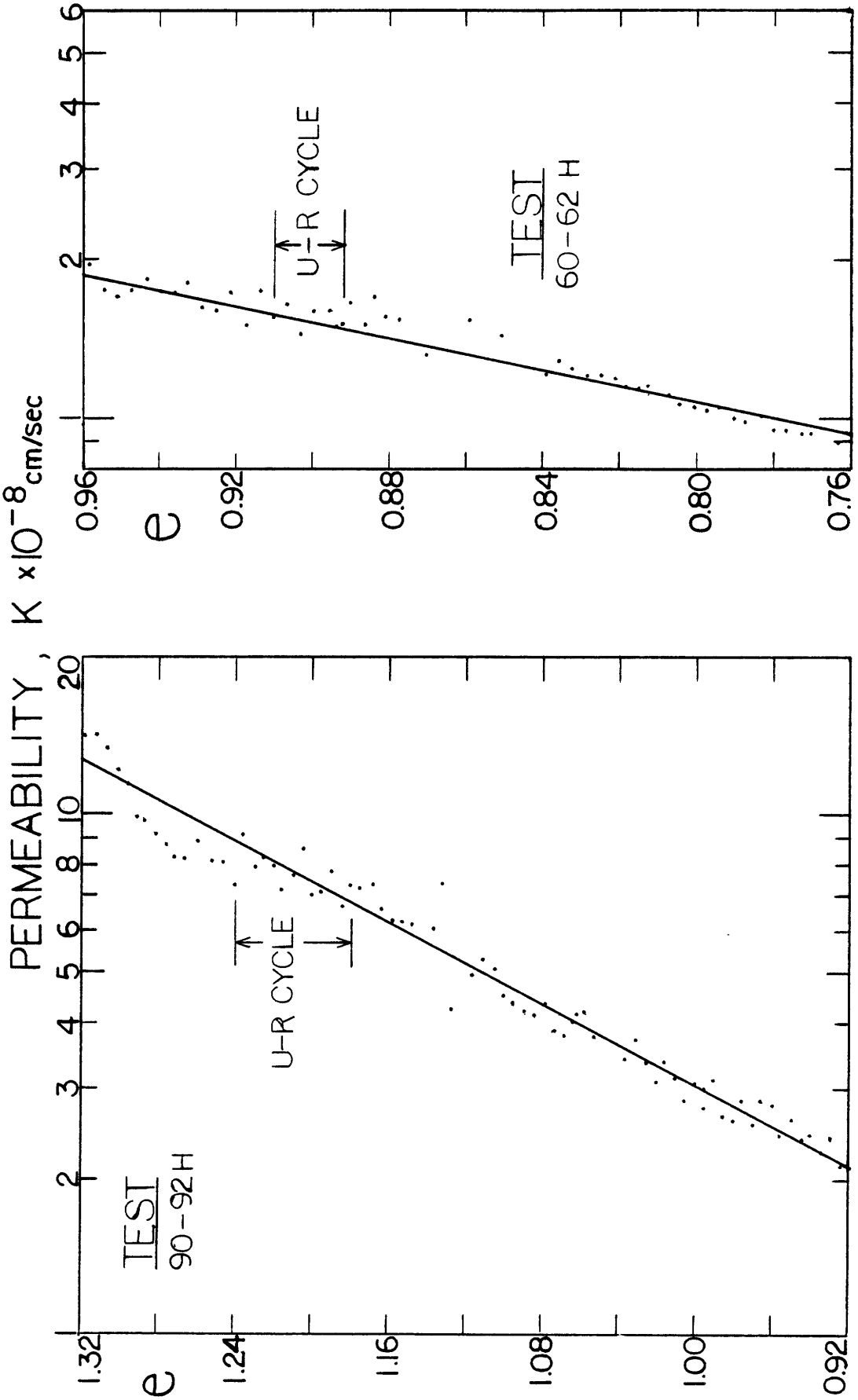

Figure 5.9 e Versus logk from CRSC Tests

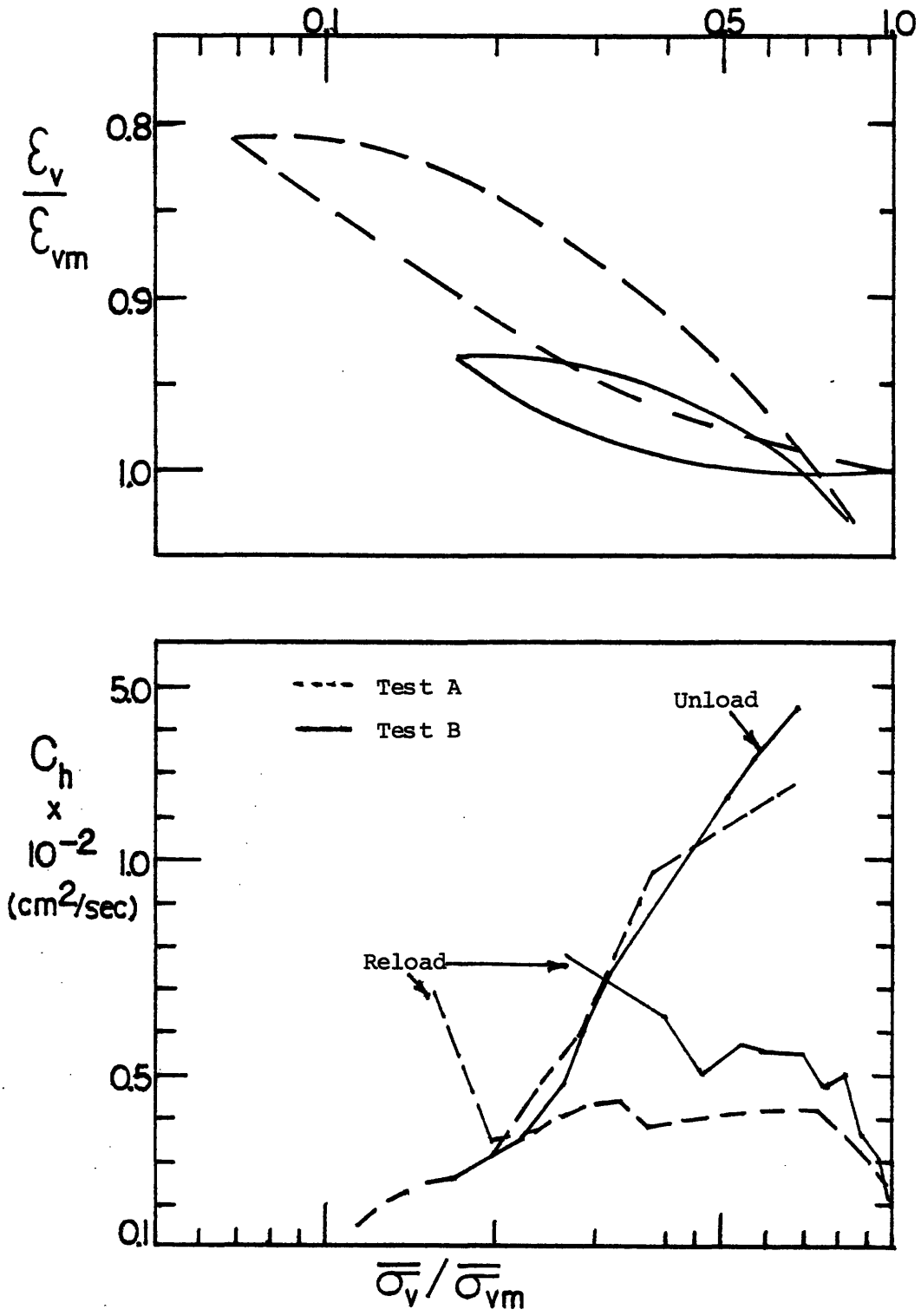

Figure 5.10 Effect of Unloading-Reloading Cycle on c_h

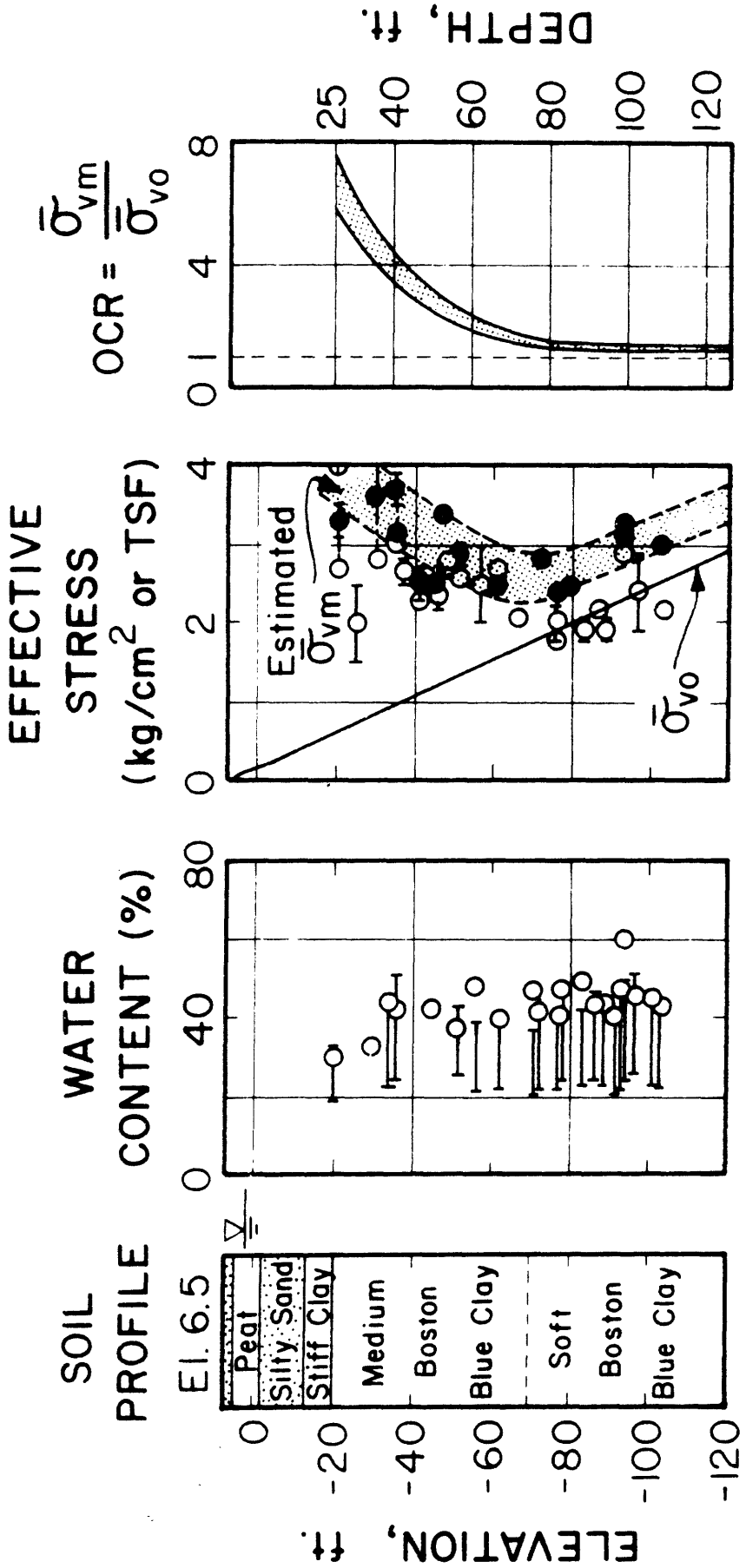

Figure 5.11 Soil Profile in Boston Blue Clay at Station 246 (from Baligh et al., 1981)

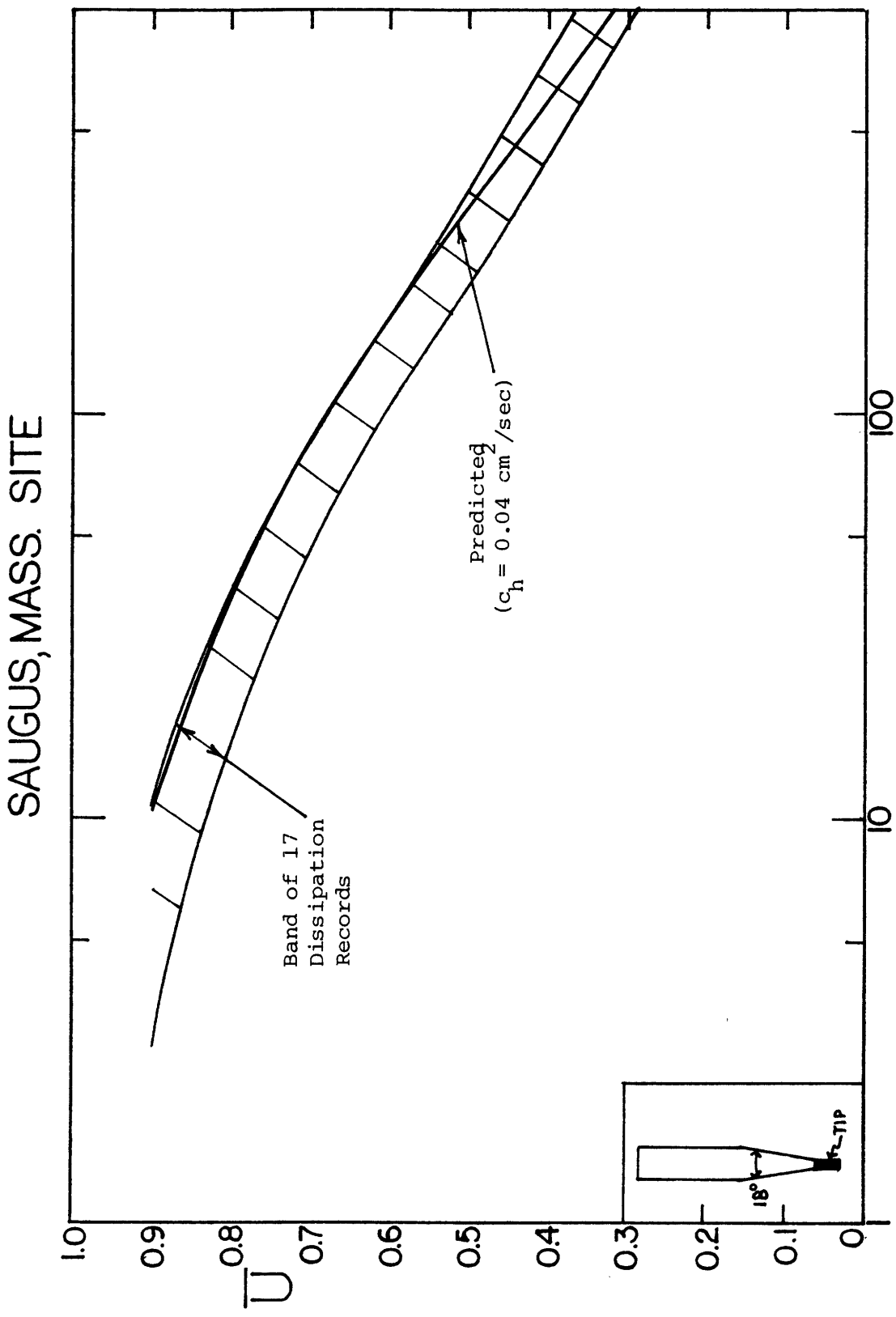

Figure 5.12 Measured Versus Predicted Dissipation Curves (from Baligh and Levadoux, 1980)

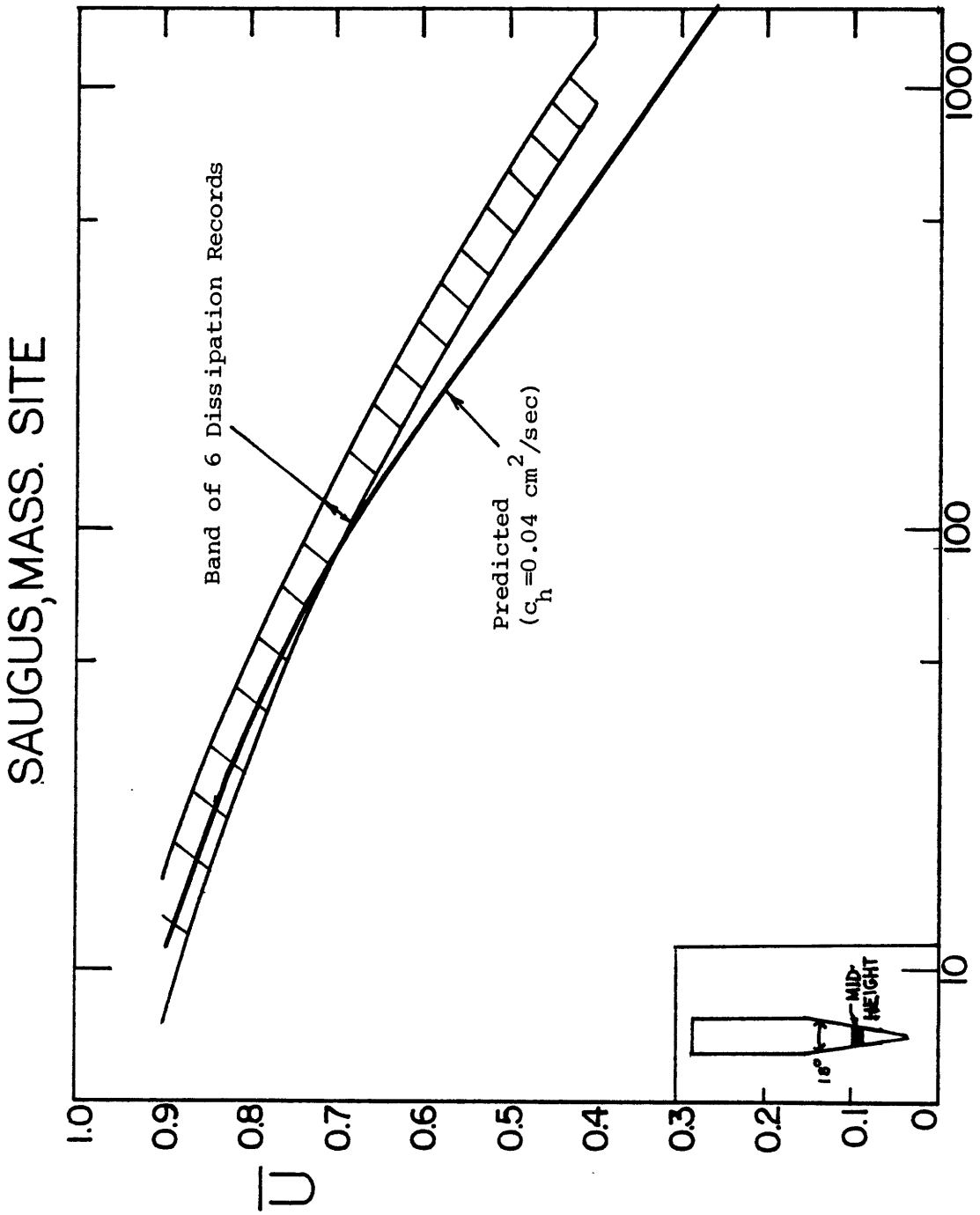

Figure 5.13 Measured Versus Predicted Dissipation Curves (from Baligh and Levadoux, 1980)

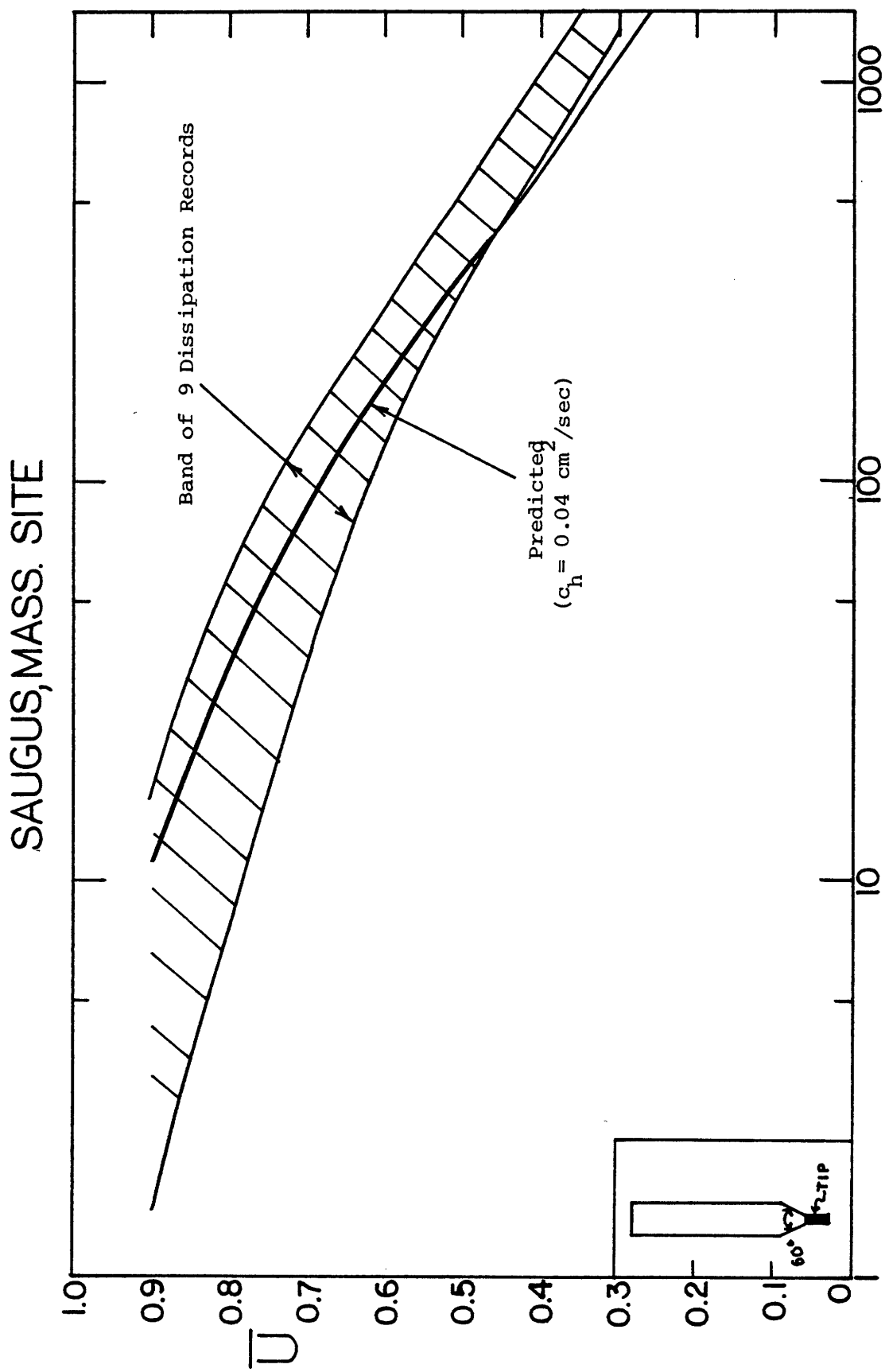

Figure 5.14 Measured Versus Predicted Dissipation Curves (from Baligh and Levadoux, 1980)

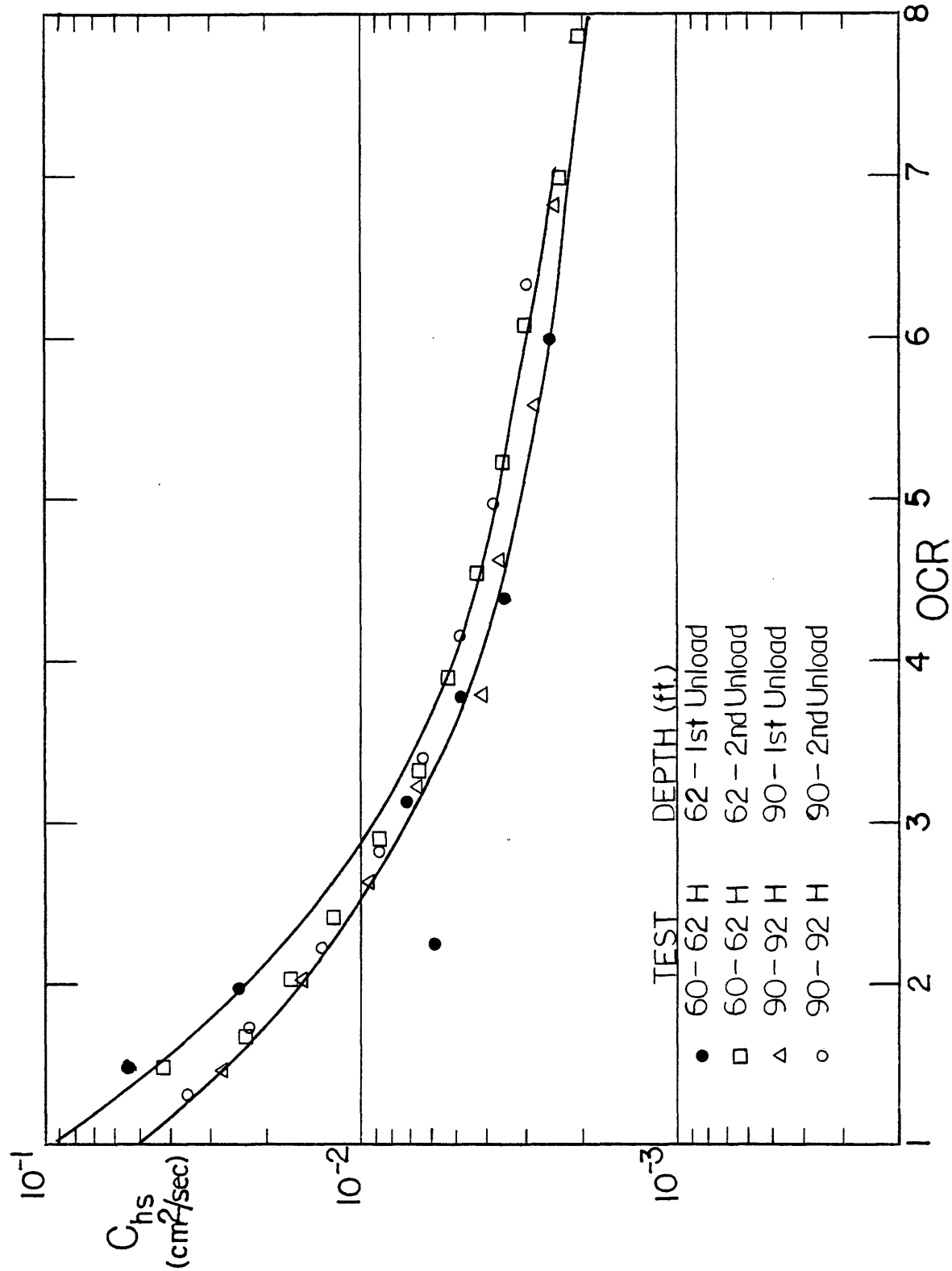

Figure 5.15 c_{hs} vs. OCR from CRSC Tests (from Ghantos, 1982)

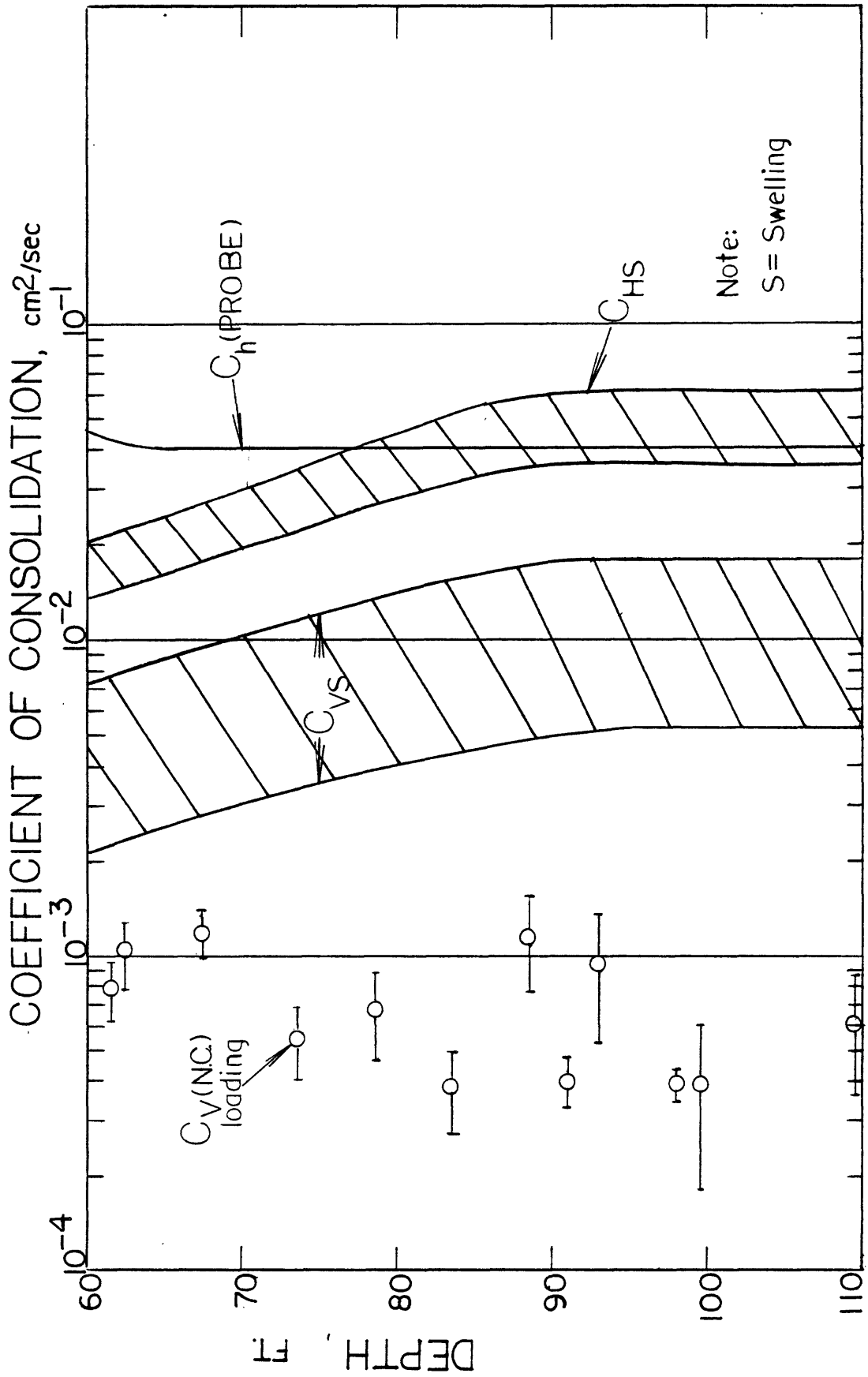

Figure 5.16 c_{hs} at the In Situ OCR vs. Depth from CRSC Tests (from Ghantos, 1982)

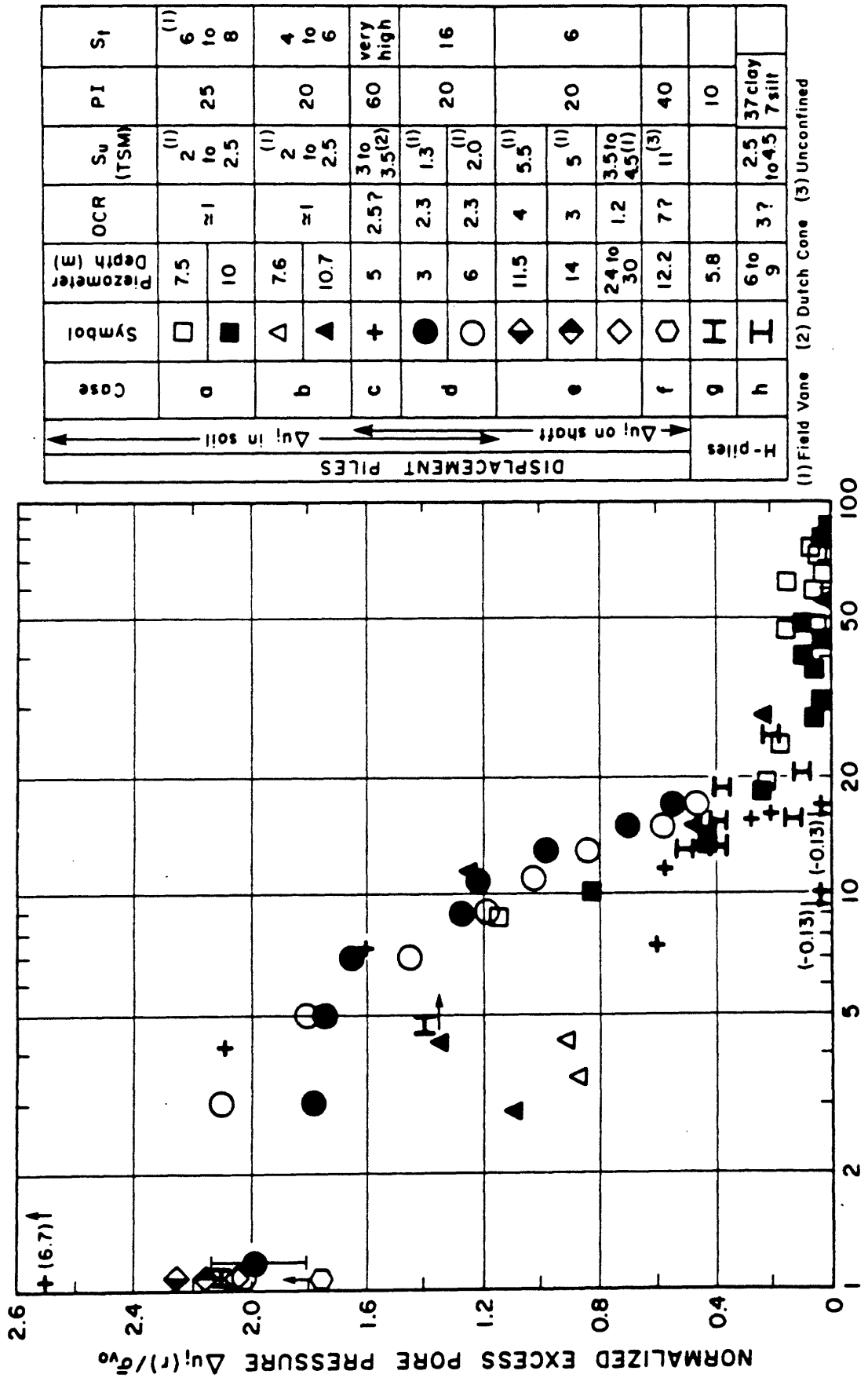

Case	Symbol	Piezometer Depth (m)	OCR	S_u (TSM)	PI	S_t
a	□	7.5	≥1	(1) 2 to 2.5	25	(1) 6 to 8
a	■	10	≥1	(1) 2 to 2.5	25	(1) 6 to 8
b	△	7.6	≥1	(1) 2 to 2.5	20	4 to 6
b	▲	10.7	≥1	(1) 2 to 2.5	20	4 to 6
c	+	5	2.5?	3 to 3.5(2)	60	very high
d	●	3	2.3	(1) 1.3	20	16
d	○	6	2.3	(1) 2.0	20	16
e	◆	11.5	4	(1) 5.5	20	6
e	◆	14	3	(1) 5	20	6
e	◇	24 to 30	1.2	3.5 to 4.5(1)	20	6
f	⬡	12.2	??	(3) 11	40	
g	H	5.8			10	
h	I	6 to 9	3?	2.5 to 4.5	37 clay 7 silt	

Figure 5.17a Excess Pore Pressure Measurements Due to Pile Installation in Clays - Case Histories (from Baligh and Levadoux, 1980)

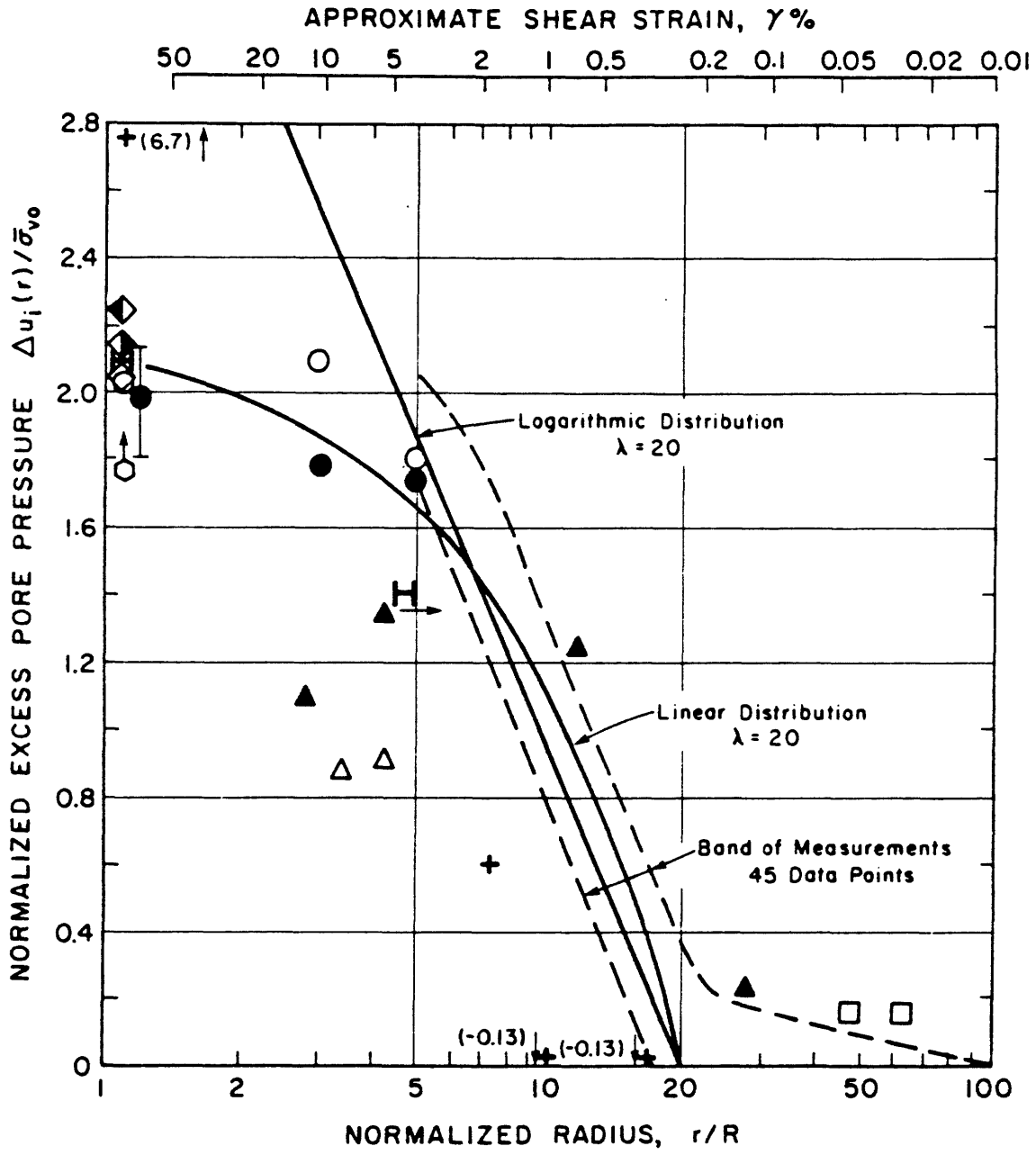

Figure 5.17b Excess Pore Pressure Measurements Due to Pile Installation in Clays - Simplified Distributions (from Baligh and Levadoux, 1980)

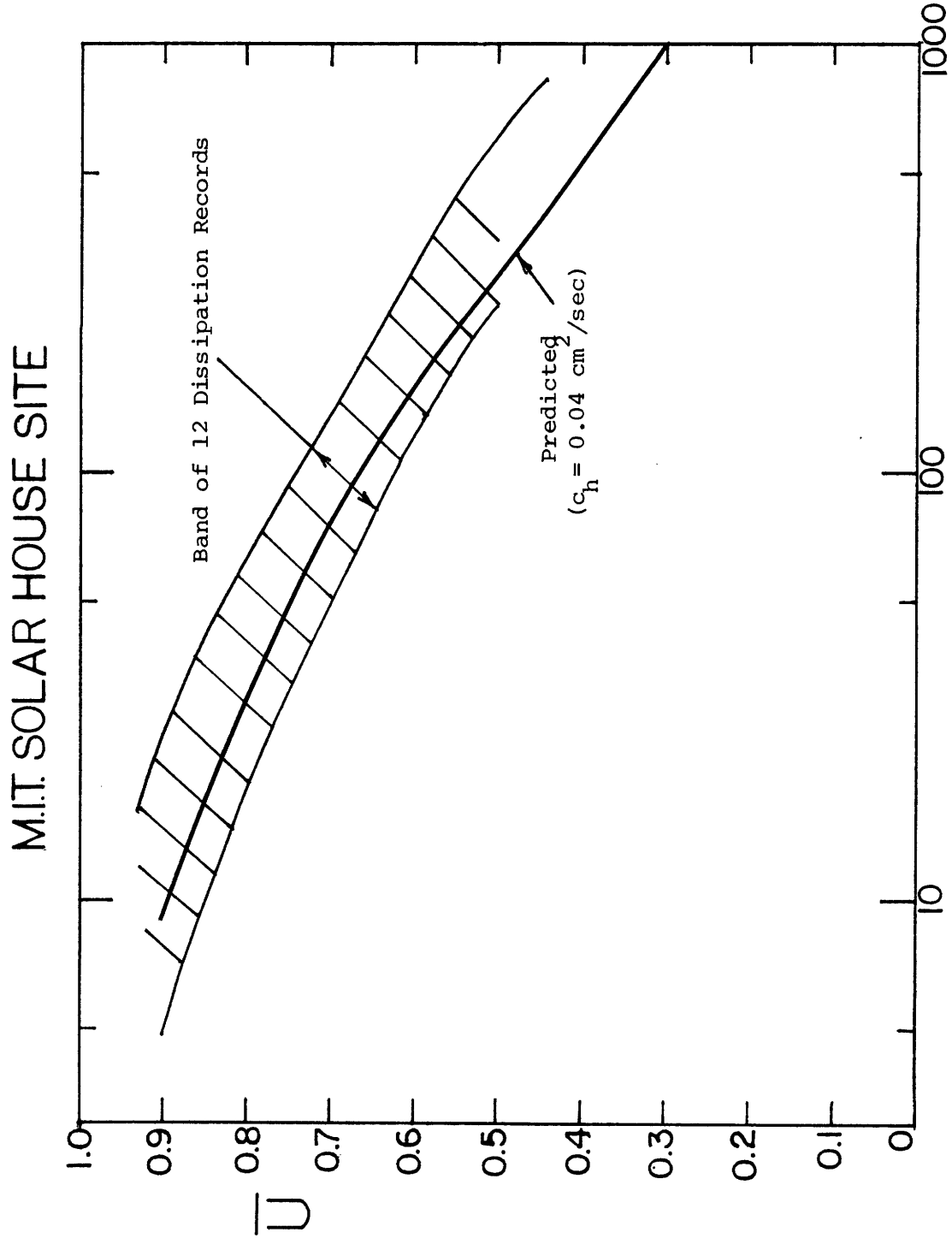

Figure 5.18 Measured Versus Predicted Dissipation Curves: MIT Solar House

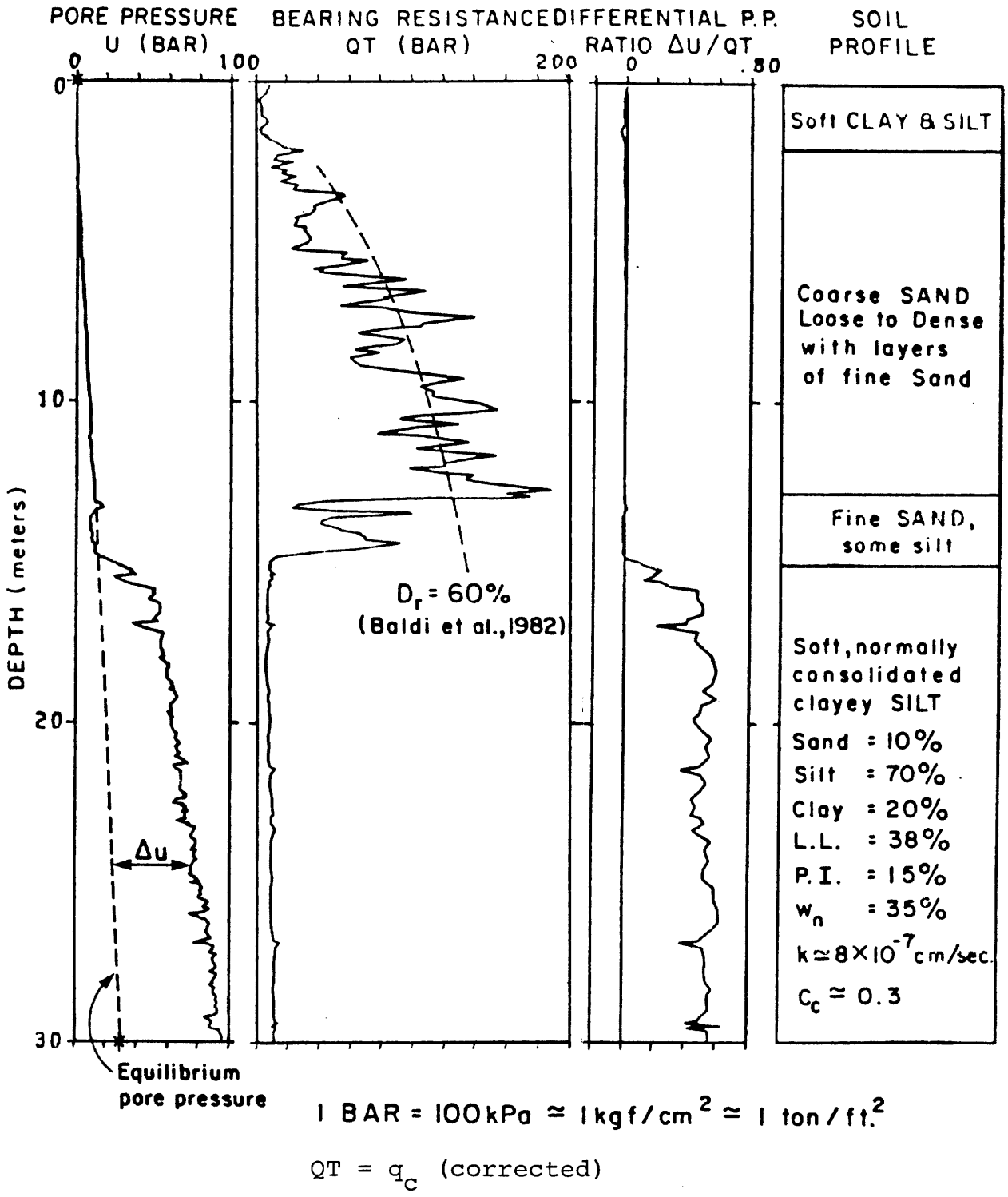

Figure 5.19 Soil Conditions at Richmond, B.C. Site (from Campanella et al., 1982)

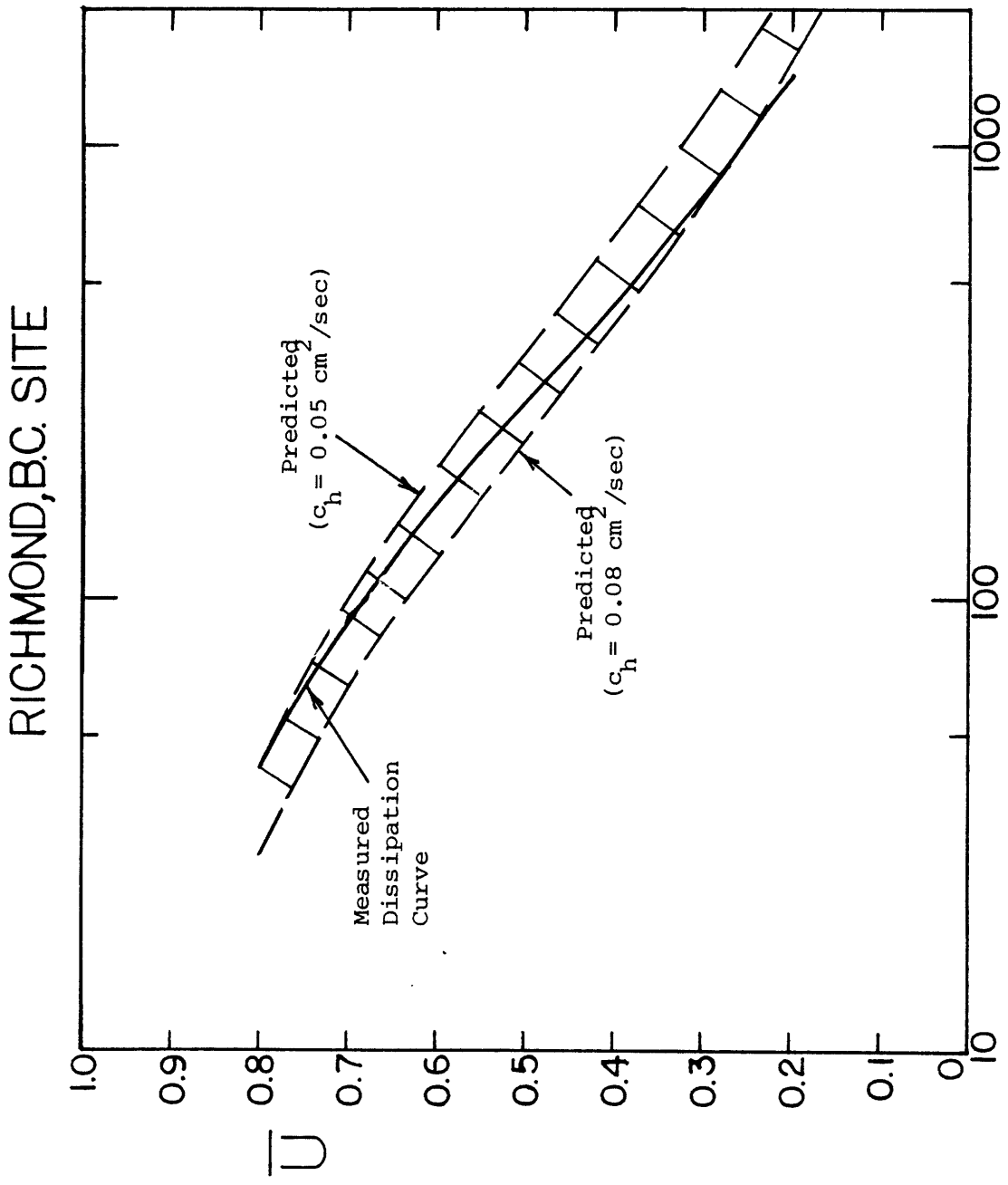

Figure 5.20 Measured Versus Predicted Dissipation Curves (from Campanella et al., 1982)

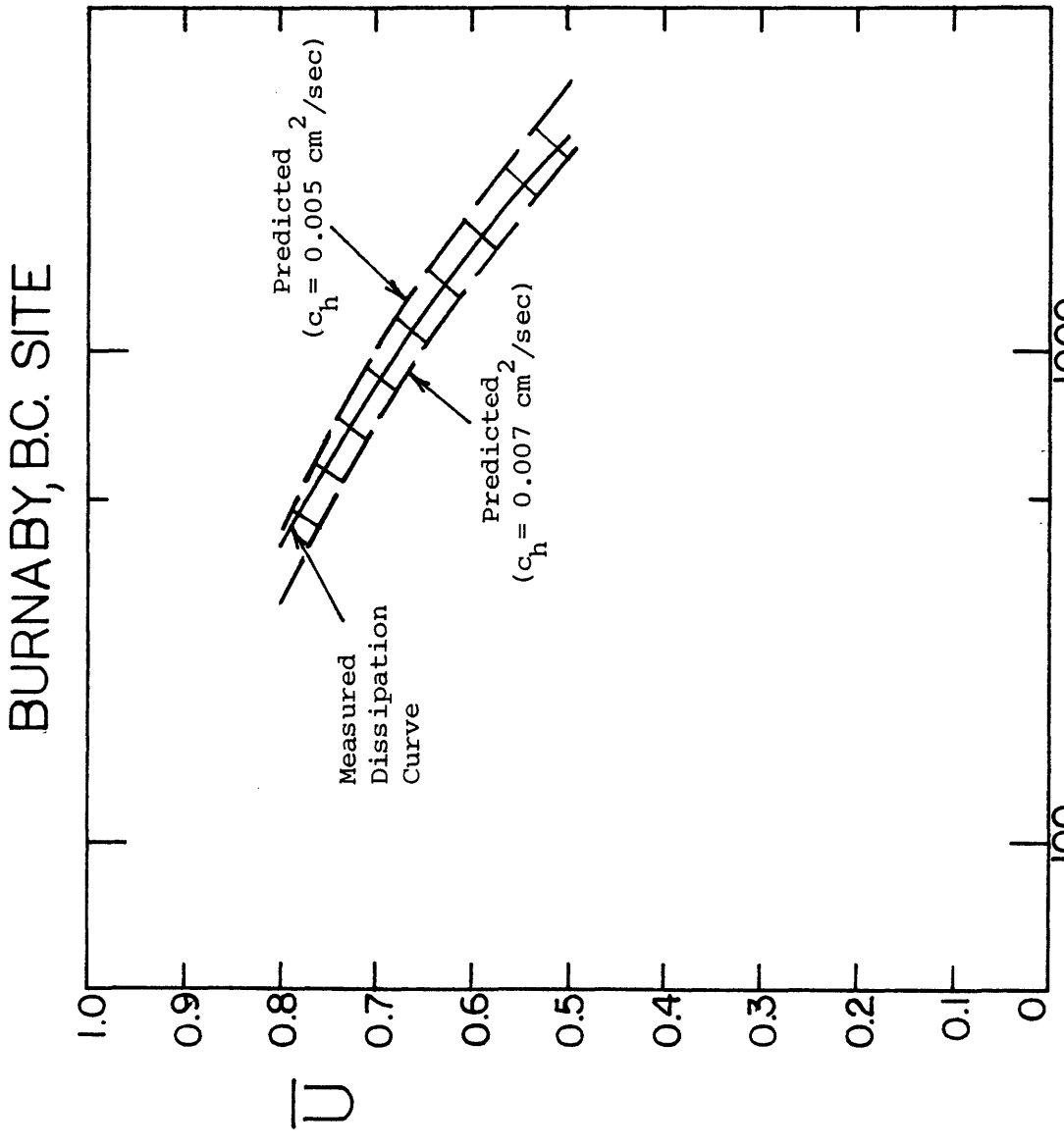

Figure 5.21 Measured Versus Predicted Dissipation Curves (from Gillespie and Campanella, 1981)

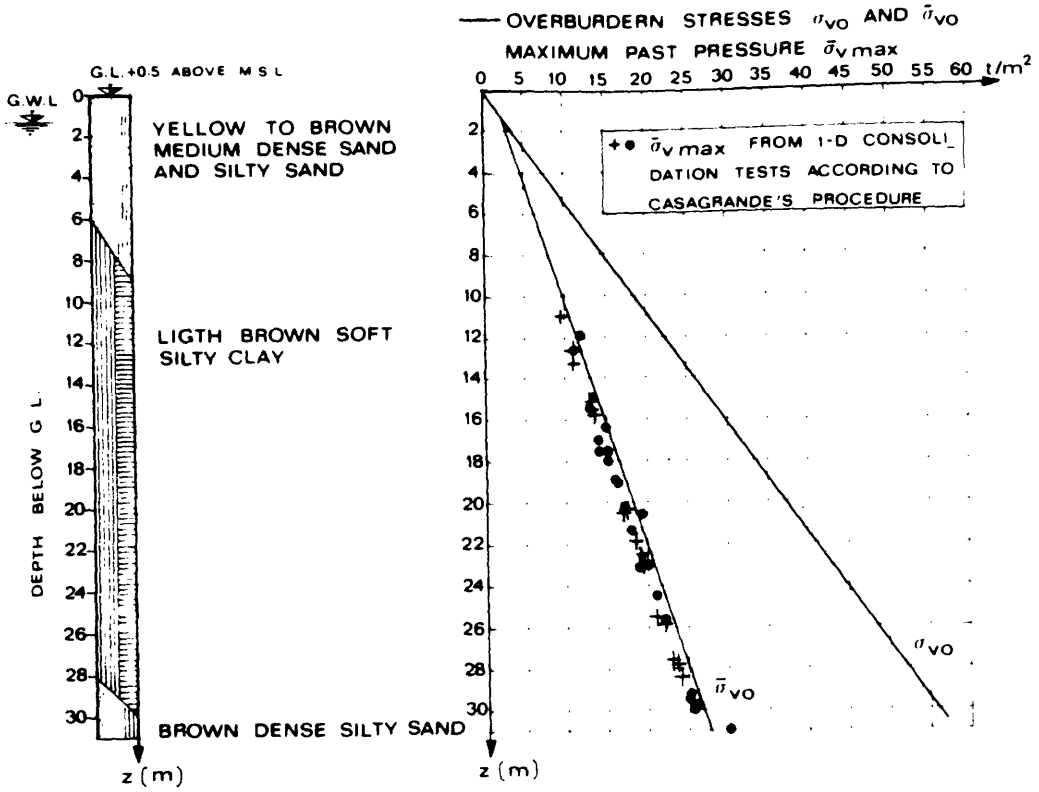

a) Porto Tolle Site

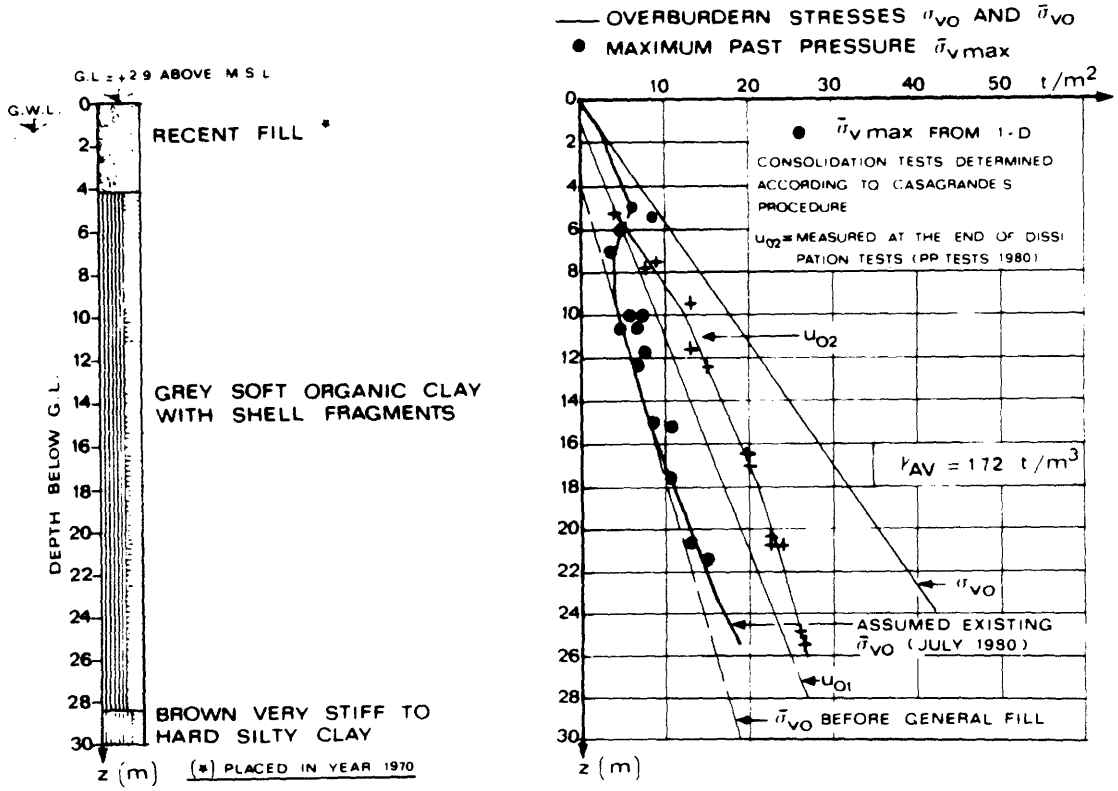

b) Trieste Site

Figure 5.22 Soil Profiles and Stress Histories of Two Italian Clays (from Battaglio et al., 1981)

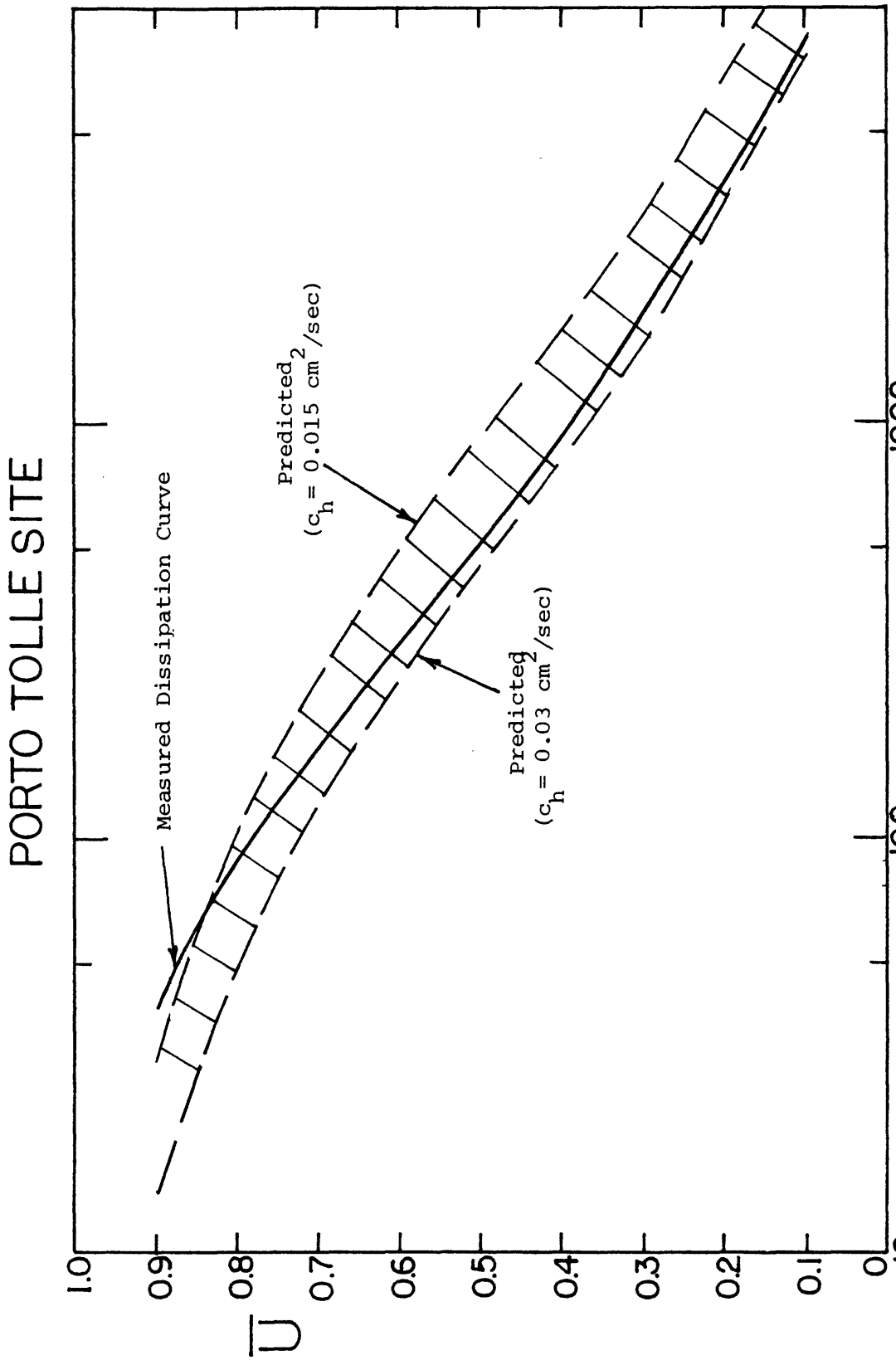

Figure 5.23 Measured Versus Predicted Dissipation Curves (from Battaglio et al., 1981)

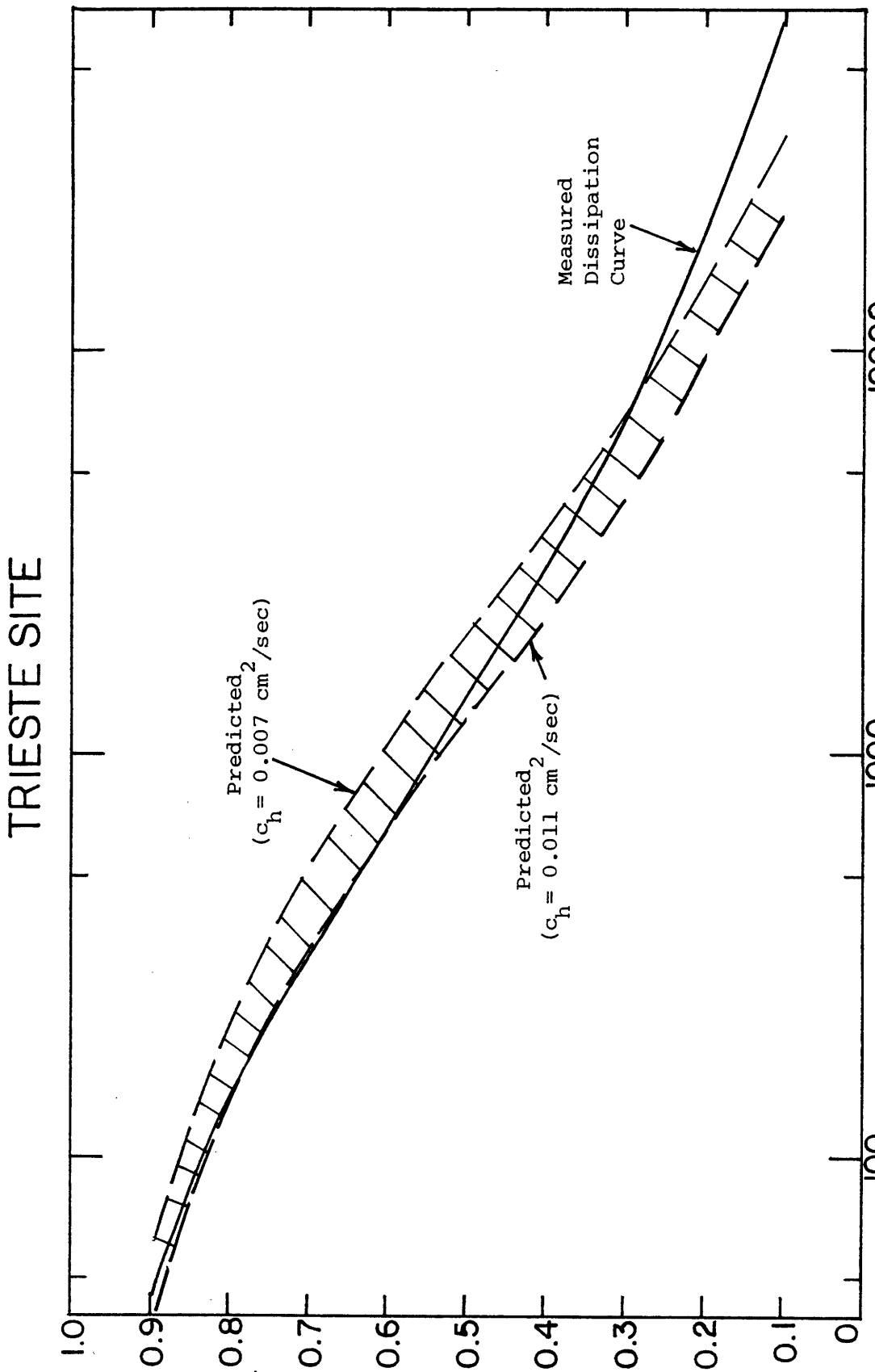

Figure 5.24 Measured Versus Predicted Dissipation Curves (from Battaglio et al., 1981)

CHAPTER 6

SUMMARY AND CONCLUSIONS

6.1 Scope and Objectives

The Piezocone Penetrometer represents an improvement over other testing devices in that it provides information which previously required two separate probes. By being able to measure cone resistance, q_c, pore pressure, u, and skin friction, f_s, it combines the measurement capabilities of the Dutch cone and piezometer probe into one tool. This thesis evaluates the adequacy of the Piezocone Penetrometer as an in situ device for evaluating engineering properties as diverse as stratigraphy, stress history, undrained shear strength, and coefficient of consolidation. This is achieved through a review of the past piezocone studies updated with the results of a recent geotechnical investigation program performed on the MIT campus. Discussions of other in situ devices for evaluating the engineering properties of clays and the soil properties below the MIT campus preceed the evaluation of the piezocone as a viable tool for soil investigation.

6.2 Review of In Situ Devices for Evaluating the Engineering Properties of Clays

In situ and laboratory testing provide two alternative approaches for evaluation of engineering properties of clays. In situ testing (e.g., penetration and field vane tests) have the advantage of making measurements on relatively undisturbed soil at substantial savings in time and cost compared to laboratory tests, but interpretation

of the data is highly empirical and often subjected to substantial uncertainty. Laboratory testing, on the other hand, offers the advantage of having well defined and directly controllable boundary conditions; however, a major problem facing most laboratory testing is the influence of sample disturbance. Disturbance reduces predictions of the maximum past pressures, $\bar{\sigma}_{vm}$, from consolidation tests and lowers the measured undrained shear strengths, s_u.

The field vane, pressuremeter, and cone penetration tests are the most commonly employed in situ tests used to evaluate the strength and consolidation characteristics of clays. These tests are quick, easy, and economical to perform and will yield semi-continuous to continuous records at a given investigation site. However, since the behavior of most clays is anisotropic and strain-rate dependent, the undrained shear strength, s_u, measured using these devices will likely be different. While all three tests can be employed to predict s_u; only the cone penetration test, supplemented with pore pressure measurements (e.g., the piezocone penetrometer) can be used to predict the consolidation characteristics of clays.

The field vane test is probably the most widely used in situ strength test in the U.S.A. The test is relatively easy and inexpensive to use, and will yield undisturbed as well as remolded s_u profiles. It is however, difficult to assess the failure mode associated with this test.

The pressuremeter tests, both the Menard Pressuremeter Test (MPT) and the Self-Boring Pressuremeter Test (SBPT), are widely used in France and England for the design of both shallow and deep foundations, but have found limited use elsewhere. The SBPT device is based on the same measurement concept as the Menard Pressuremeter; however, it can be inserted with far less disturbance. The SBPT offers the capability of making in situ measurements of strength-deformation properties of soils in greater detail and more accurately than heretofore possible. Evaluations of the SBPT show that the test yields quite reasonable estimates of the in situ total horizontal stress, especially in stiff clay, derives peak strengths in "soft" clay too high by a factor of two or more, and reasonably estimates of undrained shear modulus.

The cone penetration test (CPT), most widely performed using the electric quasi-static "Dutch" cone, yields continuous measurements of penetration resistance, q_c, and sleeve friction, f_s, as the cone penetrates through the clay strata. This data is primarily used to predict the undrained strength of clays and the friction angle and compressibility of sands. In 1975, Wissa et al. and Torstensson independently developed the piezometer probe. It consists of a fine porous element located on a conical tip connected hydraulically to an electro-mechanical pressure transducer which transmits the signal to the surface. The measured u values can give an indication of

the soil type and of changes in relative consistency or density. In addition, variations in the coefficient of consolidation of the soil layers can also be inferred from rates of pore pressure dissipation.

The Piezocone Penetrometer combines the measuring capabilities of the Dutch cone and the Piezometer Probe. In addition to its use in providing estimates of the stress history, strength and consolidation characteristics of soil (explained in detail later), the piezocone has applications in detecting failure planes from landslides or embankment failures, evaluating equilibrium groundwater conditions, and material classification.

6.3 Engineering Properties of Soils Underlying the MIT Campus

Ladd and Luscher (1965) summarized the engineering properties of the soils at several locations on the MIT campus. Since that time, soils investigations have been performed at other sites on the campus, however, aside from soil profiles, not much information regarding the engineering properties of the underlying clays were obtained from these studies.

In the fall of 1981, a geotechnical investigation program was initiated adjacent to the Solar House. The in situ testing program consisted of a total of 8 bore holes; 4 for piezocone penetration, 3 for field vane testing and one hole for undisturbed sampling. The laboratory testing program consisted of Atterberg limits, Standard Incremental Oedometer, and K_o-consolidated Direct Simple Shear tests.

Geologically, the MIT campus overlies the Boston Blue Clay formation which was formed during the wane of the late Pleistocene ice age (about 14,000 years ago) under a marine environment in the Boston Basin, probably not very far from the ice margin. The investigations at the nine sites mentioned in the text disclosed subsurface conditions that are compatible with the geologic site description. The generalized soil profile is:

Fill-mostly hydraulic, but some dumped

Loose organic silts and fine sand -some pockets of peat

Firm sand and gravel - widely varying in thickness

Boston Blue Clay -of medium consistency in higher elevations, soft in lower elevations

Glacial till - mixture of gravel, sand, silt and clay, usually very dense

Shale or slate - often weathered and/or fractured near the upper surface

6.3.1 Laboratory Testing Results

As is consistent with past Atterberg limits tests on BBC, the Plasticity Index for the Solar House clay is approximately 20%. The results of the one-dimensional consolidation tests show the clay below the MIT campus to be overconsolidated above elevation about -60 ft, with the maximum past pressure increasing as one goes up. The increased amount of precompression at the higher elevations is thought to be the result of desiccation of the upper

portion of the clay stratum. There does not appear to be any consistent variation in the degree of precompression with location, except that the clay at the Solar House may be somewhat more overconsolidated than usual above elevation -37 ft. This may be a result of recovering higher quality samples from the Solar House site as compared to other sites, which is further substantiated by the lower RR values obtained at this location. The coefficient of consolidation in the normally consolidated range, c_v(NC), averages 10.5 x 10^{-4} cm^2/sec below elevation -29 ft.

The strength testing program for the Solar House investigation consisted of twelve one-dimensionally consolidated undrained Direct Simple Shear (CK_oUDSS) tests. The tests were run according to the SHANSEP (an acronym for Stress History and Normalized Soil Engineering Properties) procedure. In all, seven different types of undrained shear strength tests were run on samples from seven different locations on the MIT campus. These test results as well as average strength profiles are presented in Chapter 3.

6.3.2 In Situ Testing

The piezocone penetrometer used for the Solar House program was penetrated at a steady rate of 2 cm/sec in the clay stratum at four different locations within the site. All cone resistance, pore pressure, and friction sleeve measurements were displayed on multi-channel high-speed

strip chart recorders for observations during field operations and were also recorded on magnetic tapes using a data logger for subsequent computer processing. Two of the four piezocone holes experienced some mechanical difficulties and yielded unreliable results.

As expected, the stiffer, more overconsolidated clays are characterized by higher point resistances and lower pore pressures than the softer, normally consolidated clays, where q_c and u exhibit linear increases with in situ effective stress and hydrostatic pore pressure, respectively. At the present time, the reliability of skin friction measurements in clay deposits seems to be questionable (Baligh et al., 1981).

Subsequent to penetration, dissipation of generated pore pressures occurs. Dissipation tests were run at 12 depths below 53 ft. From the dissipation versus time curves, the horizontal coefficient of consolidation, c_h, can be predicted utilizing one of the available theories for pore pressure dissipation (see Section 6.5).

Thirty eight field vane tests were performed within three vane test holes at the Solar House. These tests yielded peak and remolded shear strength profiles from which the sensitivity of the clay was determined.

6.4 Evaluation of Cone Resistance and Pore Pressure Measurements During Penetration

Simultaneous pore pressure, u, and cone resistance, q_c, measurements can be used to evaluate the stratigraphy,

stress history, and consolidation characteristics of soils. These penetration logs are very useful in helping to distinguish between sand, silt and clay layers in heterogeneous or stratified soil deposits. Also, the logs will identify sand and silt lenses as well as different sublayers that may exist within a homogeneous clay deposit.

Review of the u and q_c plots, and the normalized pore pressure data, $(u-u_o)/\overline{\sigma}_{vo}$, suggests that the Solar House clay can be divided into four sublayers. The top three layers indicate the "upper" clays where the soil is overconsolidated and exhibits variable behavior with depth. Below 77.5 ft, are the "lower" clays where u and q_c increase with u_o and $\overline{\sigma}_{vo}$, respectively, and $(u-u_o)/\overline{\sigma}_{vo}$ remains relatively constant. These stratifications will yield a detailed picture of soil variability which may help explain and/or verify laboratory test variability.

Simultaneous u and q_c measurements can be used to evaluate the stress history of a clay deposit. The relationship between u/q_c and overconsolidation ratio was first hypothesized by Baligh et al., (1980). High values of u/q_c should be associated with low OCR and vice-versa. Many studies have since been performed to further advance the usefulness and applicability of this relationship. While most agree that u/q_c is a good indicator of OCR, at the present time the absolute figures need as yet further discussion and research. Plots of u/q_c for the Solar House

investigation substantiate this reasoning. The relative trend of the plots supports Baligh's hypothesis; that is, as OCR decreases, u/q_c increases. When the clay becomes normally consolidated, u/q_c becomes constant at approximately 0.67. However, being that the location of the porous stone, the cone angle, and the cone shape all affect u and q_c measurements; further research is needed before u/q_c can be quantitatively related to stress history.

It has been well established, based on field and laboratory studies, that the stress-strain-strength characteristics of soft saturated clays are influenced by the mode of failure and the rate of strain (Ladd, 1975). This is extremely evident with regards to the undrained shear strength. Therefore, a problem exists in interpreting the "field strength" being measured from cone penetration tests.

Use of the penetration test (CPT) to evaluate the undrained shear strength of clays has been approached both theoretically and empirically. The theoretical approach utilizes one of the many solutions for the cone factor, N_k, for application into the equation:

$$q_c = N_k S_u + \sigma_o \qquad (6.1)$$

where, q_c = penetration resistance

s_u = undrained shear strength

σ_o = in situ total vertical, horizontal or octahedral stress

The theoretical solutions are based on three approaches that can be grouped as follows: plane strain slip-line, expansion of cavities, and steady penetration. All of these approaches rely on modifications of more rigorous solutions to simplified problems and cannot account for all of the factors which are known to influence the ultimate cone resistance (e.g., anisotropy in shear strength and cone angle).

The new two-dimensional strain path method introduced by Levadoux and Baligh (1980) was able to reasonably predict cone resistance profiles for the Saugus, Mass. site. However, the method is sophisticated and cannot be used readily in interpreting the q_c records or s_u profiles. More studies are necessary to answer what "field strength" the cone measures and which of the theoretical approaches, if any, is better suited to predict the undrained shear strength of clays.

The empirical approach to cone penetration, in lieu of directly predicting s_u utilizing a predetermined theoretical cone factor, employs a reference s_u that is determined from laboratory or field tests, to backfigure N_k utilizing equation 6.1. This N_k value will then be used on subsequent investigations to predict s_u from penetration resistance logs. The most widely reported test to estimate a reference s_u is the field vane test. Plate load, laboratory triaxial and Direct Simple Shear tests have also been used. Cone factors in the literature vary from 5-33

depending on the testing method used to predict s_u and the different clay region. For the Solar House site, cone factors were calculated using field vane as well as DSS strength results, and fall within a range of 13-22 and 18-32, respectively. Below 65 ft (OCR=2), the N_k values plot within a fairly narrow band, 18-22 for s_u(FV) and 26-32 for s_u(DSS).

When Bjerrum's correction factor is applied to cases where N_k is determined by s_u(FV), the corrected N_k values fall within a range of 14 ± 3. Obviously, this helps to reduce the scatter in cone factor values, but cannot totally account for the dependence of N_k on some of the inherent limitations of the empirical approach.

Clearly, because of the scatter of N_k values and the limitations of the empirical analysis, no single N_k value exists that will cover all types of clays, penetrometers, and test conditions. However, for a given clay deposit, a given penetrometer, and given test conditions, it seems likely that there should be a unique relationship between cone tip resistance and s_u (Kjekstad, 1978).

Recently, empirical studies have been performed to relate $\Delta u(u-u_o)$ to s_u via a pore pressure factor $N_{\Delta u}$. More research is still needed before this approach can be used in practice.

6.5 Pore Pressure Dissipation After Cone Penetration

6.5.1 Solutions to Predict the Horizontal Coefficient of Consolidation, c_h

Steady cone penetration in saturated clays causes undrained shearing and develops excess pore pressures in the soil. Once penetration is interrupted, these pore pressures will dissipate and eventually reach the equilibrium value u_o. Many authors (Soderberg, 1962; Torstensson, 1977; Randolph and Wroth, 1979; Baligh and Levadoux, 1980; Battaglio et al., 1981; and Tumay et al., 1982) have developed solutions to predict the consolidation and flow characteristics of cohesive deposits from the pore pressure dissipation data.

Torstensson suggests that the pore pressures in the soil caused by steady cone penetration can be estimated by one-dimensional (radial) solutions corresponding to cylindrical and spherical cavities. The cavity expansion model adopted predicts a logarithmic initial pore pressure distribution assuming the soil to behave as an elastic-perfectly plastic material. Torstensson utilizes linear uncoupled one-dimensional finite difference consolidation analyses to estimate normalized excess pore pressure dissipation curves. In order to estimate the coefficient of consolidation, c_h, he proposes matching of predictions and measurements at 50% consolidation ($\bar{u}$=0.5).

Baligh and Levadoux (1980) analyze the deep cone penetration in clays as an axisymmetric two-dimensional

steady-state problem with the strain path method, which assumes that strains and deformations in the soil are primarily imposed by kinematic requirements. The normalized excess pore pressures due to cone penetration were predicted on the basis of laboratory data on normally consolidated Boston Blue Clay. However, it is shown that the strain path method will predict satisfactory normalized excess pore pressures in other clays as well. Baligh and Levadoux (1980) use two-dimensional linear uncoupled finite element analyses to obtain the variation of pore pressures with time.

Predictions of c_h can be achieved graphically by comparing the measured normalized dissipation ($\bar{u}$ vs. log t) curves to the recommended curves of $\bar{u}$ vs. log T. The measured dissipation curve ($\bar{u}$ vs. log t) is plotted to the same scale of $\bar{u}$ vs. log T and translated horizontally with respect to the predicted curve (while maintaining equality of $\bar{u}$) until the best agreement is achieved.

At a given degree of consolidation, the predicted c_h (probe) is obtained from the expression:

$$c_h \text{ (probe)} = \frac{R^2 T}{t} \qquad (6.2)$$

where, R = radius of the cone shaft

t = measured time to reach this degree of consolidation

T = time factor

An analytical method to check the validity of the prediction method consists of determining c_h at different $\bar{u}$. Large differences between c_h at various degrees of consolidation indicate an inadequate initial distribution of excess pore pressure or significant coupling or creep behavior.

Several empirical and curve fitting procedures have been developed over the last few years by Battaglio et al., (1981), Jones and Van Zyl (1981), Tavenas et al. (1982), and Tumay et al., (1982) to predict c_h(probe).

Battaglio and his co-workers use a trial and error method to obtain a dimensionless u vs. T relationship which best matches the field dissipation curves. The initial excess pore pressures are estimated using the one-dimensional cavity expansion solutions and the consolidation process is modeled by means of a one-dimensional finite difference solution to Terzaghi's Equation.

The Jones and Van Zyl empirical approach simply plots time to 50% dissipation, t_{50}, versus the reciprocal of the vertical coefficient of consolidation obtained from laboratory oedometer tests, from which they compute c_v from the slope of a straight line fit through the origin of the results. Tavenas et al. state that c_h should be a function of the permeability k and the modulus of deformability of the intact clay M. In overconsolidated clays, M is related to the maximum past pressure, $\bar{\sigma}_{vm}$, by $M=m\bar{\sigma}_{vm}$ so that c_h would be more or less constant and equal to:

$$c_h = \frac{K\bar{\sigma}_{vm}\, m}{\gamma_w} \quad . \tag{6.3}$$

Tumay et al., recommend a curve fitting procedure for predicting the consolidation coefficient of cohesive deposits. They present typical theoretical dissipation curves and show that there is a straight line portion of every dissipation curve. Each of these straight lines, when extended, meet at 90% consolidation; the point of intersection called T'_{90}. Also, Tumay et al., (1982) showed that all the parameters that affect dissipation, i.e., anisotropy, disturbed zone around the cone, location of piezometric element, and cone angle, will be least pronounced during the final stages of consolidation. In other words, they feel that all dissipation curves will converge at about 90% consolidation and called this converging point T_{90}. The procedure adopted to compute the consolidation coefficient using Tumay's method is as follows:

1) Calculate the ratio of $\frac{\log T_{90}}{\log T'_{90}}$ which equals a constant A

2) Estimate t_{90} by the expression:

$$t_{90} = 10^{A \log t'_{90}}$$

where, t'_{90}=time of 90% dissipation at the straight line portion

t_{90}= actual time of 90% dissipation

3) Calculate c_h by the expression:

$$c_h = \frac{T_{90}}{t_{90}} (R^2)$$

The Tumay, Jones, and Tavenas solutions are all limited to predicting c_h at one level of dissipation. The empirical solutions of Jones and Tavenas rely mainly on laboratory test results for c_h and permeability. As will be shown in the following section, c_h values from consolidation tests can vary depending on the type of test, loading cycle, and stress level. One must first understand the consolidation process around probes and also understand the limitations of c_h(lab) values before an attempt to draw empirical relationships from the two measuring systems can be made.

Although the Battaglio solution appears to reasonably predict c_h at all levels of dissipation, and compares well with reference c_h values, use of the solution is complex and time-consuming.

6.5.2 Evaluation of c_h From Laboratory Tests

Pore pressure dissipation during early stages of consolidation around cones takes place in a recompression mode (as opposed to virgin compression) for both normally consolidated and slightly overconsolidated clays with OCR $\leq$ 4.

Therefore, the objective of a laboratory testing program should be to evaluate c_h(probe) with lab measurements of c_h obtained from tests when the soil is in the overconsolidated range, i.e., c_h(OC). In consolidation tests, this would be during an unload or a reload cycle. Initial loading is largely influenced by sample disturbance which lowers c_h(OC), Ladd (1973), and is therefore not suitable for use in evaluating c_h(probe).

Consolidation tests, either the standard incremental oedometer or the constant rate of strain consolidation, CRSC, (Wissa et al., 1971) are the laboratory techniques most widely used to evaluate c_h(OC). CRSC tests run on horizontal samples allow measurement of c_h(OC) at small stress increments. On the other hand, for the range of OCR of interest (estimated to be $\leq$ 3), the oedometer test is inadequate to evaluate c_h(OC) for the following reasons:

1) The very high gradients at the start of an unload or a reload cycle are overlooked by the curve fitting procedures used to calculate c_h which tend to emphasize the data towards the middle of the load increment.

2) Oedometer tests can only yield average values for an increment of loading.

The degree of overconsolidation at which dissipation takes place in not presently known. However, it is felt that the value of c_h at the in situ OCR is a good starting point from which to evaluate c_h(probe) until further information on this subject is known.

Furthermore, one would want to compare c_h(probe) values with c_h(lab) values measured at the in situ OCR during a reload cycle, since this best simulates the actual field occurrence. However, as was shown, attempts to evaluate c_h(lab) during recompression will lead to erroneous results because at a given OCR, c_h(reload) is a function of the size of the unload cycle. Instead, it is felt that c_h measured during unloading will yield proper values for comparison with c_h(probe).

6.5.3 Case Histories

The applicability of the Baligh and Levadoux (1980) and Torstensson's (1977) cylindrical and spherical solutions to dissipation of excess pore pressures were evaluated through a series of case studies. The first case study, Saugus, Massachusetts, showed that the Baligh and Levadoux solution not only predicts very similar c_h(probe) values for three probes, with different geometries and stone locations, but also predicts c_h(probe) values which coincide well with c_h(lab) reference values. On the other hand, it was shown that Torstensson's spherical solution does not accurately model pore pressure dissipation. At best, this solution underpredicts c_h(probe) by a factor of five. Also, it was demonstrated that Torstensson's cylindrical solution cannot accurately predict the initial excess pore pressure distribution needed to model pore pressure dissipation.

Since the Baligh and Levadoux solution accurately predicts c_h for all types of probe geometries and stone locations, and bearing in mind the shortcomings of Torstensson's solutions, the Baligh and Levadoux solution was only applied to predict c_h(probe) in the remainder of the case studies. From review of these case studies (including the MIT Solar House, two Canadian sites, and two Italian sites), it is apparent that the Baligh and Levadoux solution can predict the horizontal coefficient of consolidation of cohesive deposits with reasonable accuracy. It should be noted that this coefficient should be used in problems involving unloading or reloading.

BIBLIOGRAPHY

PROCEEDINGS

A) Proceedings of the First European Symposium on Penetration Testing, Stockholm, Sweden, June 1974, Vols. 1-2.

Vol. 2.2

1. Anagnostopoulos, A. "Evaluation of the Undrained Shear Strength from Static Cone Penetration Tests in Soft Silty Clay in Patros, Greece," pp. 13-14.

2. Eide, O., "Correlation Between Cone Tip Resistance and Field Vane Shear Strength," pp. 128-129.

3. Marsland, A., "Comparisons of the Results from Static Penetration Tests and Large in situ Plate Tests in London Clay," pp. 245-252.

B) Proceedings of the ASCE Specialty Conference on In Situ Measurement of Soil Properties, Raleigh, North Carolina, June 1975, Vol. I and II. Published by ASCE.

Vol. I

1. Massarch, K.R., Broms, B.B., and Sundquist, O., "Pore Pressure Determination with Multiple Piezometer," pp. 260-265.

2. Wissa, A.E.Z., Martin, R.T., and Garlanger, J.E., "The Piezometer Probe," pp. 536-545.

Vol. II

1. Ladd, C.C., "Discussion on Measurement of In Situ Shear Strength," pp. 153-160.

2. Schmertmann, J.H., "Measurement of In-Situ Shear Strength," pp. 57-138.

3. Torstensson, B.A., "Pore Pressure Sounding Instrument," pp. 48-54.

C) Proceedings of the ASCE convention, Session 35 on Cone Penetration Testing and Experience, St. Louis, Missouri, October, 1981. Edited by Norris, G.M. and Holtz, R.D.

1. Baligh, M.M., Azzouz, A.S., Wissa, A.E.Z., Martin, R.T., and Morrison, M.J., "The Piezocone Penetrometer," pp. 247-263.

2. Battaglio, M., Jamiolkowski, M., Lancelotta, R., and Maniscalco, R., "Piezometer Probe Test in Cohesive Deposits," pp. 264-302.

3. Campanella, R.G., and Robertson, P.K., "Applied Cone Research," pp. 343-362.

4. DeRuiter, J., "Current Penetrometer Practice," pp. 1-48.

5. Jones, G.A., Van Zyl, D., and Rust, E., "Mine Tailings Characterization by Piezometer Cone," pp. 303-324.

6. Tumay, M.T., Boggess, R.L., and Acar, Y., "Subsurface Investigations with Piezo-cone Penetrometer," pp. 325-342.

D) Proceedings of the Second European Symposium on Penetration Testing, Amsterdam, May 1982. Edited by Verruijt, A., Beringen, F.L., and DeLeeuw, E.H., publisher: A.A. Balkema, Rotterdam.

1. Campanella, R.G., Gillespie, D., and Robertson, P.K., "Pore Pressures During Cone Penetration," pp. 507-513.

2. Cancelli, A., Guadagnini, R., and Pellegrini, M., "Friction-Cone Penetration Testing in Alluvial Clays," pp. 513-518.

3. DeRuiter, J., "The Static Cone Penetration Test - State of the Art Report," pp. 389-406.

4. Jamiolkowski, M., Lancellotta, R., Tordella, L., and Battaglio, M., "Undrained Strength from CPT ," pp. 599-605.

5. Jones, G.A., and Rust, E., "Piezometer Penetration Testing CUPT," pp. 607-613.

6. Koumoto, T., amd Kaku, K., "Three-Dimensional Analysis of Static Cone Penetration into Clay," pp. 635-640.

7. Lacasse, S., and Lunne, T., "Penetration tests in two Norwegian Clays," pp. 661-670.

8. Smits, F.P., "Penetration Pore Pressure Measured with Piezometer Cones," pp. 871-876.

9. Tavenas, F., Leroueil, S., and Roy, M., "The Piezocone Test in Clays: Use and Limitations," pp. 889-894.

10. Torstensson, B.A., "A Combined Pore Pressure and Point Resistance Probe," pp. 903-908.

11. Tumay, M.T., Yilmaz, R., Acar, Y., and DeSeze, E., "Soil Exploration in Soft Clays with the Quasi-Static Cone Penetrometer," pp. 915-922.

12. Zuideberg, H.M., Schaap, L.H.J., and Beringen, F.L., "A Penetrometer for Simultaneously Measuring of Cone Resistance, Sleeve Friction and Dynamic Pore Pressures," pp. 963-970.

REFERENCES

1. Acar, Y., "Piezo-cone Penetration Testing in Soft Cohesive Soils," Internal Report, Louisiana State University, Civil Engineering Department, 1982, Activity Report No. 4, 81 p.

2. Al-Awkati, Z., "On Problems of Soil Bearing Capacity at Depth," Ph.D. Dissertation, Dept. of Civil Engineering, Duke University, 1975, 204 p.

3. ASTM, "Vane Shear and Cone Penetration Resistance Testing of In Situ Soils," ASTM STP 399, 1965, 47 p.

4. Azzouz, A.S., Baligh, M.M., and Ladd, C.C., "Cone Penetration and Engineering Properties of Soft Orinoco Clay," Proceedings, International Conference on the Behavior of Offshore Structures, Cambridge, Mass., 1982, 53 p.

5. Baligh, M.M., "Theory of Deep Site Static Cone Penetration Resistance," Research Report R75-56, No.517, September 1975, MIT, Cambridge, Mass., 133 p.

6. Baligh, M.M., and Scott, R.F., "Wedge Penetration in Clays," Geotechnique, 1976, Vol.26, No.1, pp. 185-208.

7. Baligh, M.M., Vivatrat, V., and Ladd, C.C., "Cone Penetration in Soil Profiling," Journal of the Geotechnical Engineering, ASCE, Vol.106, No.GT4, Proceeding Paper 15377, April 1978, pp. 447-461.

8. Baligh, M.M., Vivatrat, V., and Ladd, C.C., "Exploration and Evaluation of Engineering Properties for Foundation Design of Offshore Structures," Research Report R78-40, Order No.607, Department of Civil Engineering, MIT, Cambridge, Mass., Dec.1978, 268 p.

9. Baligh, M.M., and Levadoux, J.-N., "Pore Pressure Dissipation after Cone Penetration," Research Report R80-11, Order No.662, Dept. of Civil Engineering, MIT, Cambridge, Mass., April 1980, 367 p.

10. Begemann, H.K.S., "The Friction Jacket Cone as an Aid in Determining the Soil Profile," Proc., 6th International Conference on Soil Mechanics and Foundation Engineering, Montreal, Canada, 1965, Vol. 1, pp. 17-20.

11. Bishop, R.F., Hill, R., and Mott, N.F., "Theory of Indentation and Hardness Tests," Proceedings, Physical Society of London, 1945, Vol. 57, No. 321, pp. 147-159.

12. Bjerrum, L., "Embankments on Soft Ground," State-of-the-Art Report, Proceedings, ASCE Specialty Conference on Performance of Earth and Earth-Supported Structures, Layfayette, 1972, Vol. 2, pp. 1-54.

13. Durgunoglu, H.T. and Mitchell, J.K., "Static Penetration Resistance of Soils," Research Report Series 14, Issue 24, Space Science Laboratory, University of California, Berkeley, 1973, pp. 223.

14. Gibson, R.E., Discussion of G. Wilson, "The Bearing Capacity of Screw Piles and Screwcrete Cylinders," Journal of the Institute of Civil Engineers, 1950, Vol. 34, No. 4, 382p.

15. Gillespie, D. and Campanella, R.G., "Consolidation Characteristics from Pore Pressure Dissipation After Piezometer Cone Penetration," Soil Mechanics Series No. 47, Department of Civil Engineering, University of British Columbia, Vancouver, Canada, May, 1981, 18p.

16. Jones, G.A. and Van Zyl, D.J.A., "The Piezometric Probe - A Useful Investigation Tool," Proceedings, 10th International Conference on Soil Mechanics and Foundation Engineering, Stockholm, Sweden, 1981, Vol. 3, pp. 489-495.

17. Kjekstad, O., Lunne, T., and Clausen, C.J.F., "Comparison Between In-Situ Cone Resistance and Laboratory Strength for Overconsolidated North Sea Clays," Marine Geotechnology, Vol. 3, No. 1, 1978, pp. 23-36

18. Koutsoftas, D. and Fischer, T.A., "In Situ Undrained Shear Strength of Two Marine Clays," Journal of the Geotechnical Engineering Division, ASCE, Vol. 102, No. GT9, Proc. Paper 12431, September, 1976, pp. 989-1005.

19. Ladayni, B., "Expansion of a Cavity in a Saturated Clay Medium," Journal of the Soil Mechanics and Foundations Division, ASCE, Vol. 89, No. SM4, July, 1963, pp. 127-161.

20. Ladayni, B. and Eden, W.J., "Use of the Deep Penetration Test in Sensitive Clays," Proceedings, 7th International Conference on Soil Mechanics and Foundation Engineering, Mexico, 1979, Vol. 1, pp. 225-230.

21. Ladd, C.C., "Stress-Strain Modulus of Clay in Undrained Shear," Journal of Soil Mechanics and Foundations Division, ASCE, 1964, Vol. 90, No. SM5, pp. 103-132.

22. Ladd, C.C., "Strength Parameters and Stress-Strain Behavior of Saturated Clays," Research Report R71-23, Soils Publication 278, 1971.

23. Ladd, C.C., Foott, R., Ishihara, K., Schlosser, F., and Poulos, H.G., "Stress-Deformation and Strength Characteristics," Proceedings, 9th International Conference on Soil Mechanics and Foundation Engineering, Tokyo, 1977, pp. 421-494.

24. Ladd, C.C., "Estimating Settlements of Structures Supported on Cohesive Soils," 1982 Class Notes, 113p.

25. Lambe, T.W., Soil Testing For Engineers, John Wiley and Sons, New York, 1951.

26. Lambe, T.W., "Shallow Foundations on Clay," Proceedings, Symposium on Bearing Capacity and Settlement of Foundations, Duke University, Durham, N.C., 1967.

27. Leroueil, S., Tavenas, F.A., Brucy, F., LaRochelle, P., and Roy, M., "Behavior of Dectructured Natural Clays," Journal of Geotechnical Engineering Division, ASCE, Vol. 105, No. GT6, June, 1979, pp. 759-778.

28. Levadoux, J.-N. and Baligh, M.M., "Pore Pressures During Cone Penetration in Clays," Research Report R80-15, Order No. 666, Department of Civil Engineering, M.I.T., Cambridge, Mass., April, 1980, 310p.

29. Lunne, T., Eide, O., and DeRuiter, J., "Correlations Between Cone Resistance and Vane Shear Strength in Some Scandinavian Soft to Medium Stiff Clays," Canadian Geotechnical Journal, Vol. 13, 1976, pp. 430-441.

30. Marsland, A., "The Interpretation of In Situ Tests in Glacial Clays," Proceedings, Conference on Offshore Site Investigation, Society of Underwater Technology, London, England, 1979, pp. 217-230.

31. Meyerhoff, G.G., "The Ultimate Bearing Capacity of Foundations," Geotechnique, 1951, Vol. 2, No. 4, pp. 301-302.

32. Meyerhoff, G.G., "The Ultimate Bearing Capacity of Wedge-Shaped Foundations," Proceedings, 5th International Society of Soil Mechanics and Foundation Engineering, 1961, Vol. 2, pp. 105-109.

33. Randolph, M.F. and Wroth, C.P., "An Analytical Solution for the Consolidation Around a Driven Pile," International Journal for Numerical and Analytical Methods in Geomechanics, Vol. 3, 1979, pp. 217-229.

34. Roy, M., Tremblay, M., Tavenas, F., and LaRochelle, P., "Development of Pore Pressures in Quasi-Static Penetration Tests in Sensitive Clay," Canadian Geotechnical Journal, 1982, Vol. 19, pp. 124-138.

35. Roy, M., Tremblay, M., Tavenas, F., and LaRochelle, P., "Development of a Quasi-Static Piezocone Apparatus," Canadian Geotechnical Journal, 1982, Vol. 19, pp. 180-188.

36. Sanglerat, G., The Penetrometer and Soil Exploration, Elsevier Publishing Company: Amsterdam, 1972; 464p.

37. Soderberg, L.O., "Consolidation Theory Applied to Foundation Pile Time Effects," Geotechnique, Vol. 12, 1962, pp. 217-225.

38. Tavenas, F., 1982 personal correspondence.

39. Taylor, D.W., Fundamentals of Soil Mechanics, Wiley Publishing Co., New York, 700p.

40. Terzaghi, K., Theoretical Soil Mechanics, Wiley, New York, 1943.

41. Thorburn, S., Laird, C.L., and Reid, W.M., "The Importance of the Stress Histories of Cohesive Soils and the Cone Penetration Test," The Structural Engineer, Volume 59A, No. 3, March 1981, pp. 87-92.

42. Torstensson, B.-A., "The Pore Pressure Probe," Nordiske Geotekniske Mote, Oslo, Paper No. 34, 1977, pp. 34.1-34.15.

43. Tumay, M.T., Acar, Y., and Chan, A., "Analysis of Dissipation of Pore Pressures After Cone Penetration," Report FHWA/LA/LSU, Department of Civil Engineering, Louisiana State University, Baton Rouge, Louisiana, June, 1982, 131p.

44. Vesic, A.S., "Design of Pile Foundation," Synthesis of Highway Practice 42, Transportation Research Board, National Research Council, Washington, D.C., 1977, 427p.

45. Wissa, A.E.Z., Christian, J.T., Davis, E.H., and Heiberg, S., "Consolidation at Constant Rate of Strain," Journal of Soil Mechanics and Foundations Division, ASCE, Vol. 97, Oct. 1971, pp. 1393-1412.

APPENDIX A-

CONSOLIDATION TEST RESULTS

CONSOLIDATION TEST

Project _____ Type of Test Standard No. MUD 1-1g Tested by SPG Date 6/82

Soil Type BBC Location Solar House (M.I.T.) Sample Height 1.999 cm.

_____ _____ Sample Diameter 6.350 cm.

Initial w(%) _____ G_s _____ w_N(%) 30.2 w_L(%) _____ Corrections Apparatus Compressibility

Void Ratio e _____ S(%) _____ w_P(%) _____ P.I.(%) _____ Units: $\bar{\sigma}_{vc}$ kg/cm² c_v cm²/sec

$\bar{\sigma}_{vc}$	Primary			Total			C_α(%)	Coef. of Consol.		Remarks
	t(hr)	ε_v(%)	e	t(hr)	ε_v(%)	e		$\sqrt{t}$	log t	
0.026		0								
0.125		0.79						4.85 (10^{-3})	4.35 (10^{-3})	
0.250		1.20						7.06 (10^{-3})	5.18 (10^{-3})	
0.500		1.77						6.10 (10^{-3})	5.30 (10^{-3})	
1.00		2.50						6.43 (10^{-3})	5.70 (10^{-3})	
1.70		3.16						9.26 (10^{-3})	7.75 (10^{-3})	
2.89		4.04						7.76 (10^{-3})	6.63 (10^{-3})	
4.913		5.16						8.22 (10^{-3})	6.50 (10^{-3})	
8.35		6.57						6.38 (10^{-3})	5.38 (10^{-3})	
14.20		8.78						5.35 (10^{-3})	5.66 (10^{-3})	
24.14	0.077	11.82		0.75	12.15			5.80 (10^{-3})	4.40 (10^{-3})	
14.20		11.72							7.50 (10^{-3})	
8.35		11.37							6.85 (10^{-3})	
2.89		10.32							4.00 (10^{-3})	
1.00		9.02							2.06 (10^{-3})	
0.125		6.25							4.53 (10^{-4})	

GEOTECHNICAL LABORATORY
DEPT. OF CIVIL ENGR.
M.I.T.

Remarks

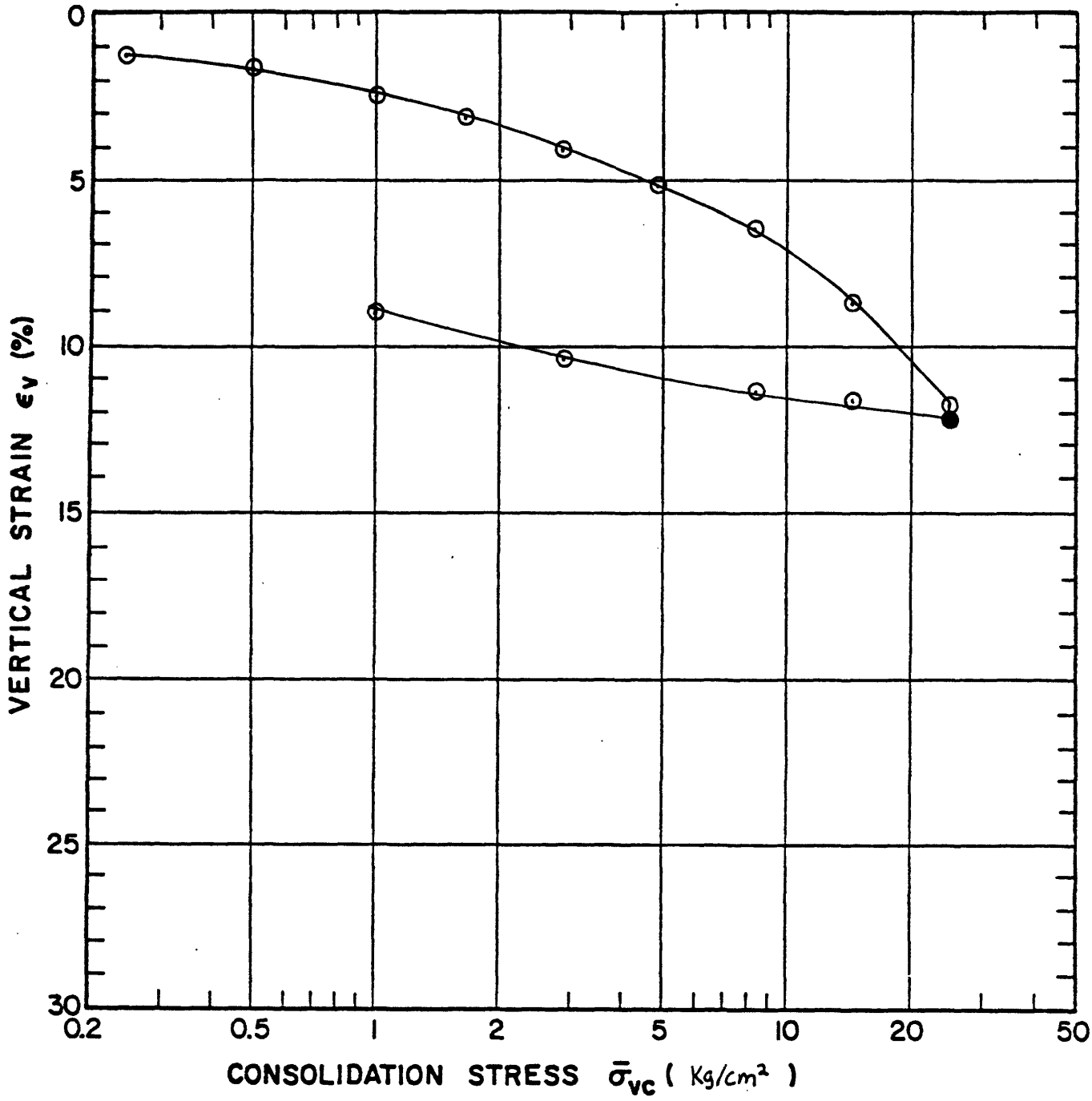

Sample No. MUD 1-1 w_N (%) 30.19 Estimated

Depth 41 ft. w_L (%) _____ $\bar{\sigma}_{vo}$ 1.5 ksc $\bar{\sigma}_{vm}$ 8.2-9.0

Soil Type BBC w_P (%) _____ CR 0.132 RR 0.015

_____ P.I.(%) _____ G_s ____ e_o ____ S(%) ____

o At t_p or ____ hr Remarks ϵ_v (%) based on d₁₀₀ from log t curve

● At ( ) hr _____

GEOTECHNICAL LABORATORY
DEPT. OF CIVIL ENGR.
M.I.T.

COMPRESSION CURVE

TEST No. Mud 1-1a

CONSOLIDATION TEST

Project _____ Type of Test Inc. Oedometer No. MU01-2a Tested by SPB Date 7/82

Soil Type BBC Location Solar House (M.I.T.) Sample Height 2.013 cm

_____ _____ Sample Diameter 6.350 cm

Initial w(%) _____ G_s _____ w_N(%) 41.1 w_L(%) _____ Corrections Apparatus Compressibility

Void Ratio e _____ S(%) _____ w_P(%) _____ P.I.(%) _____ Units: $\bar{\sigma}_{vc}$ Kg/cm² c_v cm²/sec

$\bar{\sigma}_{vc}$	Primary			Total			C_α(%)	Coef. of Consol.		Remarks
	t (hr)	ε_v(%)	e	t (hr)	ε_v(%)	e		$\sqrt{t}$	log t	
0.01		0								
0.125		0.73						3.86 (10^{-3})	5.43 (10^{-3})	
0.250		0.96						3.52 (10^{-3})	3.45 (10^{-3})	
0.500		1.30						5.82 (10^{-3})	5.50 (10^{-3})	
1.00		1.89						6.69 (10^{-3})	6.70 (10^{-3})	
1.70		2.49						5.78 (10^{-3})	5.78 (10^{-3})	
2.89		3.43						5.61 (10^{-3})	5.05 (10^{-3})	
4.91		5.09						3.71 (10^{-3})	5.55 (10^{-3})	
8.35		7.95						3.39 (10^{-3})	2.42 (10^{-3})	
14.20		11.53						2.92 (10^{-3})	2.09 (10^{-3})	
24.14	0.11	15.69		3.58	16.55			2.54 (10^{-3})	2.16 (10^{-3})	
14.20		16.25							3.35 (10^{-3})	
8.35		15.68							4.20 (10^{-3})	
2.89		14.19							1.78 (10^{-3})	
1.00		12.27							7.15 (10^{-4})	
0.125		8.91							2.13 (10^{-4})	

GEOTECHNICAL LABORATORY
DEPT. OF CIVIL ENGR.
M.I.T.

Remarks

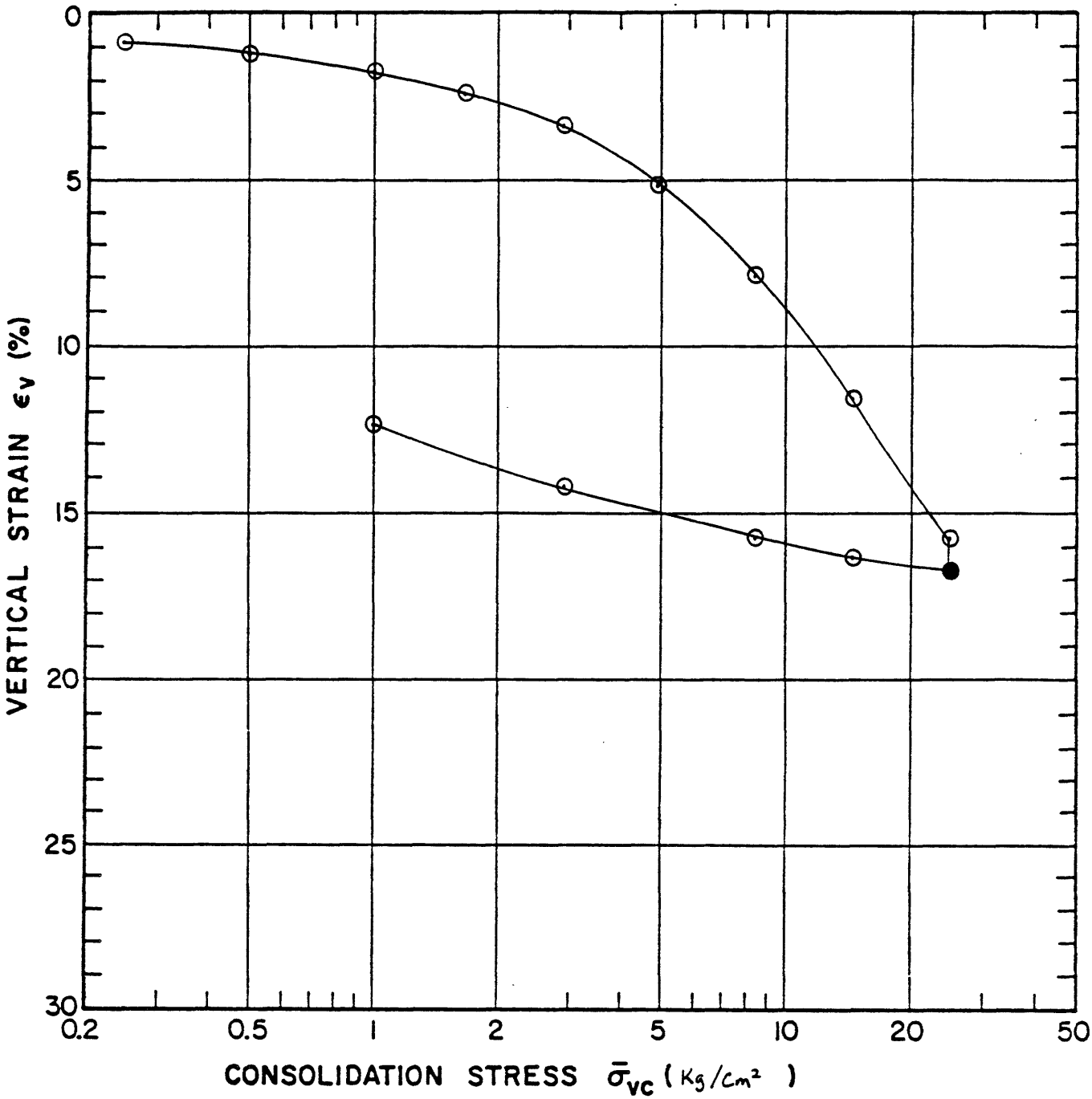

Sample No. MUD 1-2 w_N (%) 41.1 Estimated

Depth 45.5 ft. w_L (%) _____ $\bar{\sigma}_{vo}$ 1.60 ksc $\bar{\sigma}_{vm}$ 6.4-6.8

Soil Type BBC w_P (%) _____ CR 0.184 RR 0.013

_____ P.I.(%) _____ G_s ____ e_o ____ S(%) ____

o At t_p or ____ hr Remarks ϵ_v (%) based on d_{100} from log t curve

● At ( ) hr _____

GEOTECHNICAL LABORATORY
DEPT. OF CIVIL ENGR.
M.I.T.

COMPRESSION CURVE

TEST No. MUD 1-2a

CONSOLIDATION TEST

Project _____ Type of Test Incr. Oedometer No. MVO1-3a Tested by SPG Date 6/82

Soil Type BBC Location Solar House (MIT) Sample Height 2.004 cm

_____ _____ Sample Diameter 6.350 cm

Initial w(%) _____ G_s _____ w_N(%) 46.2 w_L(%) _____ Corrections Apparatus Compressibility

Void Ratio e _____ S(%) _____ w_P(%) _____ P.I.(%) _____ Units: $\bar{\sigma}_{vc}$ Kg/m² c_v cm²/sec

$\bar{\sigma}_{vc}$	Primary			Total			C_α(%)	Coef. of Consol.		Remarks
	t(hr)	ε_v(%)	e	t(hr)	ε_v(%)	e		c_v	log t	
0.026		0								
0.125		0.15						7.78 (10^{-3})	5.68 (10^{-3})	
0.250		0.44						4.61 (10^{-3})	4.20 (10^{-3})	
0.500		0.93						4.57 (10^{-3})	4.18 (10^{-3})	
1.00		1.53						8.85 (10^{-3})	5.35 (10^{-3})	
1.70		2.10						8.10 (10^{-3})	6.35 (10^{-3})	
2.89		3.12						4.15 (10^{-3})	4.60 (10^{-3})	
4.91		4.97						4.25 (10^{-3})	2.53 (10^{-3})	
8.35		8.53						1.63 (10^{-3})	1.37 (10^{-3})	
14.20		13.35						1.17 (10^{-3})	1.05 (10^{-3})	
24.14	0.23	17.86		3.50	18.49			1.39 (10^{-3})	1.12 (10^{-3})	
14.20		17.31							4.98 (10^{-3})	
8.35		16.61							2.85 (10^{-3})	
2.89		14.80							1.30 (10^{-3})	
1.00		12.67							5.45 (10^{-4})	
0.125		8.60							1.55 (10^{-4})	

GEOTECHNICAL LABORATORY
DEPT. OF CIVIL ENGR.
M.I.T.

Remarks

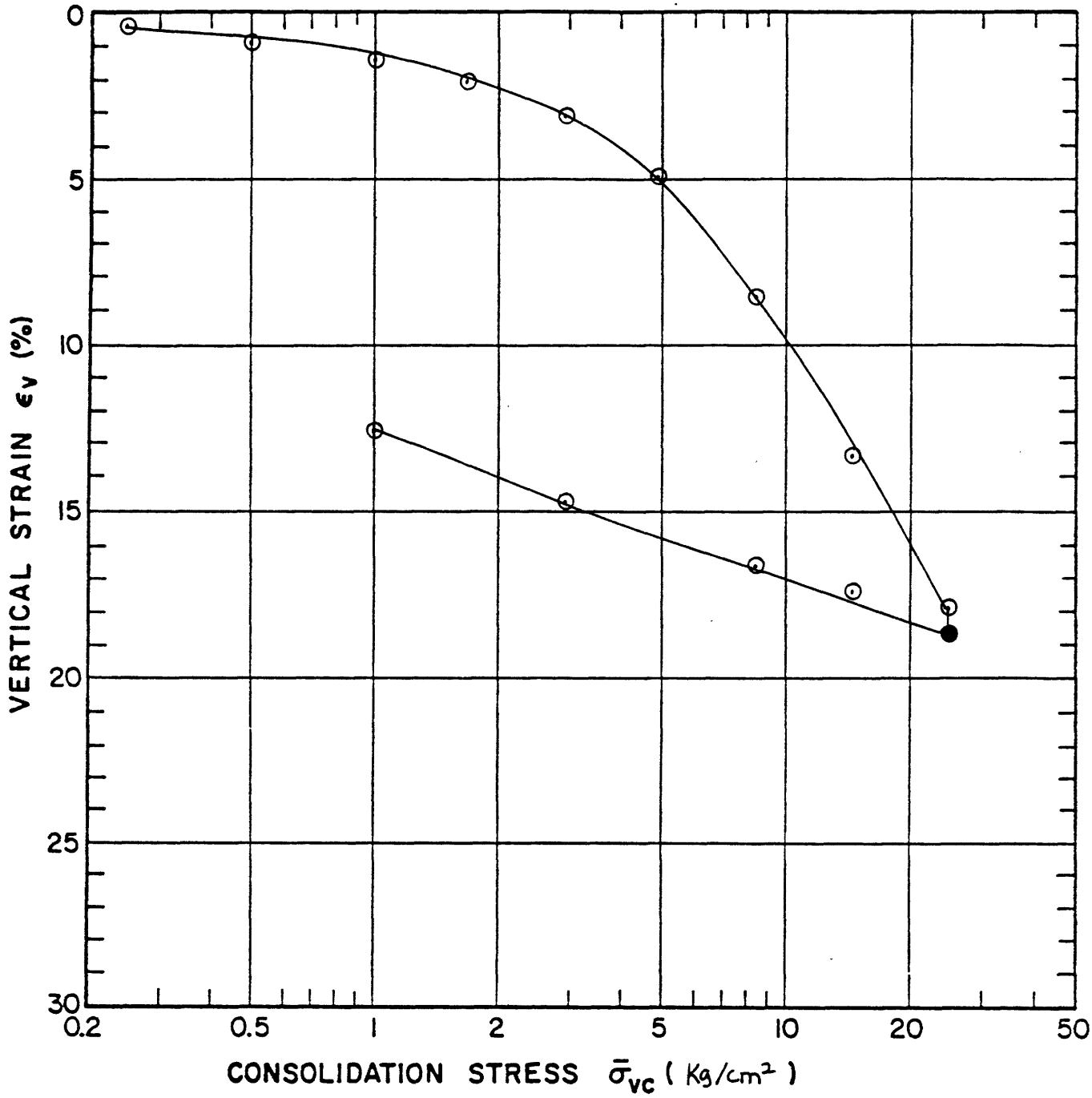

Sample No. MUD 1-3 w_N (%) 46.2 Estimated

Depth 50.5 ft. w_L (%) _____ $\bar{\sigma}_{vo}$ 1.75 ksc $\bar{\sigma}_{vm}$ 5.7-6.0

Soil Type BBC w_P (%) _____ CR 0.196 RR 0.015

_____ P.I.(%) _____ G_s ____ e_0 ____ S(%) ____

o At t_p or ____ hr Remarks ϵ_v (%) based on d_{100} from log t curve

● At ( ) hr _____

GEOTECHNICAL LABORATORY
DEPT. OF CIVIL ENGR.
M.I.T.

COMPRESSION CURVE

TEST No. MUD 1-3a

CONSOLIDATION TEST

Project _____ Type of Test Incr. Oedometer No. MUD1-4b Tested by SPG Date 6/82

Soil Type BBC Location Solar House (MIT.) Sample Height 1.963 cm

_____ _____ Sample Diameter 6.350 cm.

Initial w(%) _____ G_s _____ w_N(%) 39.1 w_L(%) _____ Corrections Apparatus Compressibility

Void Ratio e _____ S(%) _____ w_P(%) _____ P.I.(%) _____ Units: $\bar{\sigma}_{vc}$ kg/cm² c_v cm²/sec

$\bar{\sigma}_{vc}$	Primary			Total			C_α(%)	Coef. of Consol.		Remarks
	t(hr)	ε_v(%)	e	t(hr)	ε_v(%)	e		$\sqrt{t}$	log t	
0.021		0								
0.125		0.39						2.17 (10^{-3})	1.80 (10^{-3})	
0.250		0.69						1.40 (10^{-3})	1.84 (10^{-3})	
0.500		1.24						2.42 (10^{-3})	2.14 (10^{-3})	
1.00		1.92						4.30 (10^{-3})	4.45 (10^{-3})	
1.70		2.63						2.95 (10^{-3})	3.03 (10^{-3})	
2.89		3.72						3.95 (10^{-3})	2.28 (10^{-3})	
4.91		5.56						1.98 (10^{-3})	2.21 (10^{-3})	
8.35		9.14						1.30 (10^{-3})	1.33 (10^{-3})	
14.20		13.65						1.45 (10^{-3})	1.24 (10^{-3})	
24.14	0.20	17.57		1.00	17.92			1.55 (10^{-3})	1.88 (10^{-3})	
14.20		17.60							6.93 (10^{-3})	
8.35		16.96							1.81 (10^{-3})	
2.89		15.46							1.48 (10^{-3})	
1.00		13.59							5.38 (10^{-4})	
0.125		10.17							1.64 (10^{-4})	

GEOTECHNICAL LABORATORY
DEPT. OF CIVIL ENGR.
M.I.T.

Remarks

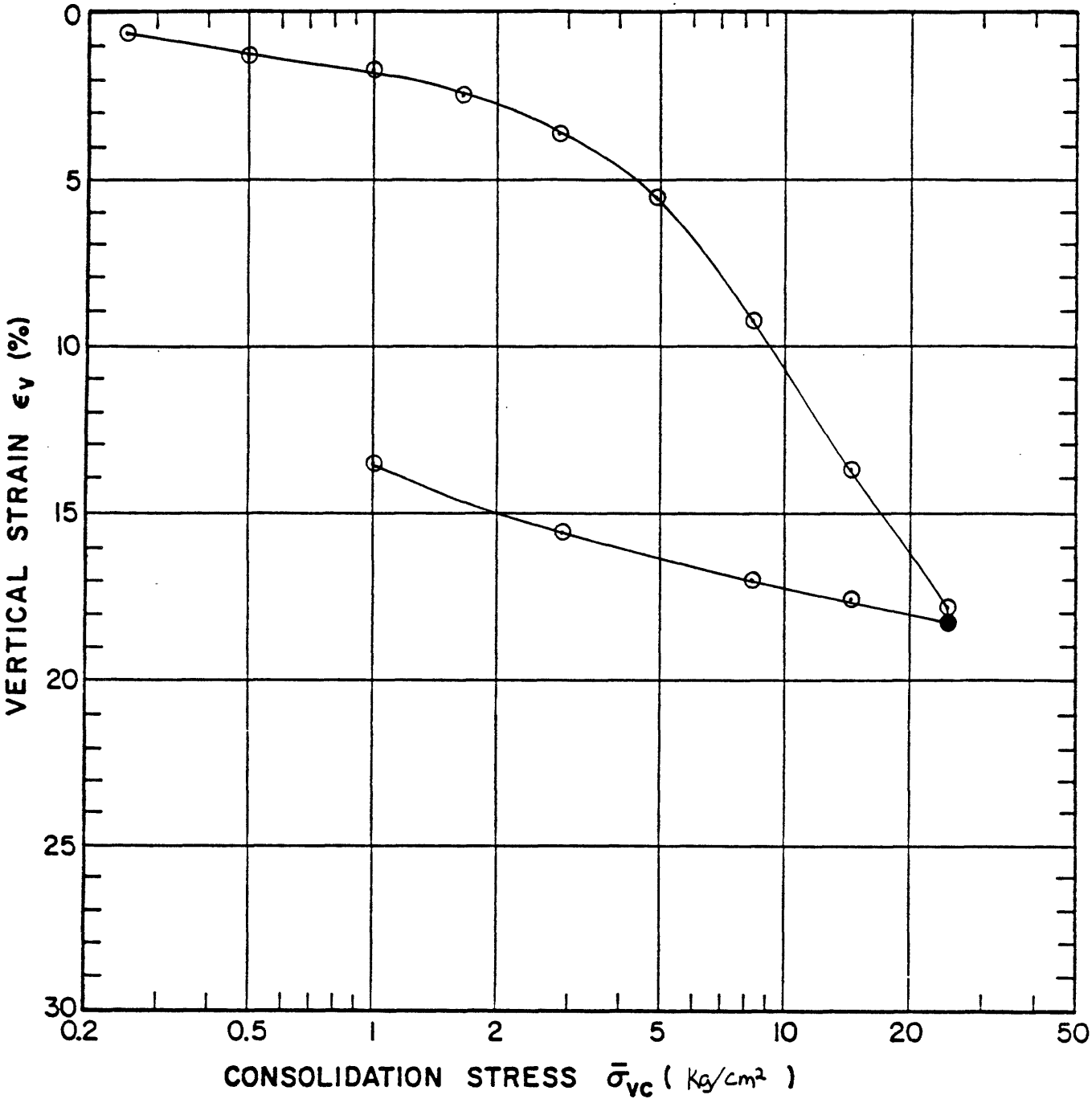

Sample No. MUD 1-4 w_N (%) 39.1 Estimated

Depth 58.5 ft. w_L (%) _____ $\bar{\sigma}_{vo}$ 1.95 ksc $\bar{\sigma}_{vm}$ 4.8-5.2

Soil Type BBC w_P (%) _____ CR 0.175 RR 0.017

_____ P.I.(%) _____ G_s ____ e_o ____ S(%) ____

o At t_p or ____ hr Remarks ϵ_v (%) based on d_{100} from log t curve

● At ( ) hr _____

GEOTECHNICAL LABORATORY
DEPT. OF CIVIL ENGR.
M.I.T.

COMPRESSION CURVE

TEST No. MUD 1-4 b

CONSOLIDATION TEST

Project _____ Type of Test Incr. Oedometer No. MUD 1-5 Tested by SPG Date 1/82

Soil Type BBC Location Solar House (M.I.T.) Sample Height 2.001 cm.

_____ _____ Sample Diameter 6.330 cm.

Initial w(%) _____ G_s _____ w_N(%) 48.7 w_L(%) _____ Corrections Apparatus Compressibility

Void Ratio e _____ S(%) _____ w_P(%) _____ P.I.(%) _____ Units: $\bar{\sigma}_{vc}$ kg/cm² c_v cm²/sec

$\bar{\sigma}_{vc}$	Primary			Total			C_α(%)	Coef. of Consol.		Remarks
	t (hr)	ε_v(%)	e	t (hr)	ε_v(%)	e		c_v	log t	
0.02		0								
0.125		0.08						6.32 (10^{-3})	3.65 (10^{-3})	
0.250		0.65						2.45 (10^{-3})	1.49 (10^{-3})	
0.500		1.31						1.33 (10^{-3})	1.08 (10^{-3})	
1.00		2.19						2.71 (10^{-3})	1.41 (10^{-3})	
2.00		3.50						2.07 (10^{-3})	1.44 (10^{-3})	
4.00		6.88						1.82 (10^{-3})	6.32 (10^{-4})	
8.00	0.87	15.17		26.42	16.07			8.01 (10^{-4})	4.52 (10^{-4})	
4.00		15.43							2.12 (10^{-3})	
2.00		14.40							9.23 (10^{-3})	
1.00		13.19							3.94 (10^{-4})	
0.500		11.90							1.87 (10^{-4})	
0.250		10.60							1.03 (10^{-4})	
0.125		9.68							1.29 (10^{-4})	

GEOTECHNICAL LABORATORY
DEPT. OF CIVIL ENGR.
M.I.T.

Remarks

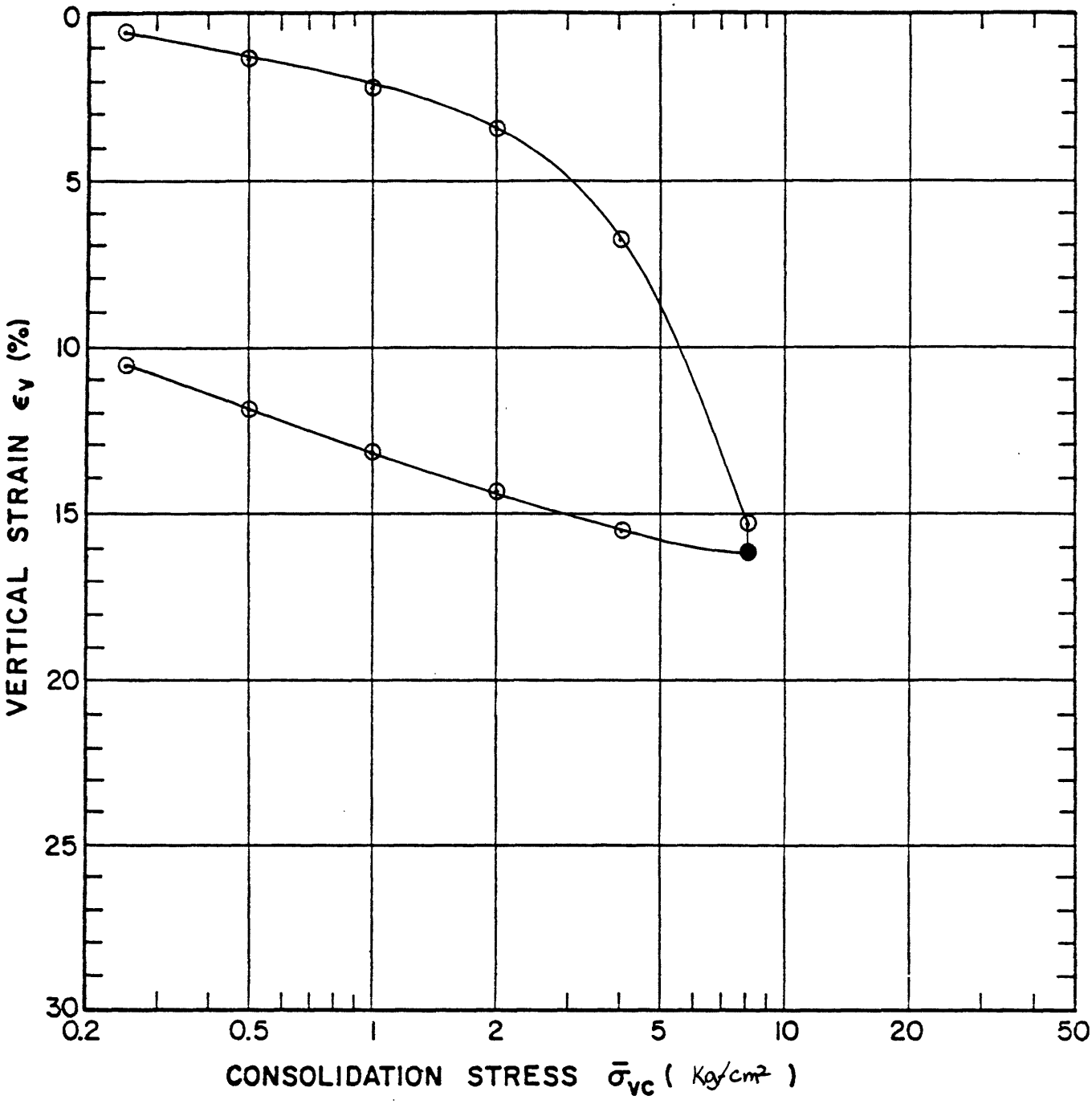

Sample No. MUD 1-5 w_N (%) 48.7 Estimated

Depth 66.0 ft. w_L (%) _____ $\bar{\sigma}_{vo}$ 2.15 ksc $\bar{\sigma}_{vm}$ 3.1-3.5

Soil Type BBC w_P (%) _____ CR 0.275 RR 0.023

_____ P.I.(%) _____ G_s ____ e_o ____ S(%) ____

o At t_p or ____ hr Remarks ϵ_v(%) based on d_{100} from log t curve

● At ( ) hr _____

GEOTECHNICAL LABORATORY
DEPT. OF CIVIL ENGR.
M.I.T.

COMPRESSION CURVE

TEST No. MUD 1-5

CONSOLIDATION TEST

Project _____ Type of Test Incr. Oedometer No. MUO 1-6 Tested by HHH Date 1/82

Soil Type BBC Location Solar House (M.I.T.) Sample Height 1.969 cm.

_____ _____ Sample Diameter 6.345 cm.

Initial w(%) _____ G_s _____ w_N(%) 40.8 w_L(%) _____ Corrections Apparatus Compressibility

Void Ratio e _____ S(%) _____ w_P(%) _____ P.I.(%) _____ Units: $\bar{\sigma}_{vc}$ Kg/cm² c_v cm²/sec

$\bar{\sigma}_{vc}$	Primary			Total			C_α(%)	Coef. of Consol.		Remarks
	t(hr)	ε_v(%)	e	t(hr)	ε_v(%)	e		c_v	log t	
0.021		0								
0.125		0.56						830 (10^{-4})	6.65 (10^{-4})	
0.250		1.09						2.34 (10^{-3})	1.25 (10^{-3})	
0.500		1.89						1.19 (10^{-3})	1.03 (10^{-3})	
1.00		3.07						2.21 (10^{-3})	1.43 (10^{-3})	
2.00		4.83						2.23 (10^{-3})	1.30 (10^{-3})	
4.00		8.74						1.52 (10^{-3})	8.73 (10^{-4})	
8.00	0.33	14.31		19.08	15.02			1.97 (10^{-3})	8.08 (10^{-4})	
4.00		14.54							4.66 (10^{-3})	
2.00		13.85							1.92 (10^{-3})	
1.00		12.91							7.54 (10^{-4})	
0.50		11.79							2.57 (10^{-4})	
0.25		10.86							1.69 (10^{-4})	
0.125		10.23							2.83 (10^{-4})	

GEOTECHNICAL LABORATORY
DEPT. OF CIVIL ENGR.
M.I.T.

Remarks

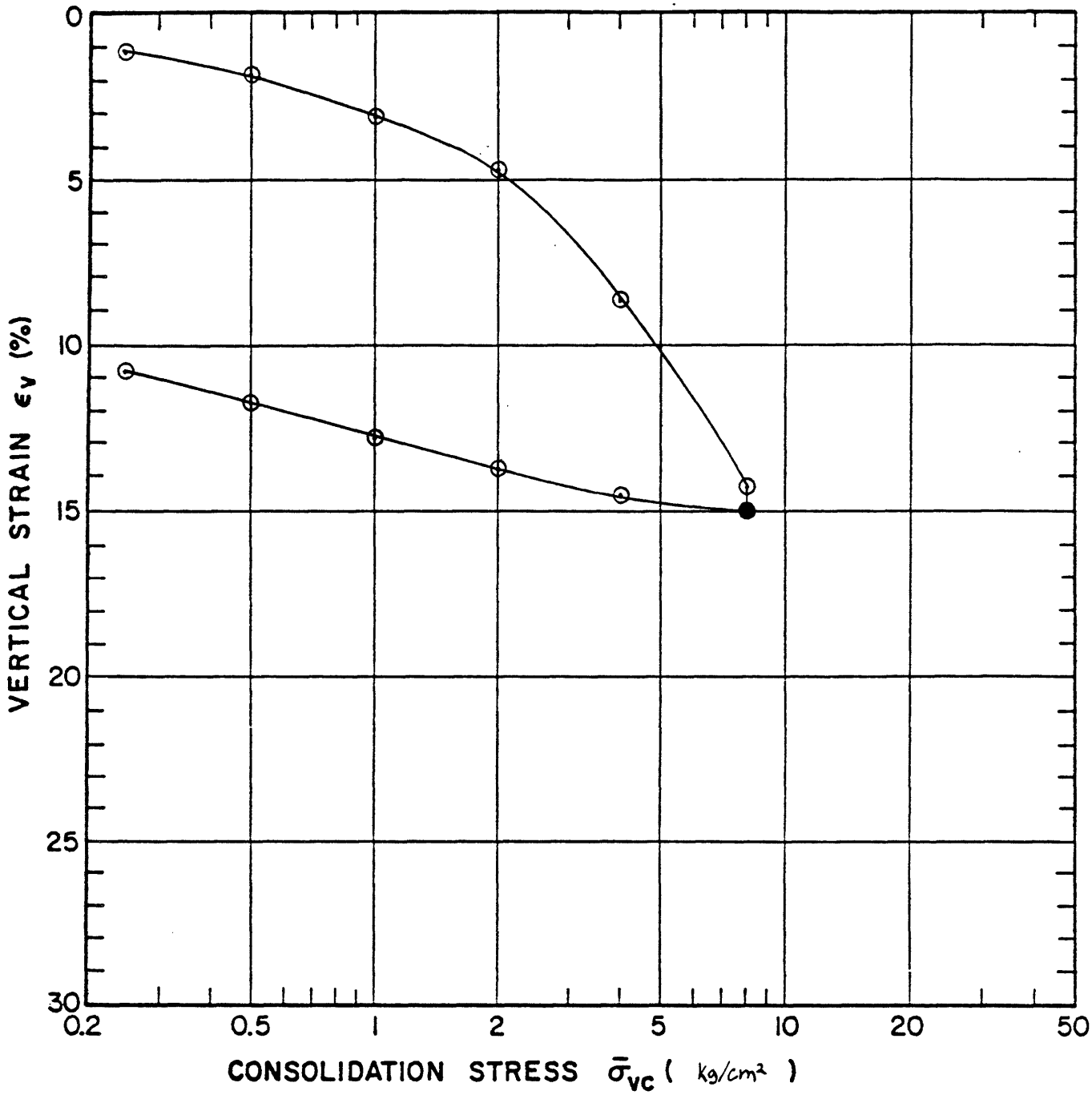

Sample No. MUD 1-6 w_N (%) 40.79 Estimated

Depth 74.0 ft. w_L (%) _____ $\bar{\sigma}_{vo}$ 2.38 ksc $\bar{\sigma}_{vm}$ 2.6-3.0

Soil Type BBC w_P (%) _____ CR 0.185 RR 0.028

_____ P.I.(%) _____ G_s ____ e_0 ____ S(%) ____

o At t_p or ____ hr Remarks ϵ_v(%) based on d_{100} from log t curve

● At ( ) hr _____

GEOTECHNICAL LABORATORY
DEPT. OF CIVIL ENGR.
M.I.T.

COMPRESSION CURVE

TEST No. MUD 1-6

CONSOLIDATION TEST

Project _____ Type of Test Incr. Oedometer No. MO1-7a Tested by SPG Date 6/82

Soil Type BBC Location Solar House (M.I.T.) Sample Height 1.984 cm

_____ _____ Sample Diameter 6.350 cm.

Initial w(%) _____ G_s _____ w_N(%) 48.7 w_L(%) _____ Corrections Apparatus Compressibility

Void Ratio e _____ S(%) _____ w_P(%) _____ P.I.(%) _____ Units: $\bar{\sigma}_{vc}$ kg/cm² c_v cm²/sec

$\bar{\sigma}_{vc}$	Primary			Total			C_α(%)	Coef. of Consol.		Remarks
	t (hr)	ε_v(%)	e	t (hr)	ε_v(%)	e		$\sqrt{t}$	log t	
0.021		0								
0.125		0						2.23 (10^{-3})	1.44 (10^{-3})	
0.25		0.77						1.35 (10^{-3})	1.13 (10^{-3})	
0.50		1.64						2.57 (10^{-3})	1.66 (10^{-3})	
1.00		2.82						2.31 (10^{-3})	1.93 (10^{-3})	
1.70		3.83						3.60 (10^{-3})	2.75 (10^{-3})	
2.89		5.63						2.39 (10^{-3})	1.73 (10^{-3})	
4.91		10.45						1.15 (10^{-3})	6.83 (10^{-4})	
8.35		15.54						1.10 (10^{-3})	9.40 (10^{-4})	
14.20	0.27	20.28		10.75	20.96			1.50 (10^{-3})	9.93 (10^{-4})	
8.35		20.38						1.56 (10^{-2})	5.41 (10^{-3})	
2.89		18.92						2.25 (10^{-3})	1.67 (10^{-3})	
1.00		17.04						7.43 (10^{-4})	6.23 (10^{-4})	
0.125		13.11						2.45 (10^{-4})	1.79 (10^{-4})	

GEOTECHNICAL LABORATORY
DEPT. OF CIVIL ENGR.
M.I.T.

Remarks

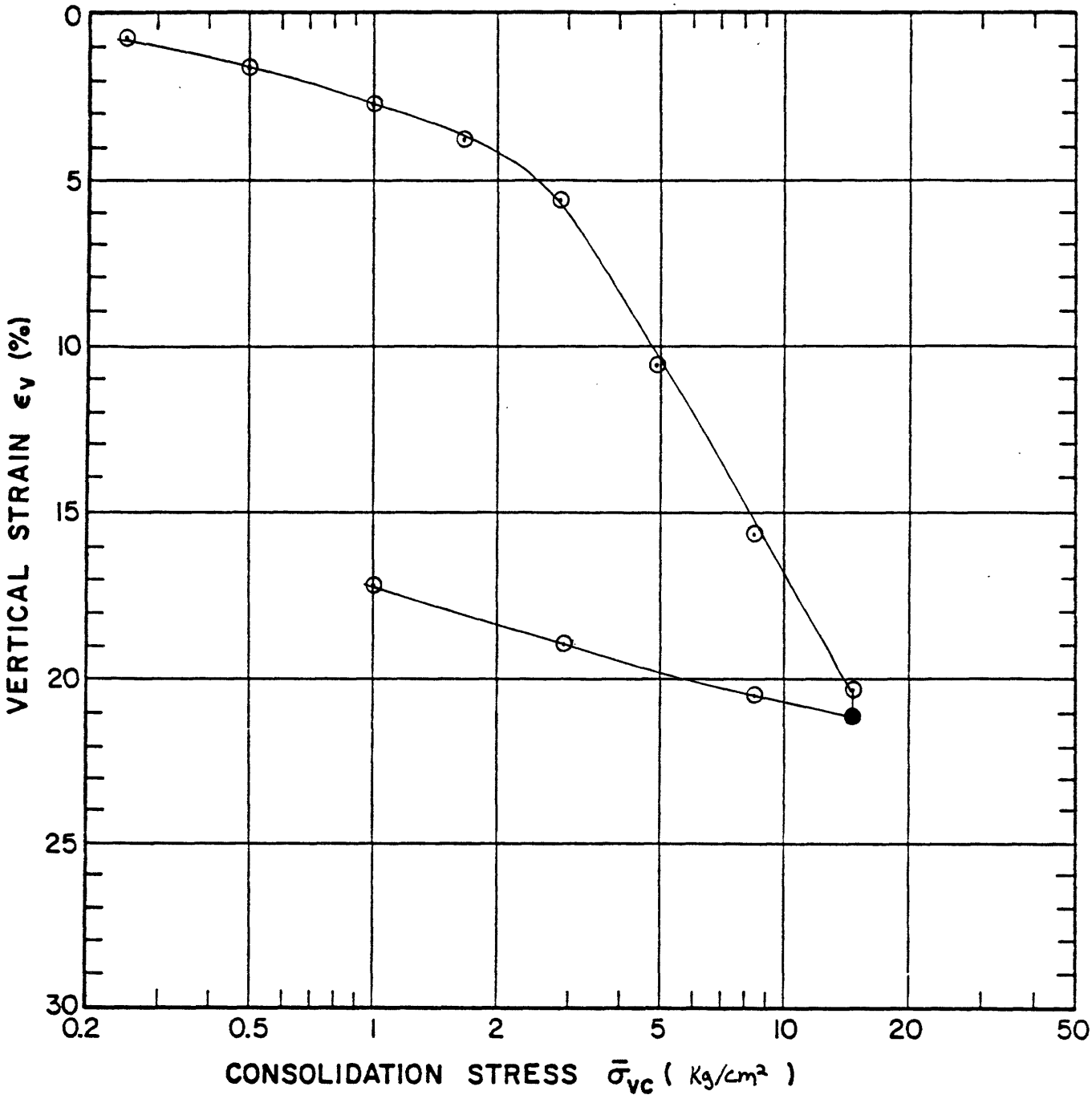

Sample No. MUD 1-7 w_N (%) 48.7 Estimated

Depth 84.5 ft. w_L (%) _____ $\bar{\sigma}_{vo}$ 2.58 ksc $\bar{\sigma}_{vm}$ 2.7-3.1

Soil Type BBC w_P (%) _____ CR 0.212 RR 0.031

_____ P.I.(%) _____ G_s ____ e_o ____ S(%) ____

o At t_p or ____ hr Remarks ϵ_v(%) based on diou from logt curve

● At ( ) hr _____

GEOTECHNICAL LABORATORY
DEPT. OF CIVIL ENGR.
M.I.T.

COMPRESSION CURVE

TEST No. MUD 1-7a

CONSOLIDATION TEST

Project _____ Type of Test Incr. Oedometer No. MUO 1-8 Tested by HHH Date 1/82

Soil Type BBC Location Solar House (M.I.T.) Sample Height 2.007 cm.

_____ _____ Sample Diameter 6.353 cm.

Initial w(%) _____ G_s _____ w_N(%) 47.1 w_L(%) _____ Corrections Apparatus Compressibility

Void Ratio e _____ S(%) _____ w_P(%) _____ P.I.(%) _____ Units: $\bar{\sigma}_{vc}$ kg/cm² c_v cm²/sec

$\bar{\sigma}_{vc}$	Primary			Total			C_α(%)	Coef. of Consol.		Remarks
	t (hr)	ε_v(%)	e	t (hr)	ε_v(%)	e		$\sqrt{t}$	log t	
0.022		0								
0.125		0.12						3.55 (10^{-3})	4.13 (10^{-3})	
0.25		0.54						3.87 (10^{-3})	3.29 (10^{-3})	
0.50		1.05						3.21 (10^{-3})	2.30 (10^{-3})	
1.00		1.78						3.75 (10^{-3})	3.21 (10^{-3})	
2.00		2.67						3.12 (10^{-3})	4.74 (10^{-3})	
4.00		9.01						1.55 (10^{-3})	2.09 (10^{-4})	
8.00	0.67	17.19		38.92	17.54			7.69 (10^{-4})	4.97 (10^{-4})	
4.00		17.05							1.51 (10^{-3})	
2.00		16.25							1.72 (10^{-3})	
1.00		15.19							5.64 (10^{-4})	
0.50		13.99							2.68 (10^{-4})	
0.25		12.95							1.91 (10^{-4})	
0.125		11.77							1.02 (10^{-4})	

GEOTECHNICAL LABORATORY
DEPT. OF CIVIL ENGR.
M.I.T.

Remarks

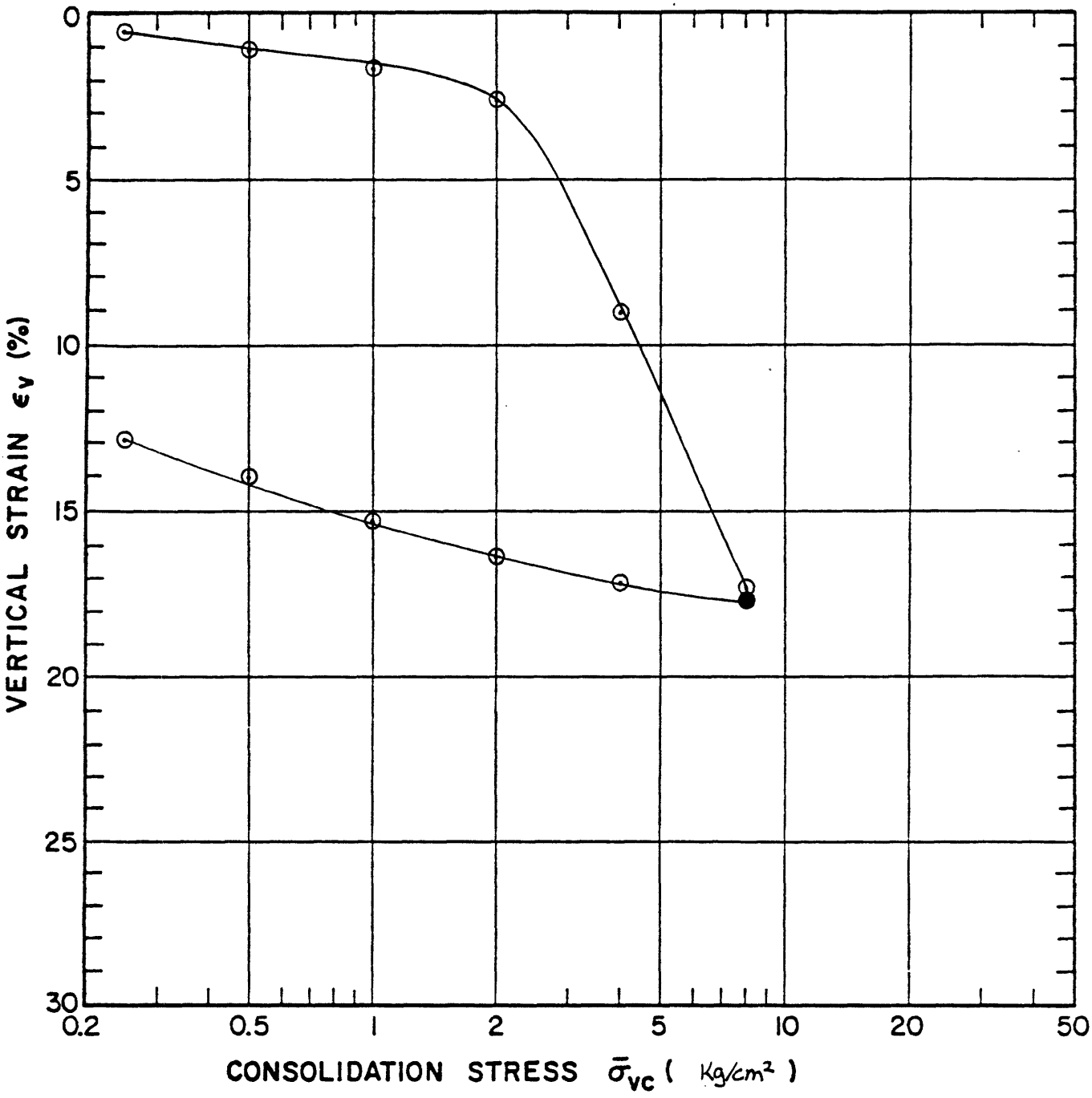

Sample No. MUD 1-8 w_N (%) 47.1 Estimated

Depth 90.0 ft w_L (%) _____ $\bar{\sigma}_{vo}$ 2.72 Ksc $\bar{\sigma}_{vm}$ 2.4-2.65

Soil Type BBC w_P (%) _____ CR 0.272 RR 0.018

_____ P.I.(%) _____ G_s ____ e_o ____ S(%) ____

o At t_p or ____ hr Remarks ϵ_v(%) based on drop from log t curve

● At ( ) hr _____

GEOTECHNICAL LABORATORY
DEPT. OF CIVIL ENGR.
M.I.T.

COMPRESSION CURVE

TEST No. MUD 1-8

CONSOLIDATION TEST

Project _____ Type of Test Incr. Oedometer No. DGL-4 Tested by DGL Date 1/20/83

Soil Type BBC Location Solar House (MIT) Sample Height 2.007 cm.

_____ _____ Sample Diameter 6.35 cm.

Initial w(%) _____ G_s _____ w_N(%) 37.8 w_L(%) _____ Corrections Apparatus Compressibility

Void Ratio e _____ S(%) _____ w_P(%) _____ P.I.(%) _____ Units: $\bar{\sigma}_{vc}$ Kg/cm² c_v cm²/sec

$\bar{\sigma}_{vc}$	Primary			Total			C_α(%)	Coef. of Consol.		Remarks
	t(hr)	ε_v(%)	e	t(hr)	ε_v(%)	e		$\sqrt{t}$	log t	
0.125		0.46								
0.250		0.722								
0.500		1.22								
1.00		1.80								
1.75		2.73								
3.00		3.73								
4.75		6.66						1.84 (10^{-3})	7.20 (10^{-4})	
8.00		12.23		11.72	13.19			8.01 (10^{-4})	5.66 (10^{-4})	
4.00		12.76								
2.00		12.05								
1.00		11.22								
0.50		10.22								
1.00		10.60								
2.00		11.25								
4.00		12.43								
8.00		14.06								
16.00		17.91		11.83	18.56			1.89 (10^{-3})	1.48 (10^{-3})	
8.00		18.09								

GEOTECHNICAL LABORATORY
DEPT. OF CIVIL ENGR.
M.I.T.

Remarks Sample MUD 1-9

CONSOLIDATION TEST

Project _____ Type of Test _____ No. DGL-4 Tested by DGL Date _____

Soil Type _____ Location _____ Sample Height _____

_____ _____ Sample Diameter _____

Initial w(%) _____ G_s _____ w_N(%) ___ w_L(%) ___ Corrections _____

Void Ratio e _____ S(%) _____ w_P(%) ___ P.I.(%) ___ Units: $\bar{\sigma}_{vc}$ _____ c_v _____

$\bar{\sigma}_{vc}$	Primary			Total			C_α(%)	Coef. of Consol.		Remarks
	t (hr)	ε_v(%)	e	t (hr)	ε_v(%)	e		$\sqrt{t}$	log t	
4.00		17.77								
2.00		16.59								
1.00		15.60								
0.50		14.98								

GEOTECHNICAL LABORATORY
DEPT. OF CIVIL ENGR.
M.I.T.

Remarks

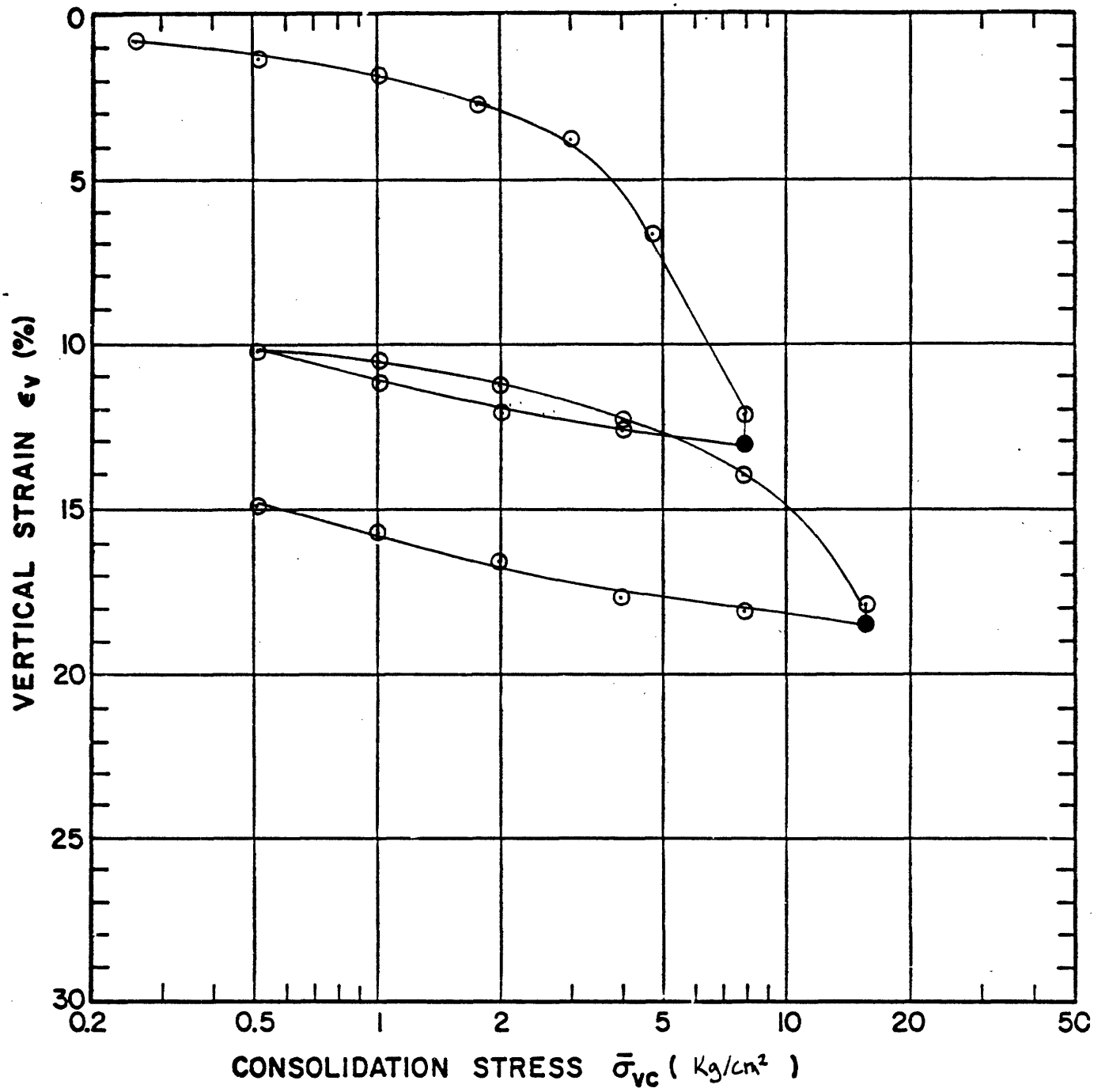

Sample No. MVD 1-9 w_N (%) 37.8 Estimated

Depth 94-96 ft w_L (%) _____ $\bar{\sigma}_{vo}$ 2.85 ksc $\bar{\sigma}_{vm}$ 3.5-3.85 ksc

Soil Type BBC w_P (%) _____ CR 0.246 RR 0.015

_____ P.I.(%) _____ G_s ____ e_o ____ S(%) ____

o At t_p or ____ hr Remarks ϵ_v (%) based on d_{100} from log t curves

● At ( ) hr _____

GEOTECHNICAL LABORATORY
DEPT. OF CIVIL ENGR.
M.I.T.

COMPRESSION CURVE

TEST No. OGL-4

CONSOLIDATION TEST

Project _____ Type of Test Incr. Oedometer No. OGL-2 Tested by OGT Date 1/83

Soil Type BBC Location Solar House (M.I.T.) Sample Height 1.994 cm.

_____ _____ Sample Diameter 6.35 cm.

Initial w(%) _____ G_s _____ w_N(%) 267 w_L(%) _____ Corrections Apparatus Compressibility

Void Ratio e _____ S(%) _____ w_P(%) _____ P.I.(%) _____ Units: $\bar{\sigma}_{vc}$ kg/cm² c_v cm²/sec

$\bar{\sigma}_{vc}$	Primary			Total			C_α(%)	Coef. of Consol.		Remarks
	t (hr)	ε_v(%)	e	t (hr)	ε_v(%)	e		VT	log t	
0.125		0.23								
0.25		0.64								
0.50		1.11								
1.00		1.58								
1.75		2.14								
3.00		2.92								
4.75		3.94								
8.00		6.90		1.50	7.36					
4.00		7.22								
2.00		7.08								
1.00		6.88								
0.50		6.65								
1.00		6.74								
2.00		6.92								
4.00		7.17								
6.77		7.57								
13.54		9.36		17.07	10.00					
6.77		9.89								

GEOTECHNICAL LABORATORY
DEPT. OF CIVIL ENGR.
M.I.T.

Remarks Sample MUD 1-10
Cv calculations innacurrate

CONSOLIDATION TEST

Project _____ Type of Test _____ No. DGL-2 Tested by _____ Date _____

Soil Type _____ Location _____ Sample Height _____

_____ _____ Sample Diameter _____

Initial w(%) _____ G_s _____ w_N(%) _____ w_L(%) _____ Corrections _____

Void Ratio e _____ S(%) _____ w_P(%) _____ P.I.(%) _____ Units: $\bar{\sigma}_{vc}$ _____ c_v _____

$\bar{\sigma}_{vc}$	Primary			Total			C_α(%)	Coef. of Consol.		Remarks
	t(hr)	ε_v(%)	e	t(hr)	ε_v(%)	e		$\sqrt{t}$	log t	
4.00		9.72								
2.00		9.53								
1.00		9.27								
0.50		9.10								
0.25		–								

GEOTECHNICAL LABORATORY
DEPT. OF CIVIL ENGR.
M.I.T.

Remarks

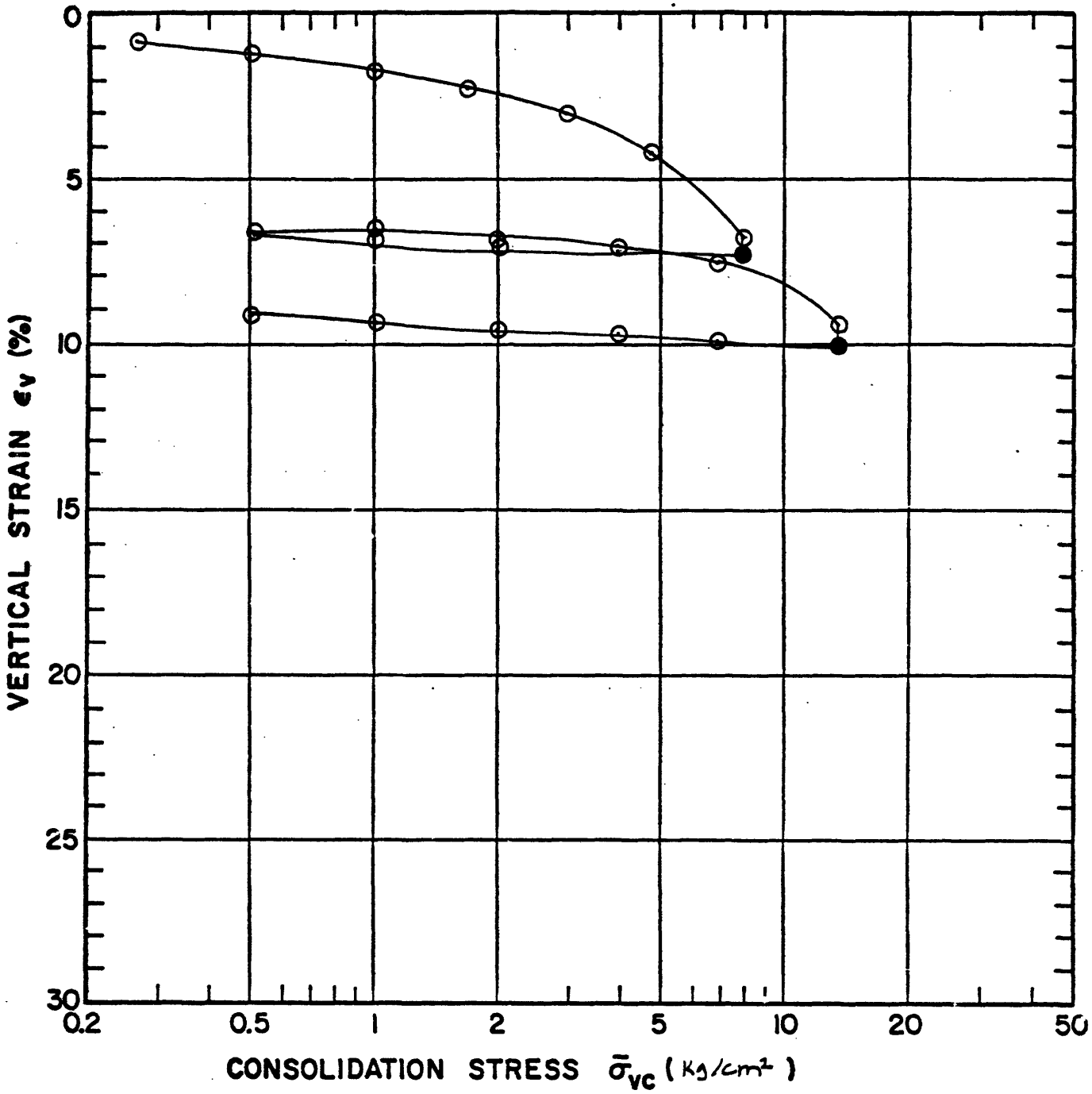

Sample No. MUD 1-10 w_N (%) 26.7 Estimated

Depth 100-102 ft. w_L (%) _____ $\bar{\sigma}_{vo}$ 3.00 $\bar{\sigma}_{vm}$ 3.9-4.2 ksc

Soil Type BBC w_P (%) _____ CR 0.131 RR 0.015

_____ P.I.(%) _____ G_s ____ e_o ____ S(%) ____

o At t_p or ____ hr Remarks δ_v (%) based on dips from log-t curves

● At ( ) hr _____

GEOTECHNICAL LABORATORY
DEPT. OF CIVIL ENGR.
M.I.T.

COMPRESSION CURVE

TEST No. OGL-2

CONSOLIDATION TEST

Project _____ Type of Test Incr. Oedometer No. 06L-3 Tested by 06L Date 1/83

Soil Type BBC Location Solar House (M.I.T.) Sample Height 1.97 cm.

_____ _____ Sample Diameter 6.35 cm.

Initial w(%) _____ G_s _____ w_N(%) 24.6 w_L(%) _____ Corrections Apparatus Compressibility

Void Ratio e _____ S(%) _____ w_P(%) _____ P.I.(%) _____ Units: $\bar{\sigma}_{vc}$ Kg/cm² c_v cm²/sec

$\bar{\sigma}_{vc}$	Primary			Total			C_α(%)	Coef. of Consol.		Remarks
	t (hr)	ε_v(%)	e	t (hr)	ε_v(%)	e		$\sqrt{t}$	log t	
0.125		0.31								
0.250		0.62								
0.500		1.13								
1.000		1.76								
1.75		2.63								
3.00		3.49								
4.75		4.53						1.73 (10^{-2})	1.61 (10^{-2})	
8.00		5.97		3.52	6.35			1.22 (10^{-2})	1.87 (10^{-2})	
4.00		6.30								
2.00		6.19								
1.00		6.09								
0.50		5.92								
1.00		5.92								
2.00		6.04								
4.00		6.23								
8.00		6.67								
16.00		7.94		1.67	8.34			1.03 (10^{-2}	1.58 (10^{-2})	
8.00		8.22								

GEOTECHNICAL LABORATORY
DEPT. OF CIVIL ENGR.
M.I.T.

Remarks Sample MUD I-11

CONSOLIDATION TEST

Project _____ Type of Test _____ No. 06L-3 Tested by _____ Date _____

Soil Type _____ Location _____ Sample Height _____

_____ _____ Sample Diameter _____

Initial w(%) _____ G_s _____ w_N(%) ___ w_L(%) ___ Corrections _____

Void Ratio e _____ S(%) ___ w_P(%) ___ P.I.(%) ___ Units: $\bar{\sigma}_{vc}$ _____ c_v _____

$\bar{\sigma}_{vc}$	Primary			Total			C_α(%)	Coef. of Consol.		Remarks
	t (hr)	ε_v(%)	e	t (hr)	ε_v(%)	e		$\sqrt{t}$	log t	
4.00		8.08								
2.00		7.92								
1.00		7.77								
0.50		7.59								

GEOTECHNICAL LABORATORY
DEPT. OF CIVIL ENGR.
M.I.T.

Remarks

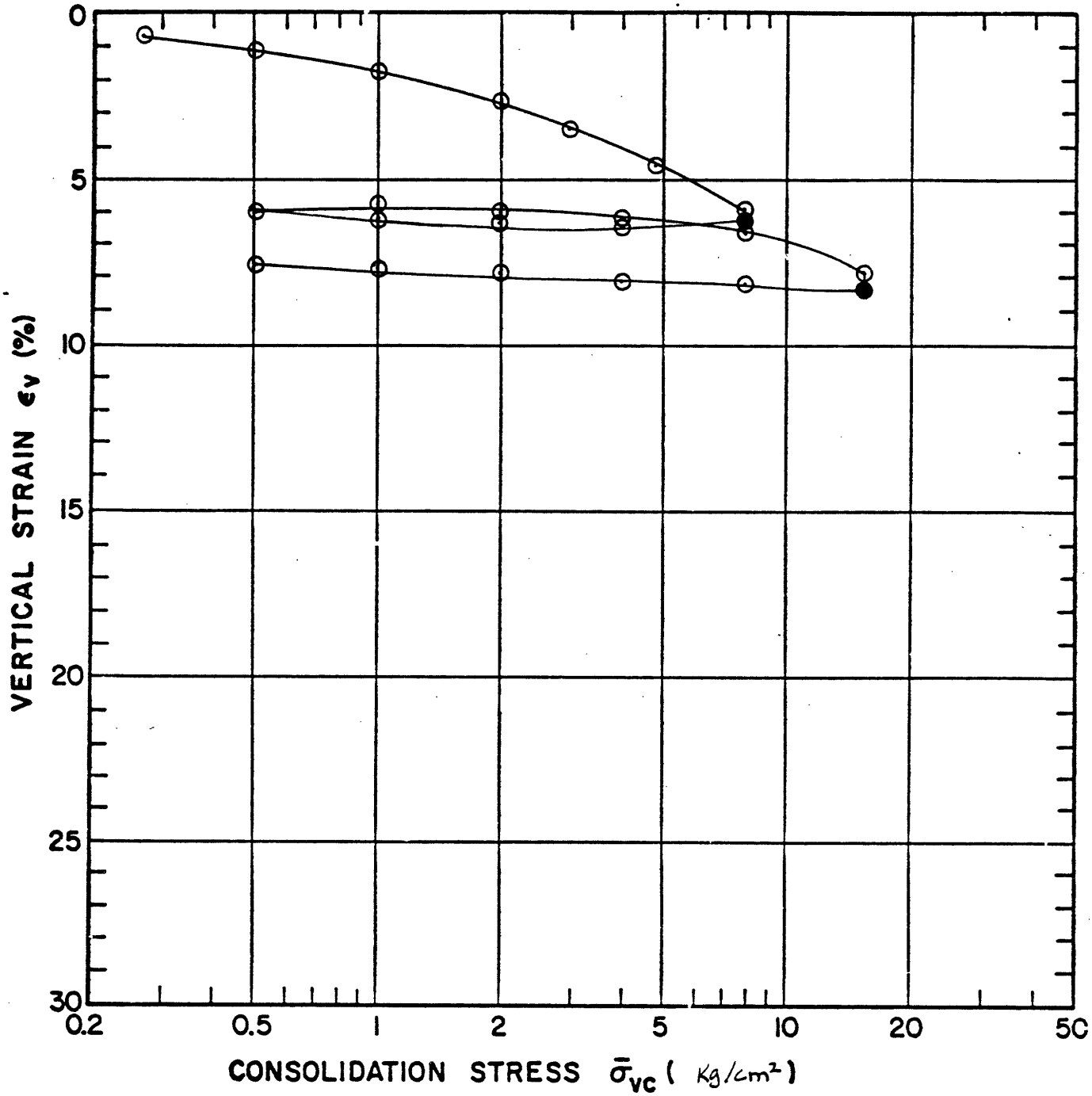

Sample No. MVO 1-11 w_N (%) 24.6 Estimated

Depth 105-107 ft. w_L (%) _____ $\bar{\sigma}_{vo}$ 3.12 KSC $\bar{\sigma}_{vm}$ 2.5-2.95 KSC

Soil Type BBC w_P (%) _____ CR 0.065 RR 0.016

_____ P.I.(%) _____ G_s ____ e_o ____ S(%) ____

○ At t_p or ____ hr Remarks ϵ_v (%) based on d_{100} from log t curves

● At ( ) hr _____

GEOTECHNICAL LABORATORY
DEPT. OF CIVIL ENGR.
M.I.T.

COMPRESSION CURVE

TEST No. DGL-3

CONSOLIDATION TEST

Project _____ Type of Test Incr. Oedometer No. DGL-1 Tested by DGL Date 1/19/83

Soil Type BBC Location Solar House (M.I.T.) Sample Height 1.827 cm

_____ _____ Sample Diameter 6.35 cm.

Initial w(%) _____ G_s _____ w_N(%) 51.2 w_L(%) _____ Corrections Apparatus Compressibility

Void Ratio e _____ S(%) _____ w_p(%) _____ P.I.(%) _____ Units: $\bar{\sigma}_{vc}$ Kg/cm² c_v cm²/sec

$\bar{\sigma}_{vc}$	Primary			Total			C_α(%)	Coef. of Consol.		Remarks
	t (hr)	ε_v(%)	e	t (hr)	ε_v(%)	e		$\sqrt{t}$	log t	
0.125		0.28								
0.250		0.74								
0.500		1.31								
1.00		2.31								
1.75		3.06								
3.00		5.34						1.26 (10^{-3})	1.17 (10^{-3})	
4.75		10.39						4.14 (10^{-4})	3.60 (10^{-4})	
8.00		16.39		16.75	17.44			5.42 (10^{-4})	4.79 (10^{-4})	
4.00		16.74								
2.00		15.75								
1.00		14.49								
0.50		13.17								
1.00		13.54								
2.00		14.14								
4.00		16.20								
8.00		18.37								
16.00		22.82		18.02	23.58			2.74 (10^{-3})	8.16 (10^{-4})	
8.00		23.00								

GEOTECHNICAL LABORATORY
DEPT. OF CIVIL ENGR.
M.I.T.

Remarks Sample MUD 1-7

CONSOLIDATION TEST

Project _____ Type of Test _____ No. D6L-1 Tested by _____ Date _____

Soil Type _____ Location _____ Sample Height _____

_____ _____ Sample Diameter _____

Initial w(%) _____ G_s _____ w_N(%) ____ w_L(%) ____ Corrections _____

Void Ratio e _____ S(%) _____ w_P(%) ____ P.I.(%) _____ Units: $\bar{\sigma}_{vc}$ _____ c_v _____

$\bar{\sigma}_{vc}$	Primary			Total			C_α(%)	Coef. of Consol.		Remarks
	t(hr)	ε_v(%)	e	t(hr)	ε_v(%)	e		$\sqrt{t}$	log t	
4.00		21.82								
2.00		20.77								
1.00		19.41								
0.50		18.19								

GEOTECHNICAL LABORATORY
DEPT. OF CIVIL ENGR.
M.I.T.

Remarks

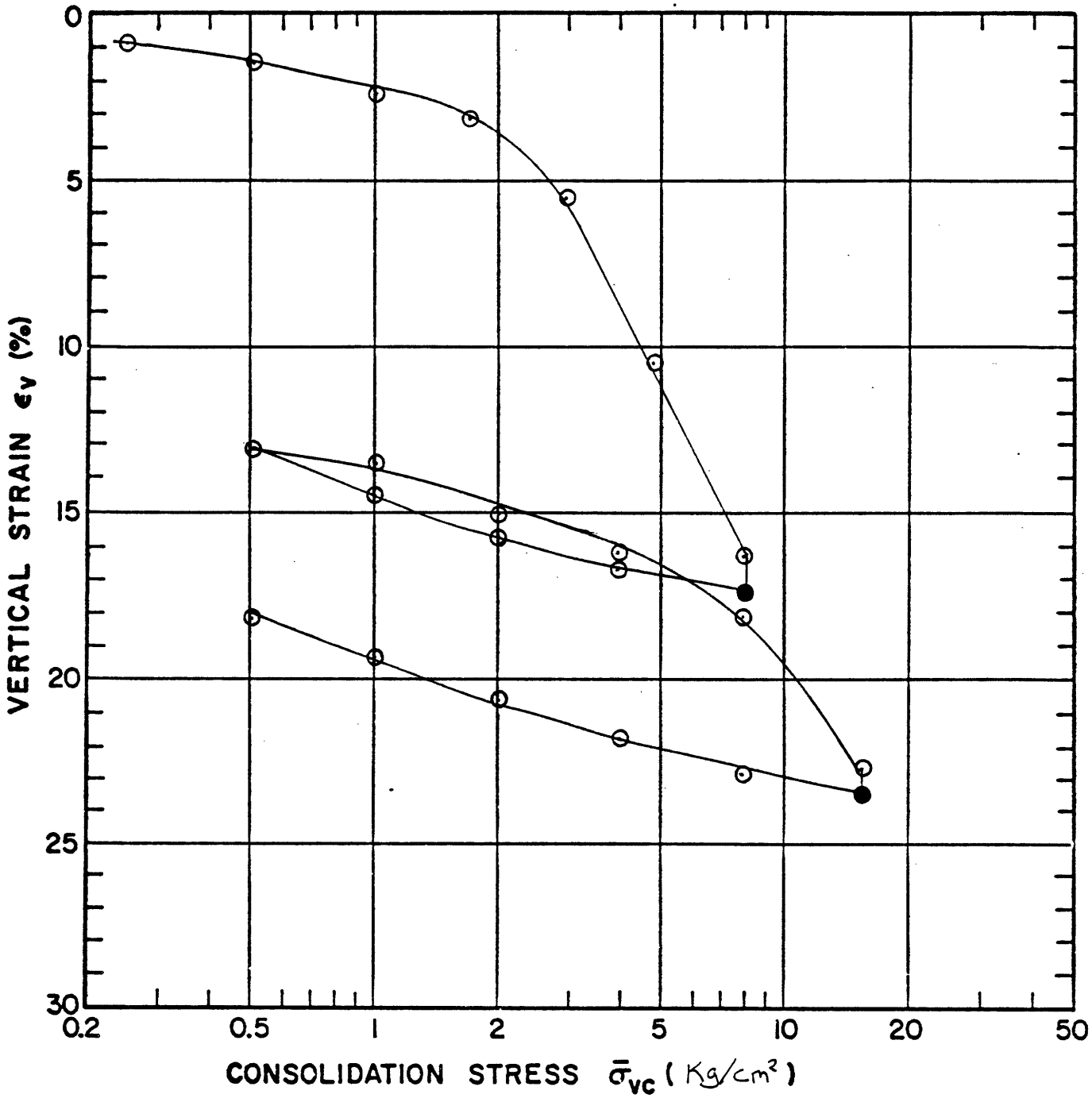

Sample No. MUD 1-7 w_N (%) 51.2% Estimated

Depth 84 - 86 ft. w_L (%) _____ $\bar{\sigma}_{vo}$ 2.58 ksc $\bar{\sigma}_{vm}$ 2.75-2.95 ksc

Soil Type BBC w_P (%) _____ CR 0.265 RR 0.026

_____ P.I.(%) _____ G_s ____ e_o ____ S(%) ____

o At t_p or ____ hr Remarks ϵ_v (%) based on d_{100} from log t curves

● At ( ) hr _____

GEOTECHNICAL LABORATORY
DEPT. OF CIVIL ENGR.
M.I.T.

COMPRESSION CURVE

TEST No. DGL-1

CONSOLIDATION TEST

Project _____ Type of Test Standard No. MUDI-9 Tested by HHH Date 1/82

Soil Type BBC Location Solar House (M.I.T.) Sample Height 2.009 cm.

_____ _____ Sample Diameter 6.35 cm.

Initial w(%) _____ G_s _____ w_N(%) 40.4 w_L(%) _____ Corrections Apparatus Compressibility

Void Ratio e _____ S(%) _____ w_P(%) _____ P.I.(%) _____ Units: $\bar{\sigma}_{vc}$ kg/cm² c_v cm²/sec

$\bar{\sigma}_{vc}$	Primary			Total			C_α(%)	Coef. of Consol.		Remarks
	t (hr)	ε_v(%)	e	t (hr)	ε_v(%)	e		c_v	log t	
0.018		0								
0.125		0.49						9.08 (10^{-3})	4.44 (10^{-3})	
0.25		0.94						5.85 (10^{-3})	5.83 (10^{-3})	
0.50		1.60						4.59 (10^{-3})	3.23 (10^{-3})	
1.00		2.16						4.54 (10^{-3})	4.56 (10^{-3})	
2.00		3.13						5.35 (10^{-3})	5.21 (10^{-3})	
4.00		7.94						2.31 (10^{-3})	2.46 (10^{-4})	
8.00	0.65	15.10		48.92	15.91			1.06 (10^{-2})	5.90 (10^{-4})	
4.00		14.67							5.33 (10^{-4})	
2.00		14.04							2.00 (10^{-3})	
1.00		13.10							7.07 (10^{-4})	
0.50		12.15							5.06 (10^{-4})	
0.25		11.22							1.72 (10^{-4})	
0.125		10.08							7.35 (10^{-5})	

GEOTECHNICAL LABORATORY
DEPT. OF CIVIL ENGR.
M.I.T.

Remarks

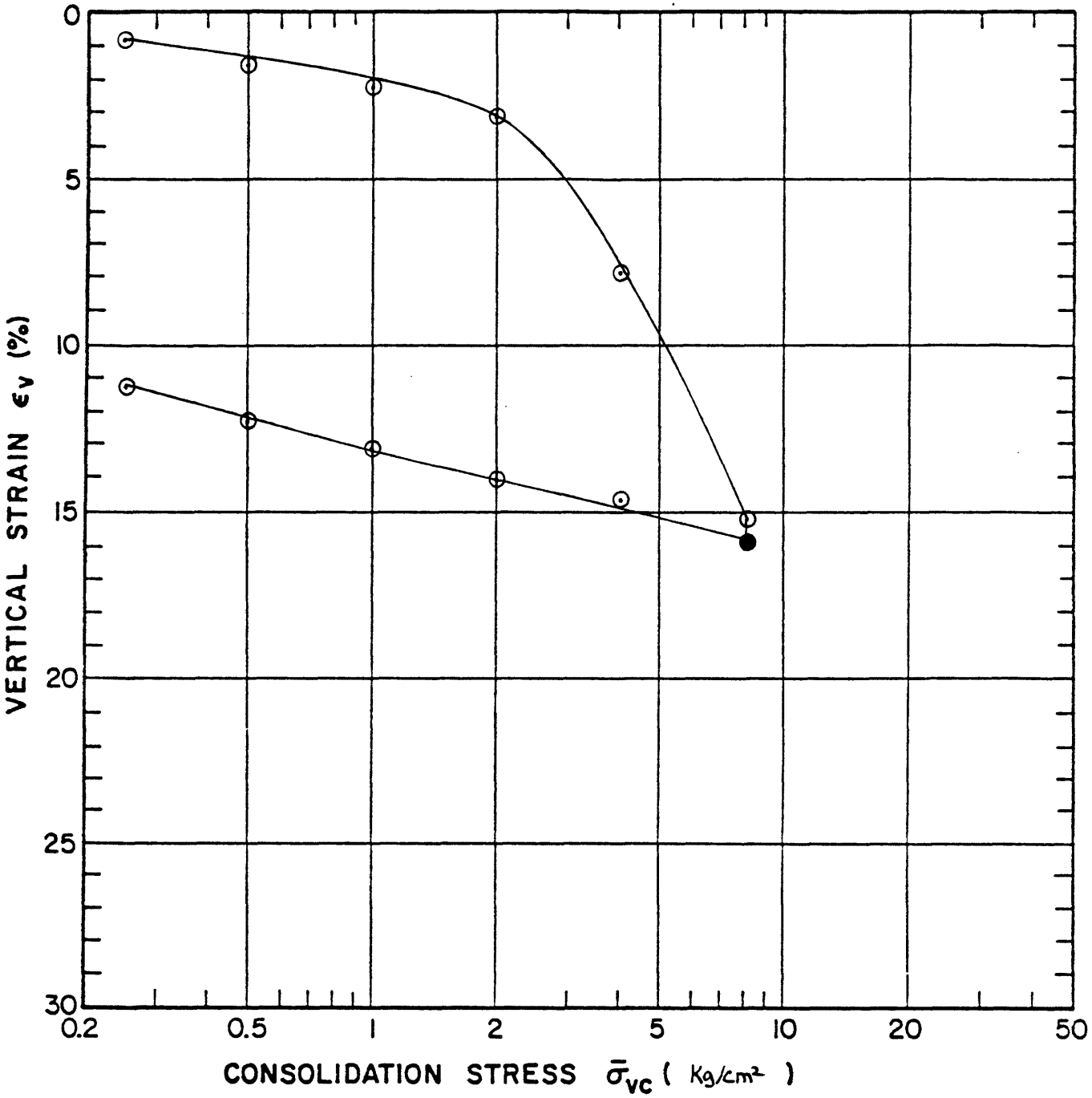

Sample No. MUD 1-9 w_N (%) 40.4 Estimated

Depth 95.0 ft. w_L (%) _____ $\bar{\sigma}_{vo}$ 2.85 ksc $\bar{\sigma}_{vm}$ 2.6-2.8

Soil Type BBC w_P (%) _____ CR 0.338 RR 0.018

_____ P.I.(%) _____ G_s ____ e_o ____ S(%) ____

o At t_p or ____ hr Remarks ϵ_v(%) based on drop from log t curve

● At ( ) hr _____

GEOTECHNICAL LABORATORY
DEPT. OF CIVIL ENGR.
M.I.T.

COMPRESSION CURVE

TEST No. MUD 1-9

CONSOLIDATION TEST

Project _____ Type of Test Incr. Oedometer No. MUDH10a Tested by SPG Date 6/82

Soil Type BBC Location Solar House (M.I.T.) Sample Height 1.993 cm.

_____ _____ Sample Diameter 6.35 cm.

Initial w(%) _____ G_s _____ w_N(%) 30.4 w_L(%) _____ Corrections Apparatus Compressibility

Void Ratio e _____ S(%) _____ w_P(%) _____ P.I.(%) _____ Units: $\bar{\sigma}_{vc}$ kg/cm² c_v cm²/sec

$\bar{\sigma}_{vc}$	Primary			Total			C_α(%)	Coef. of Consol.		Remarks
	t (hr)	ε_v(%)	e	t (hr)	ε_v(%)	e		$\sqrt{t}$	log t	
0.026		0								
0.125		0.71						5.44 (10^{-3})	6.60 (10^{-3})	
0.250		1.35						5.37 (10^{-3})	3.75 (10^{-3})	
0.500		2.06						8.68 (10^{-3})	5.73 (10^{-3})	
1.00		2.88						6.35 (10^{-3})	5.08 (10^{-3})	
1.70		3.77						5.83 (10^{-3})	4.05 (10^{-3})	
2.89		5.22						3.70 (10^{-3})	5.40 (10^{-3})	
4.91		7.81						3.40 (10^{-3})	2.37 (10^{-3})	
8.35		10.36						4.83 (10^{-3})	3.38 (10^{-3})	
14.20	0.068	12.86		1.25	13.31			5.67 (10^{-3})	5.00 (10^{-3})	
8.35		13.16							6.18 (10^{-3})	
2.89		12.75							4.50 (10^{-3})	
1.00		12.14							2.80 (10^{-3})	
0.125		10.93							8.50 (10^{-4})	

GEOTECHNICAL LABORATORY
DEPT. OF CIVIL ENGR.
M.I.T.

Remarks

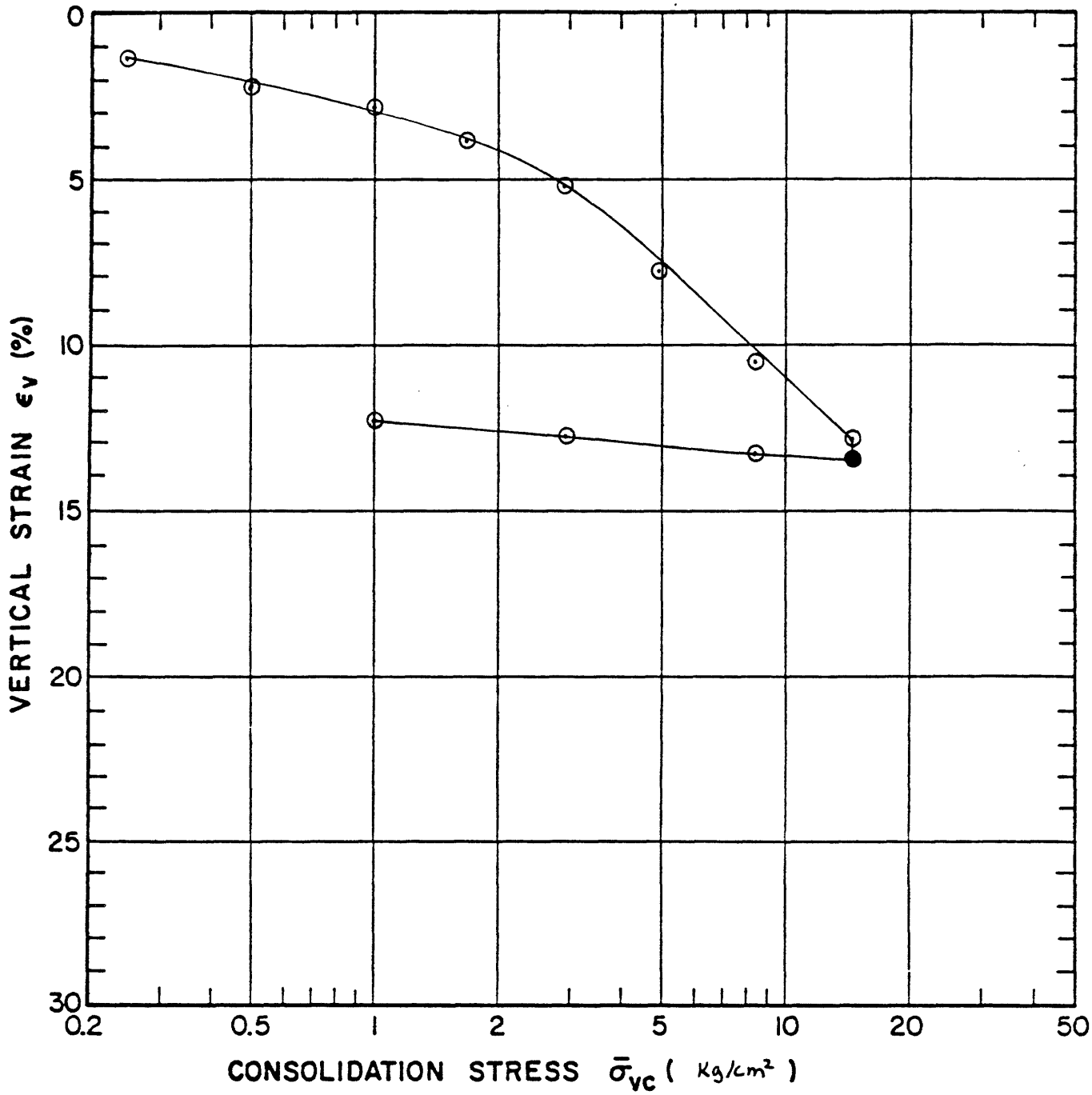

Sample No. MUD 1-10 w_N (%) 30.4 Estimated

Depth 100.5 ft. w_L (%) _____ $\bar{\sigma}_{vo}$ 3.00 ksc $\bar{\sigma}_{vm}$ 2.5-2.8

Soil Type BBC w_P (%) _____ CR 0.109 RR 0.024

_____ P.I.(%) _____ G_s ____ e_o ____ S(%) ____

o At t_p or ____ hr Remarks ϵ_v(%) based on d100 from log t curve

● At ( ) hr _____

GEOTECHNICAL LABORATORY
DEPT. OF CIVIL ENGR.
M.I.T.

COMPRESSION CURVE

TEST No. MUD 1-10a

CONSOLIDATION TEST

Project _____ Type of Test Standard No. MUD1-11 Tested by HHH Date 1/82

Soil Type BBC Location Solar House (M.I.T.) Sample Height 2.008 cm.

_____ _____ Sample Diameter 6.347 cm.

Initial w(%) _____ G_s _____ w_N(%) 36.8 w_L(%) _____ Corrections Apparatus Compressibility

Void Ratio e _____ S(%) _____ w_P(%) _____ P.I.(%) _____ Units: $\bar{\sigma}_{vc}$ Kg/cm² c_v cm²/sec

$\bar{\sigma}_{vc}$	Primary			Total			C_α(%)	Coef. of Consol.		Remarks
	t(hr)	ε_v(%)	e	t(hr)	ε_v(%)	e		$\sqrt{t}$	log t	
0.022		0								
0.125		1.02						1.68 (10^{-3})	1.07 (10^{-3})	
0.25		1.68						8.66 (10^{-4})	3.75 (10^{-4})	
0.50		2.40						1.18 (10^{-3})	7.75 (10^{-4})	
1.00		3.47						2.39 (10^{-3})	1.09 (10^{-3})	
2.00		4.66						2.84 (10^{-3})	1.86 (10^{-3})	
4.00		8.06						1.55 (10^{-2})	5.92 (10^{-4})	
8.00	0.50	13.68		24.42	14.61			9.90 (10^{-4})	6.04 (10^{-4})	
4.00		14.26							4.37 (10^{-3})	
2.00		13.71							1.75 (10^{-3})	
1.00		13.01							6.71 (10^{-4})	
0.50		12.17							2.50 (10^{-4})	
0.25		11.34							1.41 (10^{-4})	
0.125		10.58							1.14 (10^{-4})	

GEOTECHNICAL LABORATORY
DEPT. OF CIVIL ENGR.
M.I.T.

Remarks

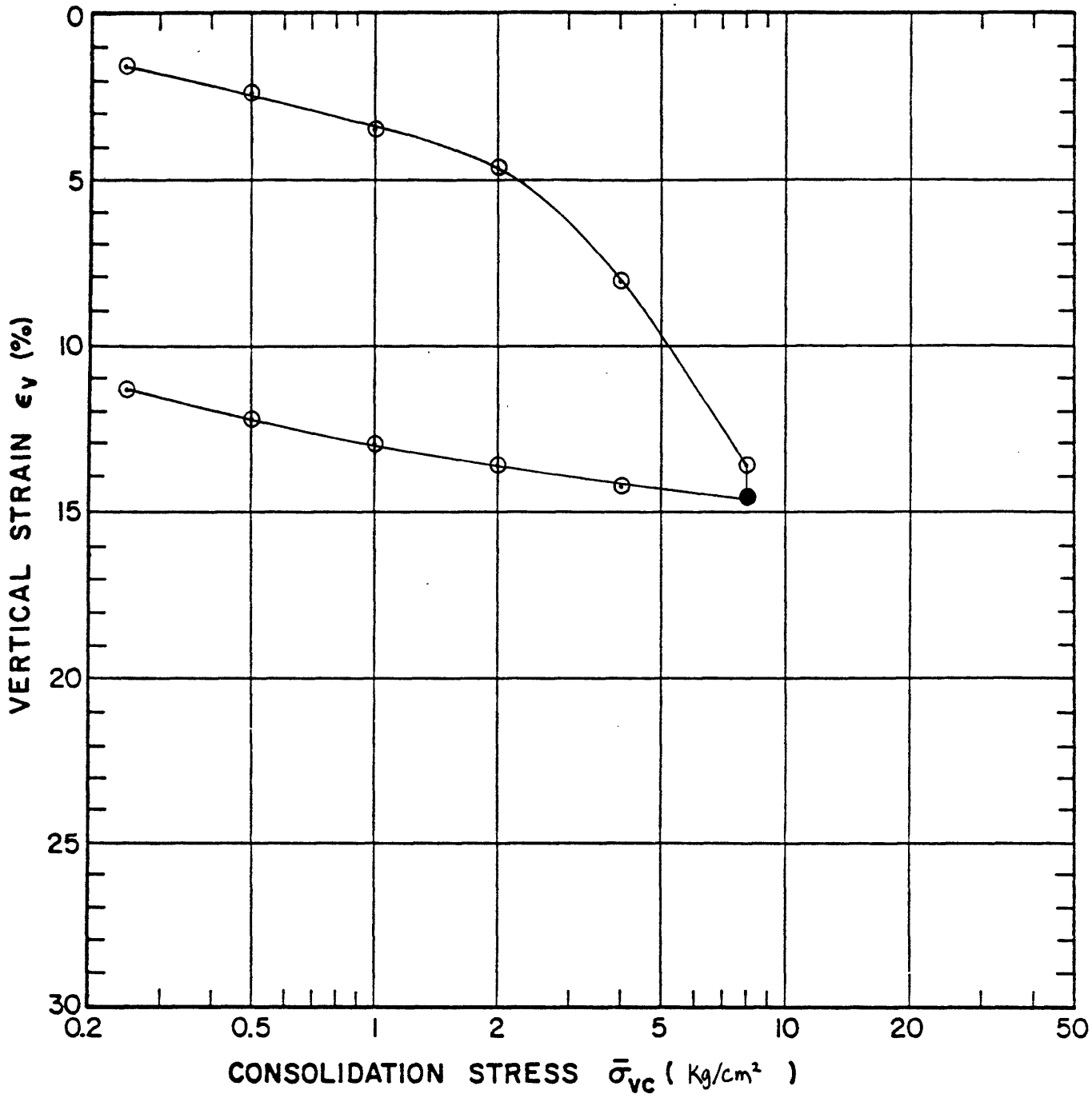

Sample No. MUD 1-11 w_N (%) 36.8 Estimated

Depth 105.0 ft. w_L (%) _____ $\bar{\sigma}_{vo}$ 3.12 kgc $\bar{\sigma}_{vm}$ 2.8-3.1

Soil Type BBC w_P (%) _____ CR 0.187 RR 0.027

_____ P.I.(%) _____ G_s ____ e_o ____ S(%) ____

o At t_p or ____ hr Remarks ϵ_v(%) based on d_{100} from log t curve

● At ( ) hr _____

GEOTECHNICAL LABORATORY
DEPT. OF CIVIL ENGR.
M.I.T.

COMPRESSION CURVE

TEST No. MUD 1-11

APPENDIX B-

K_o-CONSOLIDATED DIRECT SIMPLE SHEAR (CK_oUDSS) TEST RESULTS

DIRECT - SIMPLE SHEAR TEST

PROJECT _____ TYPE OF TEST $\overline{CK_oU}$ DSS NO. 1 OCR 1.00

SOIL TYPE BBC TESTED BY SPG DEVICE Geonor DATE 6/82

LOCATION Solar House (M.I.T.)

CONSOLIDATION (Stresses in kg/cm²)

$\overline{\sigma}_{vc}$ 4.57 τ_{hc} — $\overline{\sigma}_{vm}$ 4.57

t_c(Day) 0.66 ε_v(%) 9.47 γ_c(%) — t_c(Day) _____

	W,%	e	S,%	H (mm)
Initial	40.1			23.000
Preshear				20.823
Final	34.9			

DURING SHEAR
Controlled Strain ✓ Stress _____
Rate (% / Hr.) _____

TIME (Hr.)	STRAIN (%)	$\frac{\tau_h}{\overline{\sigma}_{vc}}$	$\frac{\Delta u}{\overline{\sigma}_{vc}}$	$\frac{\overline{\sigma}_v}{\overline{\sigma}_{vc}}$	$\frac{\tau_h}{S_u}$	$\frac{\tau_h}{\overline{\sigma}_{vm}}$	$\frac{\overline{\sigma}_v}{\overline{\sigma}_{vm}}$	REMARKS
0.00	0.00	0.000	0.000	1.000	0.000			
	0.05	0.028	0.024	0.976				
	0.073	0.037	0.039	0.961	0.21			
	0.10	0.050	0.050	0.950	0.28			
	0.14	0.062	0.055	0.945	0.35			
	0.17	0.070	0.055	0.945	0.39			
	0.23	0.084	0.070	0.930	0.47			
	0.31	0.099	0.084	0.916	0.55			
	0.36	0.106	0.094	0.906	0.60			
	0.45	0.116	0.109	0.891	0.65			
	0.65	0.132	0.140	0.860	0.74			
	1.02	0.151	0.187	0.813	0.85			
	1.67	0.167	0.249	0.751				
	2.04	0.171	0.281	0.719				
	2.62	0.176	0.328	0.672				
	3.76	0.178	0.403	0.597				
1.83	4.50	0.179	0.447	0.553				Peak
	5.95	0.178	0.500	0.500				
	7.40	0.176	0.532	0.468				
	8.83	0.174	0.563	0.437				
	10.98	0.172	0.602	0.398				
	13.21	0.165	0.640	0.360				
	15.41	0.160	0.677	0.323				
	17.68	0.151	0.703	0.297				
5.33	19.18	0.153	0.719	0.281				

SOIL MECHANICS LABORATORY
DEPT. OF CIVIL ENGINEERING
MASSACHUSETTS INSTITUTE OF TECHNOLOGY

REMARKS: $\frac{E_u}{S_u} = \frac{3\tau_h}{S_u \cdot \text{strain}}$

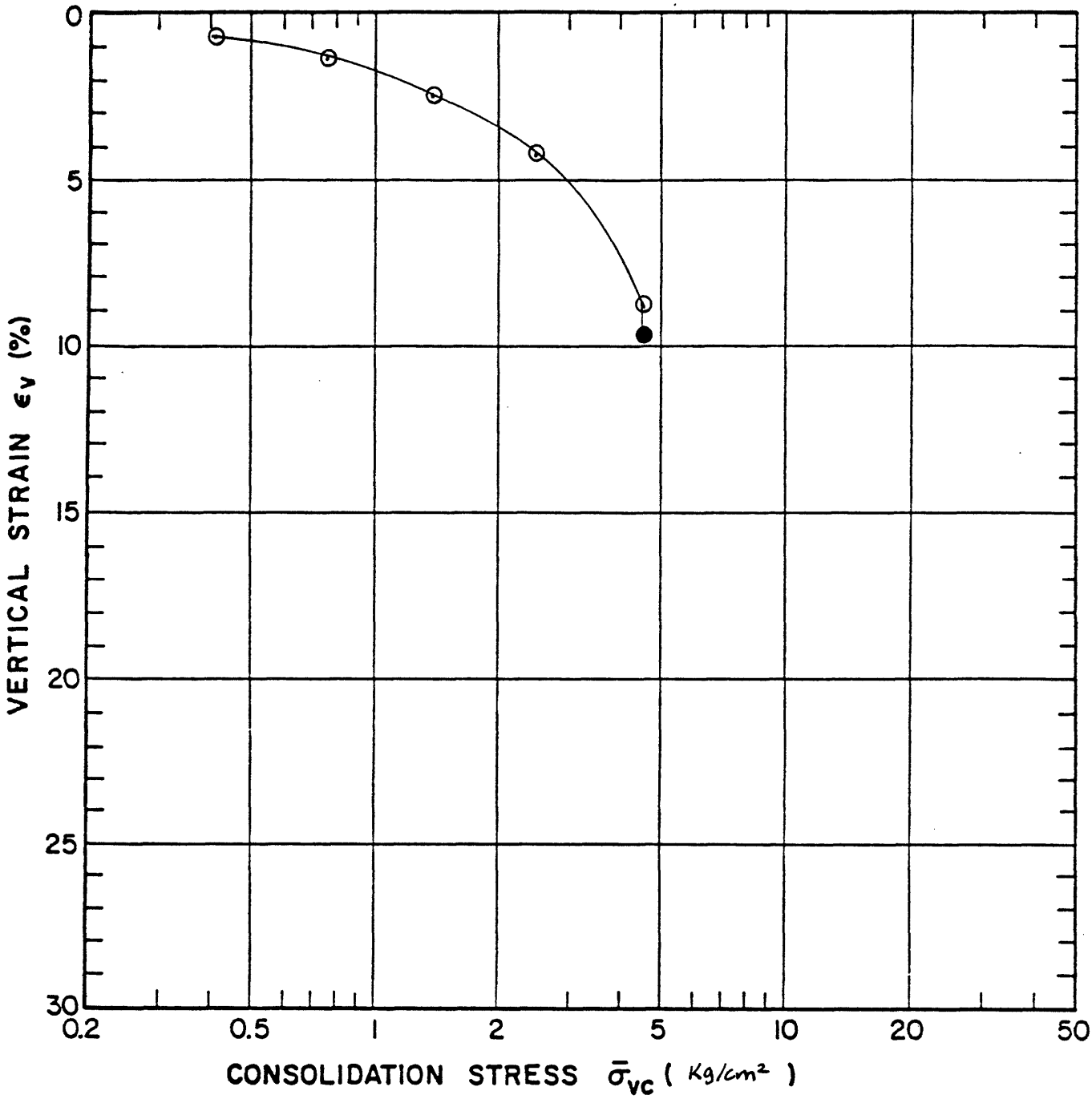

Sample No. MUD 1-7 w_N (%) 40.1 Estimated

Depth 85.0 ft. w_L (%) _____ $\bar{\sigma}_{vo}$ 2.58 ksc $\bar{\sigma}_{vm}$ _____

Soil Type BBC w_P (%) _____ CR _____ RR _____

_____ P.I.(%) _____ G_s _____ e_o _____ S(%) _____

o At t_p or ____ hr Remarks ϵ_v(%) based on dlog t curve

● At ( ) hr _____

GEOTECHNICAL LABORATORY
DEPT. OF CIVIL ENGR.
M.I.T.

COMPRESSION CURVE

TEST No. DSS-1

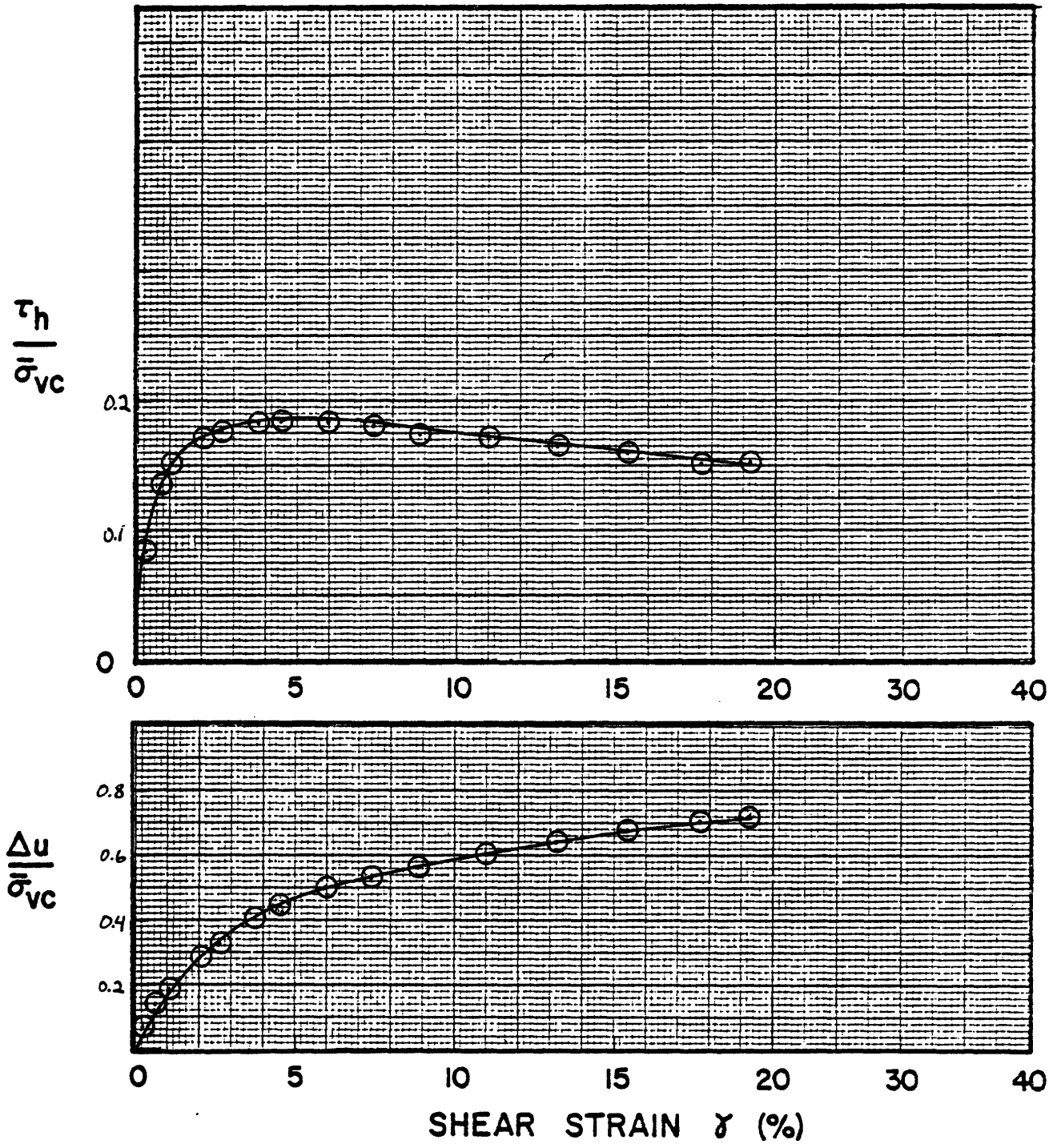

Sample No. MV01-7 w_N(%) 40.1 $\bar{\sigma}_{vc}$(Kg/cm²) 4.57 t_c(Days) 0.66

Depth 85.0 ft. w_L(%) _____ $\bar{\sigma}_{vm}$(Kg/cm²) 4.57 OCR 1.00

Soil Type BBC w_P(%) _____ Estimated $\bar{\sigma}_{vo}$(Kg/cm²) 2.58

GEOTECHNICAL LABORATORY
DEPT. OF CIVIL ENGR.
M.I.T.

NORMALIZED STRESS VS STRAIN
CK_oUDSS TEST NO. 1

FIGURE

Test No.	Sample No.	Depth ft.	w_N (%)	$\bar{\sigma}_{vc}$ (kg/cm^2)	$\bar{\sigma}_{vm}$ (kg/cm^2)	OCR	Symbol
1	MUD 1-7	85.0	40.1	4.57	4.57	1.00	

GEOTECHNICAL LABORATORY
DEPT. OF CIVIL ENGR.
M.I.T.

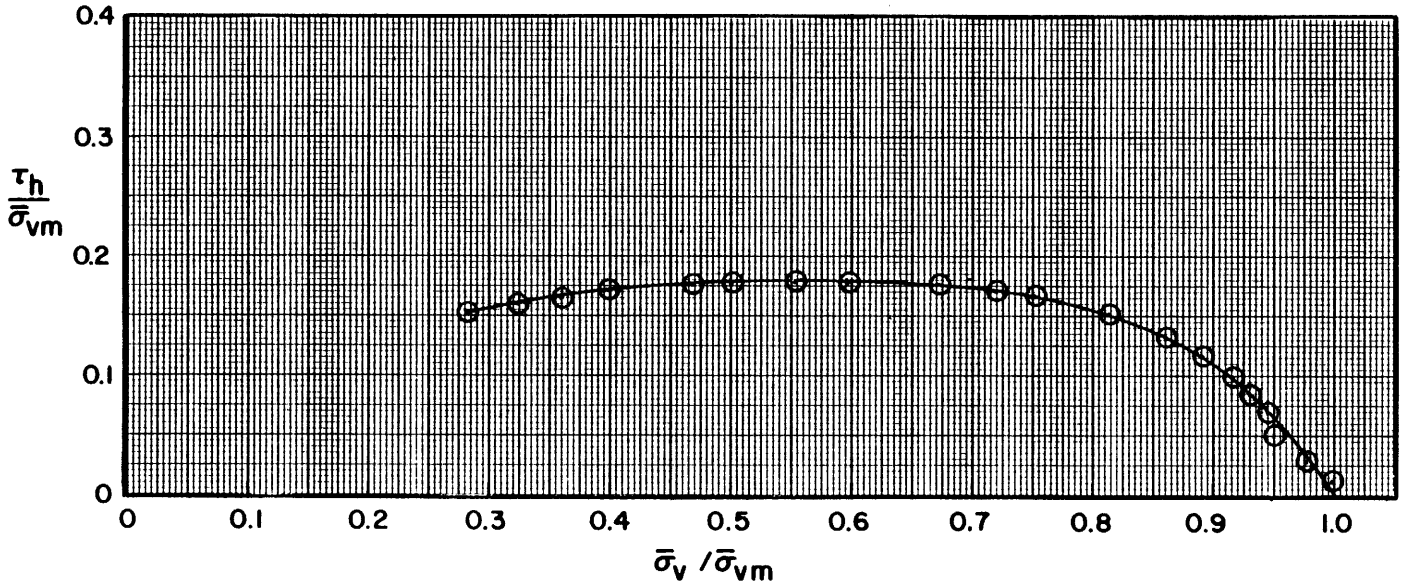

FIGURE

NORMALIZED STRESS PATHS FROM CK_0UDSS TESTS

Boring MUD 1 Soil Type BBC

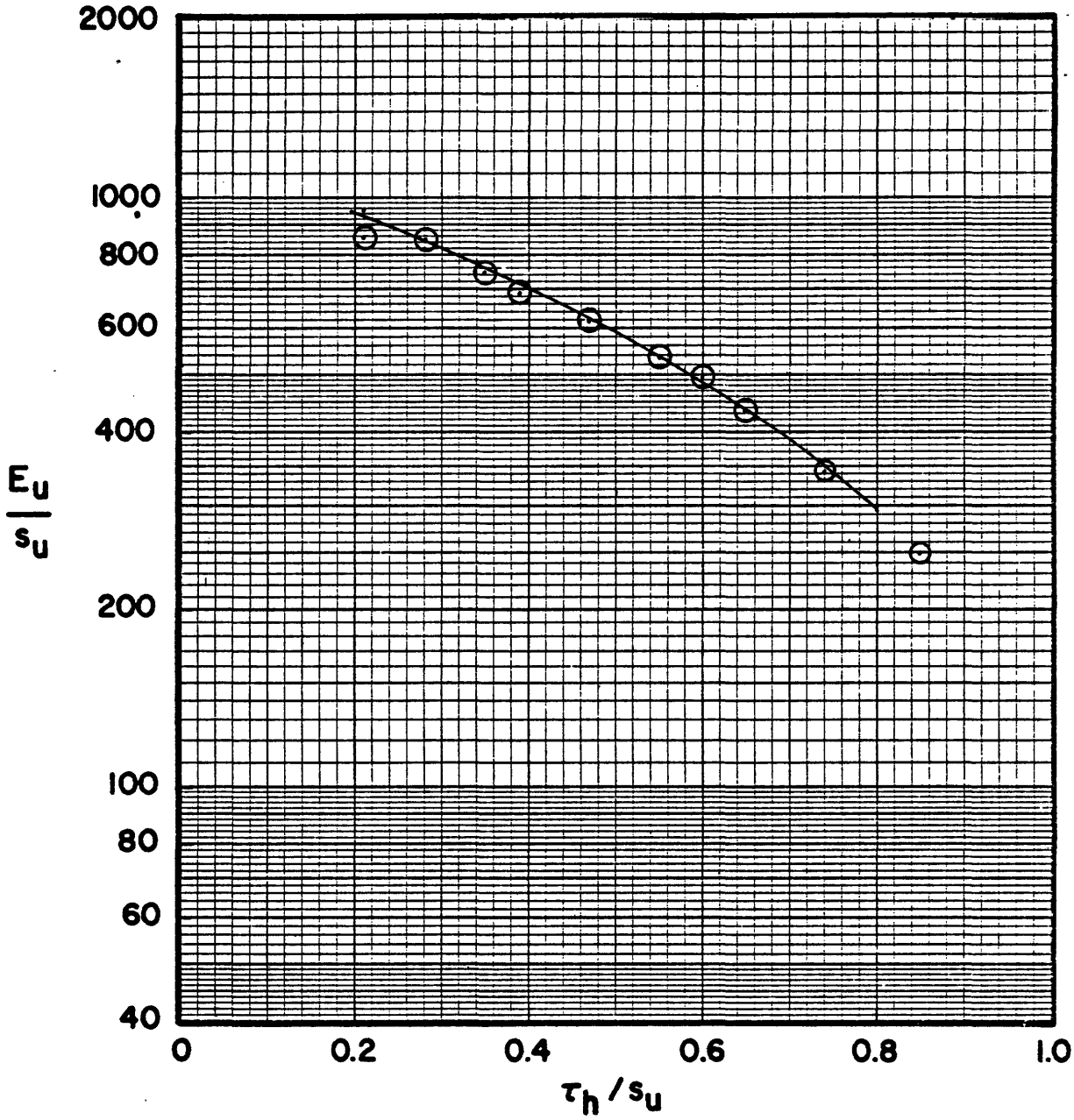

Test No.	Sample No.	Depth	w_N (%)	σ_{vc} (ksc)	OCR	Symbol
1	MUD 1-7	85.0 ft	40.1	4.57	1.00	

NORMALIZED MODULUS FROM CK_oUDSS TESTS

BORING MUD 1 SOIL TYPE BBC

DIRECT - SIMPLE SHEAR TEST

PROJECT _____ TYPE OF TEST $\overline{CK_oU}$ DSS NO. 2a OCR 1.00

SOIL TYPE BBC TESTED BY SPG DEVICE Geonor DATE 7/82

LOCATION Solar House (M.I.T.)

CONSOLIDATION (Stresses in kg/cm²)

$\overline{\sigma}_{vc}$ 6.04 τ_{hc} — $\overline{\sigma}_{vm}$ 6.04

t_c(Day) 0.50 ε_v(%) 17.4 γ_c(%) ___ t_c(Day) _____

	W,%	e	S,%	H (mm)
Initial	41.4			25.308
Preshear				20.912
Final	37.9			

DURING SHEAR
Controlled Strain ✓ Stress ____
Rate (% / Hr.) ____

TIME (Hr.)	STRAIN (%)	$\frac{\tau_h}{\overline{\sigma}_{vc}}$	$\frac{\Delta u}{\overline{\sigma}_{vc}}$	$\frac{\overline{\sigma}_v}{\overline{\sigma}_{vc}}$	$\frac{\tau_h}{S_u}$	$\frac{\tau_h}{\overline{\sigma}_{vm}}$	$\frac{\overline{\sigma}_v}{\overline{\sigma}_{vm}}$	REMARKS
0.00	0.00	0.000	0.000	1.000	0.000			
	0.02	0.023	0.000	1.000	0.132			
	0.06	0.036	0.000	1.000	0.206			
	0.12	0.050	-0.013	1.013	0.290			
	0.17	0.059	-0.010	1.010	0.341			
	0.24	0.067	-0.013	1.013	0.389			
	0.34	0.078	-0.017	1.017	0.451			
	0.42	0.087	-0.020	1.020	0.502			
	0.62	0.103	0.012	0.988	0.577			
	0.98	0.118	0.058	0.942	0.679			
	1.38	0.134	0.104	0.896	0.773			
	1.84	0.148	0.146	0.854	0.853			
	2.35	0.159	0.189	0.811				
	3.01	0.164	0.232	0.768				
	4.02	0.169	0.311	0.689				
	5.03	0.170	0.349	0.651				
	5.70	0.172	0.381	0.619				
2.25	6.42	0.173	0.417	0.583				Peak
	7.12	0.172	0.447	0.553				
	8.89	0.170	0.520	0.480				
	10.05	0.166	0.560	0.440				
	11.18	0.162	0.598	0.402				
	12.76	0.159	0.596	0.404				
	14.18	0.159	0.609	0.391				
4.37	15.63	0.158	0.621	0.379				

SOIL MECHANICS LABORATORY
DEPT. OF CIVIL ENGINEERING
MASSACHUSETTS INSTITUTE OF TECHNOLOGY

REMARKS: $\frac{E_u}{S_u} = \frac{3\tau_h}{S_u \cdot \text{strain}}$

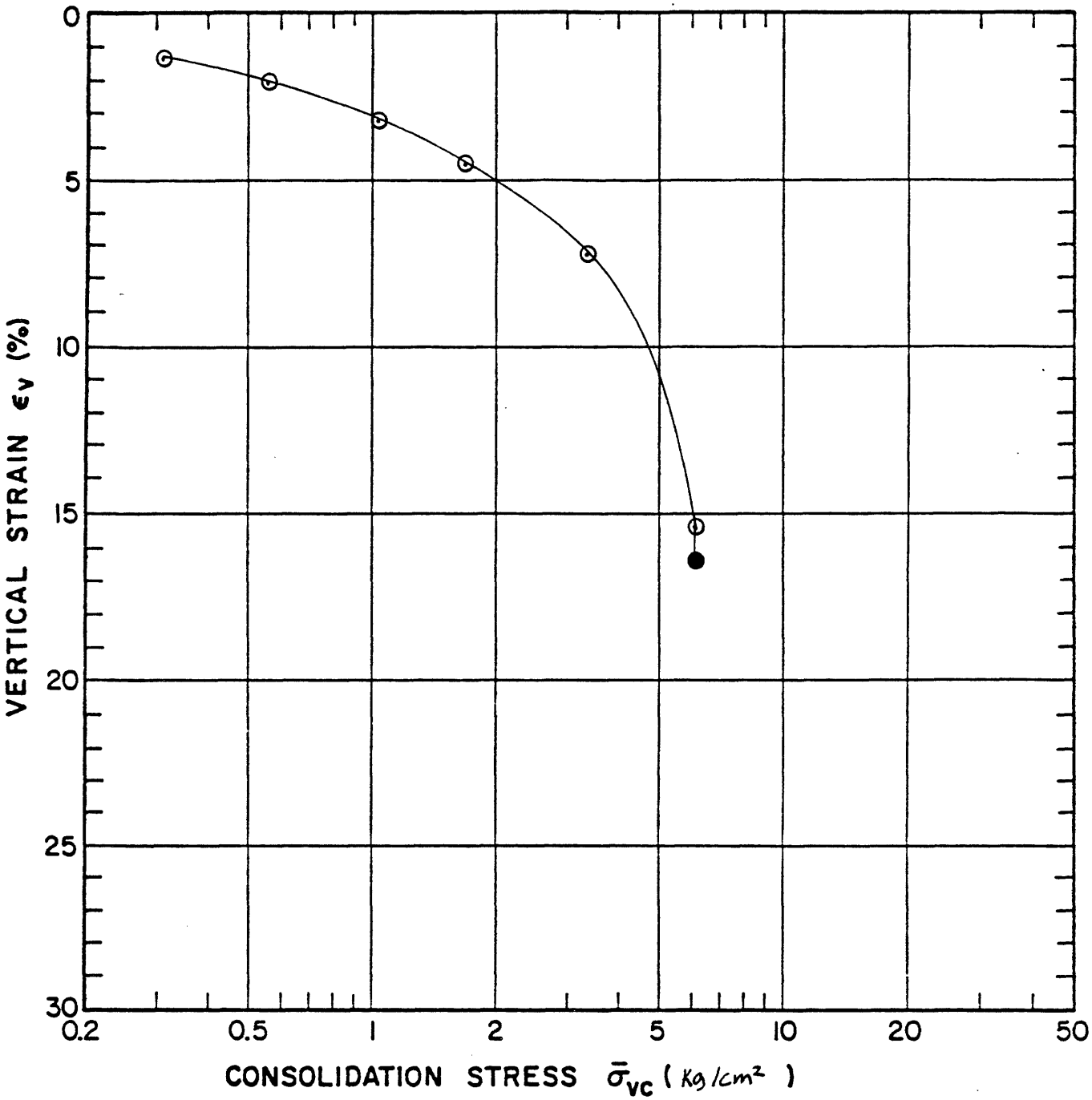

Sample No. MUD 1-7 w_N (%) 41.4 Estimated

Depth 85.0 ft. w_L (%) _____ $\bar{\sigma}_{vo}$ 2.58 kg/cm² $\bar{\sigma}_{vm}$ _____

Soil Type _____ w_P (%) _____ CR _____ RR _____

_____ P.I.(%) _____ G_s _____ e_o _____ S(%) _____

o At t_p or ____ hr Remarks ϵ_v (%) based on slope from log t curve

● At ( ) hr _____

GEOTECHNICAL LABORATORY
DEPT. OF CIVIL ENGR.
M.I.T.

COMPRESSION CURVE

TEST No. DSS-2a

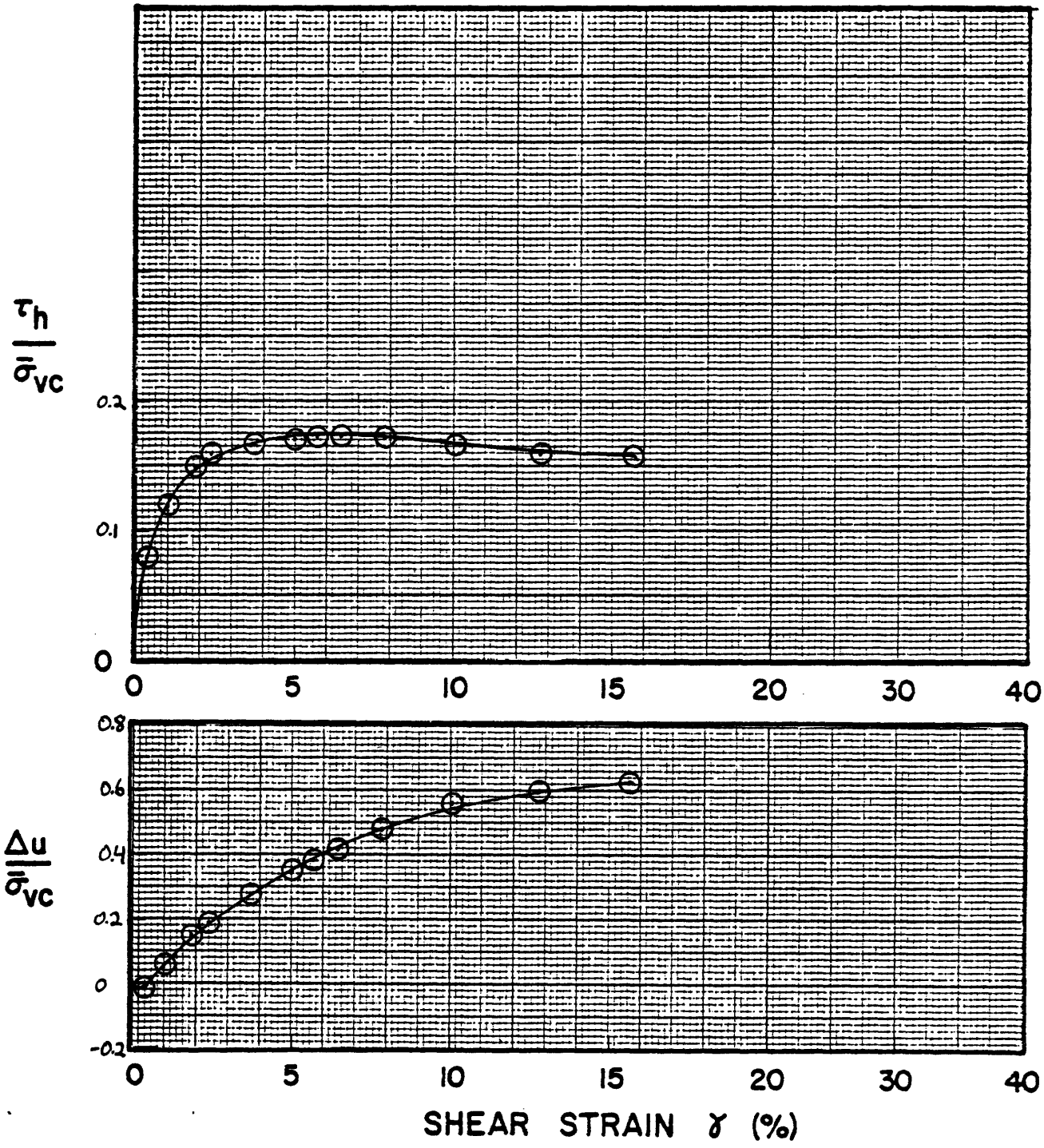

Sample No. MUD-7 w_N(%) 41.4 $\bar{\sigma}_{vc}$(Kg/cm²) 6.04 t_c(Days) 0.50

Depth 85.0 w_L(%) ____ $\bar{\sigma}_{vm}$(Kg/cm²) 6.04 OCR 1.00

Soil Type ____ w_P(%) ____ Estimated $\bar{\sigma}_{vo}$(Kg/cm²) 2.58

GEOTECHNICAL LABORATORY
DEPT. OF CIVIL ENGR.
M.I.T.

NORMALIZED STRESS VS STRAIN

CK_oUDSS TEST NO. 2a

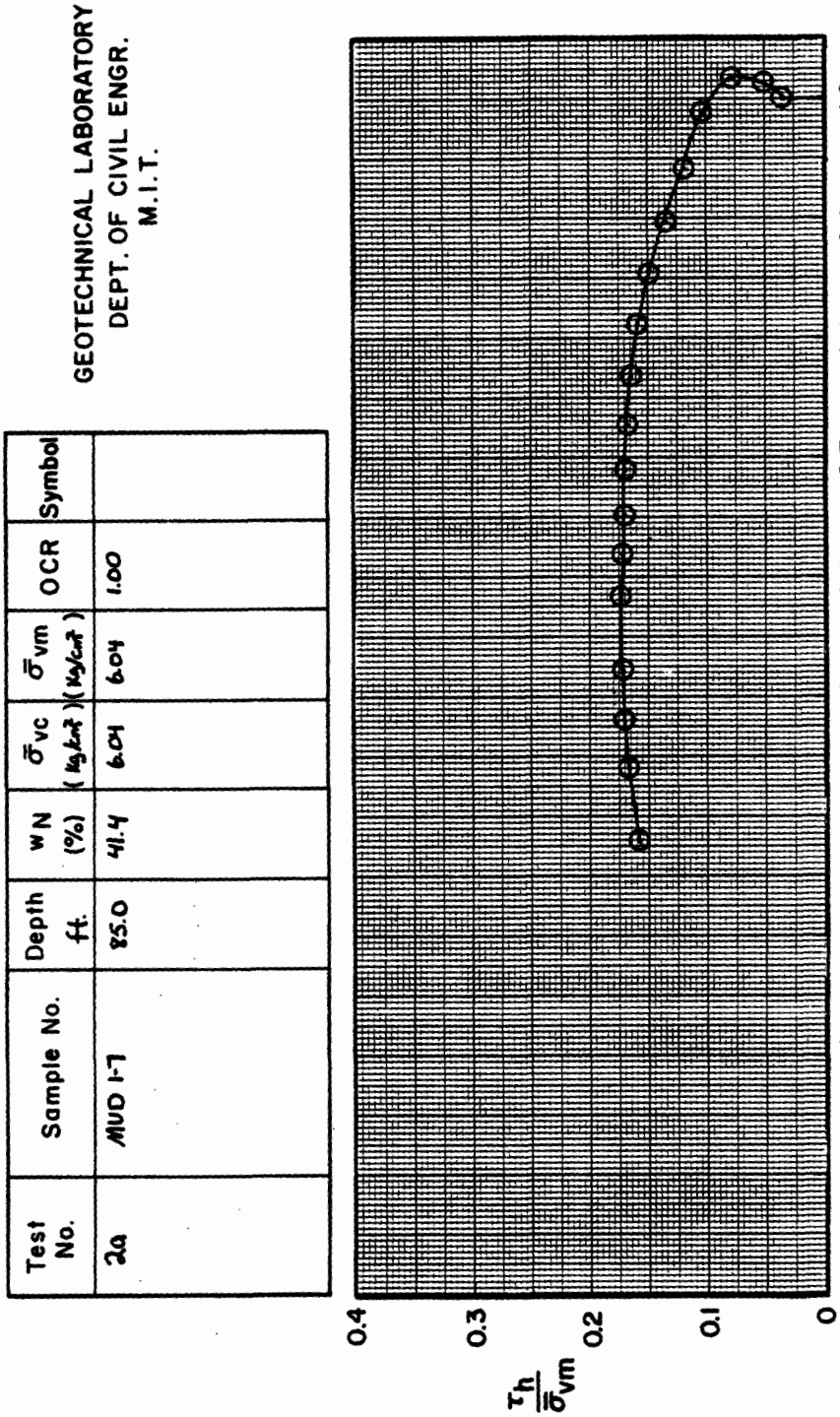

NORMALIZED STRESS PATHS FROM CK_oUDSS TESTS

Boring MUD 1 Soil Type BBC

FIGURE

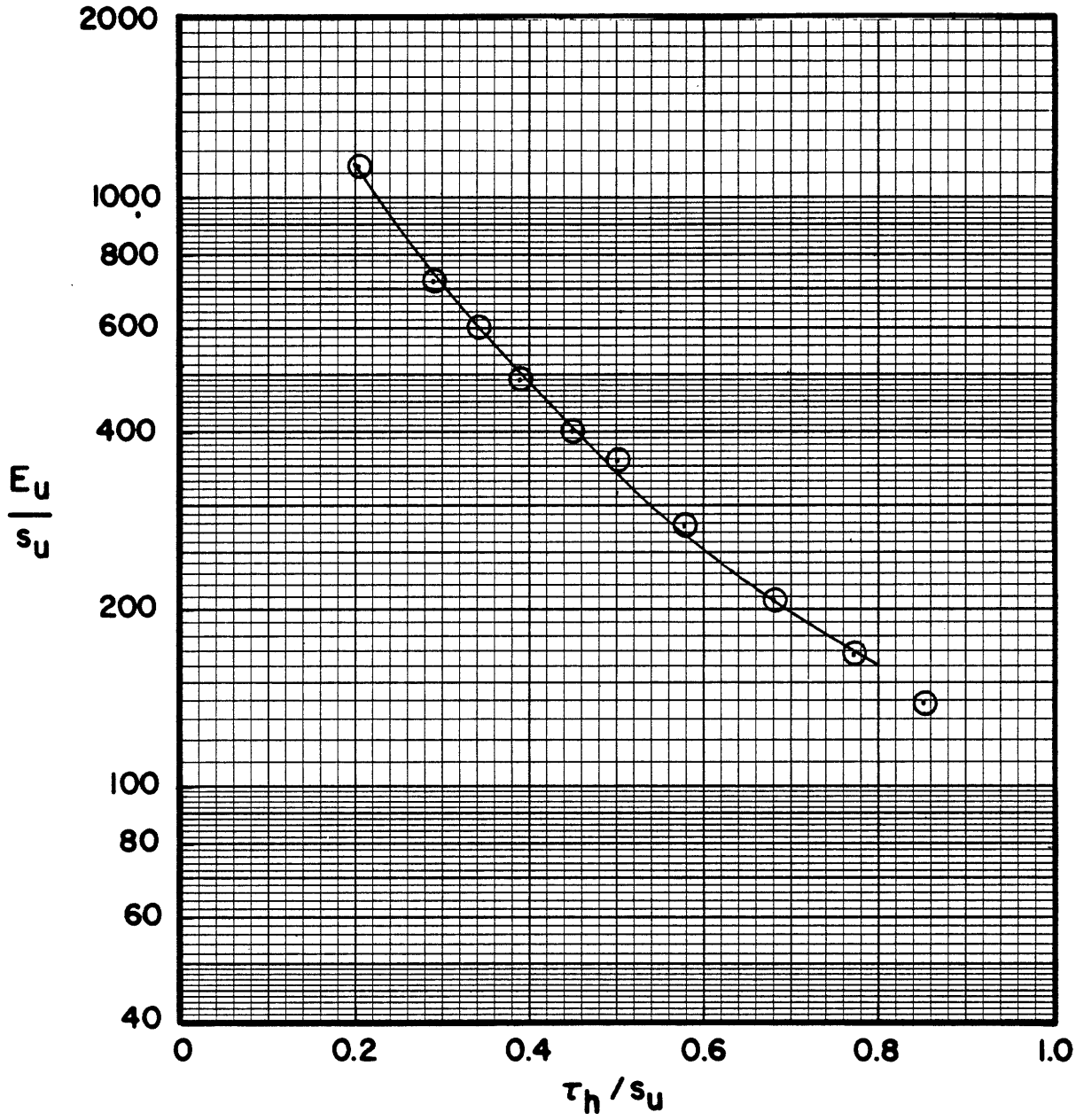

Test No.	Sample No.	Depth ft.	w_N (%)	σ_{vc} (kg/cm²)	OCR	Symbol
2a	MUD 1-7	85.0	41.4	6.04	1.00	

NORMALIZED MODULUS FROM CK_oUDSS TESTS

BORING MUD 1 SOIL TYPE BBC

FIGURE

GEOTECHNICAL LABORATORY, DEPT. OF CIVIL ENGR., M.I.T.

DIRECT - SIMPLE SHEAR TEST

PROJECT _____ TYPE OF TEST $\overline{CK_oU}$ DSS NO. 5 OCR 1.00

SOIL TYPE BBC TESTED BY SPG DEVICE Geonor DATE 7/82

LOCATION Solar House (M.I.T.)

CONSOLIDATION (Stresses in kg/cm²)

$\bar{\sigma}_{vc}$ 4.54 τ_{hc} — $\bar{\sigma}_{vm}$ 4.54

t_c(Day) 0.90 ε_v(%) 11.7 γ_c(%) — t_c(Day) _____

	W,%	e	S,%	H (mm)
Initial	37.6			24.943
Preshear				22.036
Final	36.6			

DURING SHEAR

Controlled Strain ✓ Stress _____

Rate (% / Hr.) 3.7

TIME (Hr.)	STRAIN (%)	$\frac{\tau_h}{\bar{\sigma}_{vc}}$	$\frac{\Delta u}{\bar{\sigma}_{vc}}$	$\frac{\bar{\sigma}_v}{\bar{\sigma}_{vc}}$	$\frac{\tau_h}{S_u}$	$\frac{\tau_h}{\bar{\sigma}_{vm}}$	$\frac{\bar{\sigma}_v}{\bar{\sigma}_{vm}}$	REMARKS
0.00	0.00	0.000	0.000	1.000	0.000			
0.12	0.03	0.036	0.004	0.996	0.205			
	0.05	0.040	0.007	0.993	0.228			
	0.05	0.044	0.013	0.987	0.251			
	0.08	0.053	0.022	0.978	0.298			
	0.11	0.064	0.032	0.980	0.365			
	0.16	0.075	0.020	0.980	0.426			
	0.19	0.082	0.029	0.971	0.466			
	0.24	0.092	0.044	0.956	0.523			
	0.33	0.102	0.040	0.960	0.577			
	0.41	0.111	0.051	0.949	0.625			
	0.55	0.121	0.071	0.929	0.684			
	0.68	0.130	0.091	0.909	0.737			
	0.85	0.139	0.106	0.894	0.785			
	1.10	0.149	0.126	0.874	0.841			
	2.19	0.172	0.208	0.792				
	3.00	0.177	0.269	0.731				Peak
1.47	3.69	0.177	0.316	0.684				
	4.54	0.176	0.369	0.631				
	6.57	0.175	0.453	0.547				
	9.95	0.173	0.534	0.466				
	12.06	0.169	0.563	0.437				
	14.19	0.164	0.592	0.408				
	16.31	0.159	0.616	0.384				
5.07	18.77	0.153	0.647	0.353				

SOIL MECHANICS LABORATORY
DEPT. OF CIVIL ENGINEERING
MASSACHUSETTS INSTITUTE OF TECHNOLOGY

REMARKS: $\frac{E_u}{S_u} = \frac{3\tau_h}{S_u \text{ strain}}$

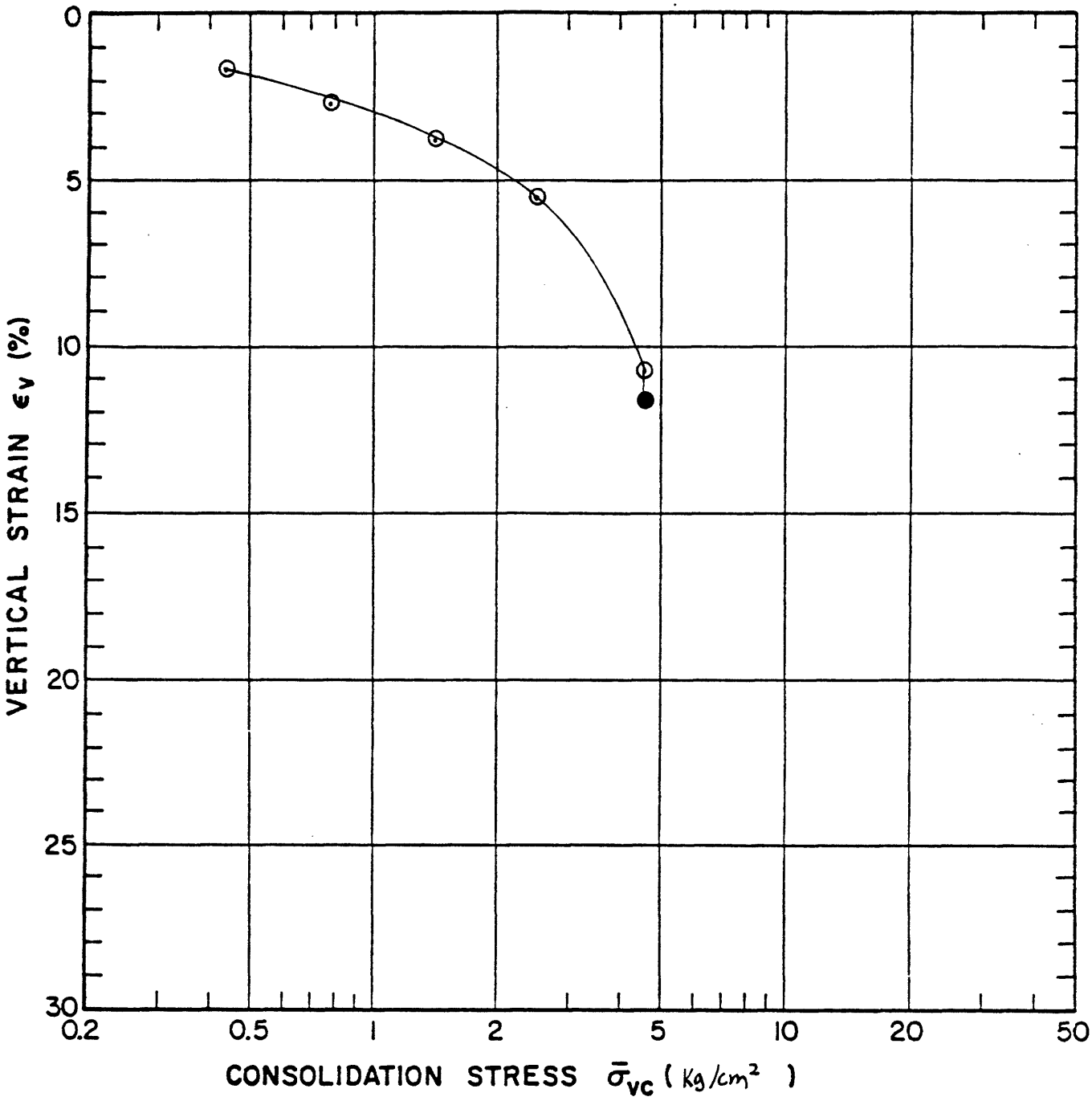

Sample No. MU01-9 w_N (%) 36.6 Estimated

Depth 96.0 ft. w_L (%) _____ $\bar{\sigma}_{vo}$ 2.85 Kg/cm² $\bar{\sigma}_{vm}$ _____

Soil Type BBC w_P (%) _____ CR _____ RR _____

_____ P.I.(%) _____ G_s _____ e_o _____ S(%) _____

o At t_p or ____ hr Remarks ϵ_v(%) based on d_{100} from log t curve

● At ( ) hr _____

GEOTECHNICAL LABORATORY
DEPT. OF CIVIL ENGR.
M.I.T.

COMPRESSION CURVE

TEST No. OSS-5

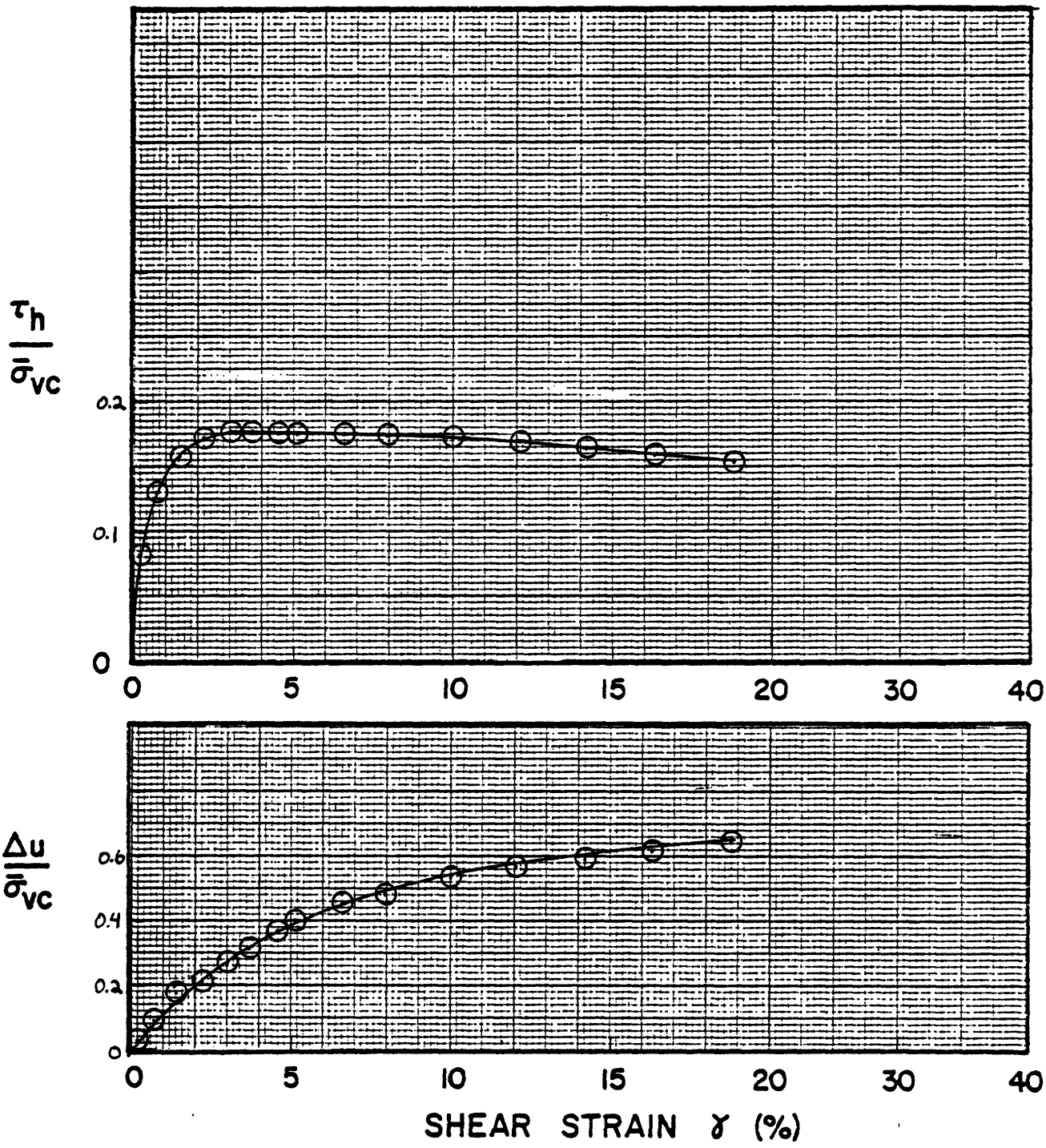

Sample No. MUD 1-9 w_N(%) 36.6 $\bar{\sigma}_{vc}$(4.54 ksc) ____ t_c(Days) 0.90

Depth 96.0 ft. w_L(%) ____ $\bar{\sigma}_{vm}$(4.54 ksc) ____ OCR 1.00

Soil Type BBC w_P(%) ____ Estimated $\bar{\sigma}_{vo}$(Kg/cm²) 2.85

GEOTECHNICAL LABORATORY
DEPT. OF CIVIL ENGR.
M.I.T.

NORMALIZED STRESS VS STRAIN

CK_oUDSS TEST NO. 5

Test No.	Sample No.	Depth	w_N (%)	$\bar{\sigma}_{vc}$ (kg/cm²)	$\bar{\sigma}_{vm}$ (kg/cm²)	OCR	Symbol
5	MUD 1-9	96.0	36.6	4.54	4.54	1.00	

GEOTECHNICAL LABORATORY
DEPT. OF CIVIL ENGR.
M.I.T.

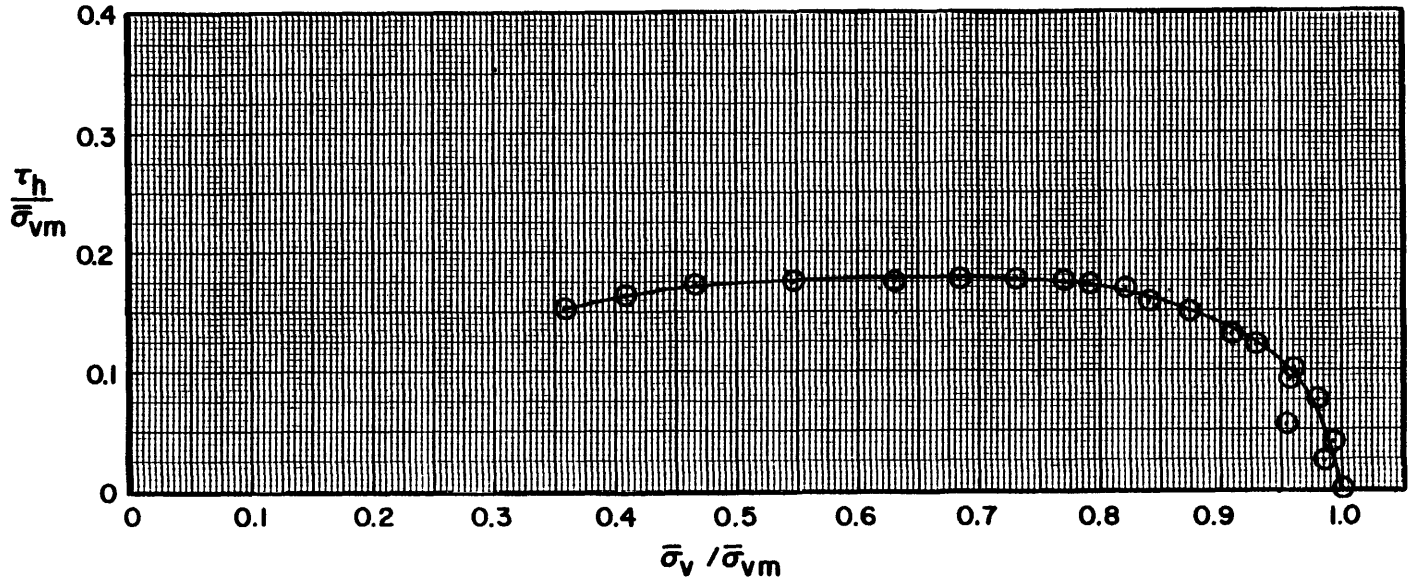

FIGURE

NORMALIZED STRESS PATHS FROM CK_0UDSS TESTS

Boring MUD 1 Soil Type BBC

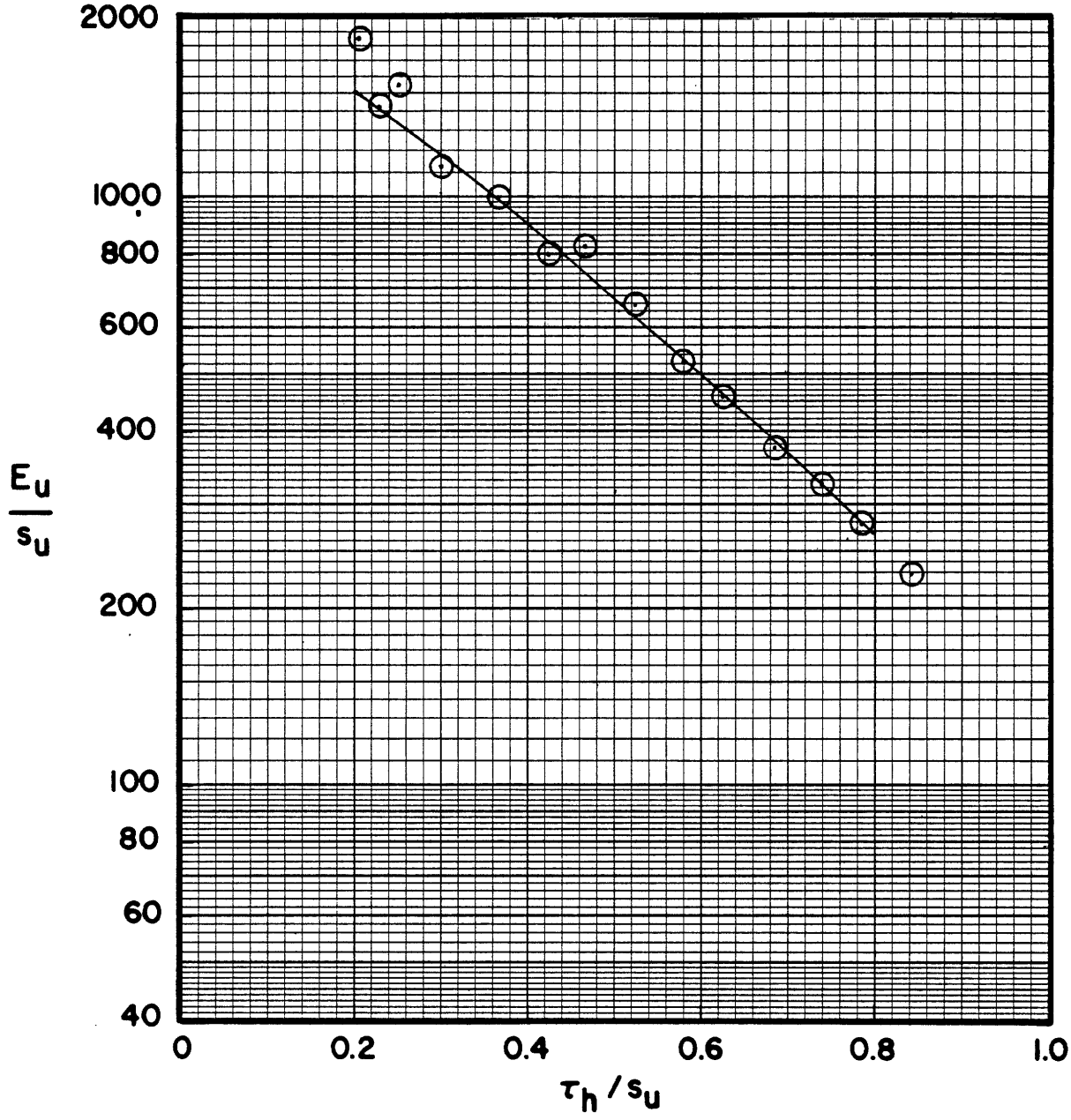

Test No.	Sample No.	Depth (ft.)	w_N (%)	σ_{vc} (kg/cm^2)	OCR	Symbol
5	MUD 1-9	96.0	36.6	4.54	1.00	

NORMALIZED MODULUS FROM CK_oUDSS TESTS

BORING MUD 1 SOIL TYPE BBC

FIGURE

GEOTECHNICAL LABORATORY, DEPT. OF CIVIL ENGR., M.I.T.

DIRECT - SIMPLE SHEAR TEST

PROJECT _____ TYPE OF TEST $\overline{CK_oU}$DSS NO. 10 OCR 2.01

SOIL TYPE BBC TESTED BY SPG DEVICE Geonor DATE 8/82

LOCATION Solar House (M.I.T.)

CONSOLIDATION (Stresses in kg/cm²)

$\bar{\sigma}_{vc}$ 4.51 τ_{hc} - $\bar{\sigma}_{vm}$ 9.06

t_c(Day) 0.76 ε_v(%) 8.7 γ_c(%) ___ t_c(Day) ___

	W,%	e	S,%	H (mm)
Initial	34.0			24.638
Preshear				22.489
Final	32.0			

DURING SHEAR
Controlled Strain ✓ Stress ___
Rate (% / Hr.) ___

TIME (Hr.)	STRAIN (%)	$\frac{\tau_h}{\bar{\sigma}_{vc}}$	$\frac{\Delta u}{\bar{\sigma}_{vc}}$	$\frac{\bar{\sigma}_v}{\bar{\sigma}_{vc}}$	$\frac{\tau_h}{S_u}$	$\frac{\tau_h}{\bar{\sigma}_{vm}}$	$\frac{\bar{\sigma}_v}{\sigma_{vm}}$	REMARKS
0.00	0.00	0.000	0.000		0.000	0.000	0.000	
	0.09	0.055			0.171			
	0.14	0.074			0.233			
	0.17	0.090			0.281			
	0.20	0.099			0.311			
	0.25	0.116			0.363			
	0.26	0.124			0.390			
	0.29	0.133			0.416			
	0.32	0.141			0.442			
	0.35	0.150			0.469			
	0.39	0.157			0.493			
	0.42	0.165			0.518			
	0.46	0.173			0.542			
	0.49	0.180			0.565			
	0.54	0.188			0.589			
	0.59	0.195			0.611			
	0.63	0.202			0.633			
	0.68	0.208			0.654			
			*Malfunction of electronic recording device					
			*Peak value obtained manually					
3.25		0.318						Peak

SOIL MECHANICS LABORATORY
DEPT. OF CIVIL ENGINEERING
MASSACHUSETTS INSTITUTE OF TECHNOLOGY

REMARKS: $\frac{E_u}{S_u} = \frac{3\tau_h}{S_u \cdot \text{strain}}$
- At maximum load, t_c = 2.1 hrs. ε_v% = 9.0

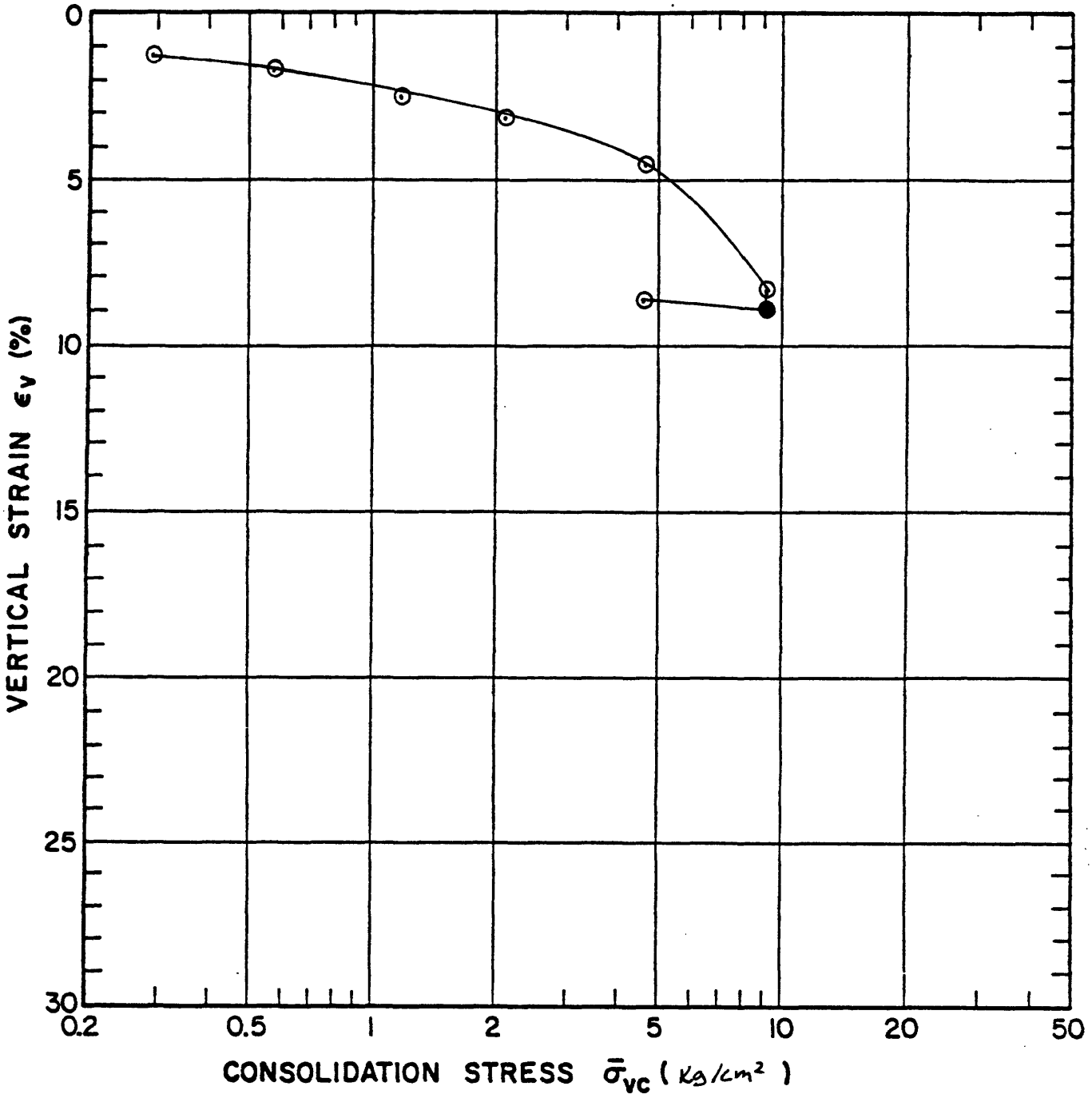

Sample No. MUD 1-4 w_N (%) 34.0 Estimated

Depth 59.0 ft. w_L (%) _____ $\bar{\sigma}_{vo}$ 1.95 ksc $\bar{\sigma}_{vm}$ _____

Soil Type _____ w_P (%) _____ CR _____ RR _____

_____ P.I.(%) _____ G_s ____ e_o ____ S(%) ____

o At t_p or ____ hr Remarks ϵ_v(%) based on d_{100} from log t curve

● At ( ) hr _____

GEOTECHNICAL LABORATORY
DEPT. OF CIVIL ENGR.
M.I.T.

COMPRESSION CURVE

TEST No. DSS-10

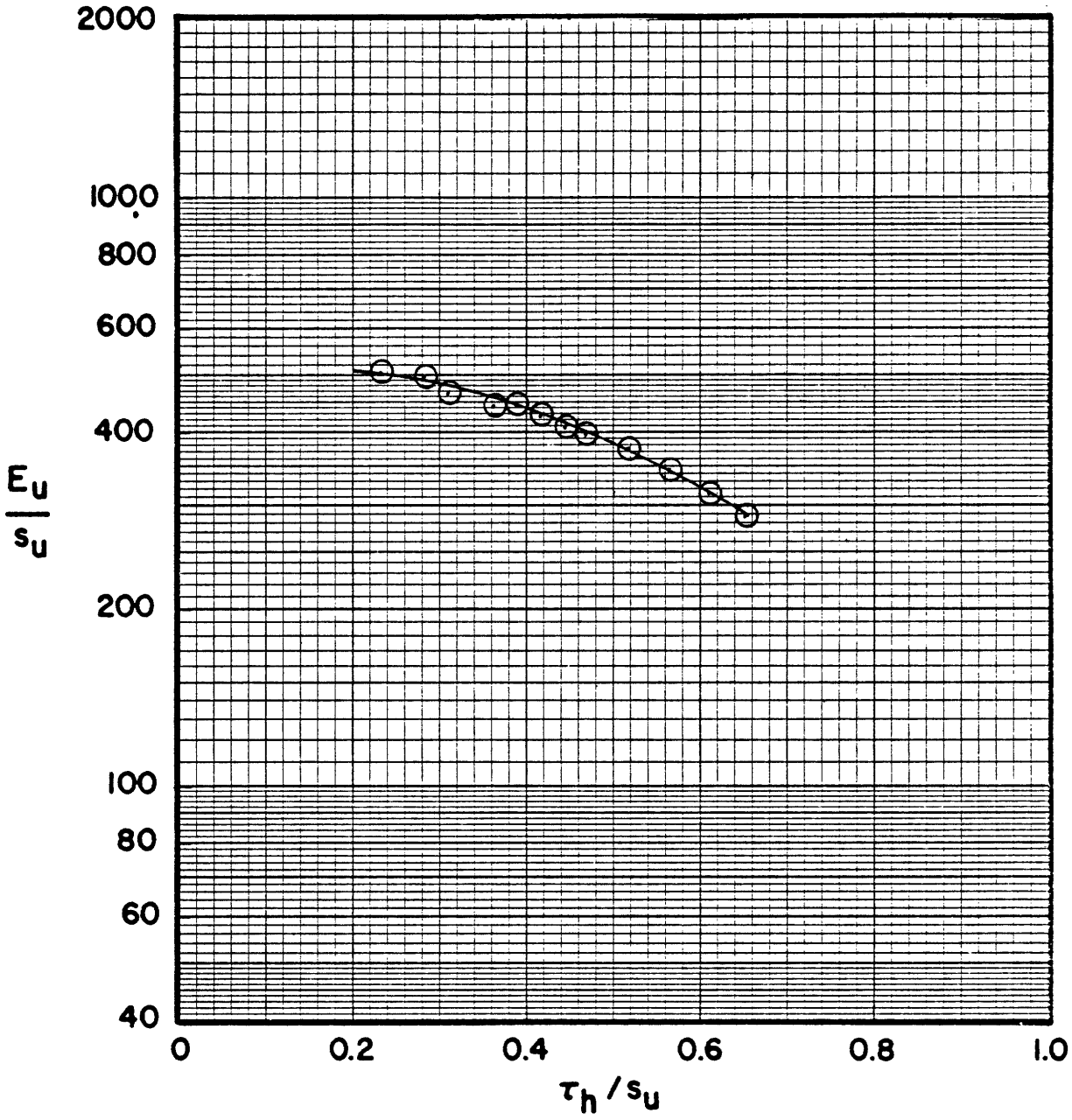

Test No.	Sample No.	Depth ft.	w_N (%)	σ_{vc} (kg/cm²)	OCR	Symbol
10	MUD 1-4	59.0	34.0	4.51	2.01	

NORMALIZED MODULUS FROM CK$_o$UDSS TESTS

BORING MUD 1 SOIL TYPE BBC

GEOTECHNICAL LABORATORY, DEPT. OF CIVIL ENGR., M.I.T.

DIRECT - SIMPLE SHEAR TEST

PROJECT _____ TYPE OF TEST $\overline{CK_oU}$ DSS NO. 12 OCR 2.00

SOIL TYPE BBC TESTED BY SPG DEVICE Geonor DATE 7/82

LOCATION Solar House (M.I.T.)

CONSOLIDATION (Stresses in kg/cm^2)

$\overline{\sigma}_{vc}$ 4.52 τ_{hc} — $\overline{\sigma}_{vm}$ 9.02

t_c(Day) 0.81 ε_v(%) 9.8 γ_c(%) ___ t_c(Day) ___

	W,%	e	S,%	H (mm)
Initial	37.6			24.771
Preshear				22.340
Final	38.1			

DURING SHEAR
Controlled Strain ✓ Stress ___
Rate (% / Hr.) ___

TIME (Hr.)	STRAIN (%)	$\frac{\tau_h}{\overline{\sigma}_{vc}}$	$\frac{\Delta u}{\overline{\sigma}_{vc}}$	$\frac{\overline{\sigma}_v}{\overline{\sigma}_{vc}}$	$\frac{\tau_h}{S_u}$	$\frac{\tau_h}{\overline{\sigma}_{vm}}$	$\frac{\overline{\sigma}_v}{\overline{\sigma}_{vm}}$	REMARKS
0.00	0.00	0.000	0.000	1.000	0.000	0.000	0.500	
	0.02	0.025	-0.019	1.019		0.012	0.510	
	0.12	0.072	-0.041	1.041	0.216	0.036	0.521	
	0.14	0.080	-0.034	1.034	0.240	0.040	0.518	
	0.16	0.089	-0.026	1.026	0.265	0.044	0.514	
	0.20	0.106	-0.022	1.022	0.318	0.053	0.512	
	0.25	0.123	-0.023	1.023	0.369	0.062	0.512	
	0.30	0.141	-0.024	1.024	0.422	0.070	0.513	
	0.36	0.157	-0.034	1.034	0.472	0.079	0.518	
	0.45	0.179	-0.038	1.038	0.536	0.090	0.520	
	0.53	0.194	-0.040	1.040	0.581	0.097	0.521	
	0.62	0.208	-0.041	1.041	0.623	0.104	0.521	
	0.73	0.221	-0.043	1.043	0.663	0.111	0.522	
	0.92	0.239	-0.045	1.045	0.717	0.120	0.523	
	1.10	0.256	-0.054	1.054	0.767	0.128	0.528	
	1.33	0.271	-0.061	1.061	0.810	0.135	0.531	
	2.00	0.298	-0.065	1.065		0.149	0.533	
	2.98	0.317	-0.038	1.038		0.158	0.520	
	4.48	0.328	+0.008	0.992		0.164	0.497	
2.62	5.97	0.334	+0.041	0.959		0.167	0.480	Peak
	7.35	0.332	0.072	0.928		0.166	0.465	
	9.28	0.332	0.116	0.884		0.166	0.443	
	12.04	0.324	0.181	0.819		0.162	0.410	
	14.88	0.309	0.236	0.764		0.155	0.382	
6.87	19.96	0.253	0.402	0.598		0.126	0.300	

SOIL MECHANICS LABORATORY
DEPT. OF CIVIL ENGINEERING
MASSACHUSETTS INSTITUTE OF TECHNOLOGY

REMARKS: $\frac{E_u}{S_u} = \frac{3\tau_h}{S_u \text{ strain}}$

— At maximum load,
t_c = 4.5 hrs.
ε_v% = 10.2

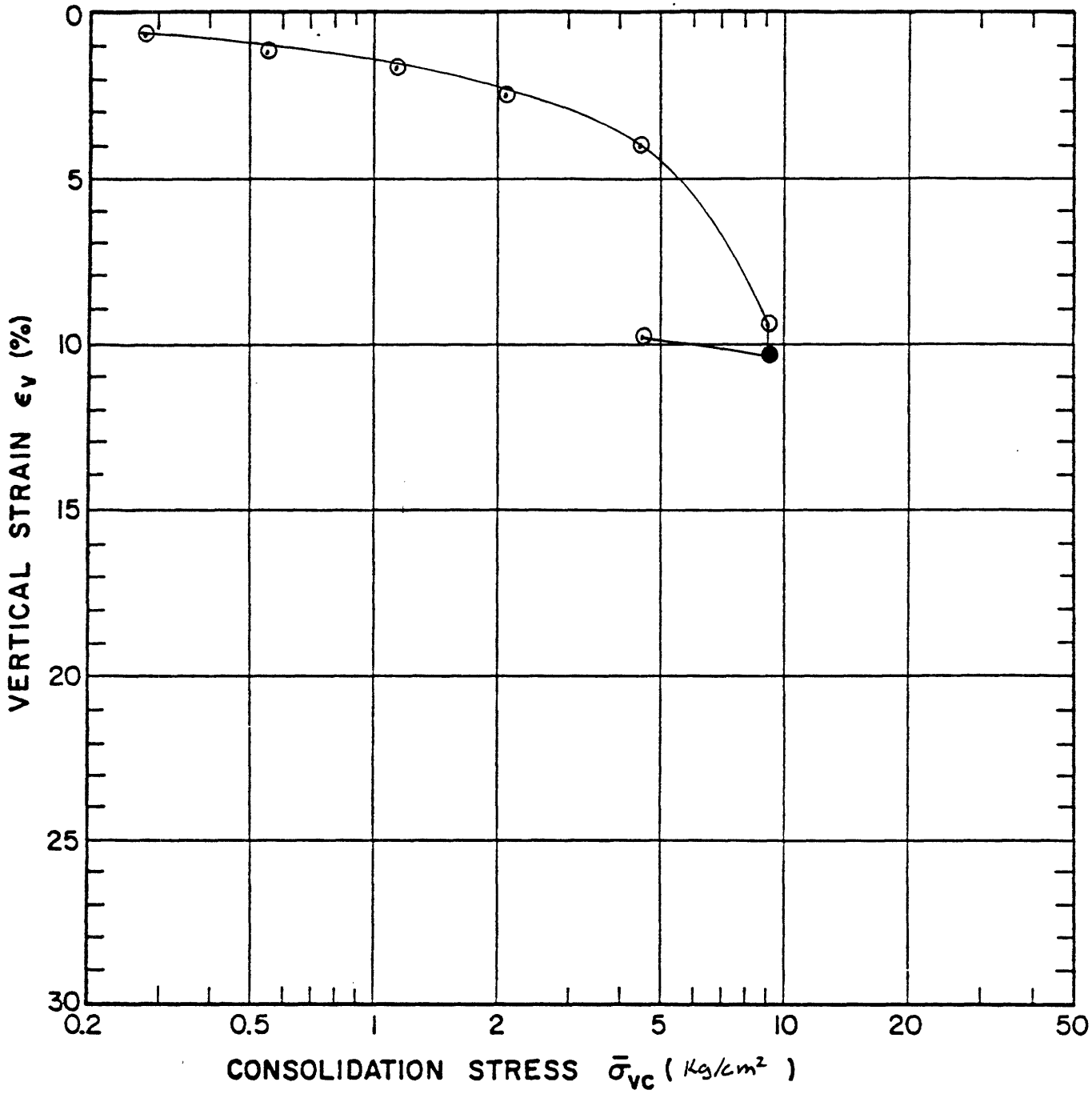

Sample No. MUD 1-4 w_N (%) 37.6 Estimated

Depth 59.0 ft. w_L (%) _____ $\bar{\sigma}_{vo}$ 1.95 ksc $\bar{\sigma}_{vm}$ _____

Soil Type BBC w_P (%) _____ CR _____ RR _____

_____ P.I.(%) _____ G_s _____ e_o _____ S(%) _____

o At tp or ____ hr Remarks ϵ_v(%) based on d100 from log t curve

● At ( ) hr _____

GEOTECHNICAL LABORATORY
DEPT. OF CIVIL ENGR.
M.I.T.

COMPRESSION CURVE

TEST No. DSS-12

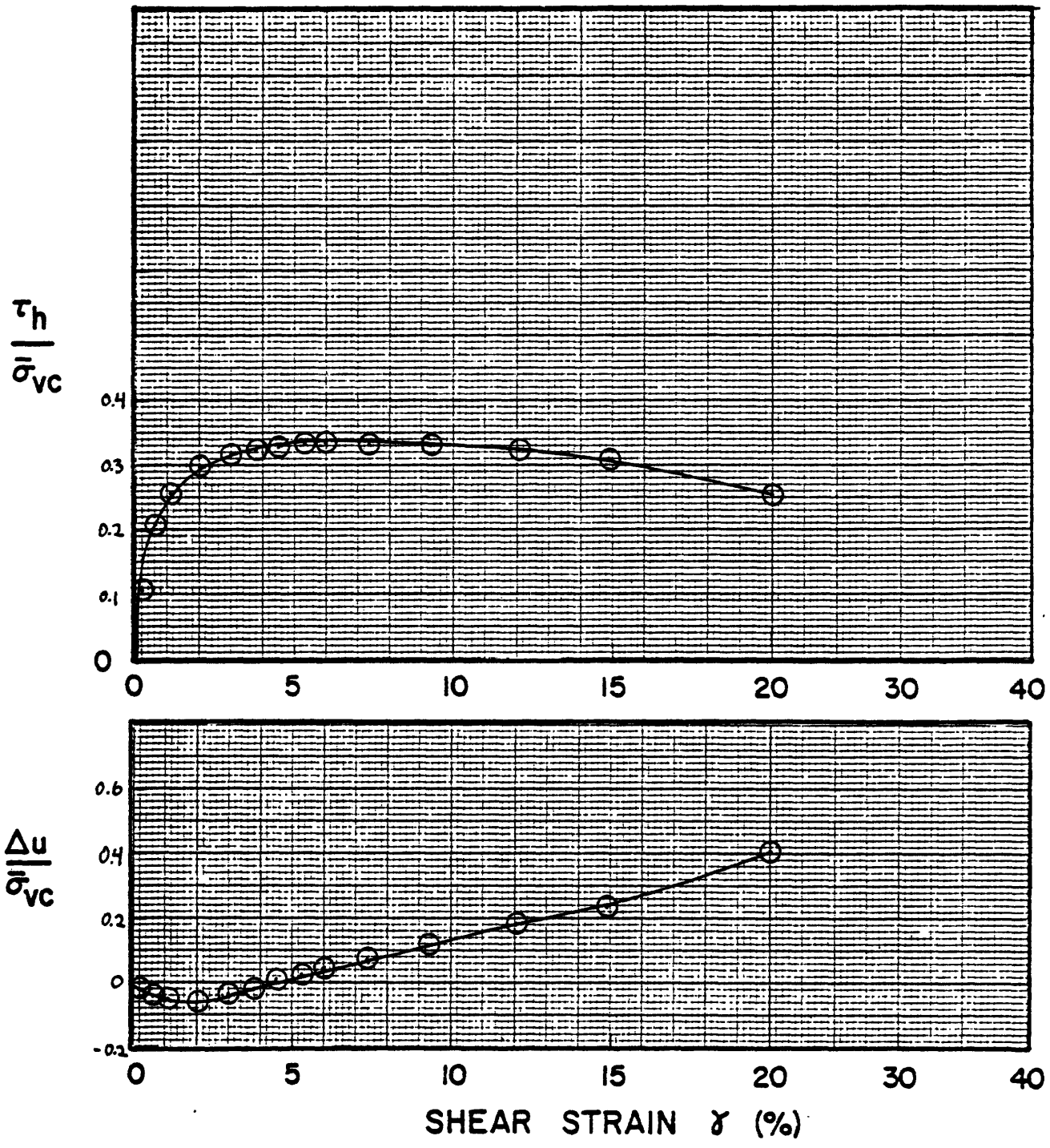

Sample No. MUD 1-4 w_N(%) 37.6 $\bar{\sigma}_{vc}$(kg/cm²) 4.52 t_c(Days) 0.81

Depth 59.0 ft w_L(%) ____ $\bar{\sigma}_{vm}$(kg/cm²) 9.03 OCR 2.00

Soil Type BBC w_P(%) ____ Estimated $\bar{\sigma}_{vo}$(kg/cm²) 1.95

GEOTECHNICAL LABORATORY
DEPT. OF CIVIL ENGR.
M.I.T.

NORMALIZED STRESS VS STRAIN
CK_oUDSS TEST NO. 12

FIGURE

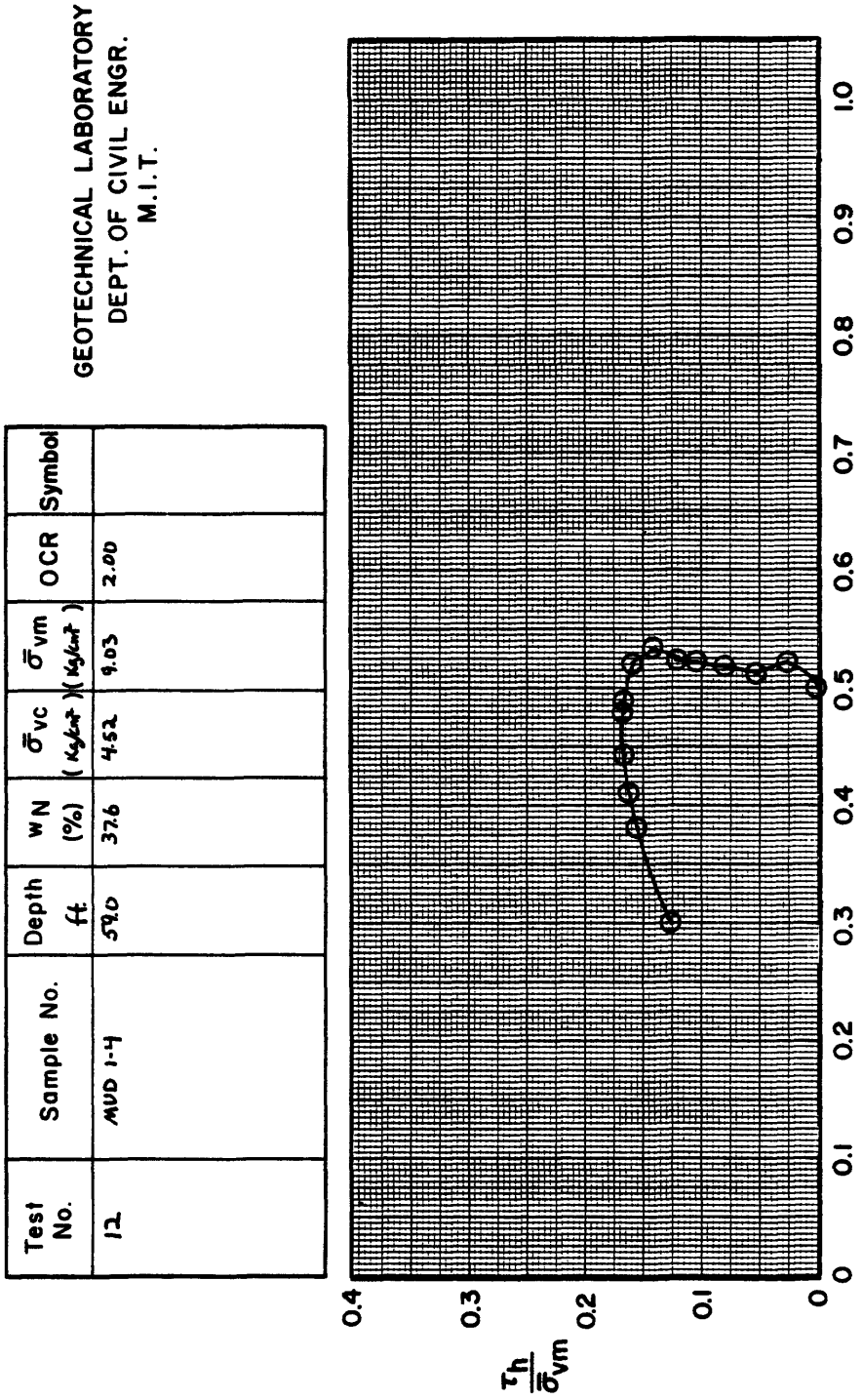

NORMALIZED STRESS PATHS FROM CK_0UDSS TESTS

Boring MUD 1 Soil Type BBC

FIGURE

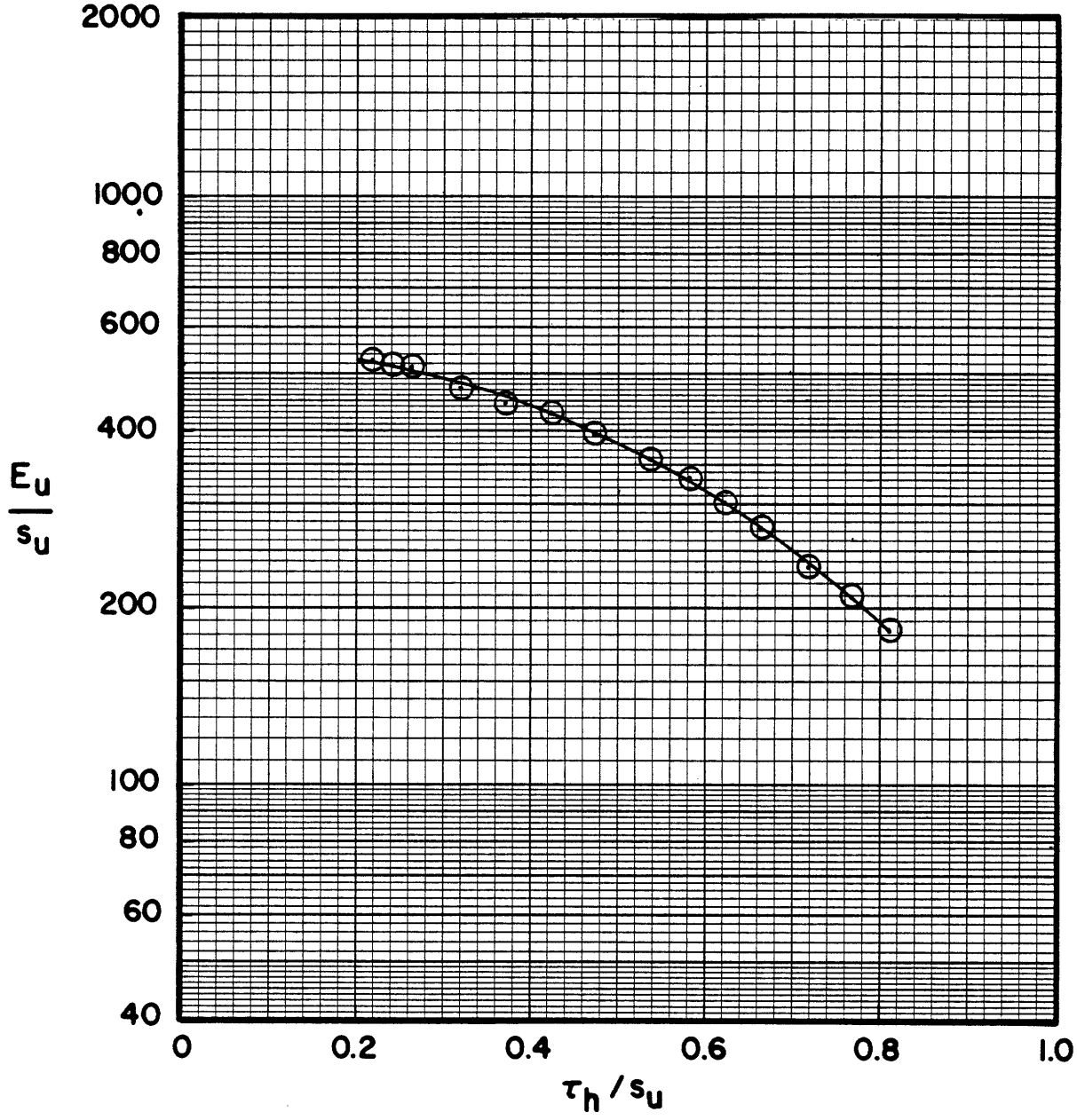

Test No.	Sample No.	Depth ft.	w_N (%)	σ_{vc} (kg/cm²)	OCR	Symbol
12	MUD 1-4	59.0	37.6	4.52	2.00	

NORMALIZED MODULUS FROM CK$_o$UDSS TESTS

BORING MUD 1 SOIL TYPE BBC

FIGURE

DIRECT - SIMPLE SHEAR TEST

PROJECT _____ TYPE OF TEST $\overline{CK_oU}$ DSS NO. 20 OCR 2.01

SOIL TYPE BBC TESTED BY SPG DEVICE Geonor DATE 10/82

LOCATION Solar House (M.I.T.)

CONSOLIDATION (Stresses in kg/cm²)

$\overline{\sigma}_{vc}$ 3.50 τ_{hc} - $\overline{\sigma}_{vm}$ 7.03

t_c(Day) 0.86 ε_v(%) 11.9 γ_c(%) ___ t_c(Day) ___

	W,%	e	S,%	H (mm)
Initial	39.0			24.524
Preshear				21.593
Final	35.2			2

DURING SHEAR
Controlled Strain ✓ Stress ___
Rate (% / Hr.) ___

TIME (Hr.)	STRAIN (%)	$\frac{\tau_h}{\overline{\sigma}_{vc}}$	$\frac{\Delta u}{\overline{\sigma}_{vc}}$	$\frac{\overline{\sigma}_v}{\overline{\sigma}_{vc}}$	$\frac{\tau_h}{S_u}$	$\frac{\tau_h}{\overline{\sigma}_{vm}}$	$\frac{\overline{\sigma}_v}{\overline{\sigma}_{vm}}$	REMARKS
0.00	0.00	0.000	0.000	1.000	0.000	0.000	0.500	
	0.09	0.062	0.000	1.000	0.193	0.031	0.500	
	0.10	0.065	0.000	1.000	0.202	0.033	0.500	
	0.11	0.069	0.000	1.000	0.214	0.034	0.500	
	0.14	0.082	0.000	1.000	0.255	0.041	0.500	
	0.19	0.101	- 0.001	1.001	0.314	0.050	0.500	
	0.25	0.124	- 0.031	1.031	0.385	0.062	0.513	
	0.30	0.142	- 0.031	1.031	0.441	0.070	0.513	
	0.36	0.158	- 0.031	1.031	0.491	0.079	0.513	
	0.50	0.187	- 0.032	1.032	0.581	0.093	0.513	
	0.61	0.207	- 0.032	1.032	0.643	0.103	0.513	
	0.75	0.224	- 0.033	1.033	0.696	0.111	0.514	
	1.00	0.245	- 0.036	1.036	0.761	0.122	0.515	
	1.25	0.261	- 0.047	1.047	0.811	0.130	0.521	
	2.00	0.293	- 0.044	1.044		0.145	0.519	
	3.00	0.308	- 0.016	1.016		0.153	0.505	
	4.00	0.314	+ 0.018	0.982		0.156	0.488	
	5.50	0.321	0.069	0.931		0.160	0.463	
	6.50	0.322	0.100	0.900		0.160	0.447	Peak
	8.00	0.320	0.155	0.845		0.159	0.420	
	10.00	0.314	0.186	0.814		0.156	0.405	
	12.00	0.310	0.231	0.769		0.154	0.382	
	14.00	0.300	0.248	0.752		0.149	0.374	
	16.00	0.290	0.304	0.696		0.144	0.346	
	20.00	0.253	0.423	0.577		0.126	0.287	

SOIL MECHANICS LABORATORY
DEPT. OF CIVIL ENGINEERING
MASSACHUSETTS INSTITUTE OF TECHNOLOGY

REMARKS: $\frac{E_u}{S_u} = \frac{3\tau_h}{S_u \text{ strain}}$

- At maximum load,
t_c = 0.81 days
$\frac{E_u}{S_u}$ = 12.6

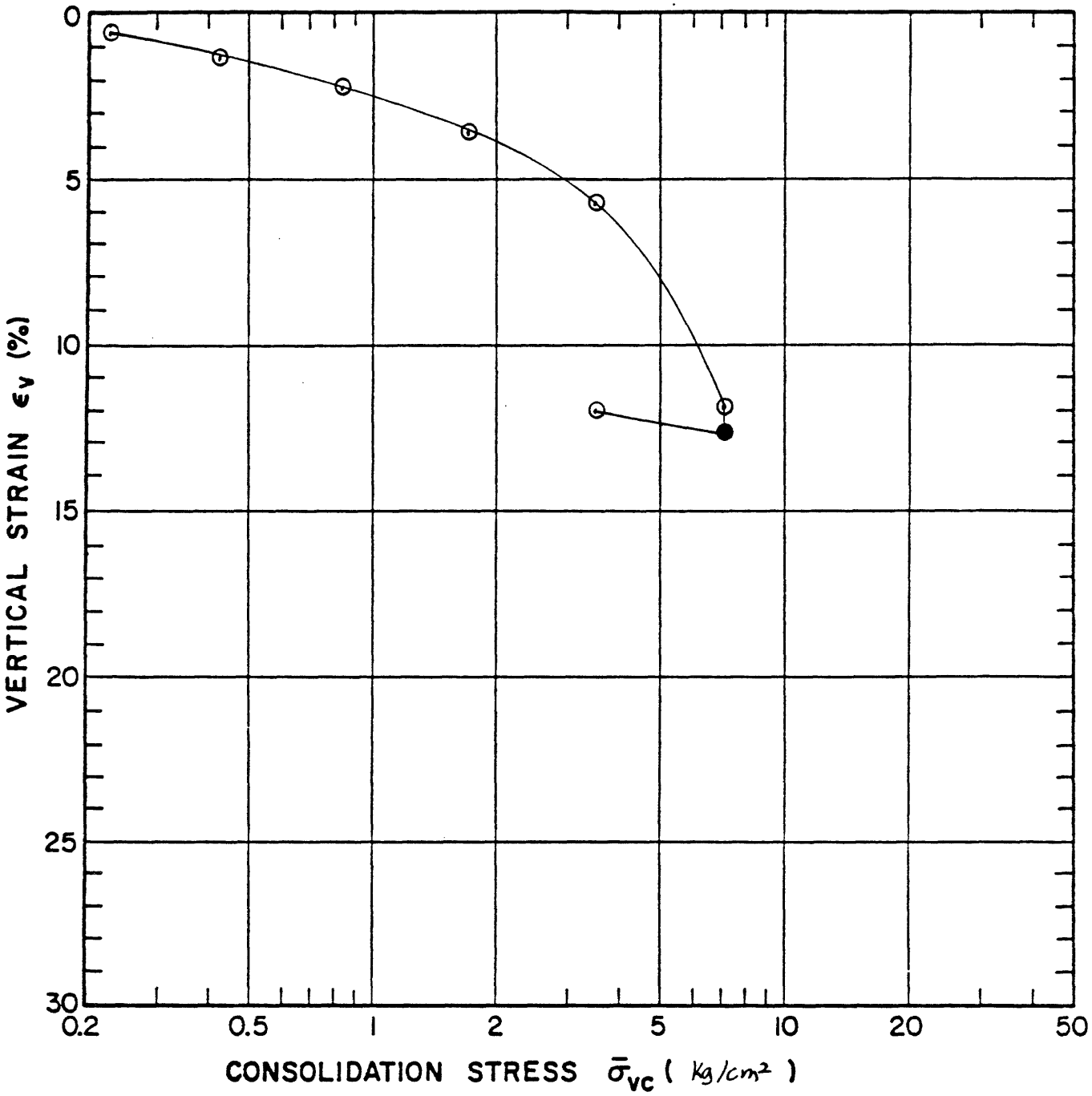

Sample No. MVO 1-5 w_N (%) 39.0 Estimated

Depth 67.0 ft. w_L (%) _____ $\bar{\sigma}_{vo}$ 2.15 ksc $\bar{\sigma}_{vm}$ _____

Soil Type BBC w_P (%) _____ CR _____ RR _____

_____ P.I.(%) _____ G_s _____ e_o _____ S(%) _____

o At t_p or _____ hr Remarks ϵ_v(%) based on d_{100} from log t curve

● At ( ) hr _____

GEOTECHNICAL LABORATORY
DEPT. OF CIVIL ENGR.
M.I.T.

COMPRESSION CURVE

TEST No. DSS-20

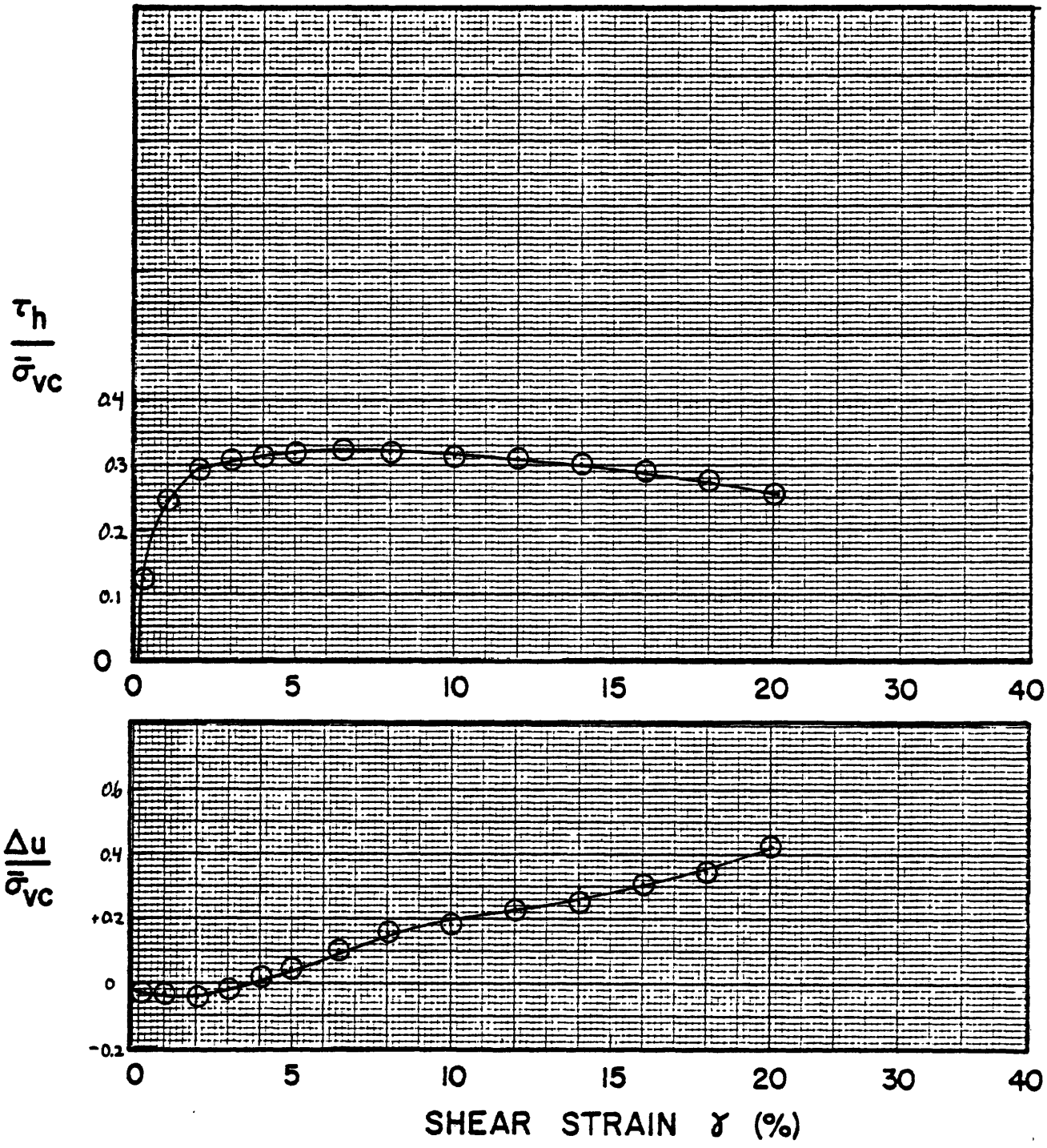

Sample No. MUD 1-5 w_N(%) 39.0 $\bar{\sigma}_{vc}$(Kg/cm²) 3.50 t_c(Days) 0.86

Depth 67.0 ft. w_L(%) _____ $\bar{\sigma}_{vm}$(Kg/cm²) 7.03 OCR 2.01

Soil Type BBC w_P(%) _____ Estimated $\bar{\sigma}_{vo}$(Kg/cm²) 2.15

GEOTECHNICAL LABORATORY
DEPT. OF CIVIL ENGR.
M.I.T.

NORMALIZED STRESS VS STRAIN
CK_oUDSS TEST NO. 20

FIGURE

Test No.	Sample No.	Depth ft.	w_N (%)	$\bar{\sigma}_{vc}$ (kg/cm²)	$\bar{\sigma}_{vm}$ (kg/cm²)	OCR	Symbol
20	MUD 1-5	67.0	39.0	3.50	7.03	2.01	

GEOTECHNICAL LABORATORY
DEPT. OF CIVIL ENGR.
M.I.T.

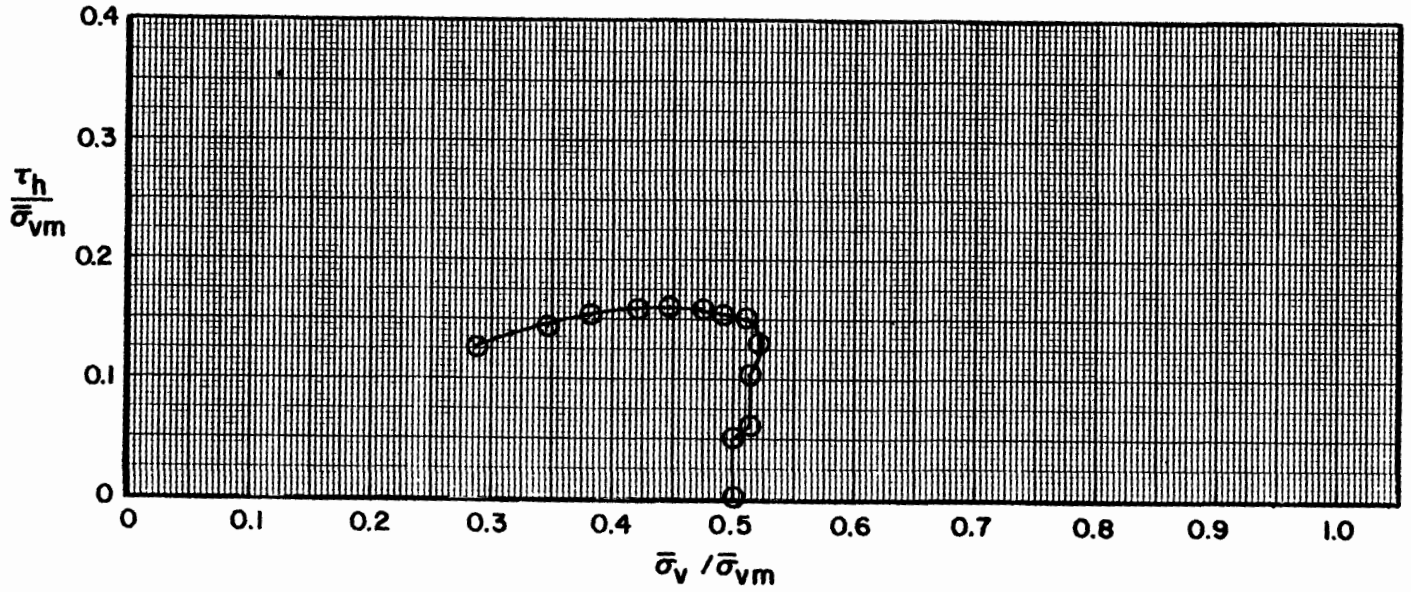

FIGURE

NORMALIZED STRESS PATHS FROM CK_0UDSS TESTS

Boring MUD 1 Soil Type BBC

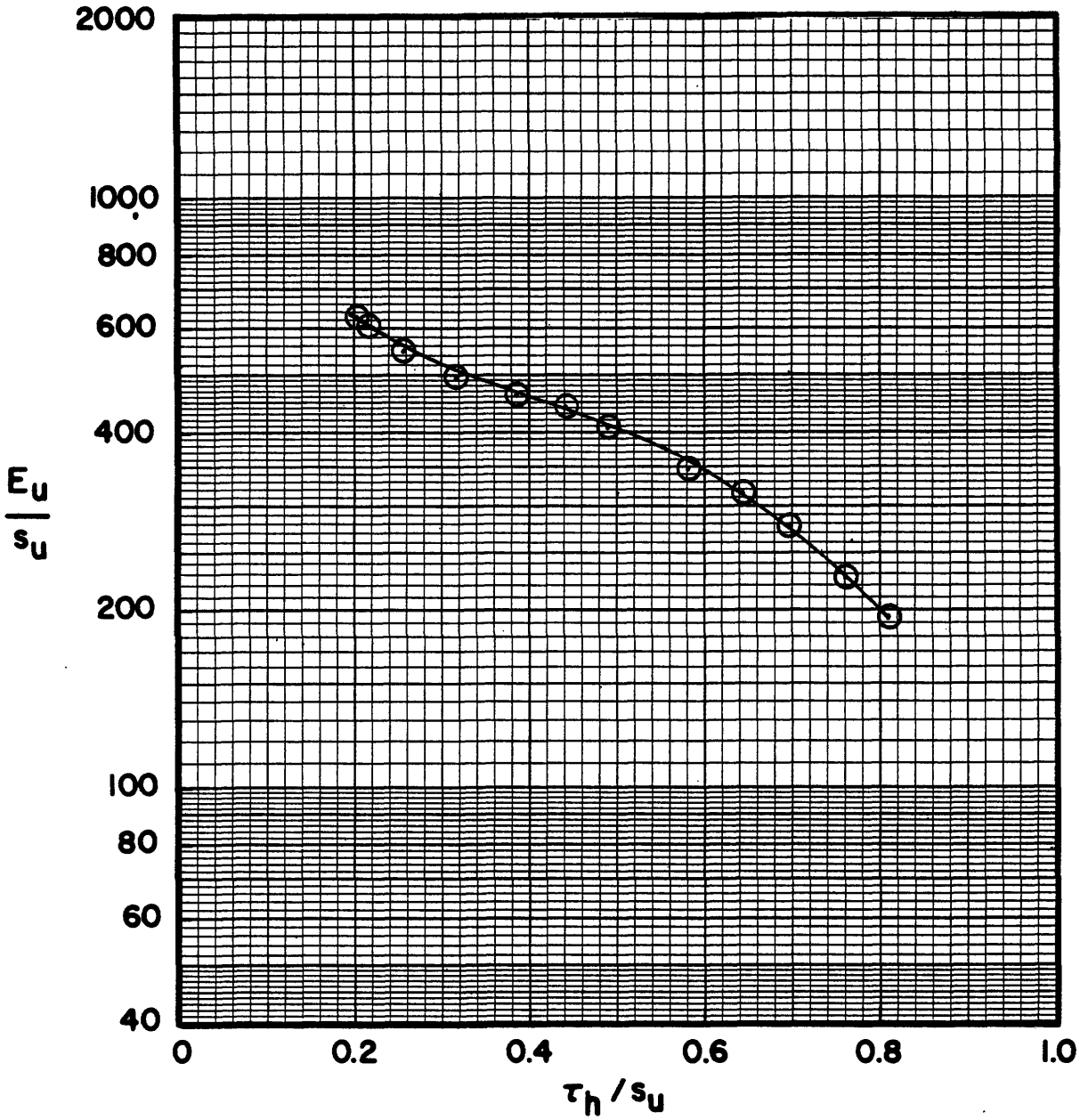

Test No.	Sample No.	Depth ft.	w_N (%)	σ_{vc} (kg/cm²)	OCR	Symbol
20	MUD 1-5	67.0	39.0	3.50	2.01	

NORMALIZED MODULUS FROM CK_oUDSS TESTS

BORING MUD 1 SOIL TYPE BBC

FIGURE

DIRECT - SIMPLE SHEAR TEST

PROJECT _____ TYPE OF TEST $\overline{CK_oU}$ DSS NO. 11 OCR 3.95

SOIL TYPE BBC TESTED BY SPG DEVICE Geonor DATE 7/82

LOCATION Solar House (M.I.T.)

CONSOLIDATION (Stresses in kg/cm²)

$\overline{\sigma}_{vc}$ 2.70. τ_{hc} - $\overline{\sigma}_{vm}$ 10.66

t_c(Day) 0.73 ε_v(%) 8.3 γ_c(%) t_c(Day) _____

	W,%	e	S,%	H (mm)
Initial	34.9			24.594
Preshear				22.556
Final	35.4			

DURING SHEAR
Controlled Strain ✓ Stress _____
Rate (% / Hr.) _____

TIME (Hr.)	STRAIN (%)	$\frac{\tau_h}{\overline{\sigma}_{vc}}$	$\frac{\Delta u}{\overline{\sigma}_{vc}}$	$\frac{\overline{\sigma}_v}{\overline{\sigma}_{vc}}$	$\frac{\tau_h}{S_u}$	$\frac{\tau_h}{\overline{\sigma}_{vm}}$	$\frac{\overline{\sigma}_v}{\overline{\sigma}_{vm}}$	REMARKS
0.00	0.00	0.000	0.000	1.000	0.000	0.000	0.252	
	0.12	0.107	-0.004	1.004	0.200	0.027	0.253	
	0.12	0.114	-0.004	1.004	0.212	0.029	0.253	
	0.18	0.147	-0.008	1.008	0.273	0.037	0.254	
	0.24	0.172	-0.024	1.024	0.320	0.044	0.258	
	0.32	0.197	-0.036	1.036	0.366	0.050	0.261	
	0.41	0.220	-0.048	1.048	0.408	0.056	0.264	
	0.51	0.241	-0.060	1.060	0.448	0.061	0.267	
	0.61	0.262	-0.071	1.071	0.487	0.066	0.270	
	0.74	0.282	-0.079	1.079	0.523	0.071	0.272	
	0.86	0.300	-0.087	1.087	0.557	0.076	0.274	
	1.07	0.326	-0.103	1.103	0.607	0.083	0.278	
	1.32	0.350	-0.115	1.115	0.651	0.089	0.281	
	1.63	0.375	-0.131	1.131	0.697	0.095	0.285	
	2.33	0.418	-0.175	1.175	0.777	0.106	0.296	
	2.79	0.439	-0.202	1.202	0.816	0.111	0.303	
	3.74	0.474	-0.238	1.238		0.120	0.312	
	4.94	0.500	-0.274	1.274		0.127	0.321	
	6.37	0.522	-0.286	1.286		0.132	0.324	
	7.84	0.535	-0.286	1.286		0.136	0.324	
3.40	9.60	0.538	-0.258	1.258		0.136	0.317	Peak
	11.17	0.529	-0.210	1.210		0.134	0.305	
	13.33	0.512	-0.147	1.147		0.130	0.289	
	16.59	0.474	-0.044	1.044		0.120	0.263	
6.27	22.0	0.398	+0.151	0.849		0.101	0.214	

SOIL MECHANICS LABORATORY
DEPT. OF CIVIL ENGINEERING
MASSACHUSETTS INSTITUTE OF TECHNOLOGY

REMARKS: $\frac{E_u}{S_u} = \frac{3\tau_h}{S_u \text{ strain}}$

- At maximum Load, t_c = 2.3 hrs. ε_v% = 9.8

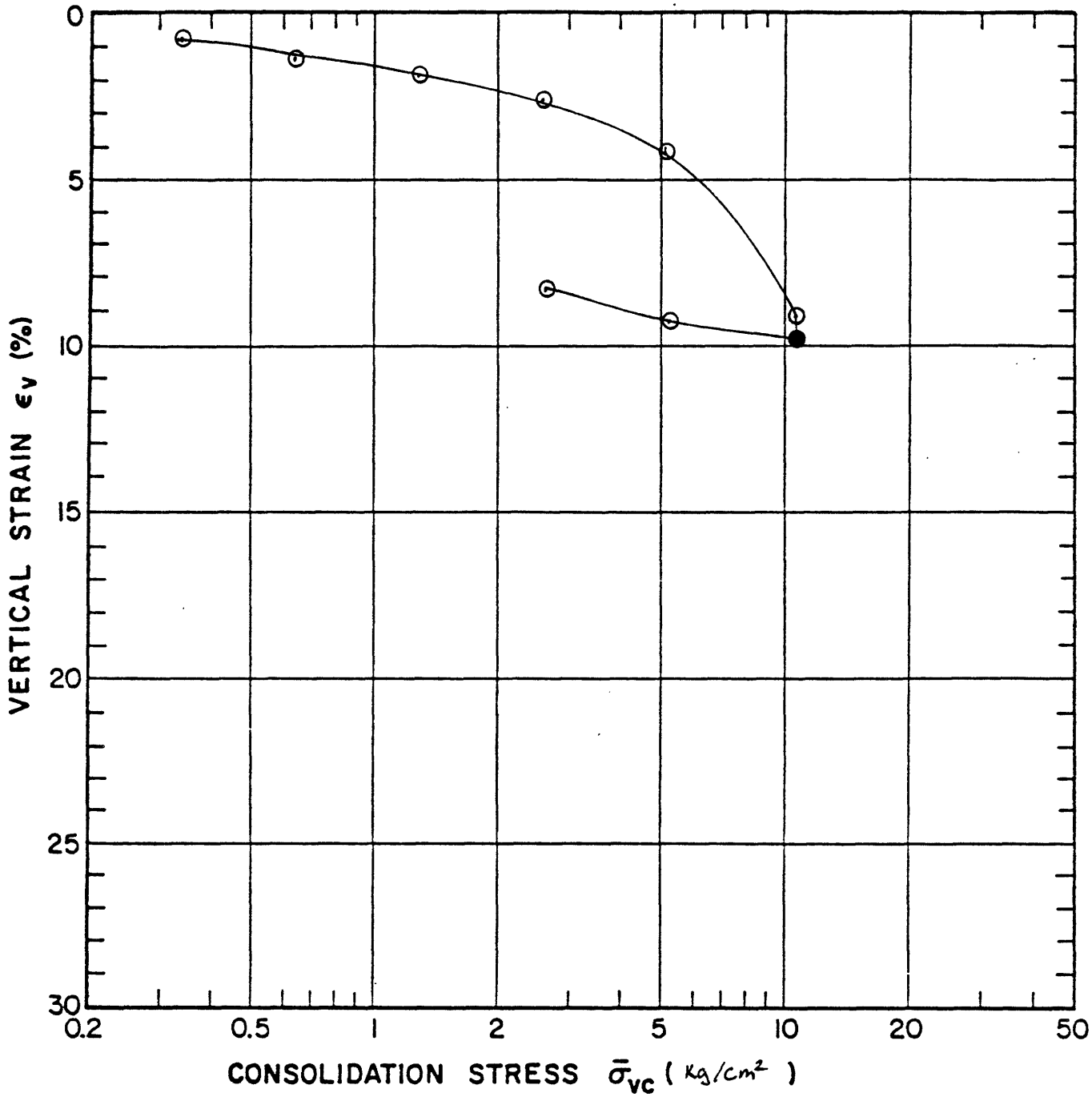

Sample No. MUO 1-2 w_N (%) 34.9 Estimated

Depth 46.0 ft. w_L (%) _____ $\bar{\sigma}_{vo}$ 1.60 ksc $\bar{\sigma}_{vm}$ _____

Soil Type BBC w_P (%) _____ CR _____ RR _____

_____ P.I.(%) _____ G_s _____ e_o _____ S(%) _____

o At t_p or ____ hr Remarks ϵ_v(%) based on diso from log t curve

● At ( ) hr _____

GEOTECHNICAL LABORATORY
DEPT. OF CIVIL ENGR.
M.I.T.

COMPRESSION CURVE

TEST No. DSS-11

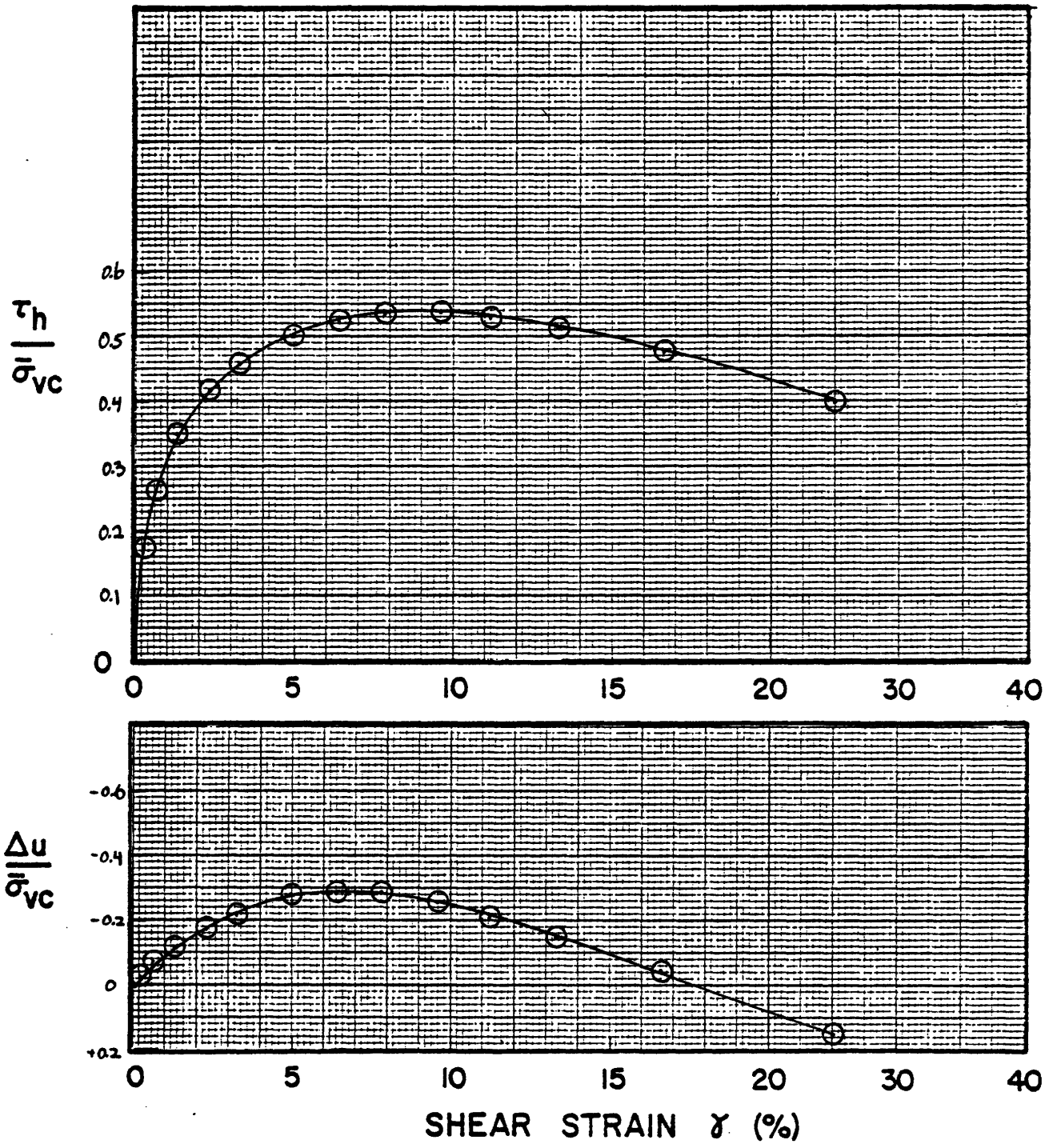

Sample No. MUD 1-2 w_N(%) 34.9 $\bar{\sigma}_{vc}$(Kg/cm²) 2.70 t_c(Days) 0.73

Depth 46.0 ft. w_L(%) ____ $\bar{\sigma}_{vm}$(Kg/cm²) 10.66 OCR 3.95

Soil Type BBC w_P(%) ____ Estimated $\bar{\sigma}_{vo}$(Kg/cm²) 1.60

GEOTECHNICAL LABORATORY
DEPT. OF CIVIL ENGR.
M.I.T.

NORMALIZED STRESS VS STRAIN
CK_oUDSS TEST NO. 11

FIGURE

Test No.	Sample No.	Depth ft.	w_N (%)	$\bar{\sigma}_{vc}$ (kg/cm²)	$\bar{\sigma}_{vm}$ (kg/cm²)	OCR	Symbol
11	MVO 1-2	46.0	34.9	2.70	10.66	3.95	

GEOTECHNICAL LABORATORY
DEPT. OF CIVIL ENGR.
M.I.T.

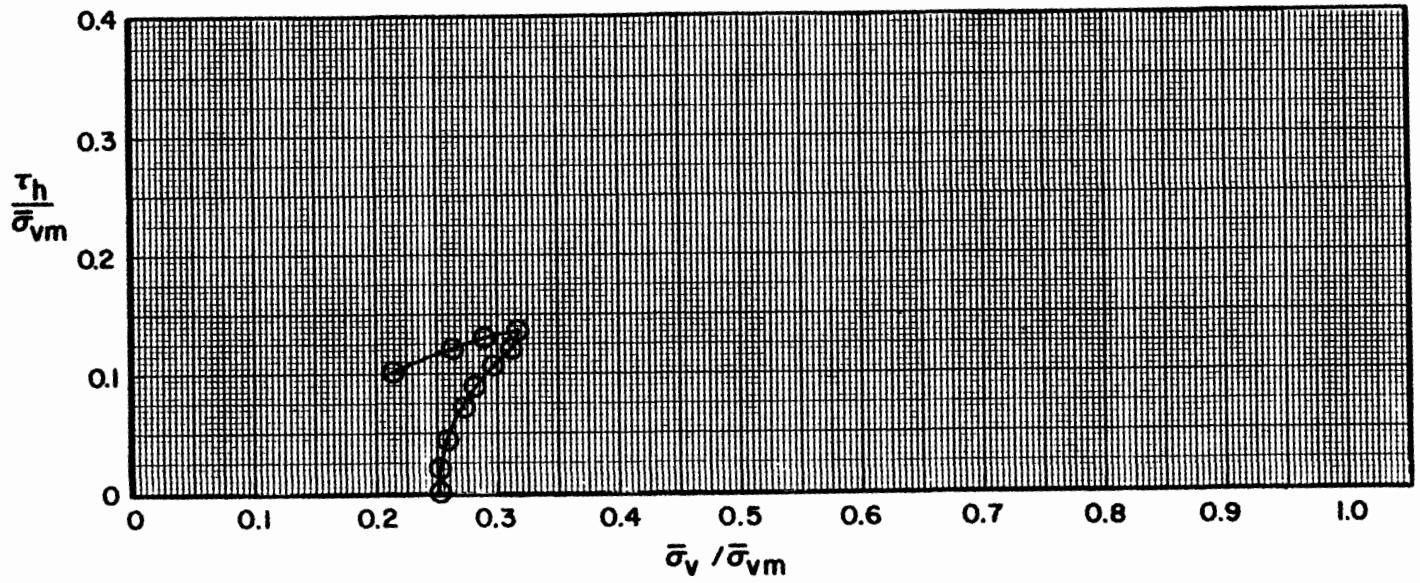

FIGURE

NORMALIZED STRESS PATHS FROM CK_oUDSS TESTS

Boring MVO 1 Soil Type BBC

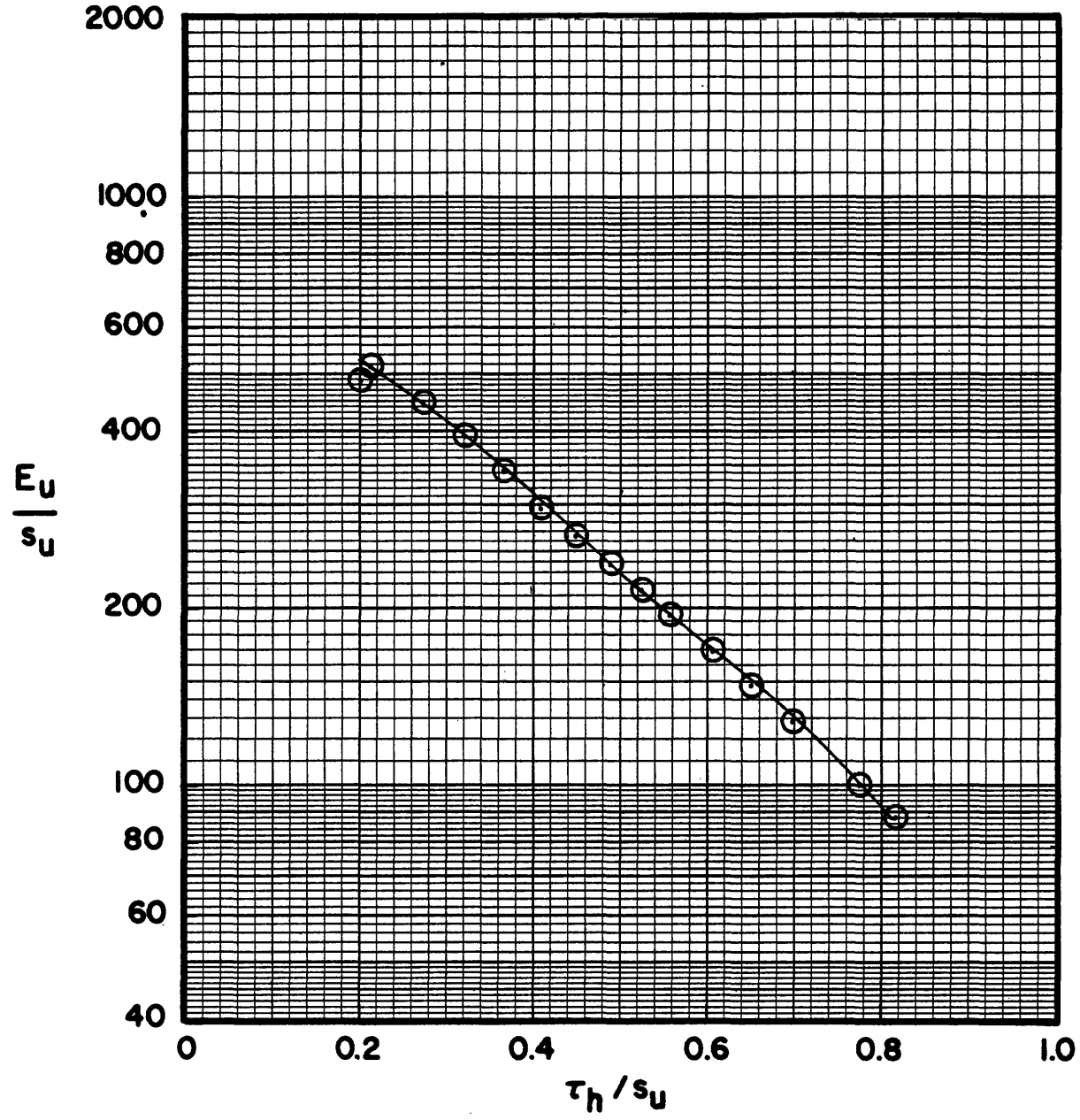

Test No.	Sample No.	Depth ft.	w_N (%)	σ_{vc} (kg/cm²)	OCR	Symbol
11	MUD 1-2	46.0	34.9	2.70	3.95	

NORMALIZED MODULUS FROM CK_oUDSS TESTS

BORING MUD 1 SOIL TYPE BBC

FIGURE

GEOTECHNICAL LABORATORY, DEPT. OF CIVIL ENGR., M.I.T.

DIRECT - SIMPLE SHEAR TEST

PROJECT _____ TYPE OF TEST $\overline{CK_oU}$ DSS NO. 13 OCR 4.04

SOIL TYPE BBC TESTED BY SPG DEVICE Geonor DATE 7/82

LOCATION Solar House (M.I.T.)

CONSOLIDATION (Stresses in Kg/cm²)

$\overline{\sigma}_{vc}$ 3.22 τ_{hc} - $\overline{\sigma}_{vm}$ 13.00

t_c(Day) 0.83 ε_v(%) 9.0 γ_c(%) t_c(Day) _____

	W,%	e	S,%	H (mm)
Initial	342			25.356
Preshear				23.078
Final	33.0			

DURING SHEAR

Controlled Strain ✓ Stress _____

Rate (% / Hr.) _____

TIME (Hr.)	STRAIN (%)	$\frac{\tau_h}{\overline{\sigma}_{vc}}$	$\frac{\Delta u}{\overline{\sigma}_{vc}}$	$\frac{\overline{\sigma}_v}{\overline{\sigma}_{vc}}$	$\frac{\tau_h}{S_u}$	$\frac{\tau_h}{\overline{\sigma}_{vm}}$	$\frac{\overline{\sigma}_v}{\overline{\sigma}_{vm}}$	REMARKS
0.00	0.00	0.000	0.000	1.000	0.000	0.000	0.247	
	0.13	0.105	-0.007	1.007	0.198	0.026	0.249	
	0.18	0.128	-0.013	1.013	0.241	0.032	0.251	
	0.24	0.149	-0.019	1.019	0.281	0.037	0.252	
	0.31	0.171	-0.024	1.024	0.322	0.042	0.253	
	0.37	0.192	-0.06	1.060	0.362	0.048	0.262	
	0.49	0.222	-0.103	1.103	0.417	0.055	0.273	
	0.63	0.252	-0.120	1.120	0.474	0.062	0.277	
	0.79	0.278	-0.128	1.128	0.523	0.069	0.279	
	1.02	0.308	-0.149	1.149	0.580	0.076	0.284	
	1.32	0.340	-0.184	1.184	0.639	0.084	0.293	
	1.66	0.372	-0.207	1.207	0.700	0.092	0.298	
	2.03	0.397	-0.233	1.233	0.748	0.098	0.305	
	2.63	0.422	-0.263	1.263	0.794	0.104	0.312	
	3.44	0.446	-0.282	1.282		0.110	0.317	
	4.40	0.471	-0.299	1.299		0.116	0.321	
	5.53	0.496	-0.322	1.322		0.123	0.327	
	6.41	0.508	-0.322	1.322		0.126	0.327	
	8.76	0.529	-0.329	1.329		0.131	0.329	
3.68	9.96	0.531	-0.312	1.312		0.131	0.325	Peak
	11.26	0.531	-0.307	1.307		0.131	0.323	
	11.93	0.528	-0.290	1.290		0.131	0.319	
	14.01	0.510	-0.232	1.232		0.126	0.305	
	15.53	0.482	-0.158	1.158		0.119	0.286	
5.75	18.72	0.437	-0.025	1.025		0.108	0.253	

SOIL MECHANICS LABORATORY
DEPT. OF CIVIL ENGINEERING
MASSACHUSETTS INSTITUTE OF TECHNOLOGY

REMARKS: $\frac{E_u}{S_u} = \frac{3\tau_h}{S_u \cdot \text{strain}}$

- At maximum load, t_c = 1 hr.
ε_v% = 10.3

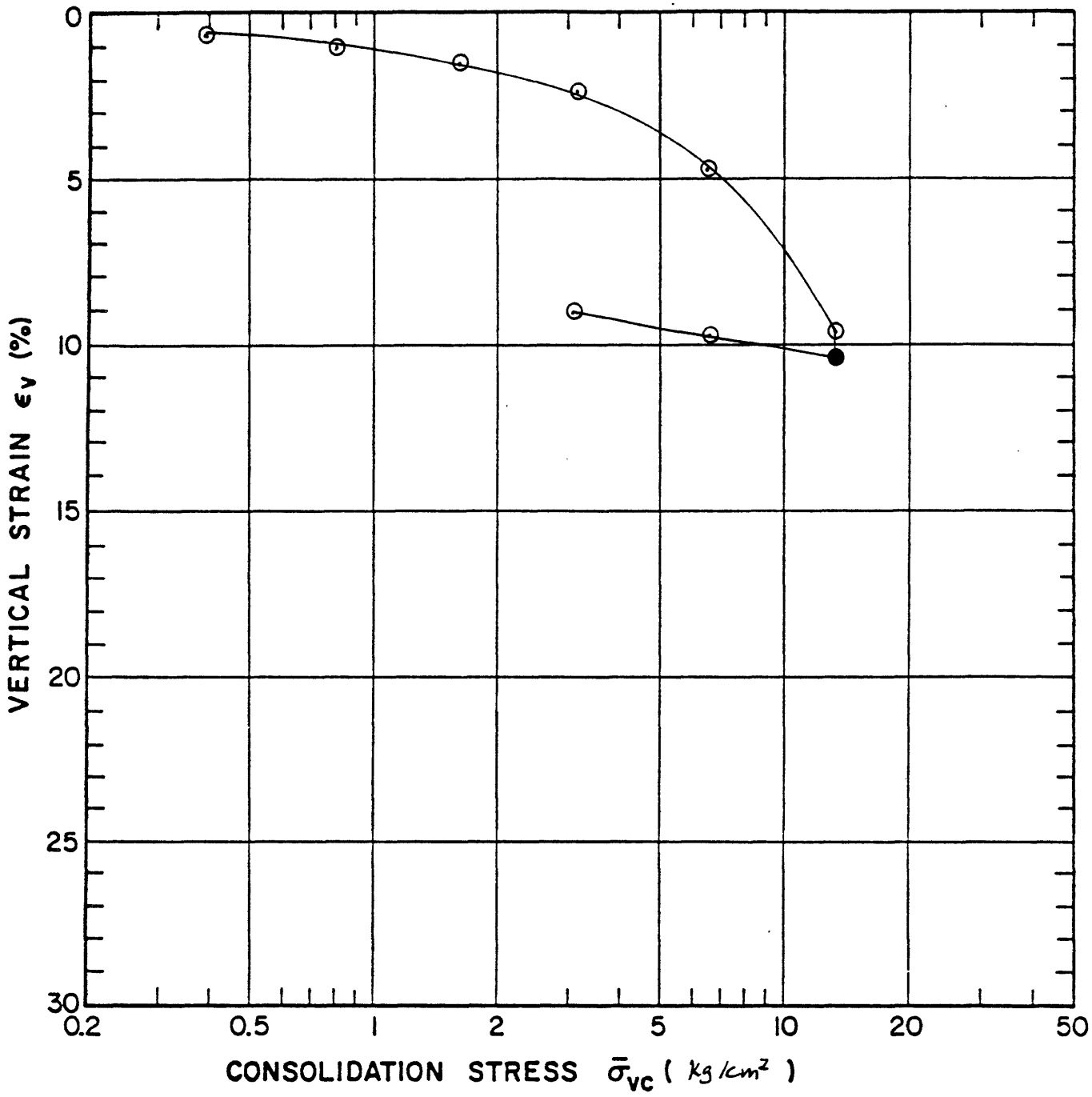

Sample No. MUD 1-2 w_N (%) 34.2 Estimated

Depth 46.0 ft. w_L (%) _____ $\bar{\sigma}_{vo}$ 1.60 Ksc. $\bar{\sigma}_{vm}$ _____

Soil Type BBC w_P (%) _____ CR _____ RR _____

_____ P.I.(%) _____ G_s _____ e_o _____ S(%) _____

o At t_p or ____ hr Remarks ϵ_v(%) based on d_{100} from log t curve

● At ( ) hr _____

GEOTECHNICAL LABORATORY
DEPT. OF CIVIL ENGR.
M.I.T.

COMPRESSION CURVE

TEST No. DSS-13

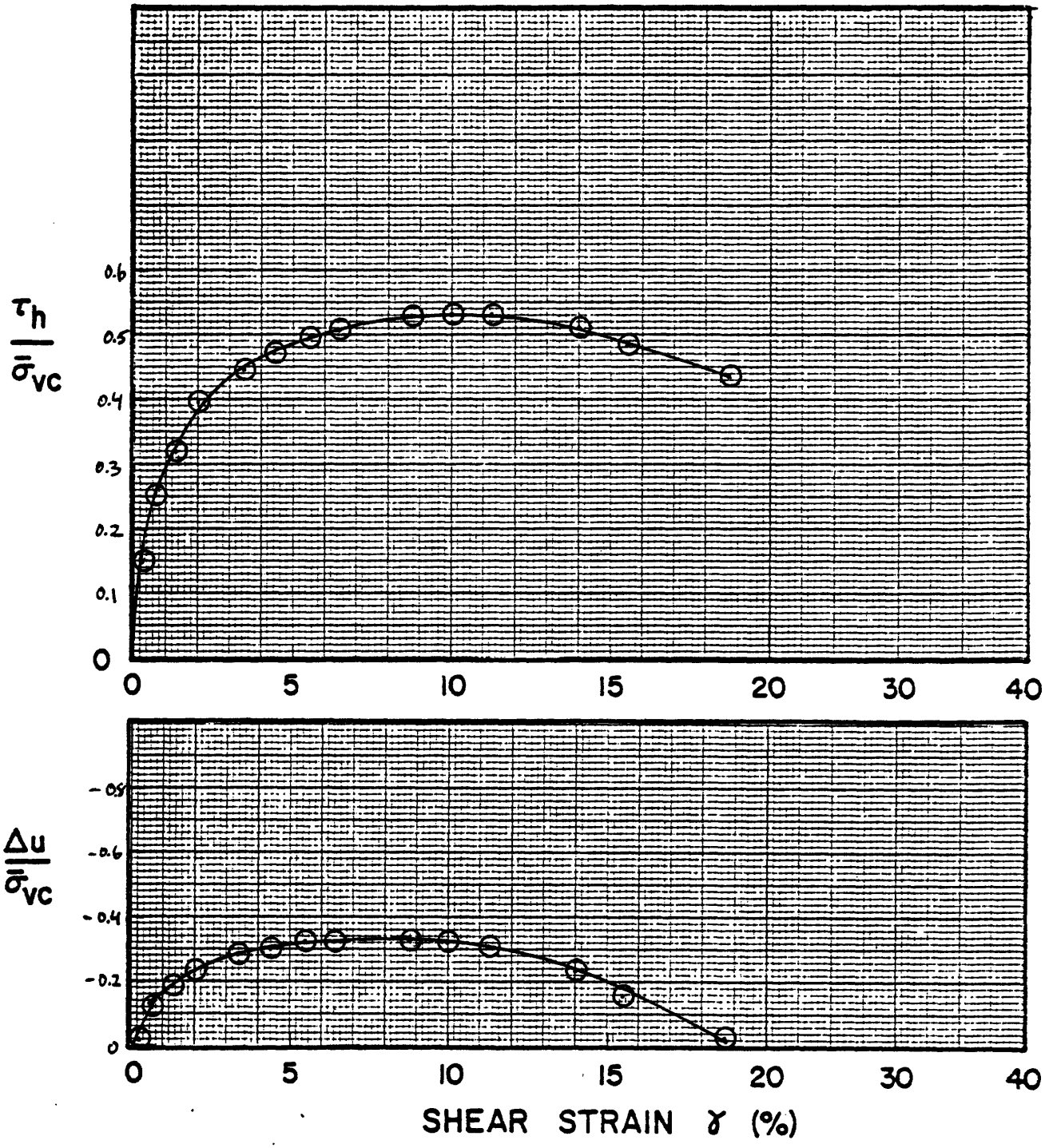

Sample No. MUD 1-2 w_N(%) 34.2 $\bar{\sigma}_{vc}$(Kg/cm²) 3.22 t_c(Days) 0.83

Depth 46.0 ft. w_L(%) ____ $\bar{\sigma}_{vm}$(Kg/cm²) 13.0 OCR 4.04

Soil Type BBC w_p(%) ____ Estimated $\bar{\sigma}_{vo}$(Kg/cm²) 1.60

GEOTECHNICAL LABORATORY
DEPT. OF CIVIL ENGR.
M.I.T.

NORMALIZED STRESS VS STRAIN

CK_oUDSS TEST NO. 13

FIGURE

Test No.	Sample No.	Depth ft.	w_N (%)	$\bar{\sigma}_{vc}$ (Kg/cm²)	$\bar{\sigma}_{vm}$ (Kg/cm²)	OCR	Symbol
13	MUD 1-2	46.0	34.2	3.22	13.0	4.04	

GEOTECHNICAL LABORATORY
DEPT. OF CIVIL ENGR.
M.I.T.

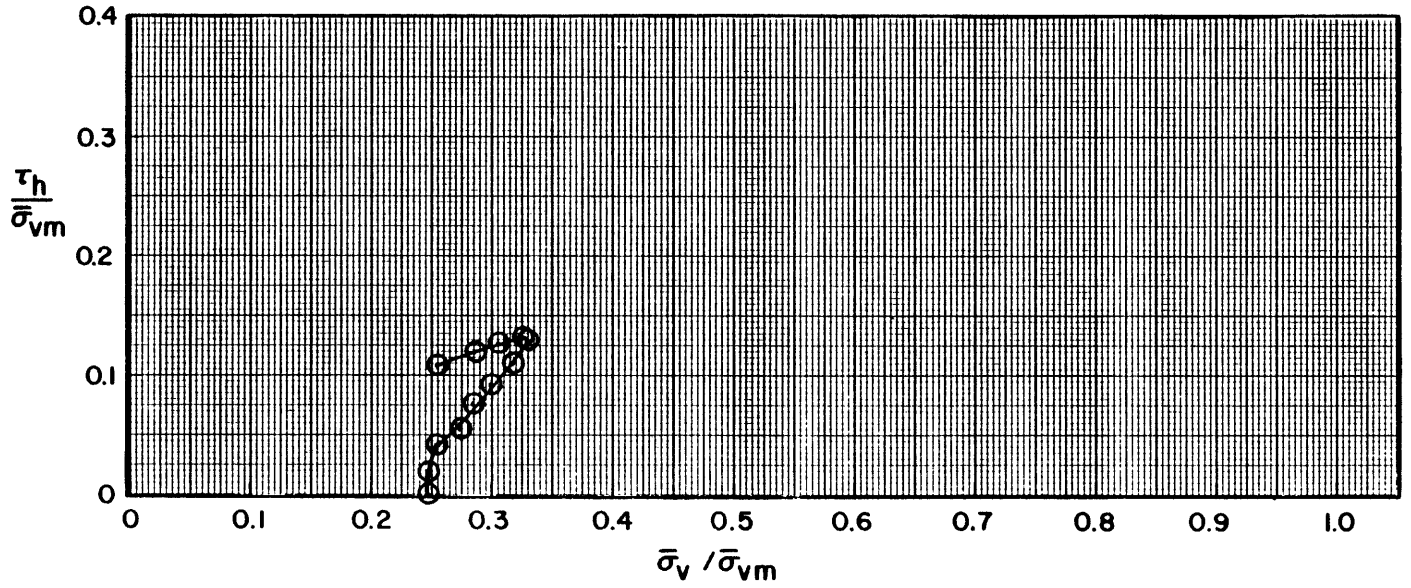

FIGURE

NORMALIZED STRESS PATHS FROM CK_0UDSS TESTS

Boring MUD 1 Soil Type BBC

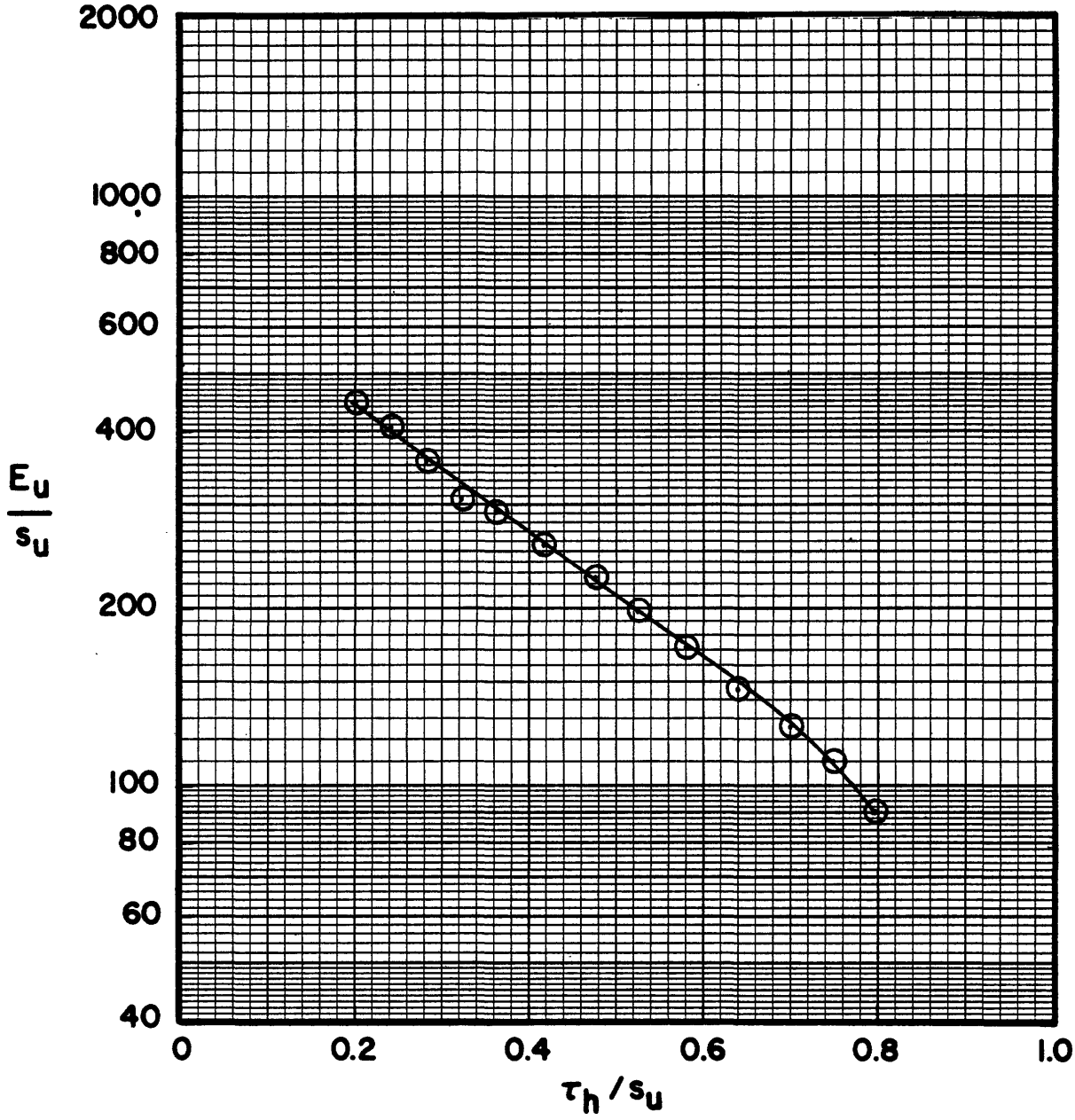

Test No.	Sample No.	Depth ft.	w_N (%)	σ_{vc} (kg/cm^2)	OCR	Symbol
13	MUD 1-2	46.0	34.2	3.22	4.04	

NORMALIZED MODULUS FROM CK_oUDSS TESTS

BORING MUD 1 SOIL TYPE BBC

FIGURE

GEOTECHNICAL LABORATORY, DEPT. OF CIVIL ENGR., M.I.T.

DIRECT - SIMPLE SHEAR TEST

PROJECT _____ TYPE OF TEST $\overline{CK_oUDSS}$ NO. 16 OCR 8.03

SOIL TYPE BBC TESTED BY SPG DEVICE Geonor DATE 8/82

LOCATION Solar House (M.I.T.)

CONSOLIDATION (Stresses in kg/cm²)

$\overline{\sigma}_{vc}$ 1.74 τ_{hc} – $\overline{\sigma}_{vm}$ 14.00

t_c(Day) 1.5 ε_v(%) 9.2 γ_c(%) ___ t_c(Day) ___

	W,%	e	S,%	H (mm)
Initial	39.8			25.641
Preshear				23.275
Final	40.8			

DURING SHEAR
Controlled Strain ✓ Stress ___
Rate (% / Hr.) ___

TIME (Hr.)	STRAIN (%)	$\frac{\tau_h}{\overline{\sigma}_{vc}}$	$\frac{\Delta u}{\overline{\sigma}_{vc}}$	$\frac{\overline{\sigma}_v}{\overline{\sigma}_{vc}}$	$\frac{\tau_h}{S_u}$	$\frac{\tau_h}{\overline{\sigma}_{vm}}$	$\frac{\overline{\sigma}_v}{\overline{\sigma}_{vm}}$	REMARKS
0.00	0.00	0.000	0.000	1.000	0.000	0.000	0.125	
	0.16	0.170	-0.027	1.027	0.191	0.021	0.128	
	0.18	0.180	-0.044	1.044	0.201	0.022	0.130	
	0.19	0.190	-0.054	1.054	0.212	0.024	0.131	
	0.28	0.237	-0.065	1.065	0.265	0.029	0.133	
	0.42	0.287	-0.082	1.082	0.321	0.036	0.135	
	0.63	0.343	-0.113	1.113	0.384	0.043	0.139	
	0.93	0.402	-0.188	1.188	0.450	0.050	0.148	
	1.25	0.457	-0.232	1.232	0.511	0.057	0.153	
	1.61	0.507	-0.291	1.291	0.566	0.063	0.161	
	2.21	0.575	-0.362	1.362	0.643	0.072	0.170	
	2.96	0.631	-0.424	1.424	0.706	0.079	0.177	
	3.72	0.683	-0.492	1.492	0.763	0.085	0.186	
	4.72	0.748	-0.584	1.584	0.836	0.093	0.197	
	5.79	0.798	-0.646	1.646	0.893	0.099	0.205	
	6.94	0.834	-0.711	1.711		0.104	0.213	
	8.14	0.861	-0.755	1.755		0.107	0.219	
	9.33	0.885	-0.789	1.789		0.110	0.223	
	9.94	0.890	-0.803	1.803		0.111	0.225	
3.78	10.57	0.894	-0.814	1.814		0.111	0.226	Peak
	11.90	0.894	-0.806	1.806		0.111	0.225	
	14.02	0.858	-0.714	1.714		0.107	0.213	
	16.24	0.801	-0.615	1.615		0.100	0.201	
	18.49	0.736	-0.509	1.509		0.092	0.188	
6.20	21.02	0.678	-0.396	1.396		0.084	0.174	

SOIL MECHANICS LABORATORY
DEPT. OF CIVIL ENGINEERING
MASSACHUSETTS INSTITUTE OF TECHNOLOGY

REMARKS: $\frac{E_u}{S_u} = \frac{3\tau_h}{S_u \text{ strain}}$

- At maximum load, t_c = 4.8 hrs. ε_v% = 12.3

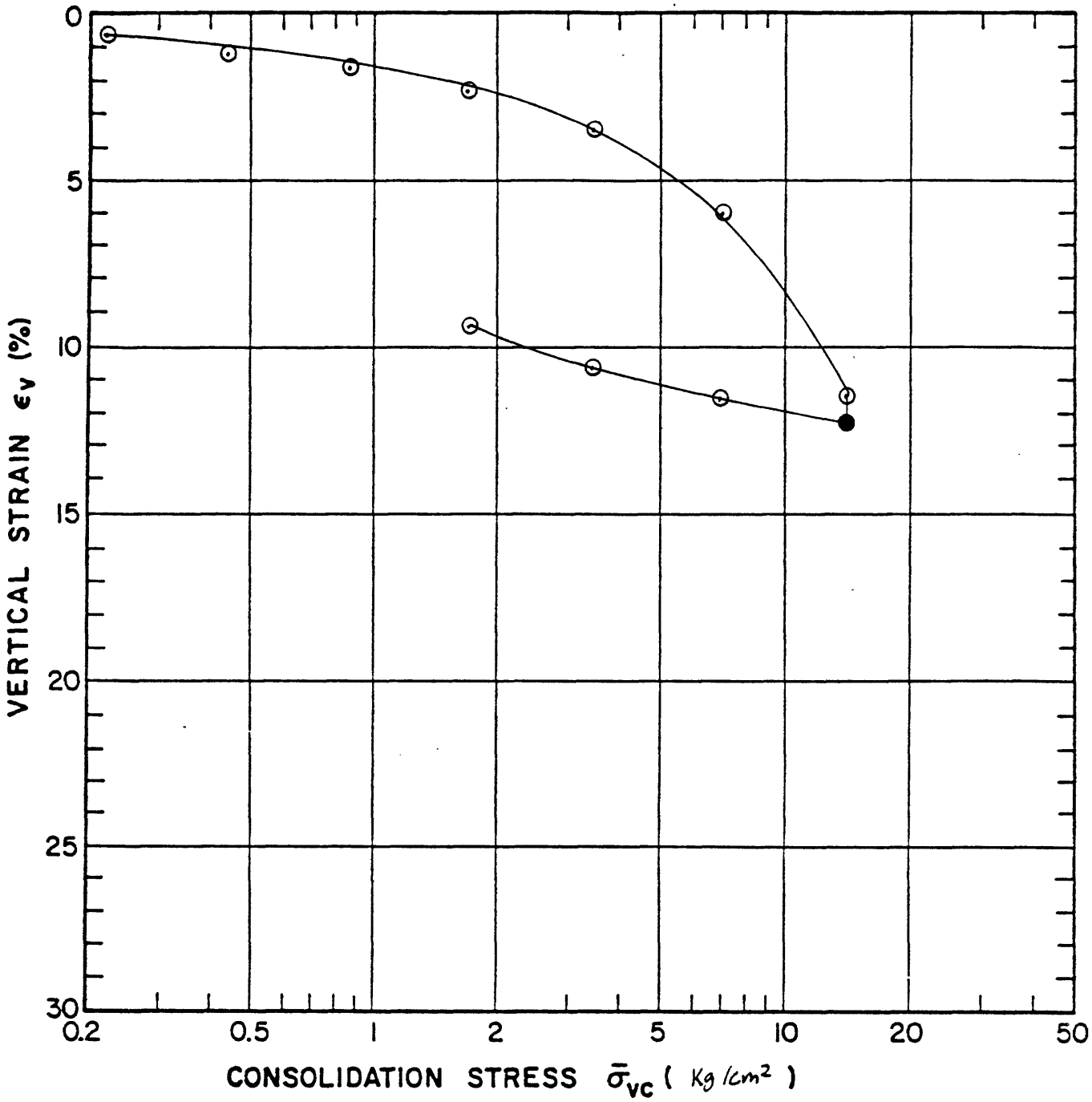

Sample No. MVO 1-1 w_N (%) 39.8 Estimated

Depth 41.5 ft w_L (%) _____ $\bar{\sigma}_{vo}$ 1.5 ksc $\bar{\sigma}_{vm}$ _____

Soil Type BBC w_P (%) _____ CR _____ RR _____

_____ P.I.(%) _____ G_s _____ e_o _____ S(%) _____

o At t_p or ____ hr Remarks Ev(%) based on dlvo from logt curve

● At ( ) hr _____

GEOTECHNICAL LABORATORY
DEPT. OF CIVIL ENGR.
M.I.T.

COMPRESSION CURVE

TEST No. OSS-16

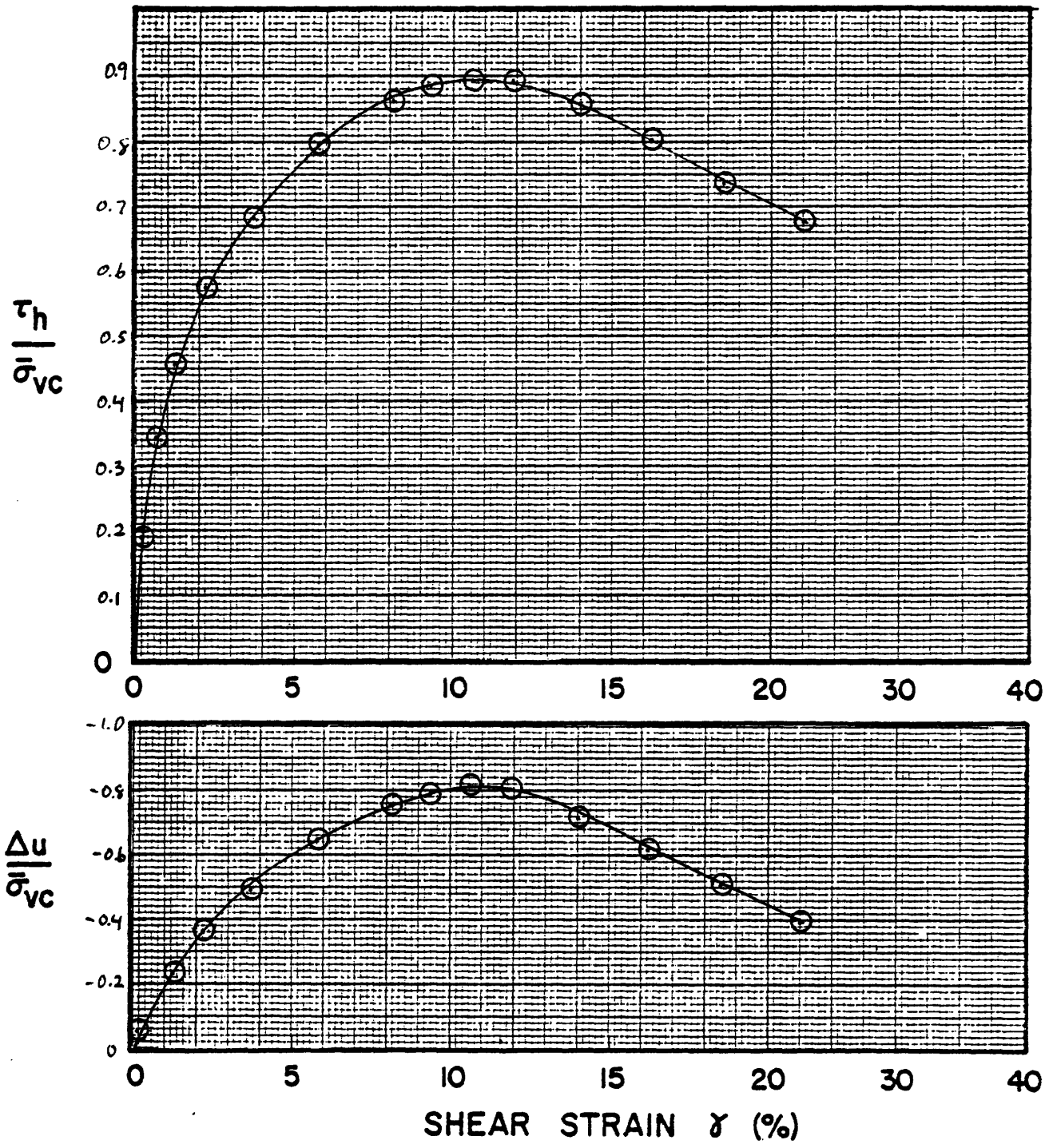

Sample No. MUD1-1 w_N(%) 39.8 $\bar{\sigma}_{vc}$(kg/cm²) 1.74 t_c(Days) 1.5

Depth 41.5 ft. w_L(%) ____ $\bar{\sigma}_{vm}$(kg/cm²) 14.00 OCR 8.03

Soil Type BBC w_P(%) ____ Estimated $\bar{\sigma}_{vo}$(kg/cm²) 1.50

GEOTECHNICAL LABORATORY
DEPT. OF CIVIL ENGR.
M.I.T.

NORMALIZED STRESS VS STRAIN

CK_oUDSS TEST NO. 16

Test No.	Sample No.	Depth ft.	w_N (%)	$\bar{\sigma}_{vc}$ (kg/cm²)	$\bar{\sigma}_{vm}$ (kg/cm²)	OCR	Symbol
16	MUD 1-1	41.5	39.8	1.74	14.00	8.03	

GEOTECHNICAL LABORATORY
DEPT. OF CIVIL ENGR.
M.I.T.

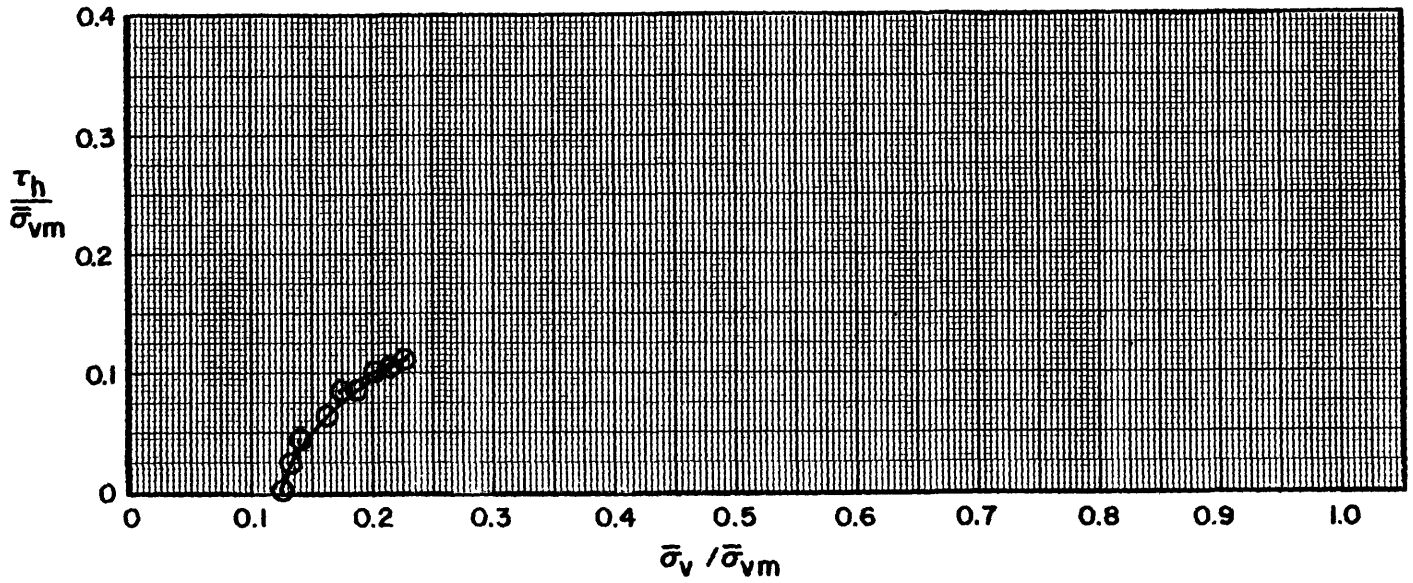

FIGURE

NORMALIZED STRESS PATHS FROM CK_0UDSS TESTS

Boring MUD 1 Soil Type BBC

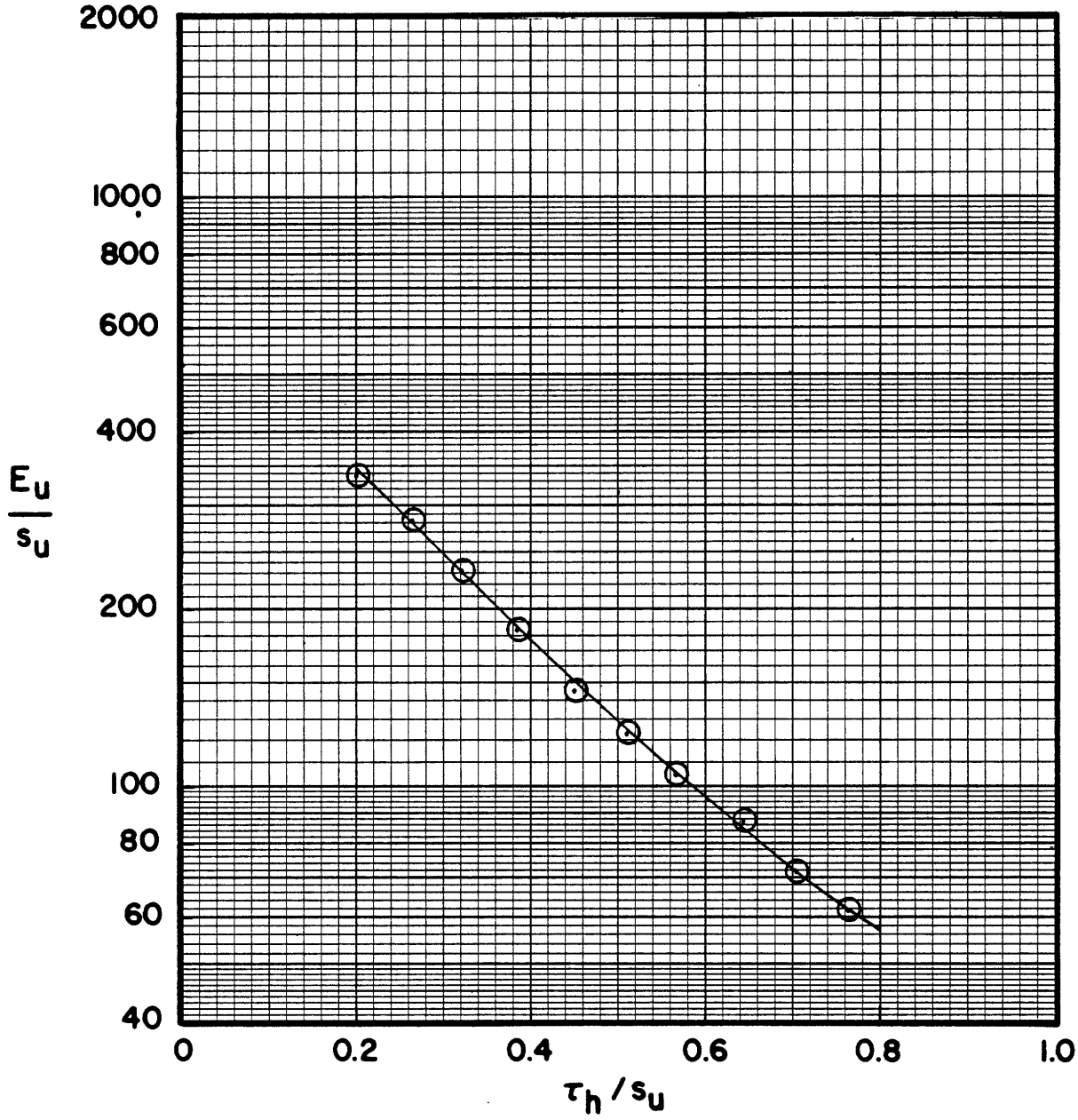

Test No.	Sample No.	Depth ft.	w_N (%)	$\bar{\sigma}_{vc}$ (kg/cm²)	OCR	Symbol
16	MUD1-1	411.5	39.8	1.74	8.03	

NORMALIZED MODULUS FROM CK_oUDSS TESTS

BORING MUD1 SOIL TYPE BBC

FIGURE

GEOTECHNICAL LABORATORY, DEPT. OF CIVIL ENGR., M.I.T.

DIRECT - SIMPLE SHEAR TEST

PROJECT _____ TYPE OF TEST $\overline{CK_oU}$ DSS NO. 19 OCR 7.97

SOIL TYPE BBC TESTED BY SPG DEVICE Geonor DATE 9/82

LOCATION Solar House (M.I.T.)

CONSOLIDATION (Stresses in kg/cm²)

$\bar{\sigma}_{vc}$ 1.79 τ_{hc} - $\bar{\sigma}_{vm}$ 14.29

t_c(Day) 0.97 ε_v(%) 1.02 γ_c(%) ___ t_c(Day) ___

	W,%	e	S,%	H (mm)
Initial	353			25.502
Preshear				22.892
Final				

DURING SHEAR
Controlled Strain ✓ Stress ___
Rate (% / Hr.) ___

TIME (Hr.)	STRAIN (%)	$\frac{\tau_h}{\bar{\sigma}_{vc}}$	$\frac{\Delta u}{\bar{\sigma}_{vc}}$	$\frac{\bar{\sigma}_v}{\bar{\sigma}_{vc}}$	$\frac{\tau_h}{S_u}$	$\frac{\tau_h}{\bar{\sigma}_{vm}}$	$\frac{\bar{\sigma}_v}{\bar{\sigma}_{vm}}$	REMARKS
0.00	0.00	0.000	0.000	1.000	0.000	0.000	0.126	
	0.33	0.184	-0.099	1.099	0.211	0.023	0.138	
	0.38	0.211	-0.109	1.109	0.243	0.026	0.139	
	0.49	0.265	-0.139	1.139	0.305	0.033	0.143	
	0.64	0.318	-0.145	1.145	0.366	0.040	0.144	
	0.83	0.371	-0.171	1.171	0.426	0.047	0.147	
	1.07	0.424	-0.218	1.218	0.487	0.053	0.153	
	1.36	0.477	-0.275	1.275	0.548	0.060	0.160	
	1.75	0.529	-0.328	1.328	0.608	0.066	0.167	
	2.19	0.582	-0.395	1.395	0.669	0.073	0.175	
	2.75	0.635	-0.455	1.455	0.730	0.080	0.183	
	3.53	0.687	-0.530	1.530	0.790	0.086	0.192	
	4.46	0.740	-0.611	1.611		0.093	0.202	
	5.63	0.793	-0.724	1.724		0.100	0.216	
	6.77	0.825	-0.746	1.746		0.104	0.219	
	8.06	0.847	-0.792	1.792		0.106	0.225	
	8.56	0.851	-0.795	1.795		0.107	0.225	
	9.04	0.855	-0.816	1.816		0.107	0.228	
	9.83	0.865	-0.816	1.816		0.109	0.228	
4.25	10.90	0.870	-0.827	1.827		0.109	0.229	Peak
	12.00	0.853	-0.783	1.783		0.107	0.224	
	14.00	0.805	-0.679	1.679		0.101	0.211	
	16.00	0.768	-0.548	1.548		0.096	0.194	
	18.00	0.735	-0.440	1.440		0.092	0.181	
6.37	20.00	0.692	-0.351	1.351		0.087	0.170	

SOIL MECHANICS LABORATORY
DEPT. OF CIVIL ENGINEERING
MASSACHUSETTS INSTITUTE OF TECHNOLOGY

REMARKS: $\frac{E_u}{S_u} = \frac{3\tau_h}{S_u \text{ strain}}$
- At maximum load, t_c = 0.70 days
ε_v(%) = 1.24

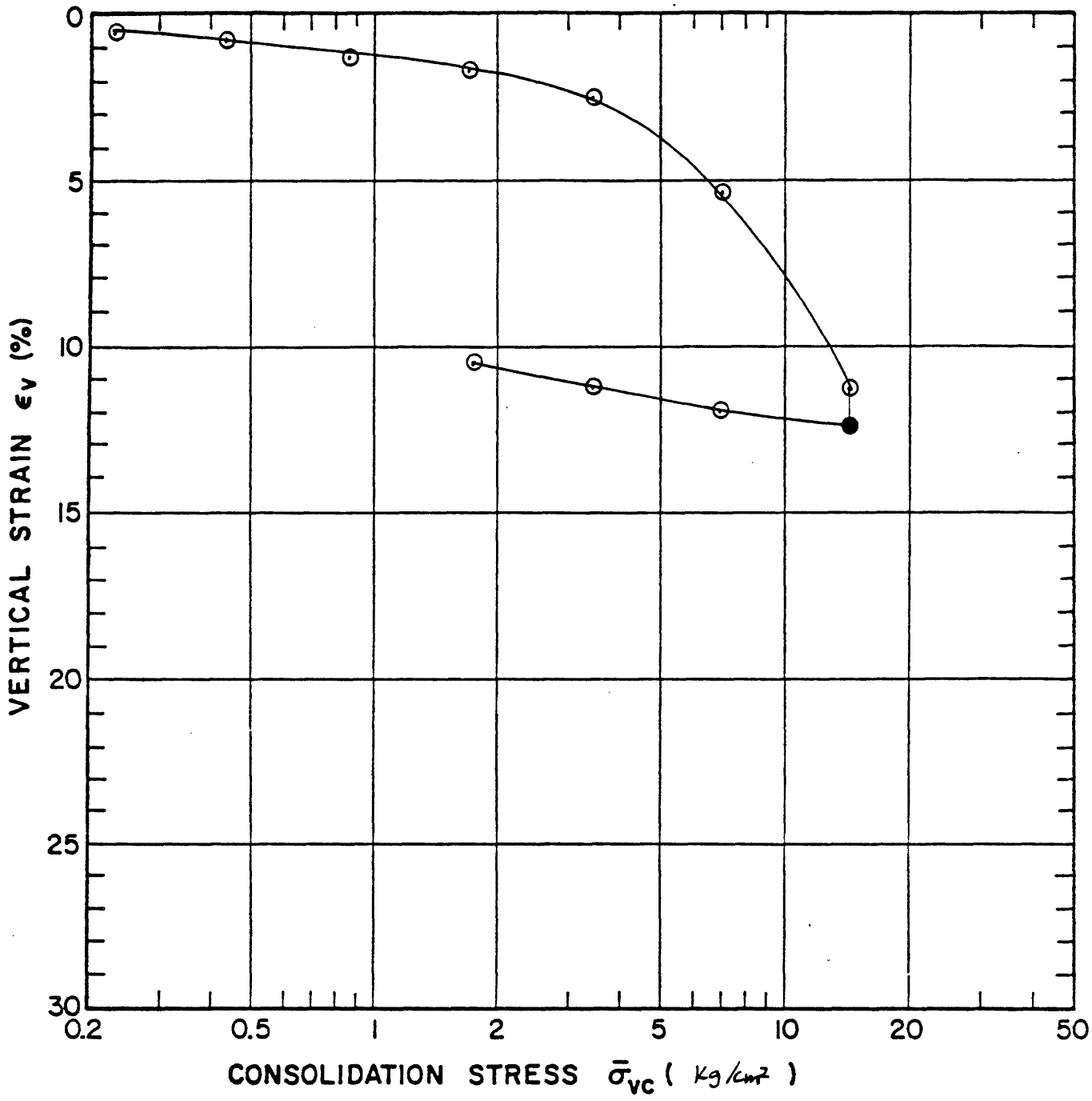

Sample No. MUD 1-2 w_N (%) 35.3 Estimated

Depth 46.0 ft. w_L (%) _____ $\bar{\sigma}_{vo}$ 1.60 ksc $\bar{\sigma}_{vm}$ _____

Soil Type BBC w_P (%) _____ CR _____ RR _____

_____ P.I.(%) _____ G_s _____ e_o _____ S(%) _____

o At t_p or ____ hr Remarks ϵ_v(%) based on disp from log t curve

● At ( ) hr _____

GEOTECHNICAL LABORATORY
DEPT. OF CIVIL ENGR.
M.I.T.

COMPRESSION CURVE

TEST No. DSS-19

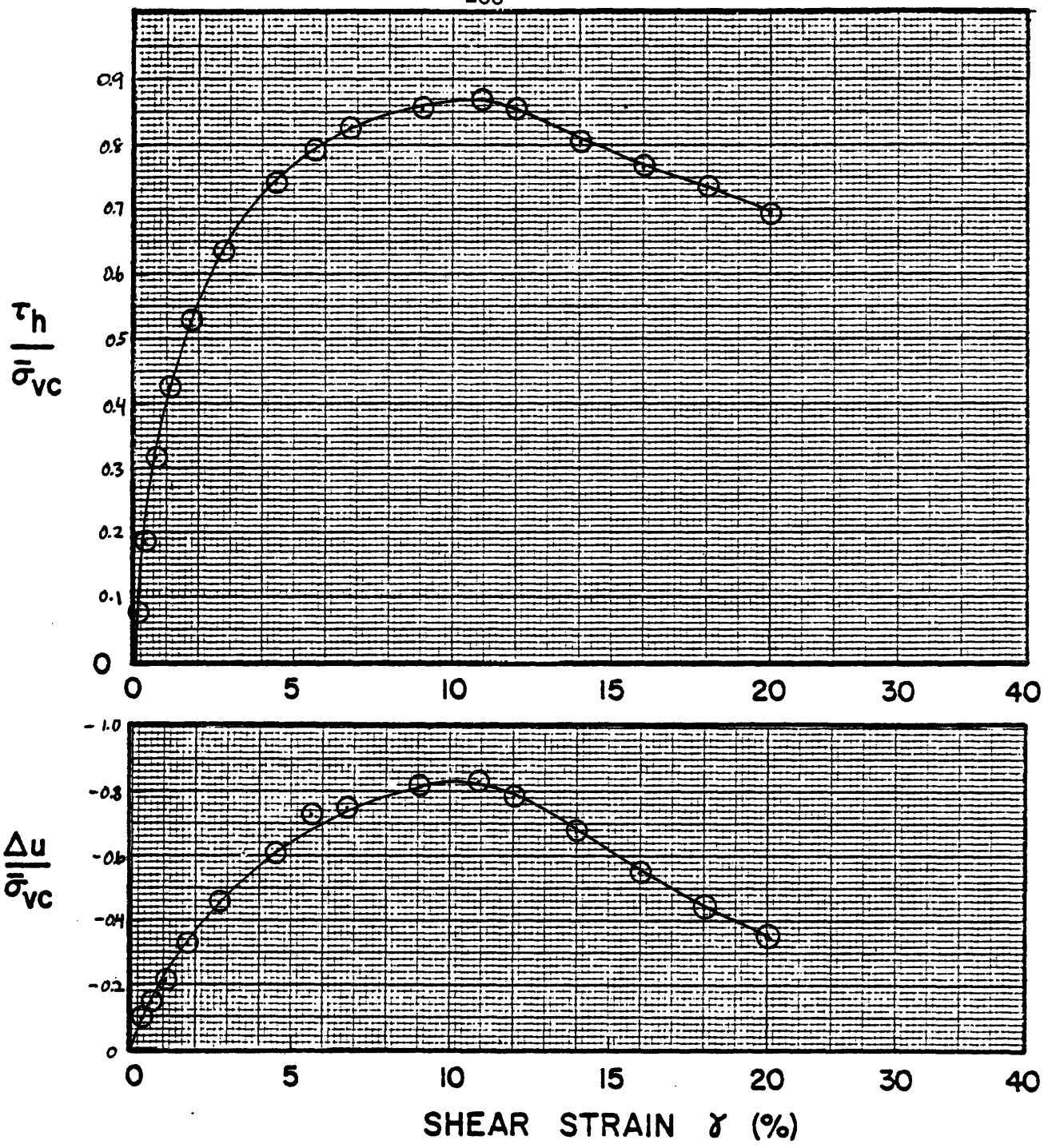

Sample No. MUD 1-2 w_N(%) 35.3 $\bar{\sigma}_{vc}$(Kg/cm²) 1.79 t_c(Days) 0.97

Depth 46.0 ft. w_L(%) ____ $\bar{\sigma}_{vm}$(Kg/cm²) 14.29 OCR 7.97

Soil Type BBC w_P(%) ____ Estimated $\bar{\sigma}_{vo}$(Kg/cm²) 1.60

GEOTECHNICAL LABORATORY
DEPT. OF CIVIL ENGR.
M.I.T.

NORMALIZED STRESS VS STRAIN
CK_oUDSS TEST NO. 19

FIGURE

Test No.	Sample No.	Depth ft.	w_N (%)	$\bar{\sigma}_{vc}$ (Kg/cm²)	$\bar{\sigma}_{vm}$ (Kg/cm²)	OCR	Symbol
19	MUD 1-2	46.0	35.3	1.79	14.29	7.97	

GEOTECHNICAL LABORATORY
DEPT. OF CIVIL ENGR.
M.I.T.

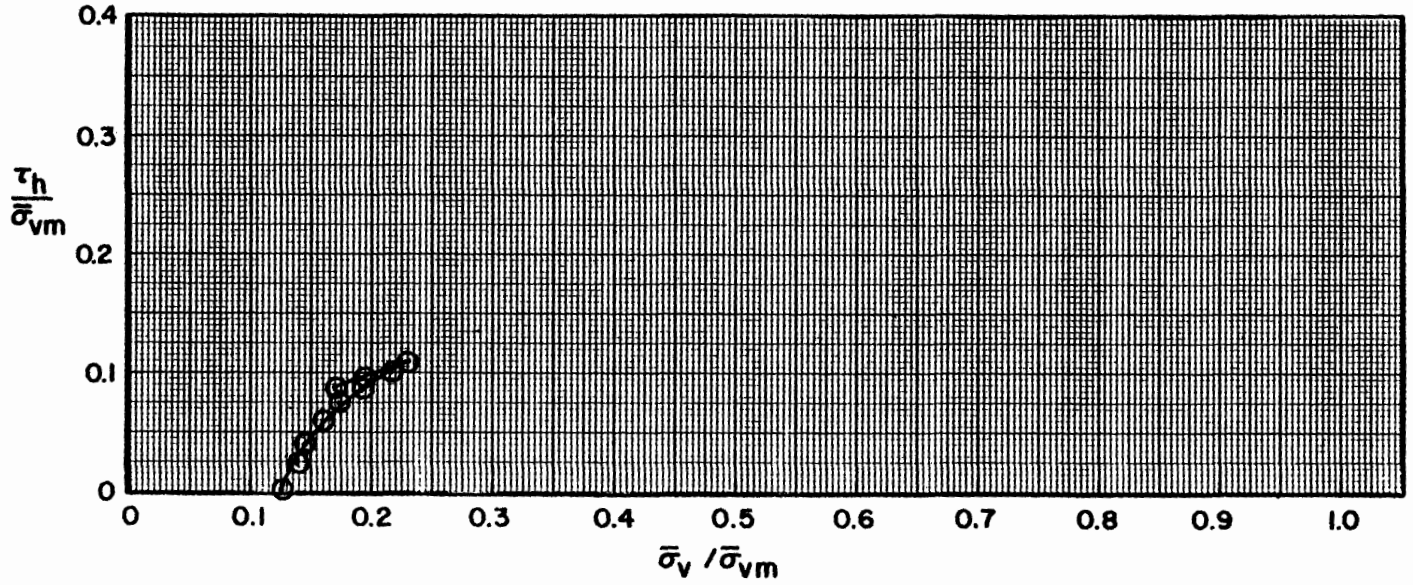

FIGURE

NORMALIZED STRESS PATHS FROM CK_0UDSS TESTS

Boring MUD 1 Soil Type BBC

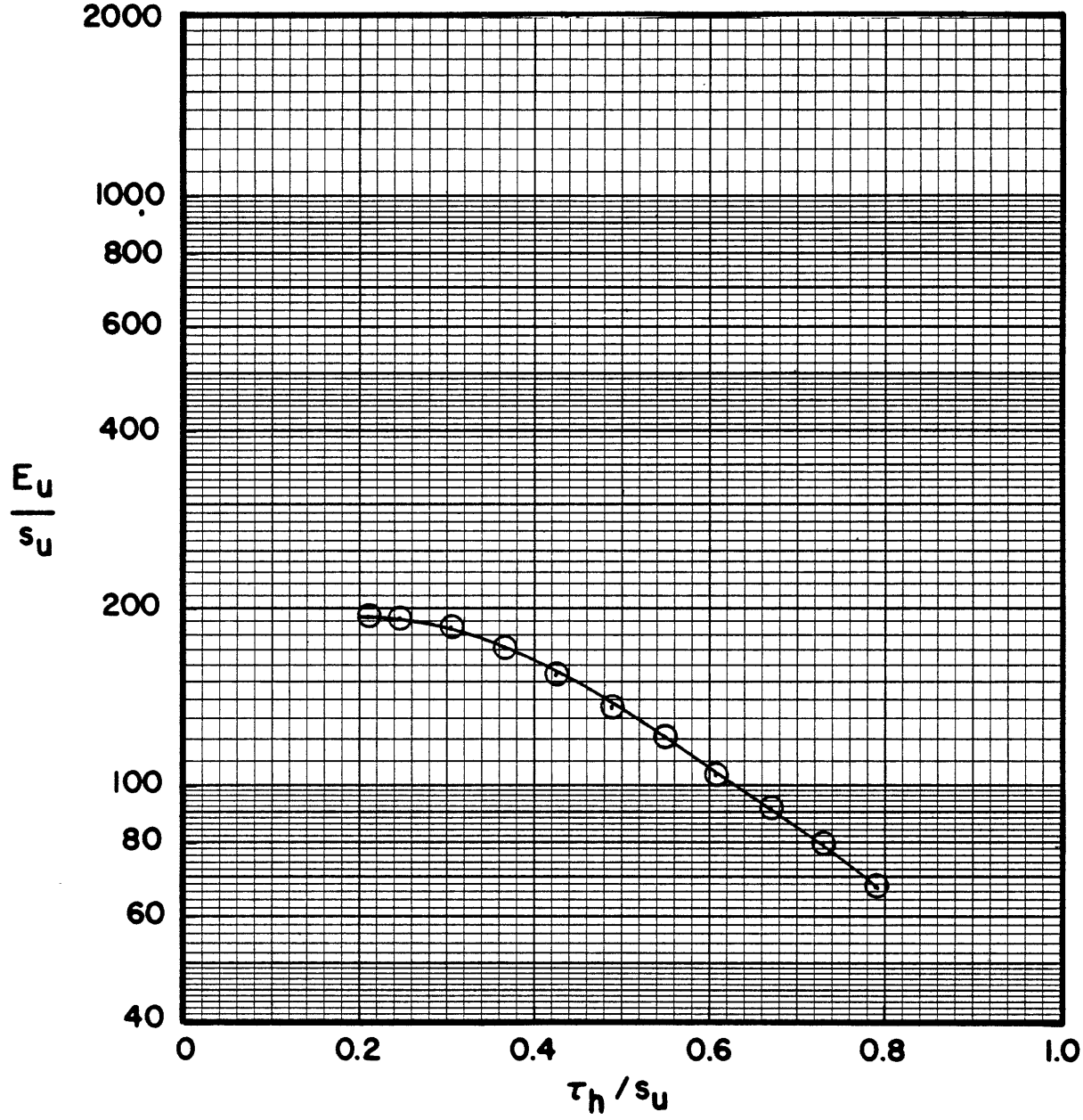

Test No.	Sample No.	Depth ft.	w_N (%)	$\bar{\sigma}_{vc}$ (Kg/cm2)	OCR	Symbol
19	MUD 1-2	46.0	35.3	1.79	7.97	

NORMALIZED MODULUS FROM CK$_o$UDSS TESTS

BORING MUD 1 SOIL TYPE BBC

FIGURE

GEOTECHNICAL LABORATORY, DEPT. OF CIVIL ENGR., M.I.T.

DIRECT - SIMPLE SHEAR TEST

PROJECT _____ TYPE OF TEST CK_oUDSS NO. X-1 OCR 1.0

SOIL TYPE BBC TESTED BY SPG DEVICE Geonor DATE 11/82

LOCATION MIT Solar House

CONSOLIDATION (Stresses in kg/cm²)

$\bar{\sigma}_{vc}$ 2.68 τ_{hc} - $\bar{\sigma}_{vm}$ 2.68

t_c(Day) 1.03 ε_v(%) 4.20 γ_c(%) ___ t_c(Day) _____

	W,%	e	S,%	H (mm)
Initial	43.0			25.349
Preshear				24.285
Final	42.0			

DURING SHEAR
Controlled Strain ✓ Stress _____
Rate (% / Hr.) _____

TIME (Hr.)	STRAIN (%)	$\frac{\tau_h}{\bar{\sigma}_{vc}}$	$\frac{\Delta u}{\bar{\sigma}_{vc}}$	$\frac{\bar{\sigma}_v}{\bar{\sigma}_{vc}}$	$\frac{\tau_h}{S_u}$	$\frac{\tau_h}{\bar{\sigma}_{vm}}$	$\frac{\bar{\sigma}_v}{\bar{\sigma}_{vm}}$	REMARKS
—	0.00	0.000	0.000	1.000	0.000			
	0.04	0.032	0.000	1.000	0.168			
	0.09	0.051	0.001	0.999	0.268			
	0.13	0.064	0.001	0.999	0.337			
	0.19	0.076	0.012	0.988	0.400			
	0.24	0.089	0.023	0.987	0.468			
	0.31	0.101	0.034	0.966	0.532			
	0.41	0.114	0.046	0.954	0.600			
	0.54	0.127	0.060	0.940	0.668			
	0.70	0.140	0.075	0.925	0.737			
	1.00	0.157	0.121	0.879	0.826			
	2.00	0.184	0.215	0.785				
	2.68	0.188	0.265	0.735				
	3.38	0.189	0.304	0.696				
	3.76	0.190	0.326	0.674				Peak
	4.62	0.190	0.378	0.622				
	5.50	0.188	0.402	0.598				
	6.50	0.187	0.438	0.562				
	7.50	0.183	0.470	0.530				
	8.50	0.181	0.481	0.519				
	10.00	0.175	0.518	0.482				
	12.00	0.168	0.557	0.443				
	14.00	0.159	0.593	0.407				
	16.00	0.149	0.630	0.370				
	18.00	0.140	0.641	0.359				

SOIL MECHANICS LABORATORY
DEPT. OF CIVIL ENGINEERING
MASSACHUSETTS INSTITUTE OF TECHNOLOGY

REMARKS: $\frac{E_u}{S_u} = \frac{3\tau_h}{S_u \text{ strain}}$

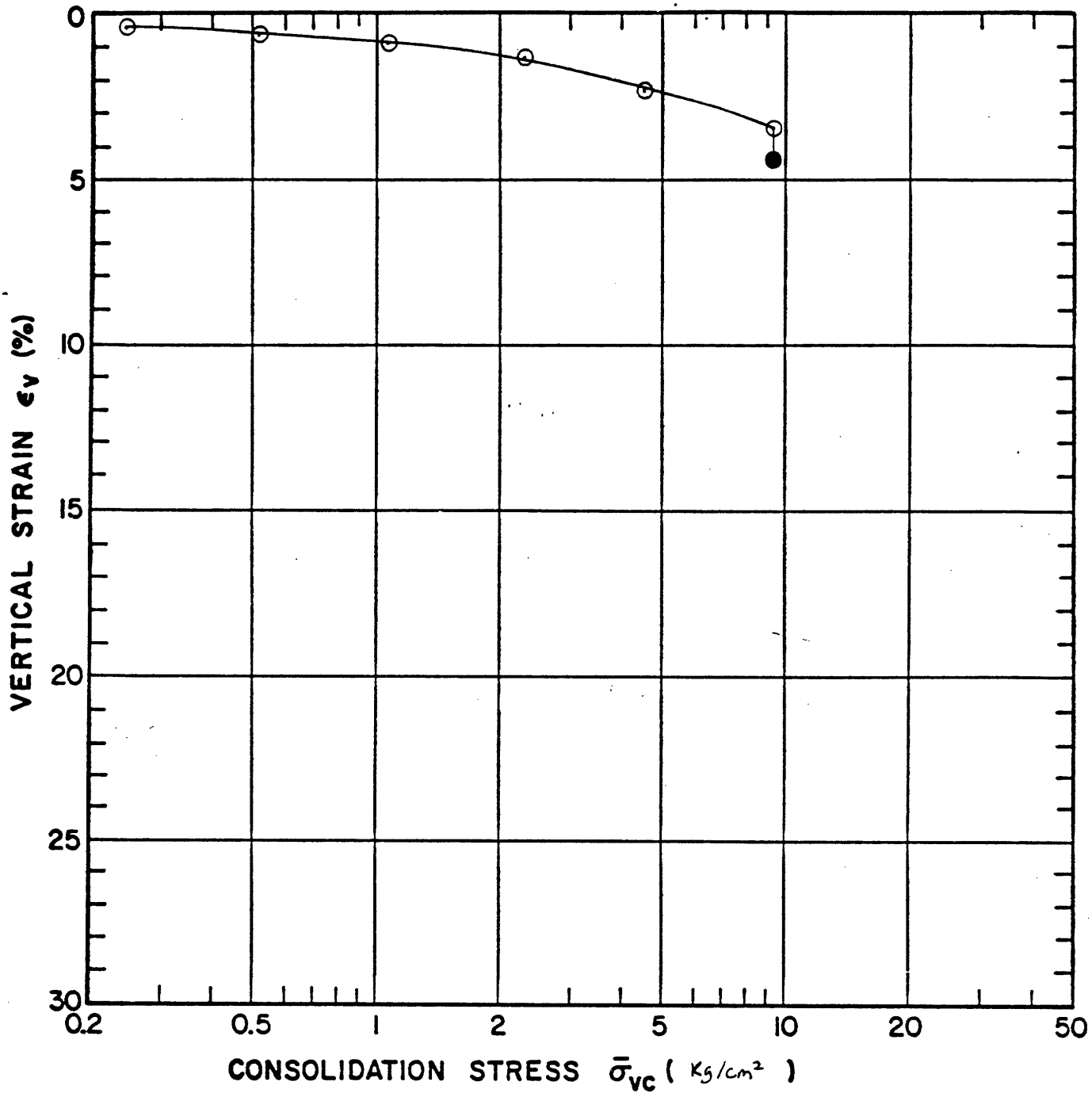

Sample No. MUD 1-8 w_N (%) 43.0 Estimated

Depth 90-92 ft. w_L (%) _____ $\bar{\sigma}_{vo}$ 2.68 ksc $\bar{\sigma}_{vm}$ _____

Soil Type BBC w_P (%) _____ CR _____ RR _____

_____ P.I.(%) _____ G_s _____ e_o _____ S(%) _____

o At t_p or _____ hr Remarks _____

● At ( ) hr _____

GEOTECHNICAL LABORATORY
DEPT. OF CIVIL ENGR.
M.I.T.

COMPRESSION CURVE

TEST No. X-1

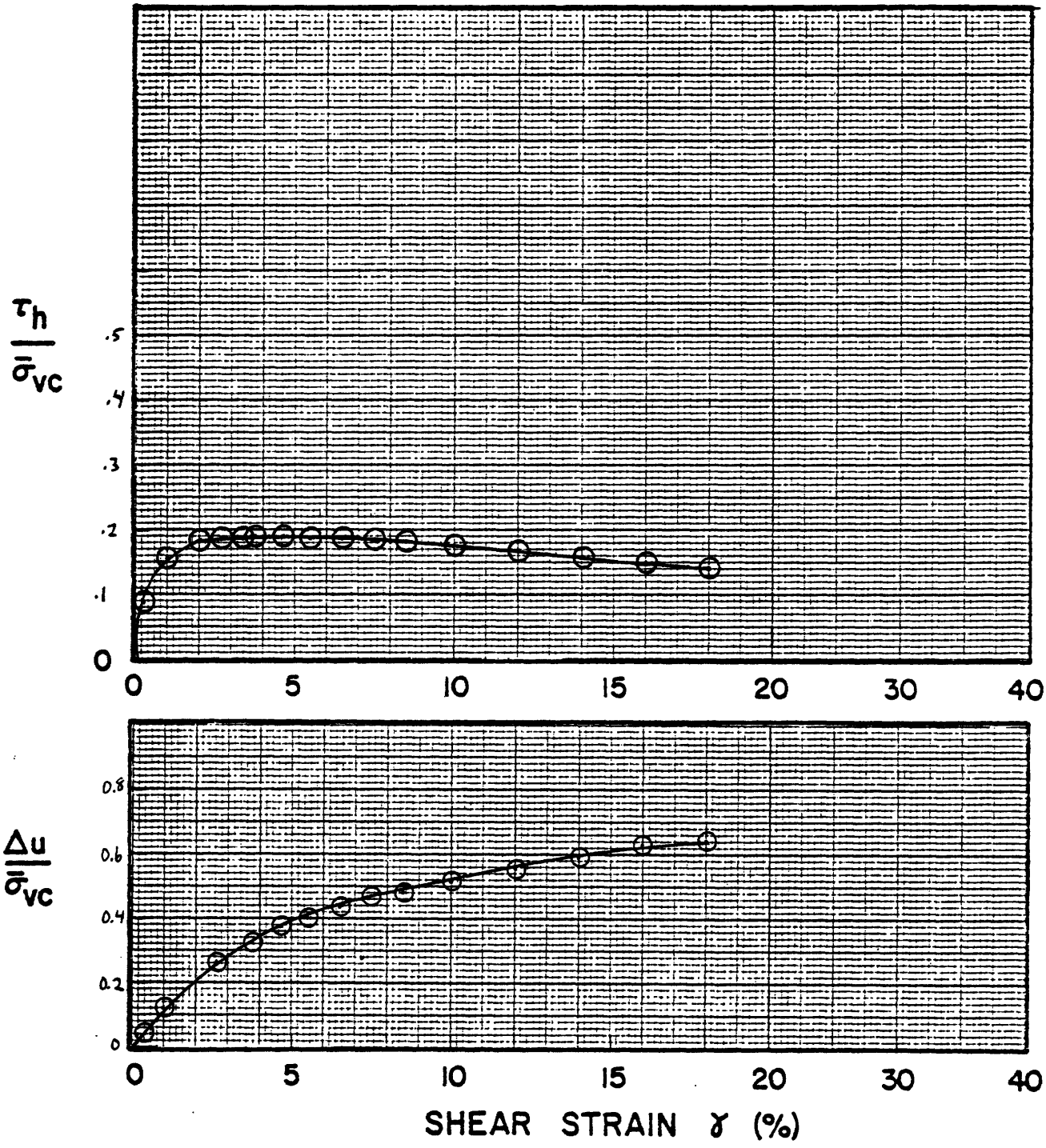

Sample No. MV0 1-8 w_N(%) 43.0 $\bar{\sigma}_{vc}$(ksc) 2.683 t_c(Days) ___

Depth 90-92 w_L(%) ___ $\bar{\sigma}_{vm}$(ksc) 2.683 OCR 1

Soil Type BBC w_P(%) ___ Estimated $\bar{\sigma}_{vo}$(2.68) ___

GEOTECHNICAL LABORATORY
DEPT. OF CIVIL ENGR.
M.I.T.

NORMALIZED STRESS VS STRAIN
CK_oUDSS TEST NO. X-1

FIGURE

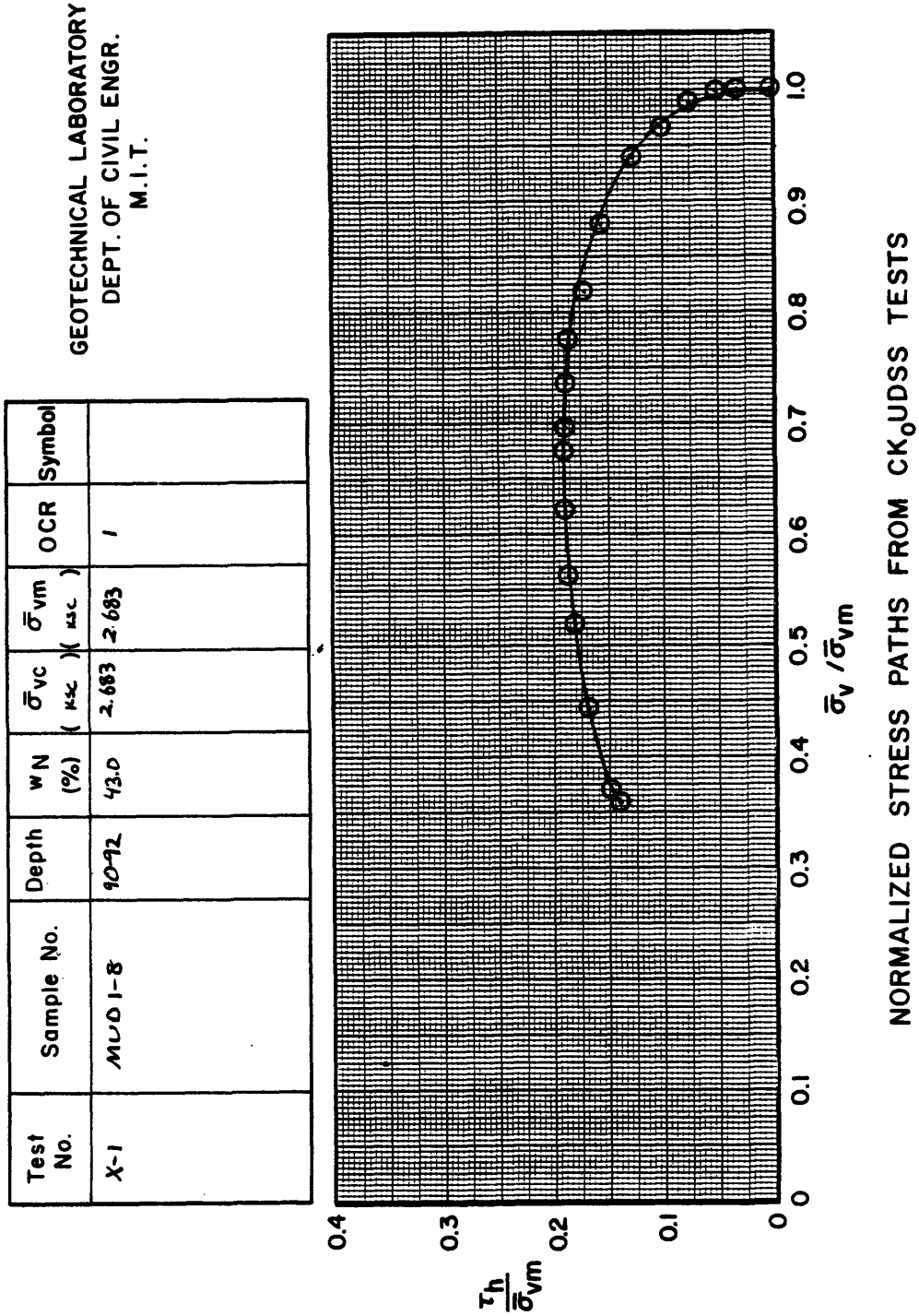

NORMALIZED STRESS PATHS FROM CK_0UDSS TESTS

Boring MUD-1 Soil Type BBC

FIGURE

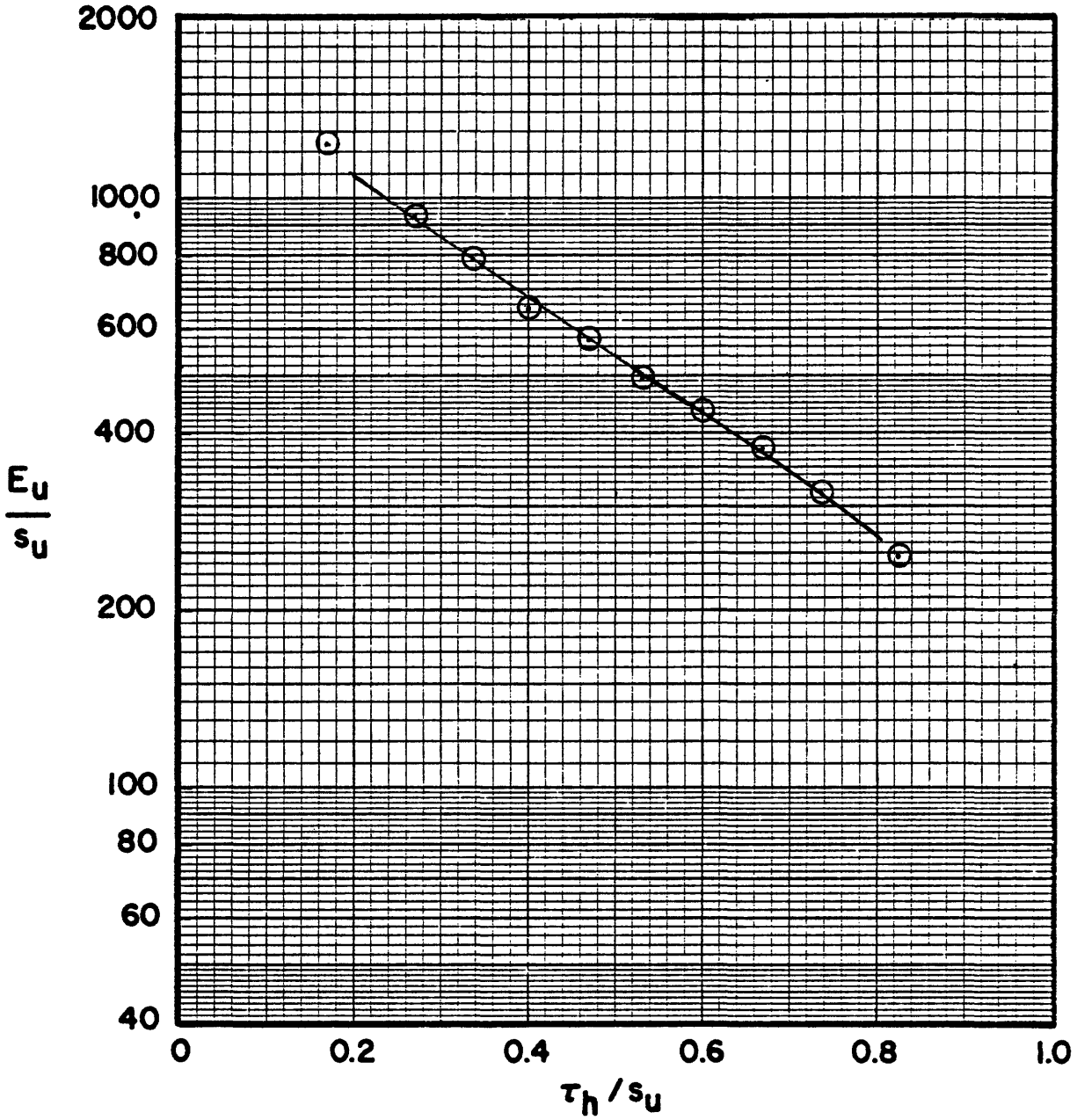

Test No.	Sample No.	Depth	w_N (%)	$\bar{\sigma}_{vc}$ (ksc)	OCR	Symbol
X-1	MUD 1-8	90-92	43.0	2.683	1	

NORMALIZED MODULUS FROM CK$_o$UDSS TESTS

BORING MUD-1 SOIL TYPE BBC

FIGURE

DIRECT - SIMPLE SHEAR TEST

PROJECT _____ TYPE OF TEST CK_oUDSS NO. X-2 OCR 1.00

SOIL TYPE BBC TESTED BY SPG DEVICE Geonor DATE 11/82

LOCATION MIT Solar House

CONSOLIDATION (Stresses in Kg/cm²)

$\bar{\sigma}_{vc}$ 1.675 τ_{hc} - $\bar{\sigma}_{vm}$ 4.675

t_c(Day) 0.92 ε_v(%) 10.3 γ_c(%) ___ t_c(Day) _____

	W,%	e	S,%	H (mm)
Initial	41.1			14.599
Preshear				13.096
Final	40.3			

DURING SHEAR
Controlled Strain ✓ Stress _____
Rate (% / Hr.) 5.17

TIME (Hr.)	STRAIN (%)	$\frac{\tau_h}{\bar{\sigma}_{vc}}$	$\frac{\Delta u}{\bar{\sigma}_{vc}}$	$\frac{\bar{\sigma}_v}{\bar{\sigma}_{vc}}$	$\frac{\tau_h}{S_u}$	$\frac{\tau_h}{\bar{\sigma}_{vm}}$	$\frac{\bar{\sigma}_v}{\bar{\sigma}_{vm}}$	REMARKS
0.00	0.00	0.000	0.000	1.000	0.000			
	0.03	0.026	0.018	0.982				
	0.07	0.035	0.026	0.974	0.204			
	0.08	0.044	0.026	0.974	0.257			
	0.12	0.053	0.026	0.975	0.309			
	0.15	0.062	0.026	0.974	0.362			
	0.21	0.071	0.042	0.958	0.414			
	0.40	0.097	0.059	0.941	0.566			
	0.60	0.112	0.088	0.912	0.653			
	1.00	0.134	0.147	0.853	0.781			
	1.40	0.146	0.167	0.833				
	2.60	0.165	0.256	0.744				
	3.00	0.168	0.280	0.720				
	3.50	0.170	0.306	0.694				
	4.00	0.171	0.331	0.669				
	4.50	0.172	0.351	0.646				Peak
	5.00	0.172	0.378	0.622				
	6.00	0.170	0.418	0.582				
	7.00	0.168	0.455	0.545				
	8.00	0.165	0.486	0.514				
	10.00	0.160	0.524	0.476				
	12.30	0.154	0.575	0.425				
	15.00	0.149	0.608	0.392				
	17.00	0.142	0.637	0.363				
3hr. 52min	20.00	0.136	0.659	0.341				

SOIL MECHANICS LABORATORY
DEPT. OF CIVIL ENGINEERING
MASSACHUSETTS INSTITUTE OF TECHNOLOGY

REMARKS: $\frac{E_u}{S_u} = \frac{3\tau_h}{S_u \text{ strain}}$

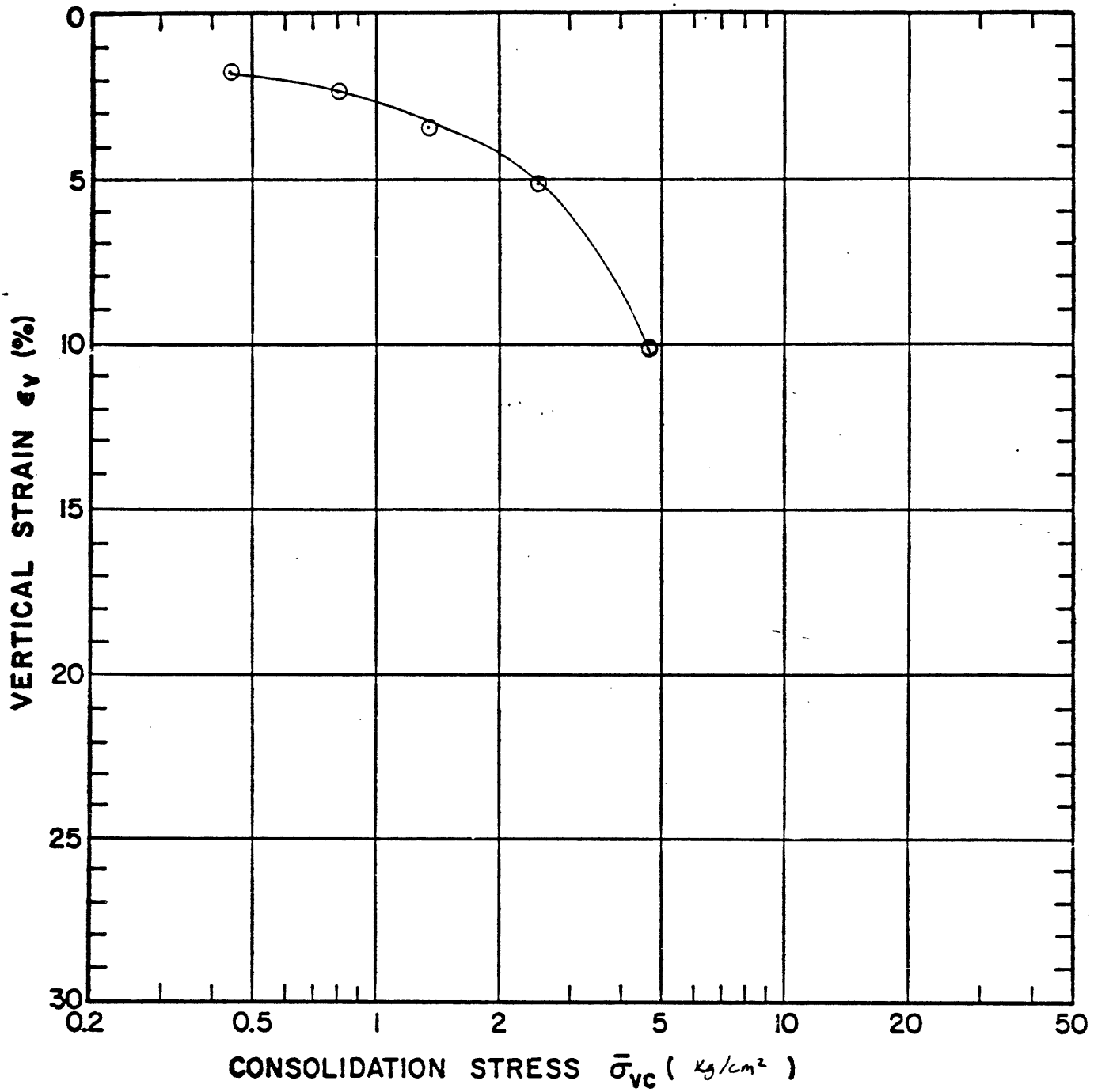

Sample No. MUD 1-9 w_N (%) 41.1 Estimated

Depth 95-97 ft. w_L (%) _____ $\bar{\sigma}_{vo}$ 2.85 ksc $\bar{\sigma}_{vm}$ _____

Soil Type BBC w_P (%) _____ CR _____ RR _____

_____ P.I.(%) _____ G_s _____ e_o _____ S(%) _____

o At t_p or _____ hr Remarks _____

● At ( ) hr _____

GEOTECHNICAL LABORATORY
DEPT. OF CIVIL ENGR.
M.I.T.

COMPRESSION CURVE

TEST No. X-2

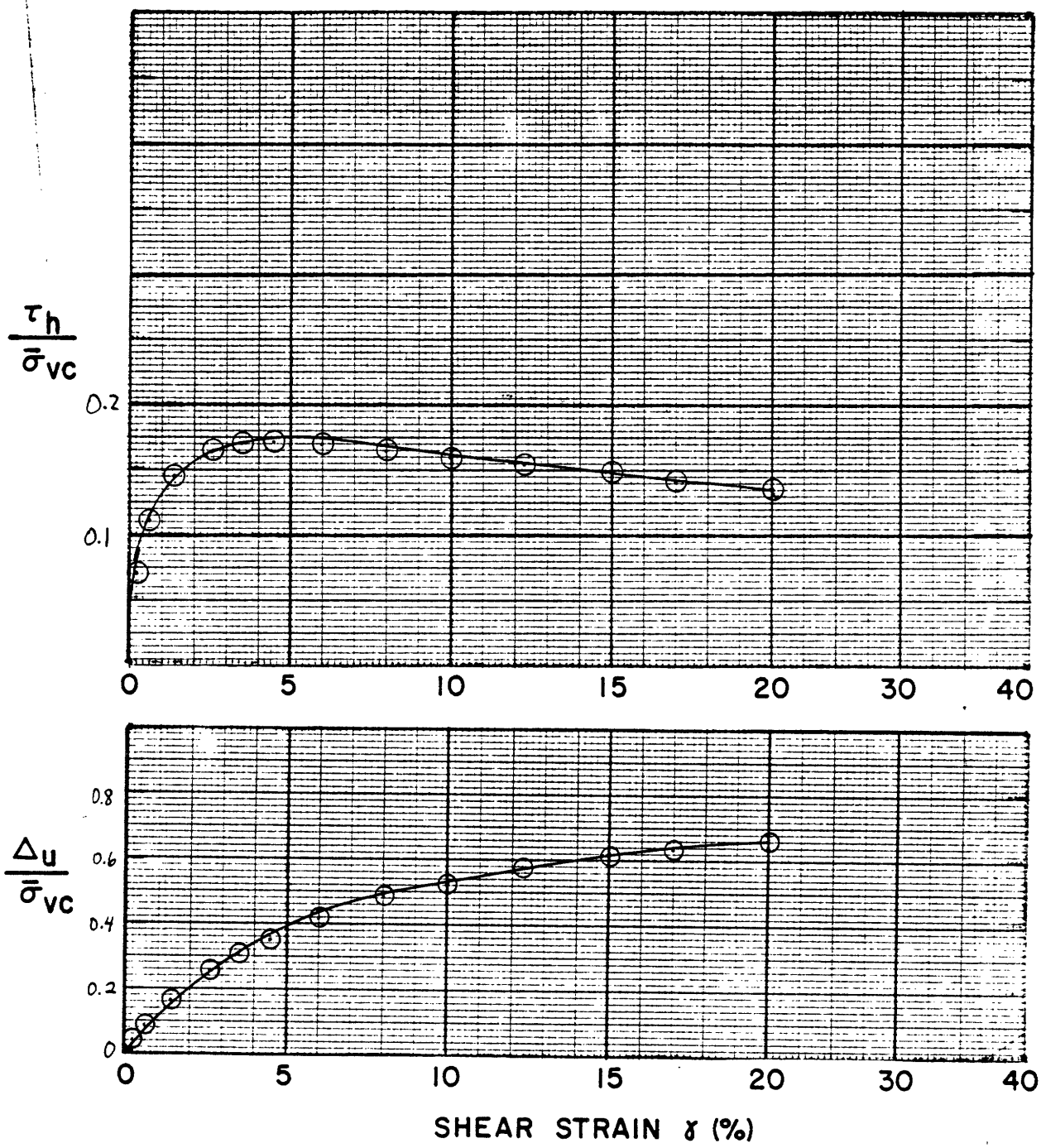

Sample No. MUD 1-9 w_N (%) 41.1 $\bar{\sigma}_{vc}$ (Kg/cm²) 4.67⁵ t_c(Days)

Depth 95-97 ft. w_L (%) $\bar{\sigma}_{vm}$ (Kg/cm²) 4.67⁵ OCR 1.00

Soil Type BBC w_P (%) Estimated $\bar{\sigma}_{vo}$ (2.85 kg/cm²)

GEOTECHNICAL LABORATORY
DEPT. OF CIVIL ENGR.
M.I.T.

NORMALIZED STRESS VS STRAIN

CK_oUDSS TEST NO. X-2

FIGURE

Test No.	Sample No.	Depth ft.	w_N (%)	$\bar{\sigma}_{vc}$ (kg/cm^2)	$\bar{\sigma}_{vm}$ (kg/cm^2)	OCR	Symbol
X-2	MUD 1-9	95-97	41.1	4.61[5]	4.61[5]	1.00	

GEOTECHNICAL LABORATORY
DEPT. OF CIVIL ENGR.
M.I.T.

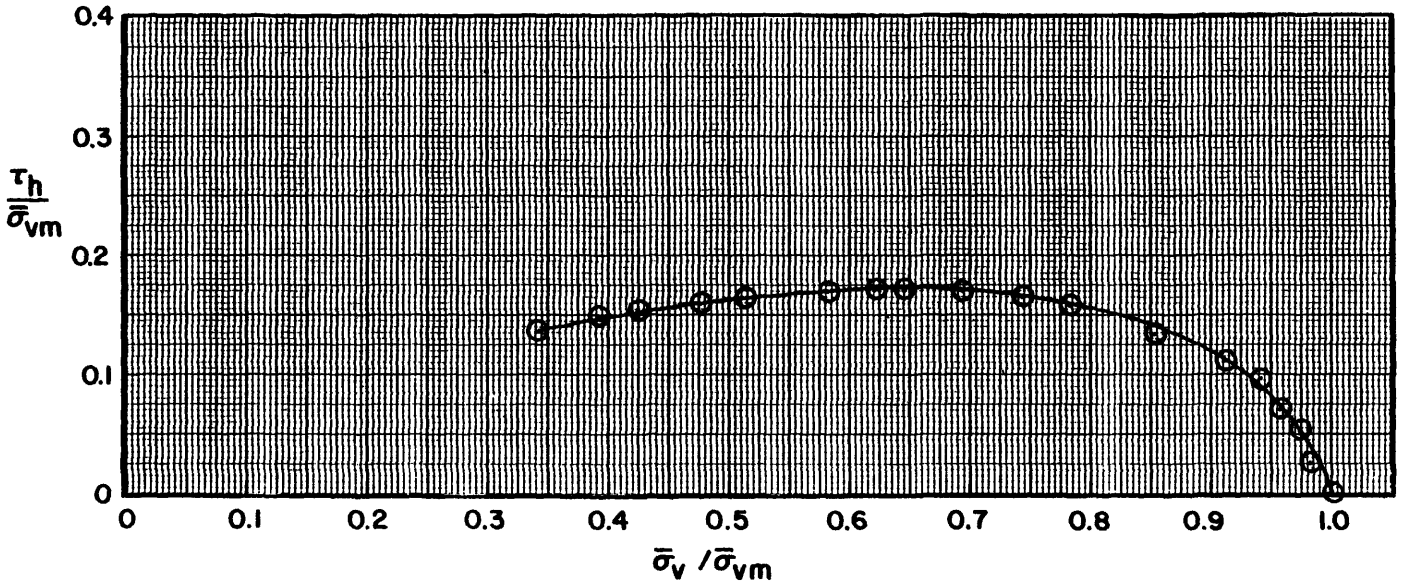

FIGURE

NORMALIZED STRESS PATHS FROM CK_0UDSS TESTS

Boring MUD-1 Soil Type BBC

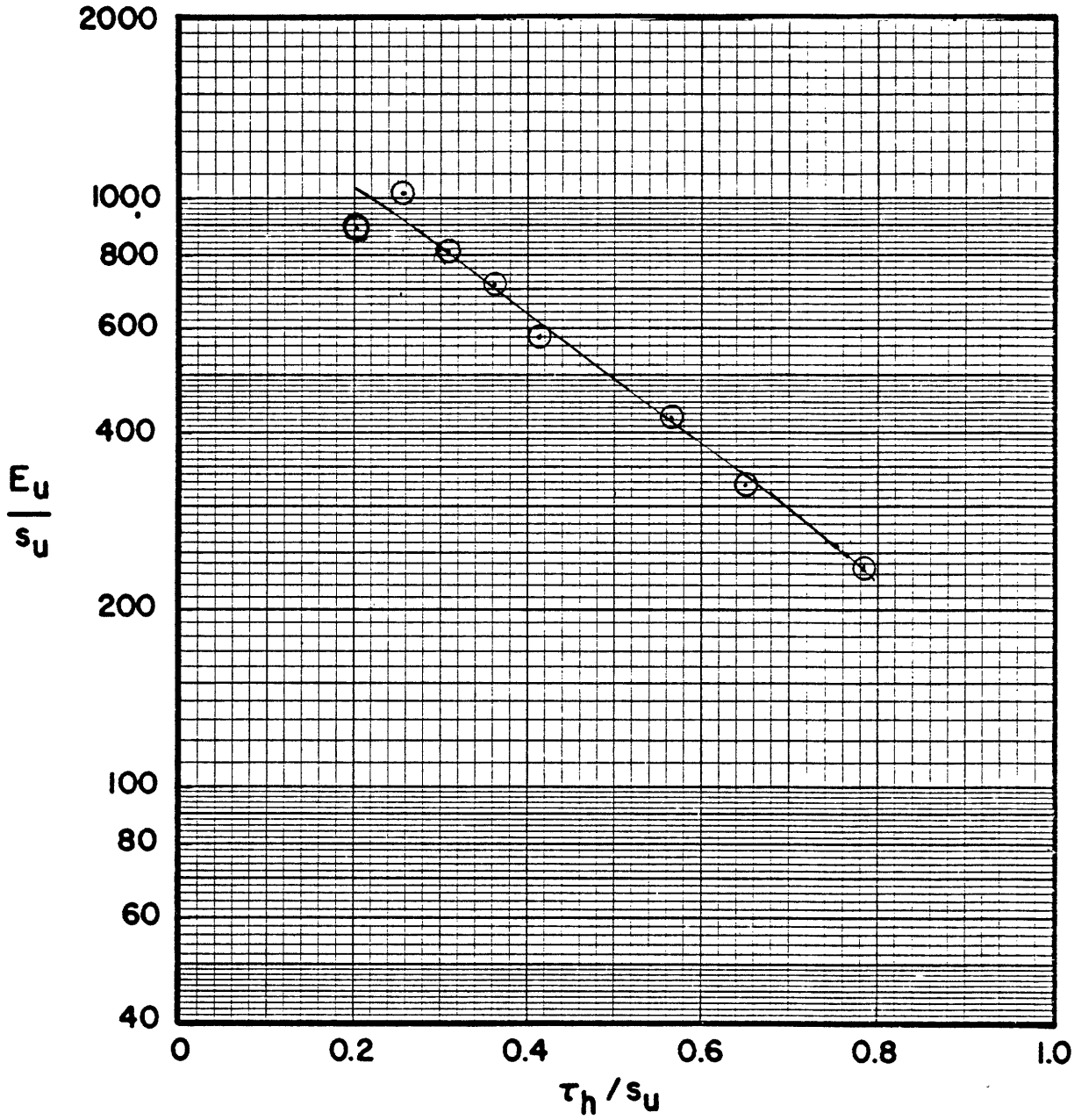

Test No.	Sample No.	Depth (ft.)	w_N (%)	$\bar{\sigma}_{vc}$ (tsc)	OCR	Symbol
X2	MUD 1-9	95-97	41.1	4.675	1.00	

NORMALIZED MODULUS FROM CK$_o$UDSS TESTS

BORING MUD1 SOIL TYPE BBC

FIGURE

GEOTECHNICAL LABORATORY, DEPT. OF CIVIL ENGR., M.I.T.